

2) Haydel
NASW-
1335

**CONTROLLED STRUCTURES TECHNOLOGY
M.I.T. SPACE ENGINEERING RESEARCH CENTER**

STEERING COMMITTEE WORKSHOP AGENDA

**January 22 and 23, 1992
(Given Room)**

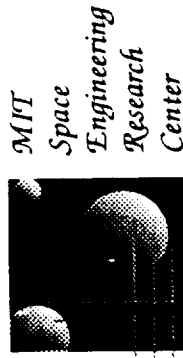
Arrive at Room 37-355 (253-8809), directions will be given

Wednesday, January 22, 1992

9:30 am	<i>Coffee</i>	
10:00-10:30	Welcome and Overview	Crawley
	<u>INTERFEROMETER TESTBED</u>	
10:30-10:45	Problem Description	Shea/Nisbet
10:45-11:20	Damping and Identification	How/Blackwood
11:20-11:40	Closed-Loop Control	Jacques
11:40-12:00	Low Authority Control	Hall/MacMartin
12:00-1:00	<i>Lunch</i>	
1:00-2:00	Lab Tour Meet at Rm. 37-372	
	<u>MIDDECK 0-GRAVITY DYNAMICS EXPERIMENT</u>	
2:15-2:45	Motivation/Background	Crawley
	MODE Program Highlights:	
	Schedule	
	Hardware	
	On-Orbit Operations	
2:45-3:00	STA	Crawley/Masters
3:00-3:15	FTA	van Schoor
3:15-3:30	<i>Break</i>	
	<u>MIDDECK ACTIVE CONTROL EXPERIMENT</u>	
3:30-3:50	Motivation/Objectives	Miller
	MACE Flight Program	
	Development Model	
	Related Research:	
3:50-4:10	Gravity Effects	Crawley/Rey
4:10-4:30	Identification for Robust Control	Karlov
4:30-5:00	<u>FUTURE PLAN-OVERVIEW</u>	Crawley

Thursday, January 23, 1992

8:00 am	<i>Coffee</i>	
	<u>ADDITIONAL RESEARCH IN PROGRESS</u>	
8:30-8:50	Multivariable Identification for Control	Athans/Lublin/Douglas
8:50-9:10	Strain Actuated Aeroelastic Control	Crawley/Lazarus
9:10-9:30	Sensor/Actuator Technology Development	Hagood/Anderson
9:30-9:50	Input Command Shaping	Seering/Chang
9:50-10:10	Other Ongoing Research	Crawley/Miller
10:10-10:20	<i>Break</i>	
10:20-11:00	<u>FUTURE PLAN-DETAIL</u>	Crawley
11:00-11:45	Workgroups	
11:45-12:15	Steering Committee Executive Session	
12:15-1:00	<i>Lunch</i>	
1:00-2:00	Steering Committee Recommendations	
2:00	<i>Conclusion</i>	



***M.I.T.
SPACE ENGINEERING RESEARCH CENTER
FOCUSED ON CONTROLLED STRUCTURES
TECHNOLOGY
1992 OVERVIEW***

Prof. Edward F. Crawley Center Director

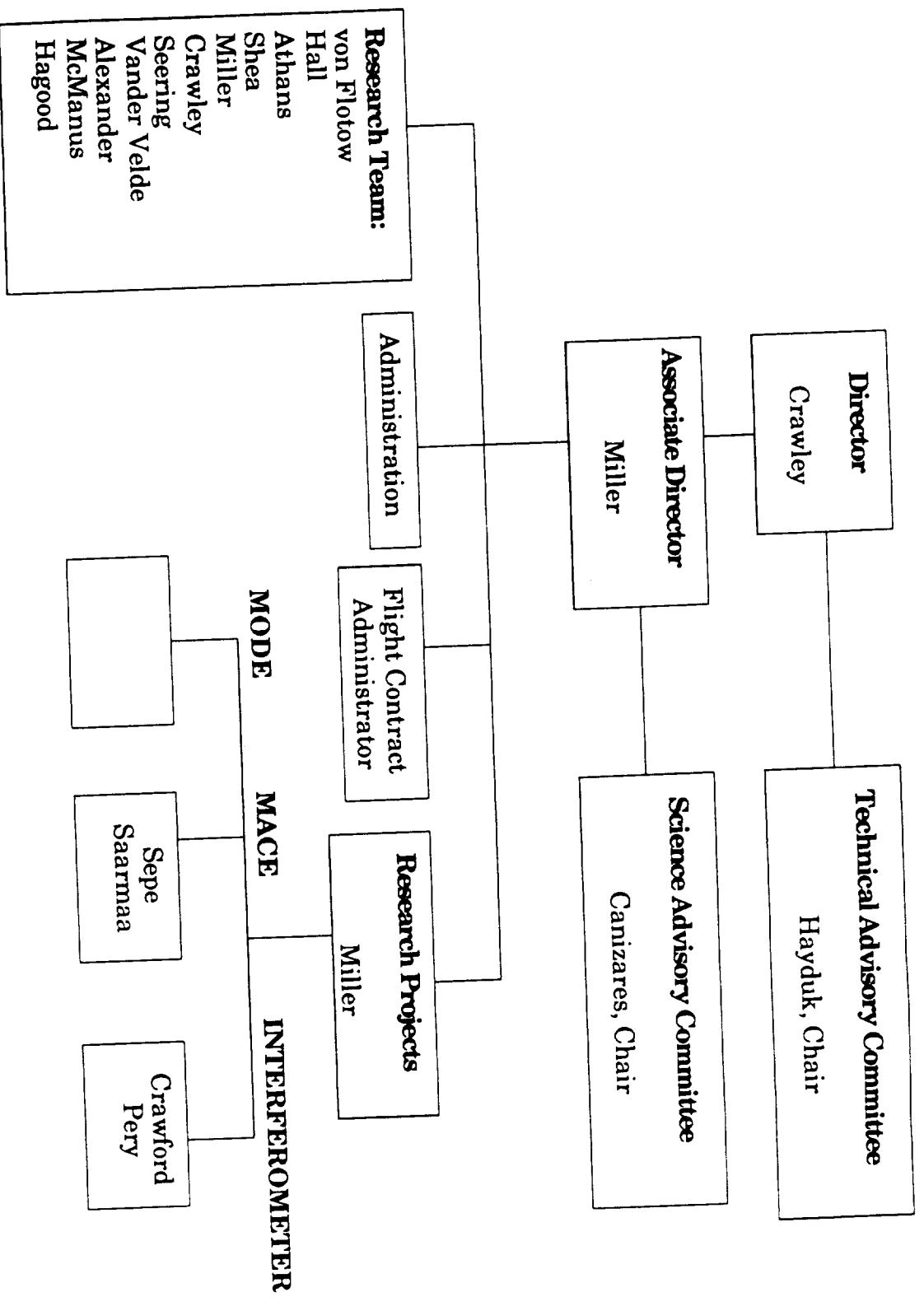
THE OBJECTIVE

To develop and demonstrate a unified technology of controlled structures, to codify and disseminate this technology, and to train a generation of skilled engineers.

APPROACH

- Form a cohesive focused interdepartmental faculty and student group.
- Identify goals by examining shortcomings of current technology and requirements of future scientific and exploration missions.
- Develop technology base research program to advance toward these goals.
- Develop hardware testbeds which mimic the requirements of relevant NASA missions.
- Promote reality by requiring students to demonstrate concepts on hardware testbeds.
- Insure coordination by working with NASA CSI field centers.
- Enable technical transfer by actively involving industrial participants.

ORGANIZATIONAL CHART



CENTER STEERING COMMITTEE

- Chairman- Vacant
- MIT Administration
- Science Advisory Representative
- Corporate Representative
(LMSC, ITEK, Draper, MDSSC, Harris, TRW)
- Center Management

TECHNICAL REPRESENTATIVE COMMITTEE

- Robert Hayduk, NASA Code RS- Chairman
- Jet Propulsion Laboratory
- Langley Research Center
- Marshall Space Flight Center

THE SCIENCE ADVISORY COMMITTEE

- Prof. Claude Canizares - Chairman

X-Ray Astronomy

- Prof. Bernard Burke

Interferometry

- Prof. Davis Staelin

Radio Astronomy

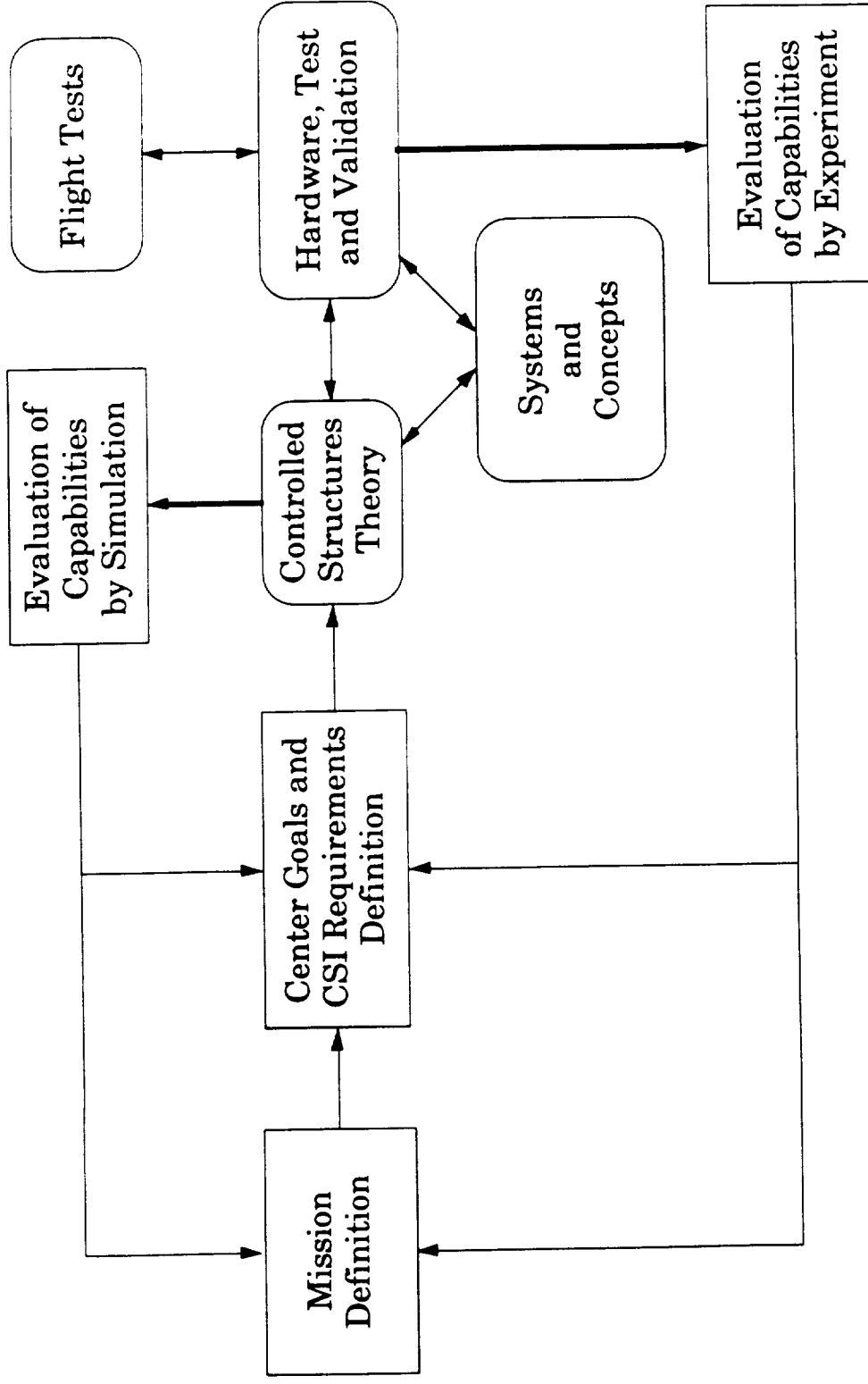
- Dr. Mike Shao

SAO/JPL

- Dr. Steve Synnott

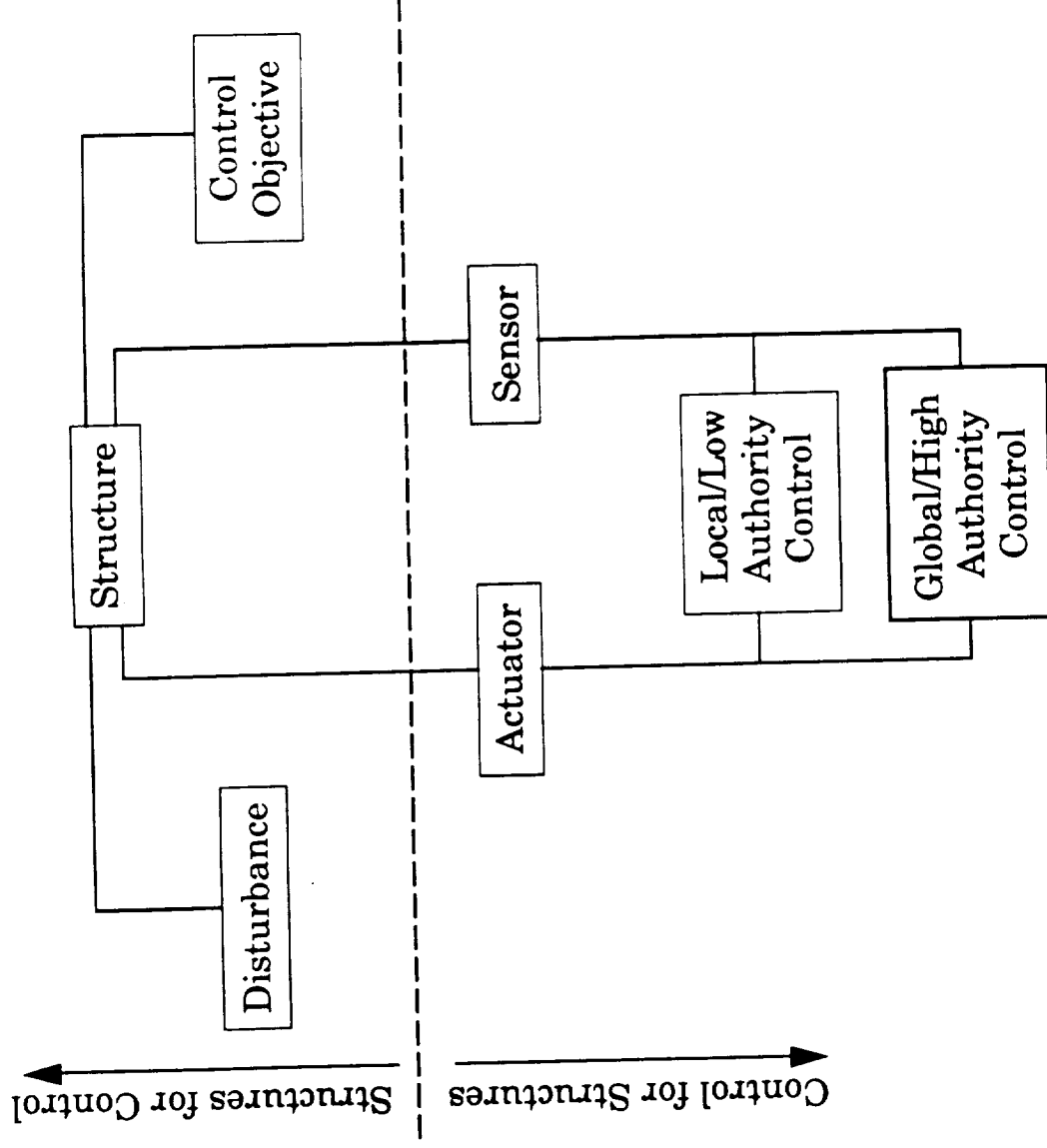
Jet Propulsion Laboratory

FUNCTIONAL ORGANIZATION



A CST DESIGN METHODOLOGY

1. Design structure.
2. Design disturbances and control objective.
3. Design actuator and sensor.
4. Design local/low authority control.
5. Design high authority control.



EVALUATION PLAN

- Internal review meeting - faculty and students present work to date, proposals for next year. Internal consensus on direction.
- Science Advisory Committee - review by leading scientists of relevance and direction of program.
- Steering/Technical Representative Committee - one day workshop presents work-to-date and consensus plans. Steering Committee (non-NASA) and TRC (NASA) caucus individually and give input to program. Director and TRC Chair concur on budget.
- Mid-summer internal review meeting - faculty and students check on progress and direction.
- Annual Symposium - mid-summer, at or near NASA center or MIT.

MAJOR INTERACTIONS WITH GOVERNMENT AND INDUSTRY

- Coordination of Interferometer Testbeds (MIT, JPL)
- Coordination of CST sample problems (MIT, JPL, LaRC, LMSC)
- Design and development of MODE flight experiment (MIT, LaRC, MDSSC, Payload Systems, Inc.)
- Design and development of MACE flight experiment (MIT, LaRC, LMSC, Payload Systems, Inc., MDSSC)
- Design and development of MACE ground test facility (ISI, CSA)
- Development and demonstration of command prefiltering for vibration reduction on Shuttle RMS (MIT, JSC, Draper)
- Guest investigator on ASTREX facility (LaRC, AFAL)
- Research funding to develop robust active vibration suppression of the AMASS program (TRW).

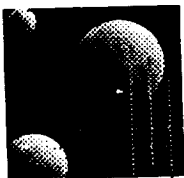
GOVERNMENT, INDUSTRY PERSONNEL AT MIT

- Short Visits from JPL, LaRC, MSFC
- Repeated Short Visits on MACE from LaRC
- Visiting Scholar from Harris (2 weeks)
- Visiting Scholar from ISI (1 week)
- Visiting Scholar from MDSSC (multiple 1x2 visits)
- Visiting Scholar from U of Colorado (4 months) — Eric Rort
- Visiting Scholar from Penn State (6 months)
- Visiting Scholar from MAI (6 months)

Massachusetts
Research Center

MIT PERSONNEL IN GOVERNMENT AND INDUSTRY

- Active at major conferences (CSI, SDM, ACC, CDC, etc.)
- Summer symposium at MIT
- Undergraduate students in residence at JPL
- MIT faculty participation in JPL interferometer design reviews
- COOP students at LaRC, JPL, ...
- Multiple students in residence at LMSC
- In the next year, hope to have longer visit at LaRC



MIT
Space
Engineering
Research
Center

INTERFEROMETER TESTBED: OVERVIEW AND HARDWARE SUMMARY

Andrew Nisbet

January 22, 1992

51-74
-1603-11
N93-27889
1-10

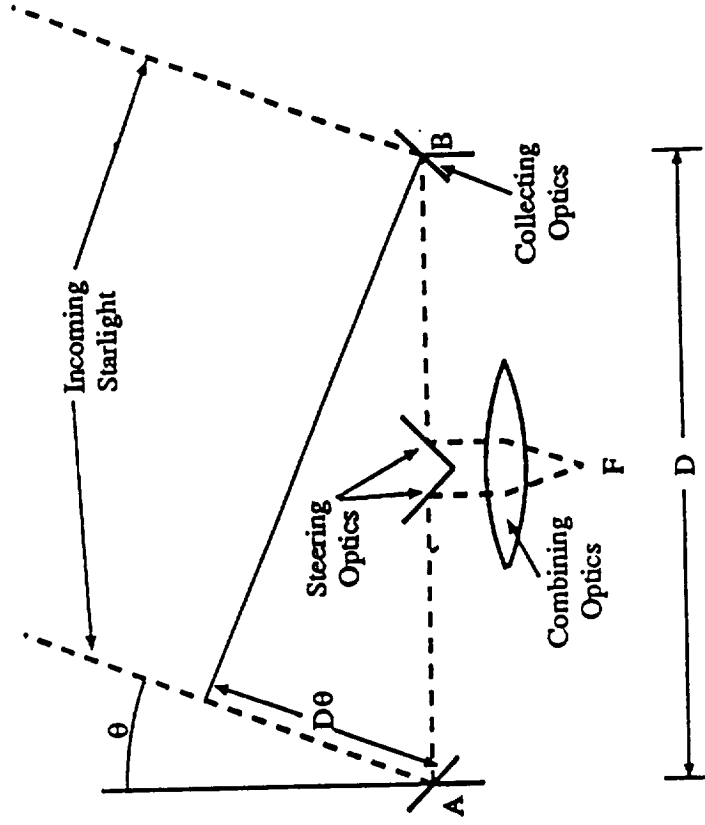
185

Reference Mission & Science Requirements

- Needed scientific reference mission to define stringent CST goals: Optical Interferometer Spacecraft
- Consultation with astronomers produced the set of mission objectives shown below. The science requirements were then derived from the mission objectives.

Mission Objectives	
Description	Value
resolution	3 m-arcsec (0.014 μ rad)
wavelength	0.5 micron
stellar magnitude	10
imaging	100% u-v plane coverage
	95% image quality

Science Requirements	
Description	Value
baseline	35 meters
high freq. DPL error	25 nm > 0.005 Hz
low freq. DPL error	10 nm < 0.005 Hz



Schematic of a two dimensional interferometer

Science Requirements Derivation

- Baseline derived from resolution objective
- $$\rho = \frac{\lambda}{D} = 0.003 \text{ arcsec}$$
- High frequency DPL limit derived from maximum intensity function

$$\begin{aligned} I_{\max} &= I_T + V(u) \cos \left(2\pi \frac{\partial \ell}{\lambda} \right) \\ &\approx I_T + V(u) \left(1 - \frac{1}{2} \left(2\pi \frac{\partial \ell}{\lambda} \right)^2 \right) \end{aligned}$$

- Low frequency DPL limited derived from phase error

$$\phi_e = 2\pi \frac{\partial \ell}{\lambda}$$

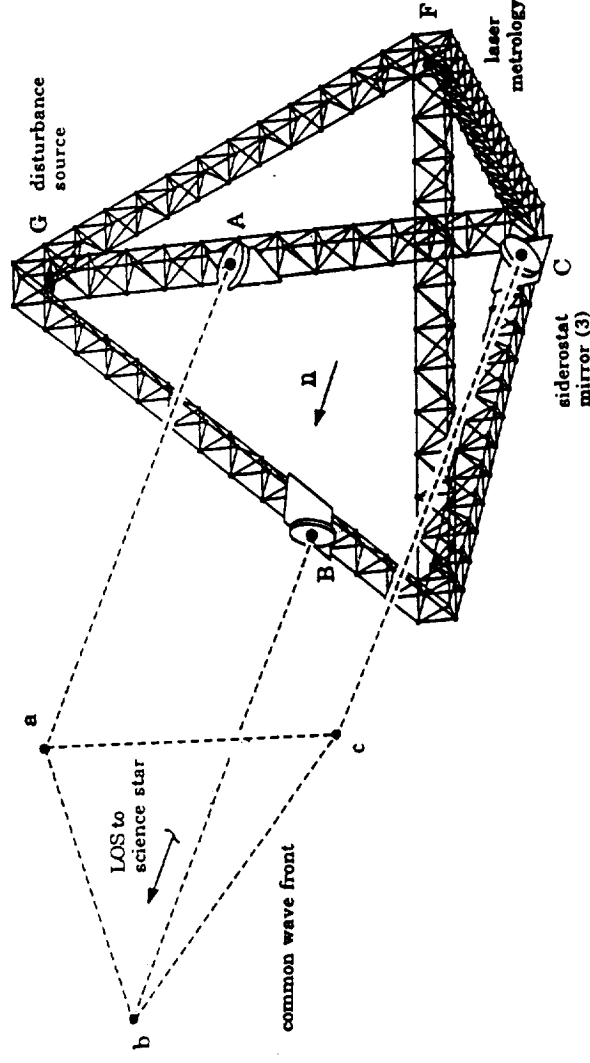
Reference Spacecraft Design Summary

Baseline	35 meters
Architecture	Deployable tetrahedral truss structure
Spacecraft Mass	3285 kg (truss) 12325 kg (total) incl. 25% margin
Payload Architecture	8 siderostats in non-redundant 2-D array
Telecommunications	TDRSS S-band compatible
Power Source	Body mounted solar arrays
Attitude Control	8 1200 Nms RWAs & mag. torque momentum dumping
Science Mode	217 sec integration time, continuous rotation about LOS

main S-band receiver

Testbed Requirements & Performance Metric

- Structure is 1/10th scale truss-work tetrahedron with three siderostat locations. Performance requirement of 50 nm RMS differential pathlength error (DPL) above 10 Hz is an order of magnitude improvement over expected disturbance environment.



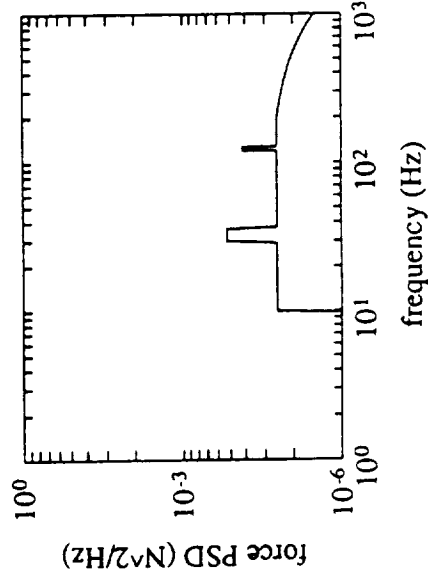
- Decision made to address only a subset of the DPL problem. Errors due only to internal flexible motion will be considered, that due to external flexible and rigid body motion are not measured.

- The performance metric as defined by internal flexible motion is measured by laser legs AF, BF, and CF. The performance goals for the testbed are:

$$\max \begin{pmatrix} (AF - BF)_{RMS} \\ (BF - CF)_{RMS} \\ (CF - AF)_{RMS} \end{pmatrix} \leq 50 \text{ nm over } 10 - 200 \text{ Hz Bandwidth}$$

Disturbance Source & Signal

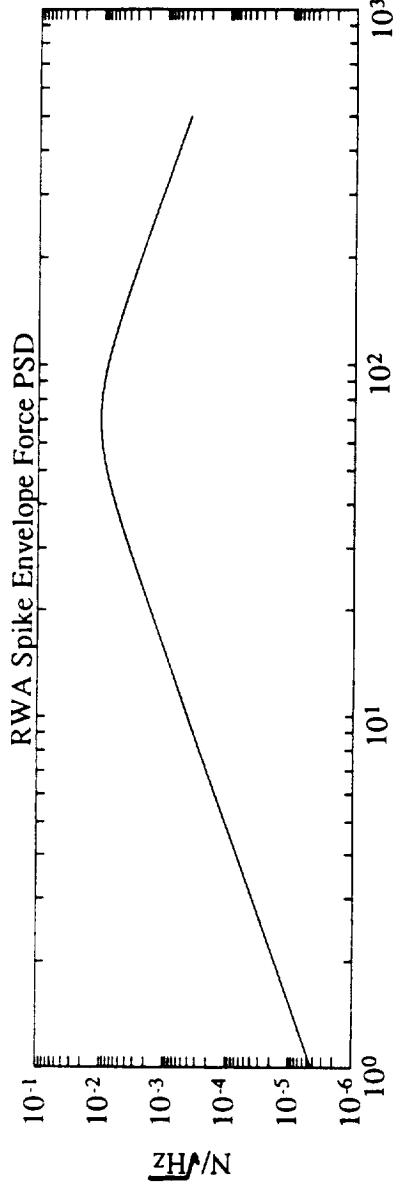
- Reference mission design identified typical spacecraft disturbances and determined DPL response of ~ 500 nm RMS on structure with nominal level of damping ($\sim 1\%$).
 - Narrow band spikes (reaction wheel imbalances)
 - Broadband (fluid flow noise)
 - Transient (solar array or antenna drives)
- Disturbance Signals Applied To Piezo-Shaker:
 - A signal to represent low broadband noise with slowly varying spikes produced insufficient excitation in structure.



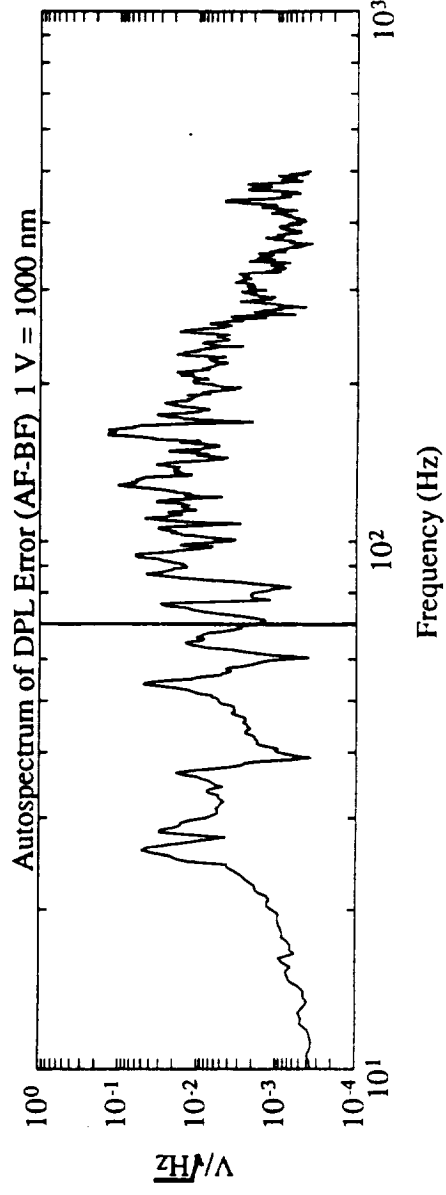
Response: only 80 - 100 nm RMS
predominantly in 20 - 50 Hz band

- Disturbance Signal (con't):

- Signal representing RWA spike envelope which increases with the square of the frequency up to wheels speed limit at 70 Hz. Some tail on the spectrum due to harmonics.



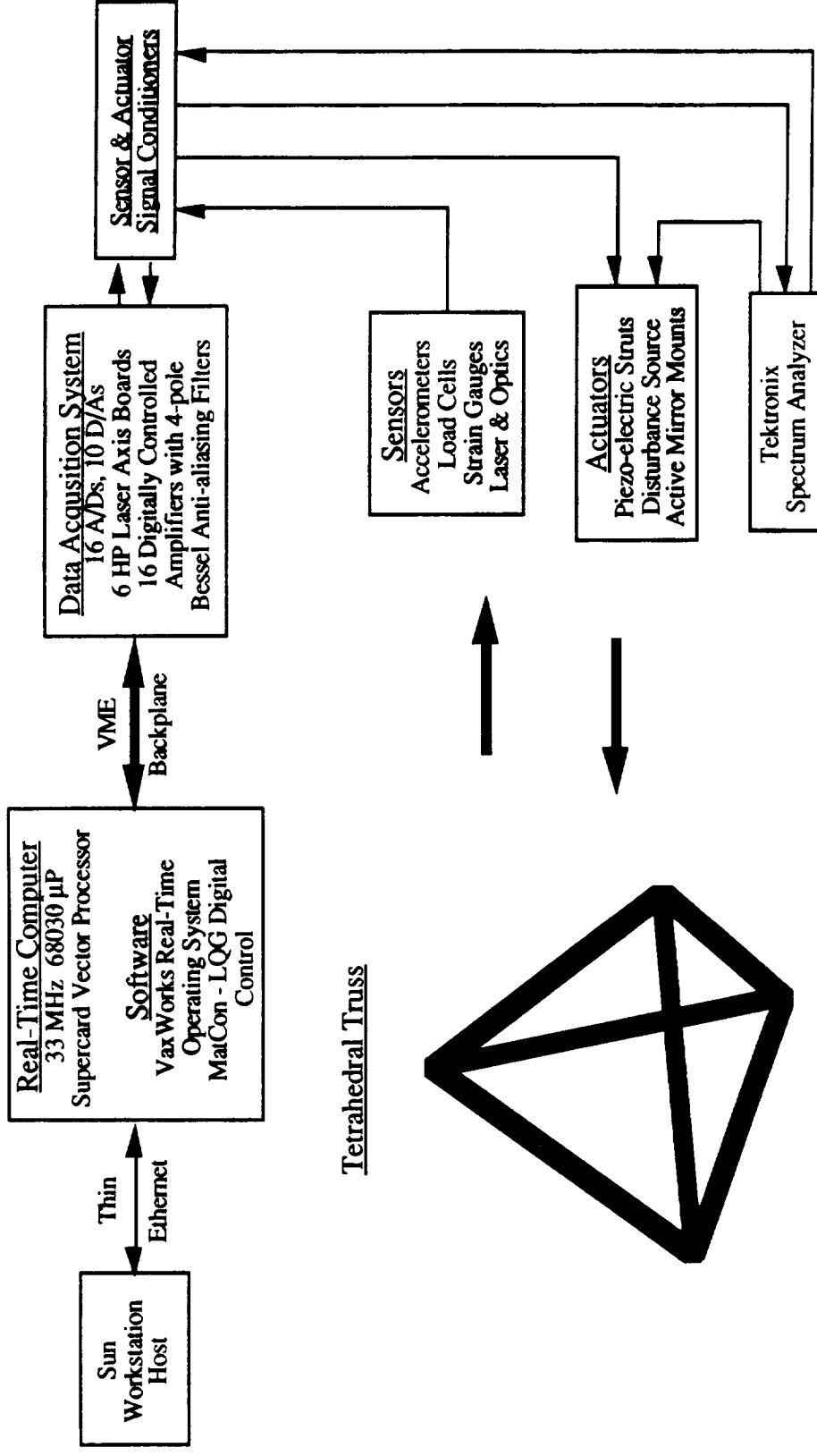
- This signal produces the following response with the desired level of disturbance (770 nm RMS). 96% of the total is below 200 Hz.

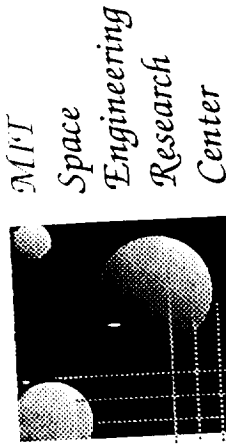




ORIGINAL PAGE IS
OF POOR QUALITY

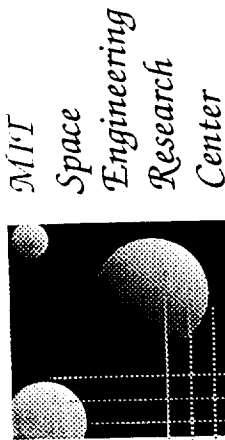
Testbed Architecture





Passive Damping in the MIT SERC Controlled Structures Testbed

Jonathan How, Gary Blackwood, and Eric Anderson
SERC Steering Committee Meeting
22 January, 1992



Finite Element Model and Identification Procedure

Jonathan P. How, Gary Blackwood, Eric Anderson, and
Etienne Balmes

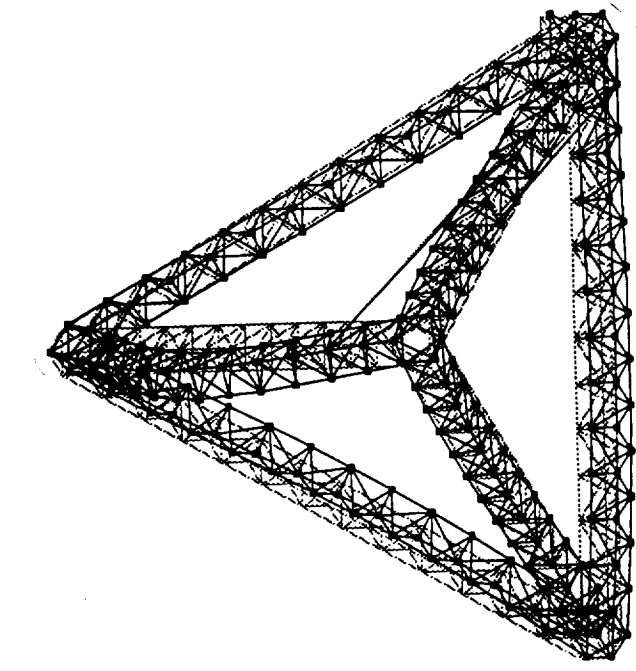
SERC Steering Committee Meeting
22 January, 1992

52-39
160312
N93-28890

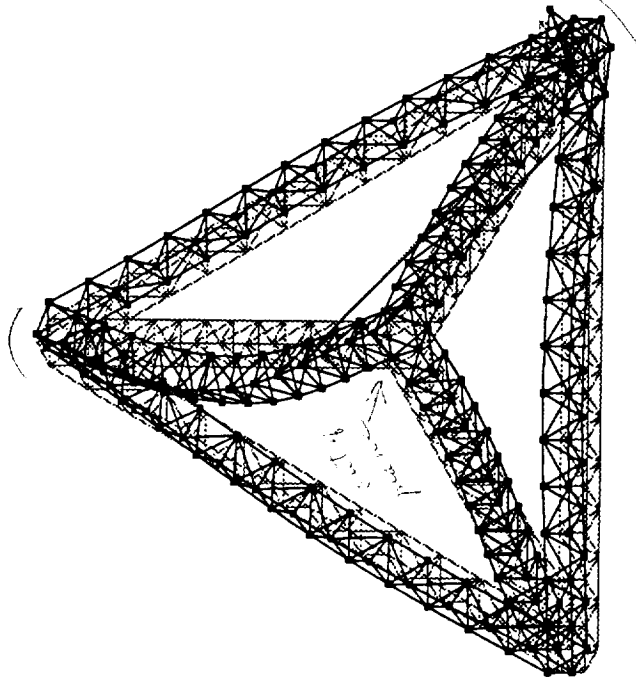
Interferometer Finite Element Model

- ADINA model, with 1500 degrees of freedom.
- Important attributes:
 - 1 beam element per strut
 - consistent mass matrix used
 - node flexibility incorporated through measured strut component test data
 - wires modelled as distributed masses
 - damping not modelled directly, included as modal damping in post processing
 - closely spaced modes due to near symmetries in structure
 - requires approximately 2 mins of Cray CPU time for the first 40 flexible modes.

Testbed Mode Shapes

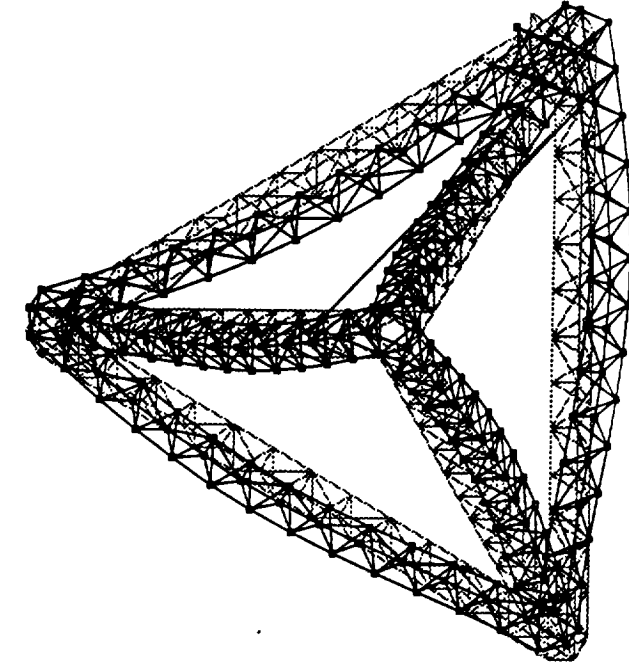


Mode 1 (25.8 Hz)

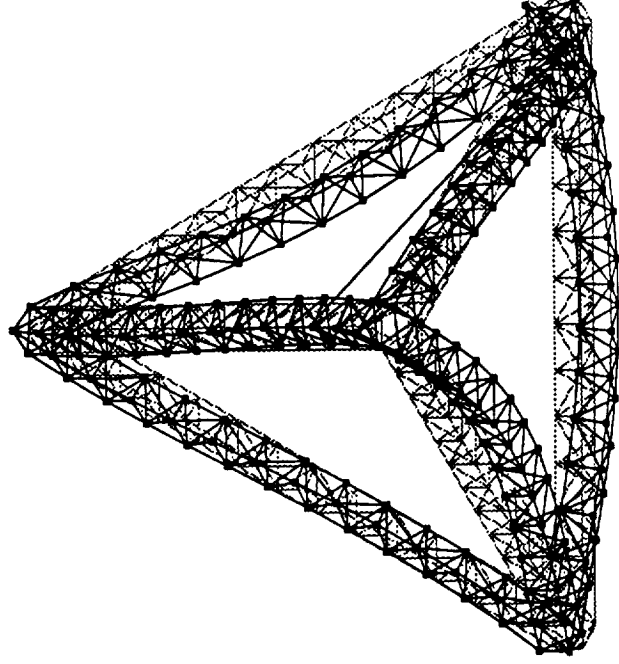


Mode 2 (27.2 Hz)

Testbed Mode Shapes



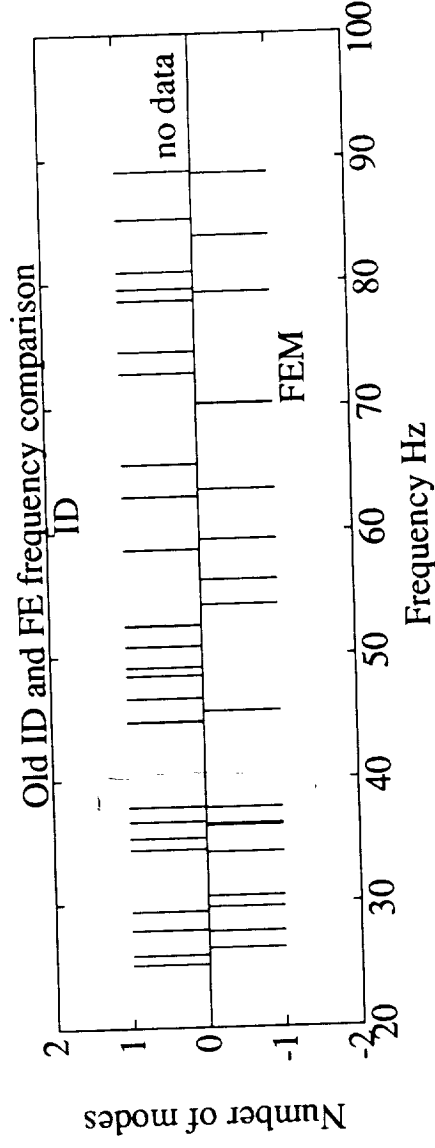
Mode 6 (36.1 Hz)



Mode 7 (36.3 Hz)

Finite Element Model Update

- Large discrepancy between finite element model and identified frequencies indicate that update required.



- Agreement of modal frequency distribution:
 - poor at high frequencies
 - better for lower frequency modes dominated by first leg bending modes.
- Better model needed for sensor, actuator, damper placement, and initial control designs.

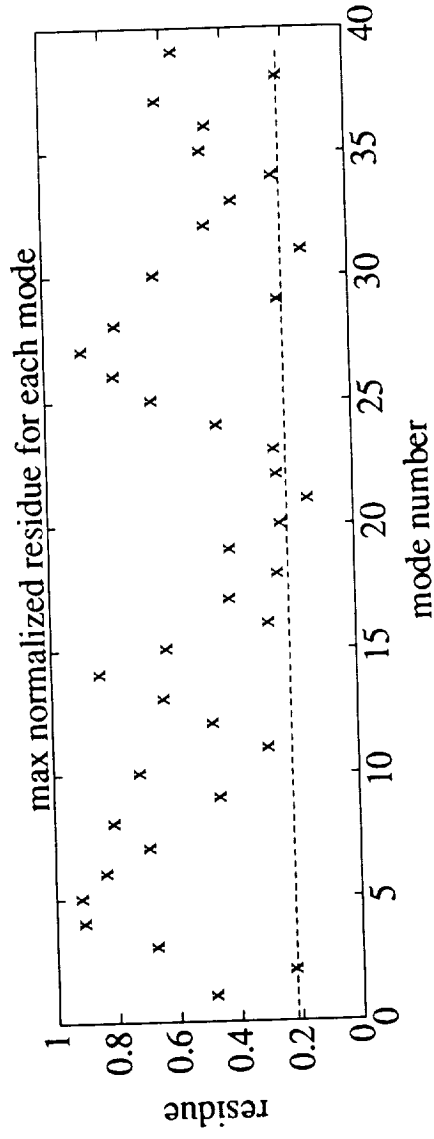
Identification Procedure

- Hardware:
 - 29 Kistler, 9 Sunstrand accelerometers
 - Bruel and Kjaer electromagnetic shaker
 - Tektronix scanner used to simultaneously measure all 38 channels.
- Selection of shaker locations: *24 locations*
 - 2142 possible locations reduced to 24 based on rankings using mean and maximum modal controllability.
 - goal: maximize controllability of least-controllable mode

$$\max_i \left(\min_r |A_i^r| \right) \quad \begin{cases} A = \text{modal residue at input} \\ i = \text{input dof (24)} \\ r = \text{mode number (20)} \end{cases} \quad (20)$$

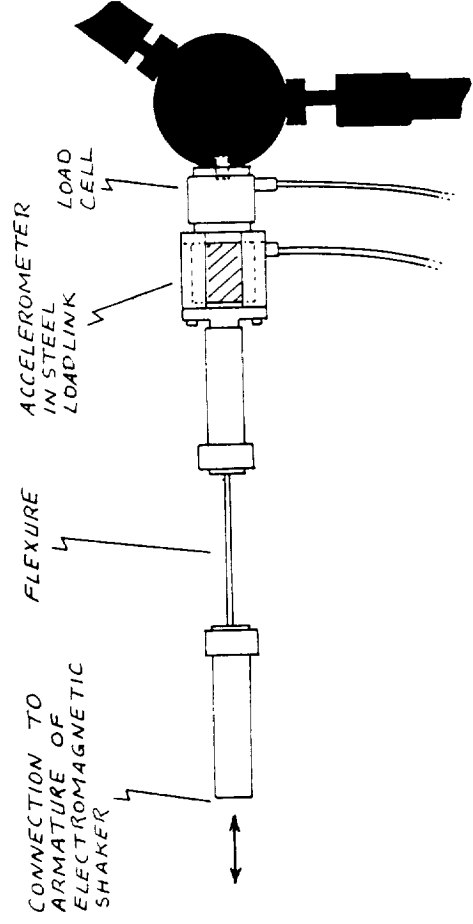
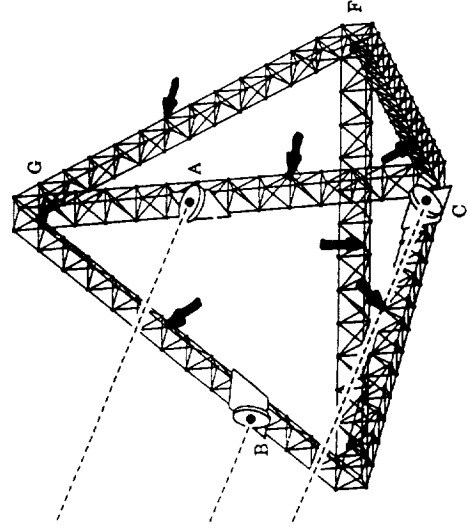
Shaker Locations

- Analysis resulted in one shaker location in each truss leg.



Shaker Tip:

- Shaker locations:



Data Analysis

- Transfer functions fit with modified least squares approach (R. Smith, UCSB).
- Leads to state space representation of measured data:

$$G_{fit}(s) := \left[\begin{array}{c|c} A & B \\ \hline C & D \end{array} \right]$$

- state space representation of each mode:

$$A_i = \begin{bmatrix} 0 & 1 \\ -\omega_i^2 & -2\zeta_i\omega_i \end{bmatrix} \quad B_i = \begin{bmatrix} 0 \\ 1 \end{bmatrix}$$

$$C_i = \begin{bmatrix} c_{1i} & c_{2i} \end{bmatrix} (38 \times 2)$$

- full model:

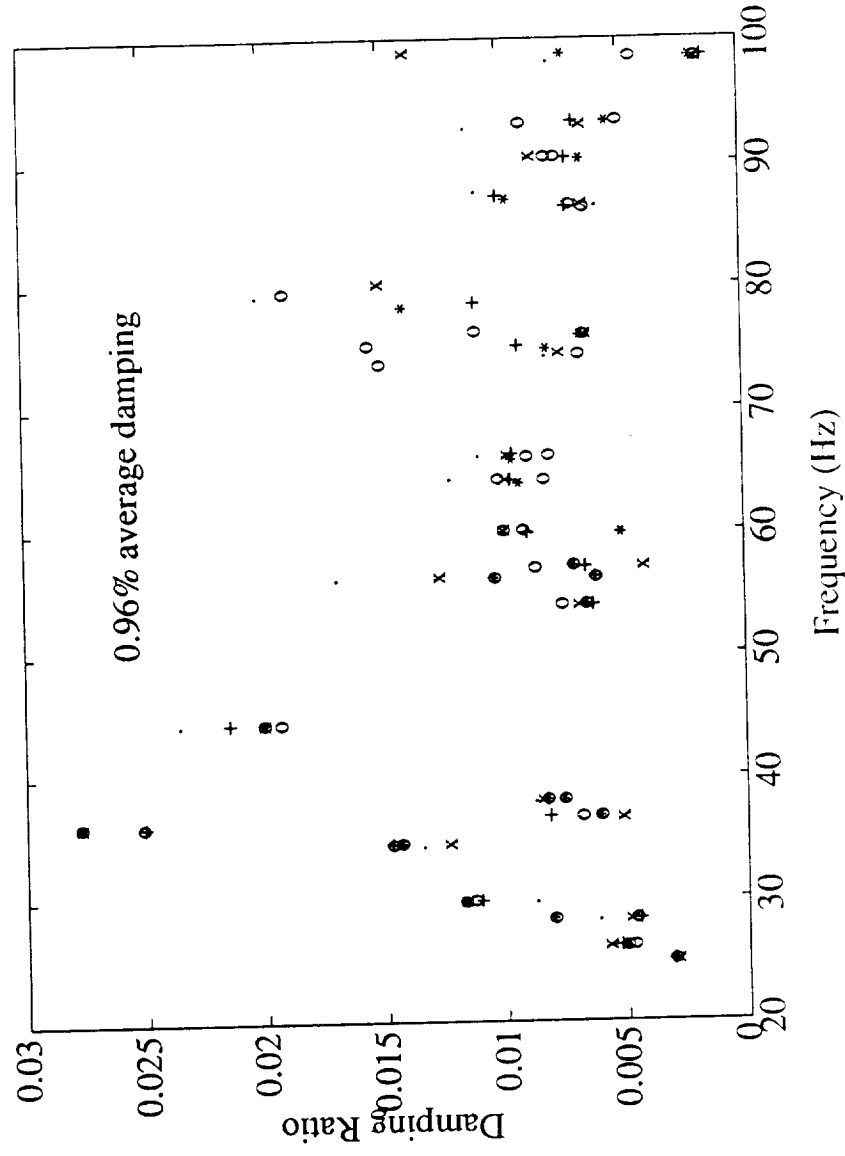
$$A = \text{BlockDiag} (A_i), \quad B = \text{Col} (B_i), \quad C = \text{Row} (C_i), \quad D$$

Data Analysis

- The A and B matrices held fixed for each shaker location.
- Full C matrix adds extra flexibility to approach.
- Modal frequency and damping computed with `invfreqs` function in MATLAB on several transfer functions.
- Note: good fits require good estimates of the frequency and damping of every mode in the frequency range of interest.
- One of several curve fitting approaches employed at SERC.

Modal Frequency and Damping Comparison

- Six A matrices agree well in frequency, less so in damping.



Computational Procedure

- C and D matrix rows independently selected for each sensor.
- Example: Pick D

$$E_r = \left(\sum_{i=1}^m \|Y(j\omega_i) - G(j\omega_i)U(j\omega_i)\|^2 \right)^{\frac{1}{2}}$$

$$\begin{aligned} Z(j\omega_i) &= Y(j\omega_i) - C_b(j\omega_i - A_b)^{-1} B_b U(j\omega_i) \\ E_r(j\omega_i) &= Z(j\omega_i) - D(j\omega_i)U(j\omega_i) \end{aligned}$$

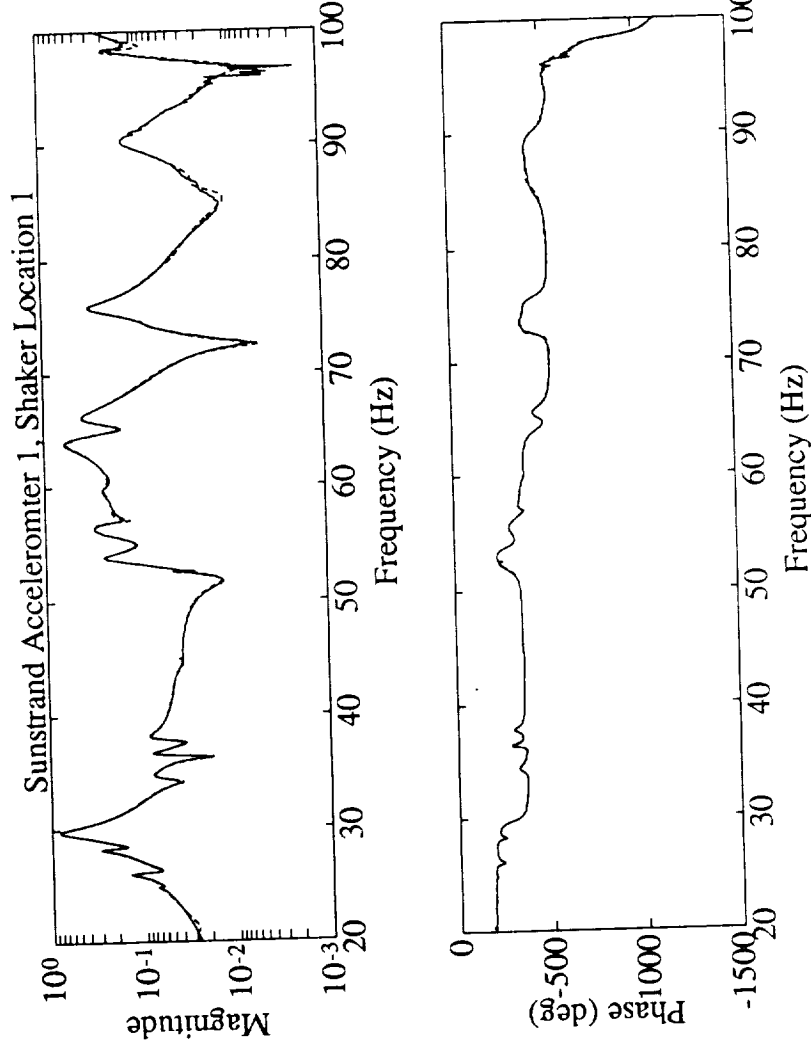
$$\text{Then } D_a = [\text{Re}(\overline{Z}) \text{ Im}(\overline{Z})] / [\text{Re}(\overline{U}) \text{ Im}(\overline{U})]$$

$$\text{where } \overline{Z} = [Z(1) \ Z(2) \ \dots \ Z(m)]$$

- Similar for the C matrix. Several iterations required.
- Software exists to perform an overall A matrix update.

Fit Comparison

- Final fit comparison:



- Procedure effectively fits hundreds of transfer functions.
Results good enough for control designs.

Residue Analysis

- Need to compute displacement residues from approximate accelerometer transfer function.

$$G_{fit}(s) = \sum_{i=1}^m \frac{c_{1i} + c_{2i}s}{s^2 + 2\zeta_i\omega_i s + \omega_i^2} + d \approx \ddot{y} \frac{1}{f}$$

$$\overline{G}_{fit}(s) = \sum_{i=1}^m \frac{b_{1i} + b_{2i}s}{s^2 + 2\zeta_i\omega_i s + \omega_i^2} + \frac{h(s)}{s^2} \approx \frac{y}{f}$$

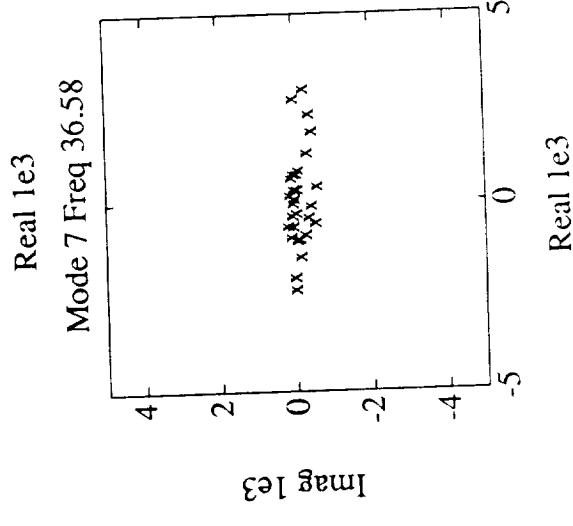
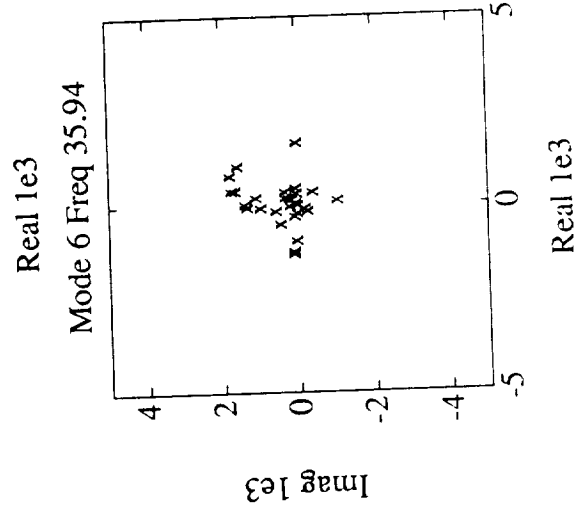
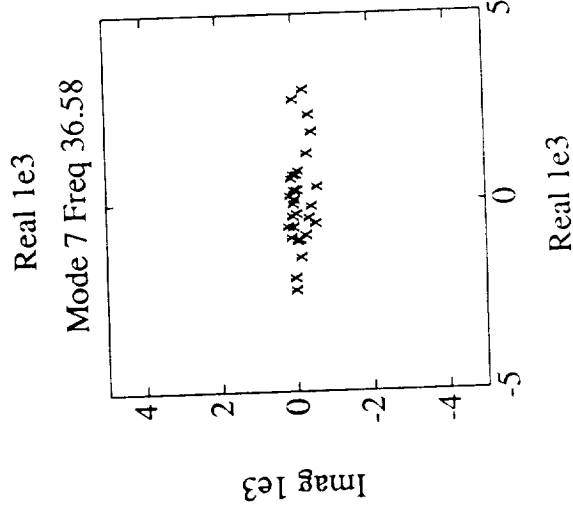
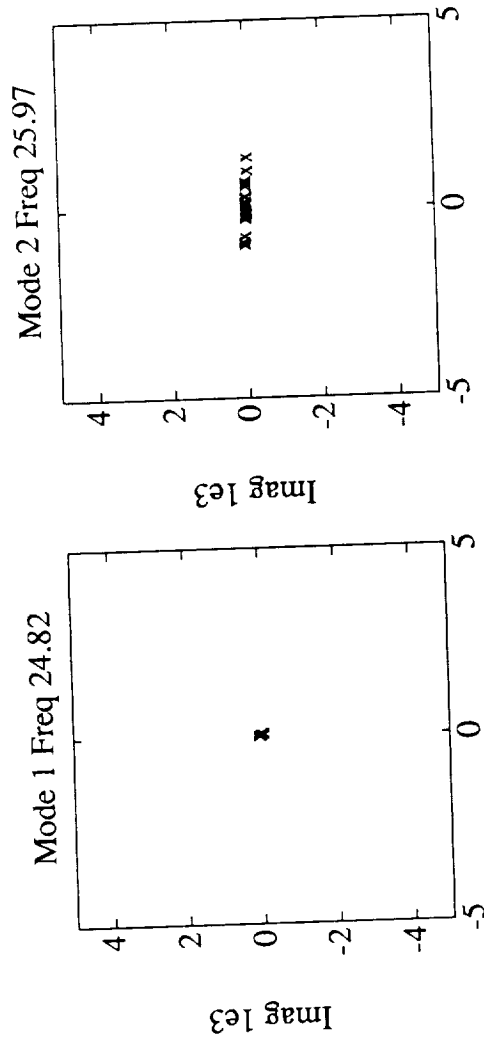
$$\text{where } b_{1i} = -\frac{(1 - 4\zeta^2)}{\omega_i^2} c_{1i} - \frac{2\zeta}{\omega_i} c_{2i}$$

$$b_{2i} = \frac{2\zeta}{\omega_i^3} c_{1i} - \frac{1}{\omega_i^2} c_{2i}$$

$$\text{Residue : } \phi_i(x_{act})\phi_i(x_{sens})^H = (b_{1i} + b_{2i}s) \big|_{s=j\omega_i}$$

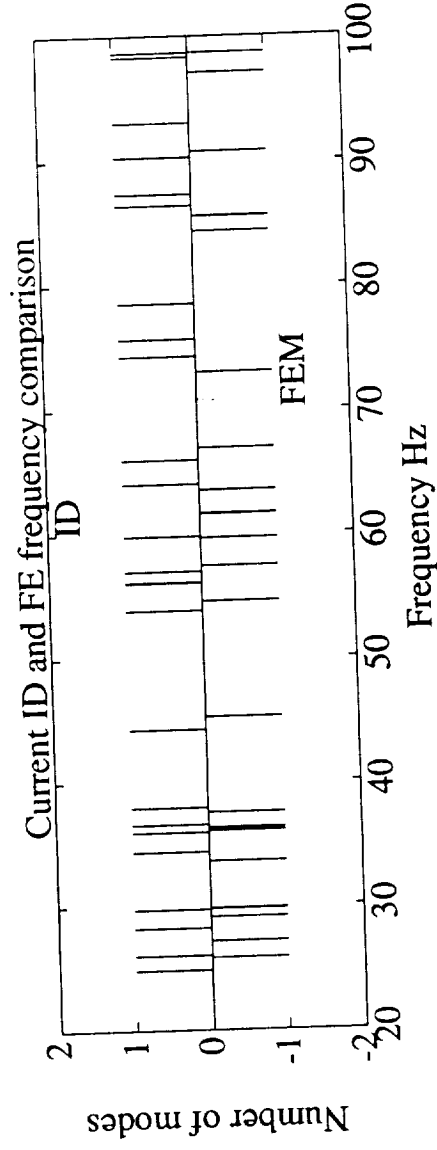
Typical Residues

- Residues rotated by phase at sensor collocated with shaker.



Current Status

- Frequency comparison after structural and model updates:

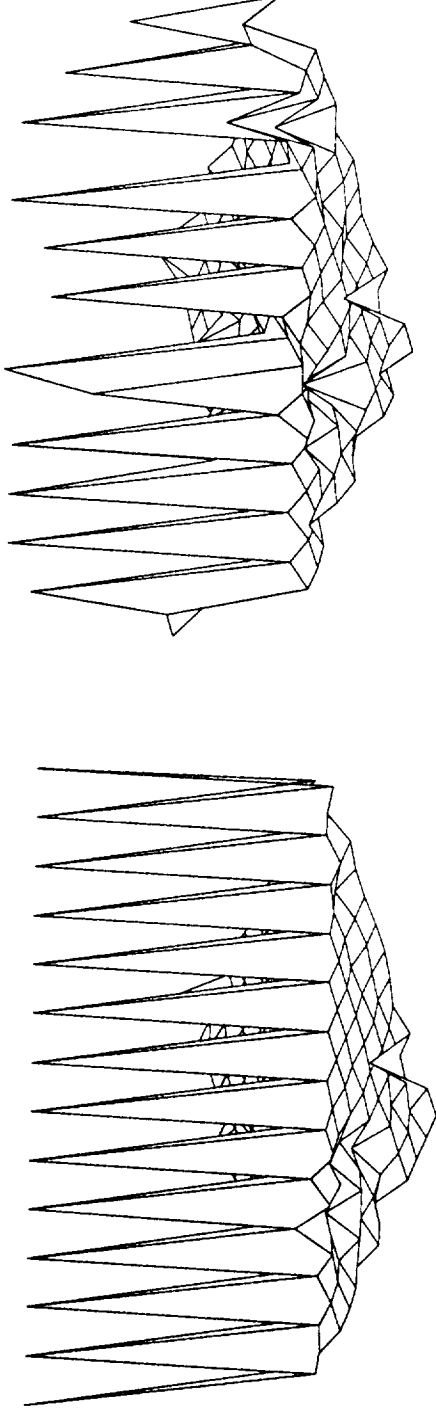


- Modifications:
 - eigenvector studies illustrated importance of plate flexibility, inclusion in the FEM lead to improved frequency agreement (4 % error in first 9)
 - fourth vertex stiffened to improve optical alignment, and better agreement indicates prior presence of local modes.

Identification/FEM Residual Comparison

- Correlate identified and FEM residues for first 14 modes.
- Modal Assurance Criterion:

$$\text{mac}(x_1, x_2) = \frac{\| \sum_{i=1}^m \phi(x_1)_i \phi(x_2)_i^H \|^2}{(\sum_{j=1}^m \phi(x_1)_j \phi(x_1)_j^H) (\sum_{j=1}^m \phi(x_2)_j \phi(x_2)_j^H)}$$

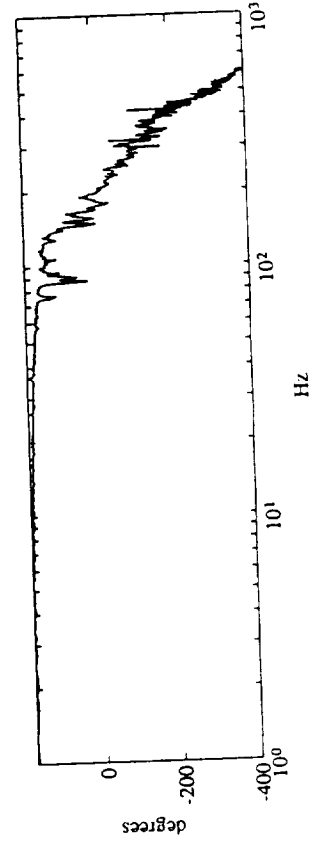
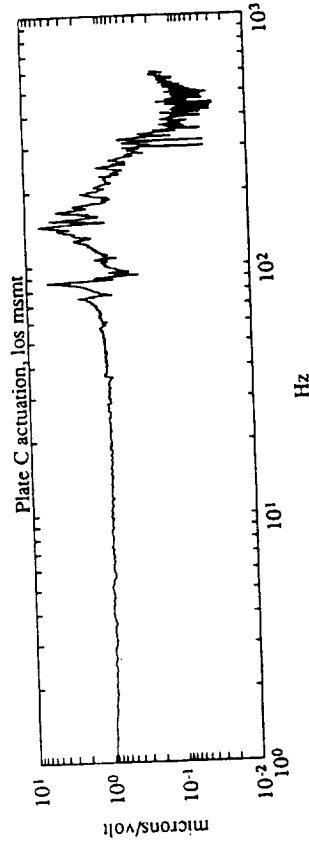
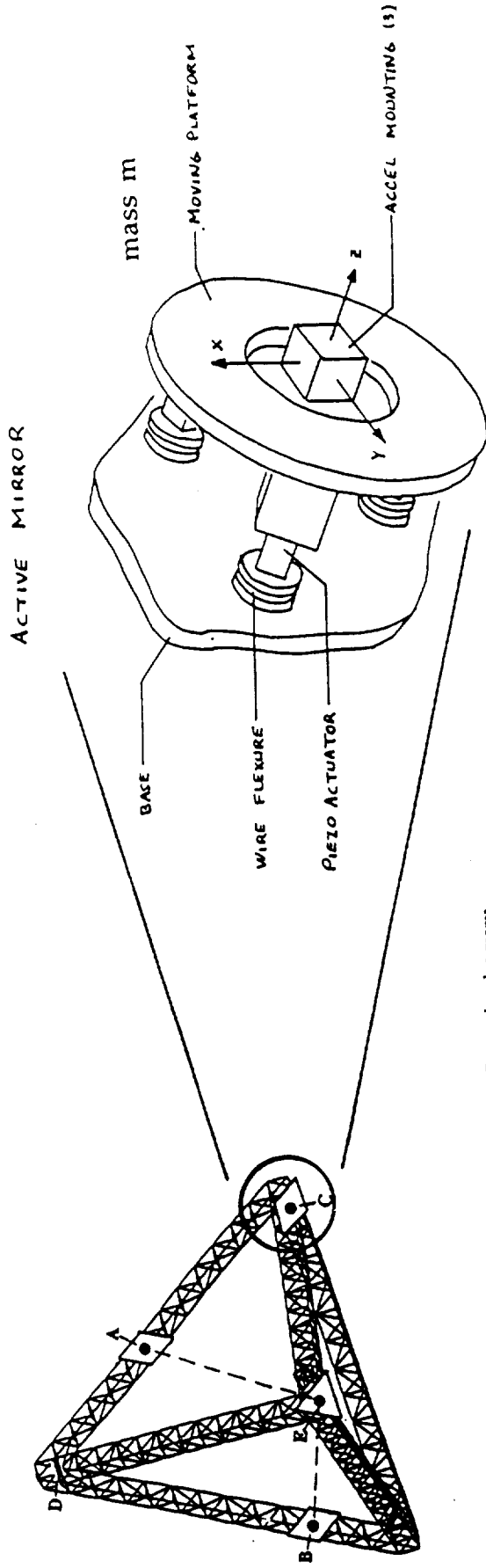


- Issue: FEM modes real, measured residues complex.

Future Work

- Continue coarse FEM changes to correct plate flexibility and mass distribution assumptions.
- Apply gradient type updates on the stiffness and mass matrices to match residues of higher frequency modes.
- Improve FEM suspension model with ID data.
- Develop state space model that can be used for sensor, actuator, damper placement, and initial control designs.

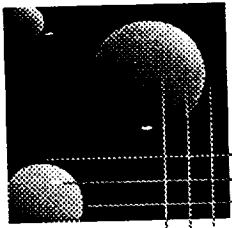
Pathlength Control Using Isolation Mounts



Input: piezo voltage

Output: pathlength C-E (microns)

MIT
Space
Engineering
Research
Center



Control Design for the SERC Experimental Testbeds

Steering Committee Presentation

Robert Jacques
Gary Blackwood
Douglas MacMartin
Jonathan How
Eric Anderson

January 22, 1992

S3-35
-160313
N93-27891

Approaches

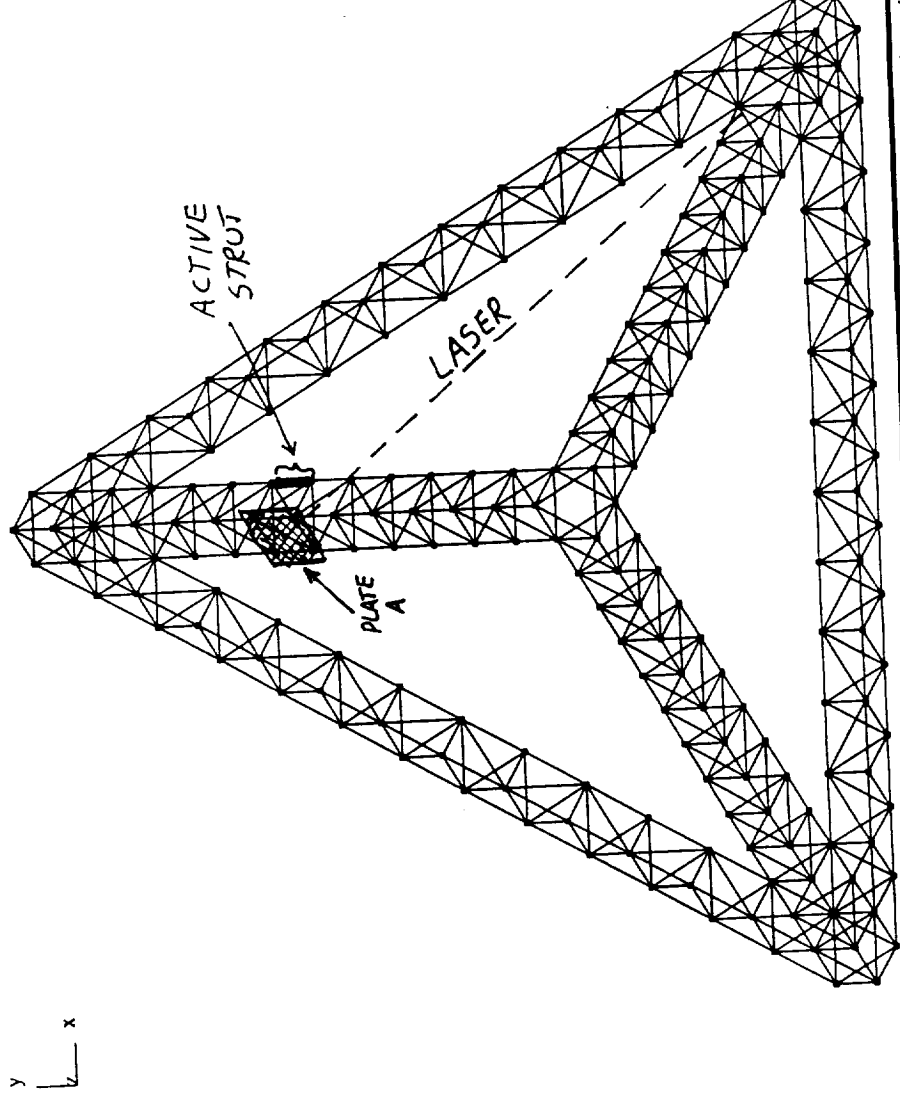
- Global control loops from lasers to active struts
- Local control loop wrapped around active struts
- Isolation at the performance outputs
- Phase 0 testbed - *integrated system*

SISO Control Design and Results

- Hardware:
 - Actuator: active strut
 - Sensor: Laser Leg
- Assumptions
 - Disturbance source and actuator collocated
 - Performance metric and sensor collocated
- Control design method
 1. Measure transfer function from actuator to sensor
 2. Use nonlinear curve fitting technique to obtain state space model of system
 3. Reduce model order
 4. Design LQG controller
 5. Remove dynamics from controller which do not contribute to stability and affect the performance only slightly

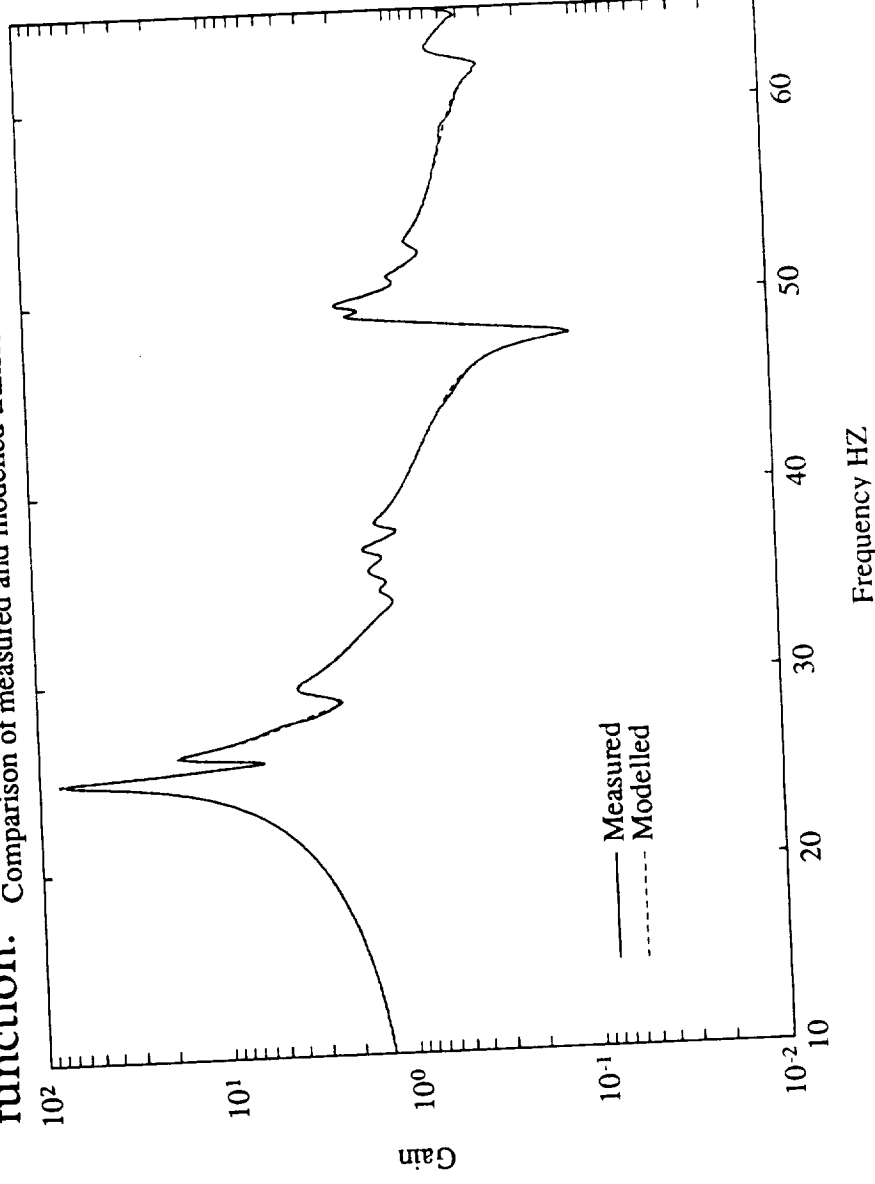
Sensor and Actuator Locations

- Sensor: Laser from fourth vertex to plate A
- Actuator: Active strut placed to maximize modal residues in transfer function from strut to laser



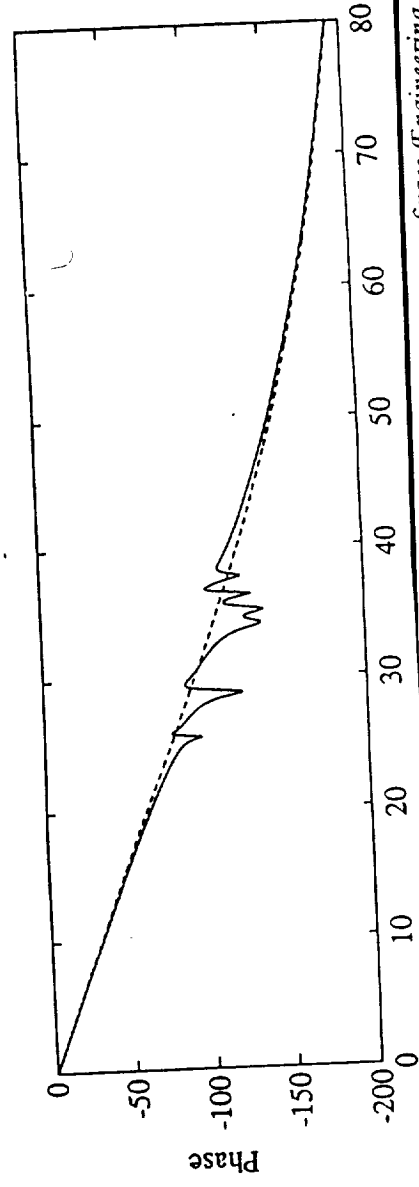
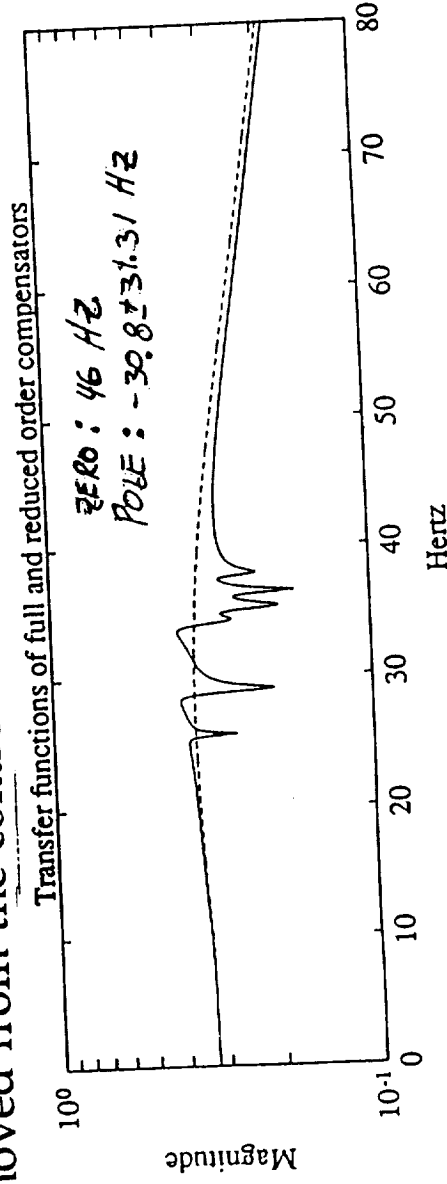
Model Identification

- Averaged empirical transfer function estimate from actuator to sensor obtained using Tektronix box.
- Nonlinear algorithm used to fit poles and zeros to transfer function. Comparison of measured and modelled transfer functions



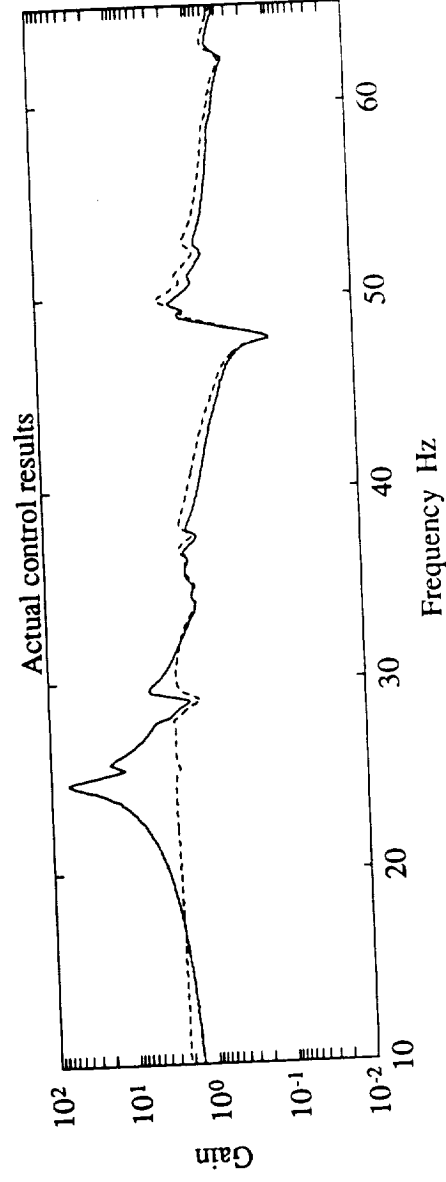
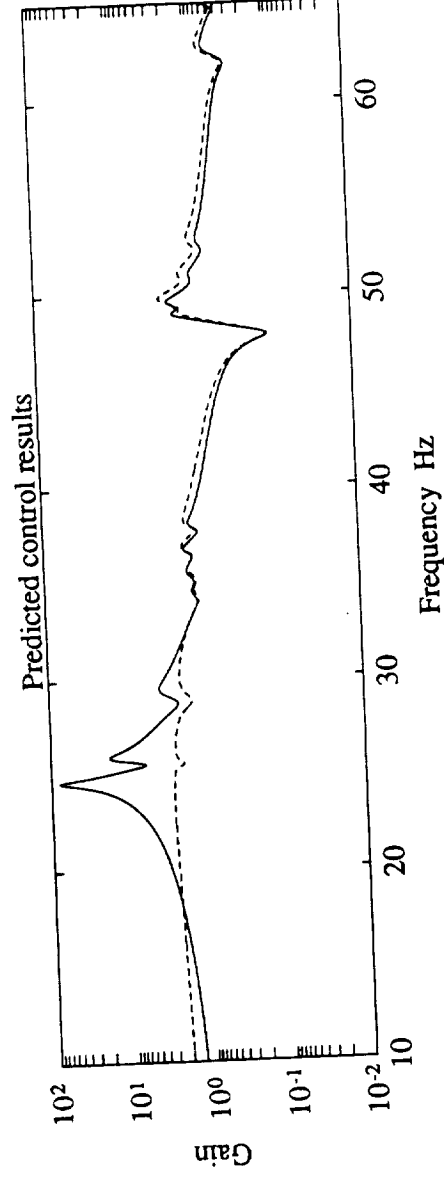
Control Design

- Model truncated at 80 Hz
- LQG controller had some slight notching which did not improve stability and affected the cost slightly. These dynamics were removed from the controller.



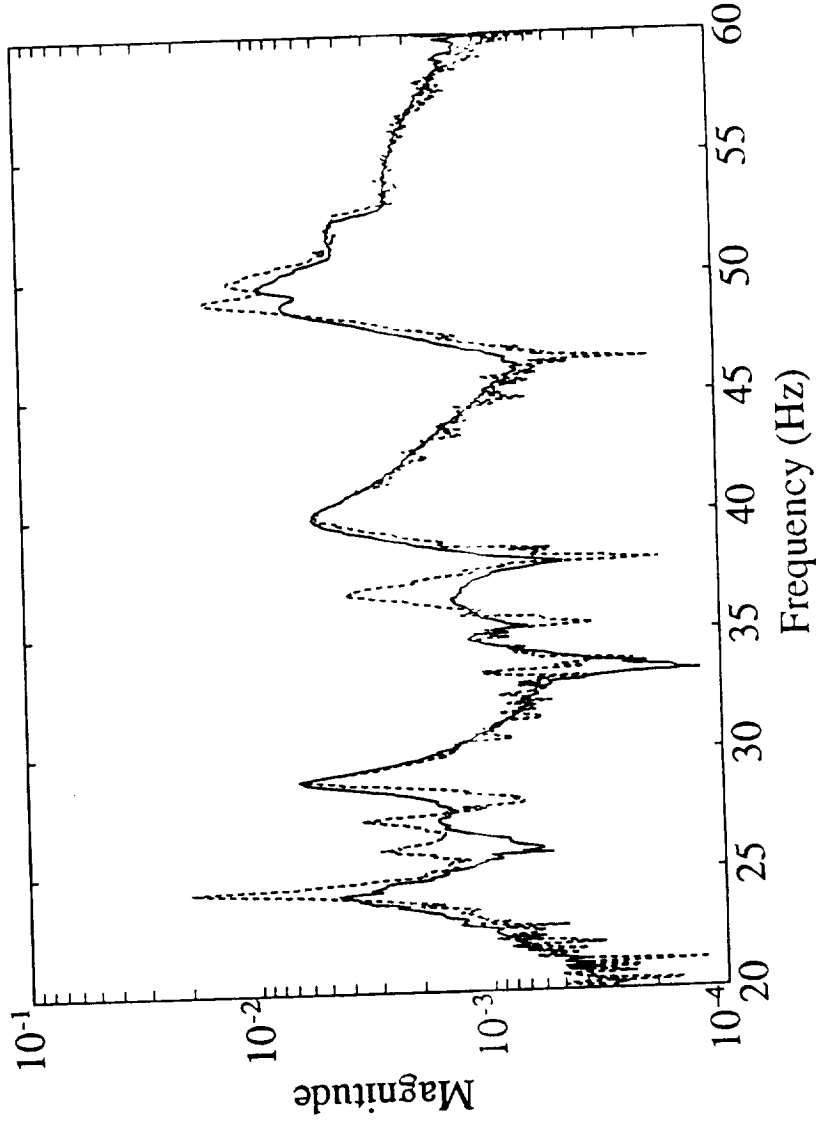
Experimental Results

- Controller digitized and implemented on real time computer at 2000 Hz.



Preliminary LAC Experimental Results

- Single collocated rate feedback loop closed around active strut to demonstrate active damping.
- Open and closed loop transfer functions from disturbance source to siderostat acceleration.



Active Vibration Isolation

Problem Statement

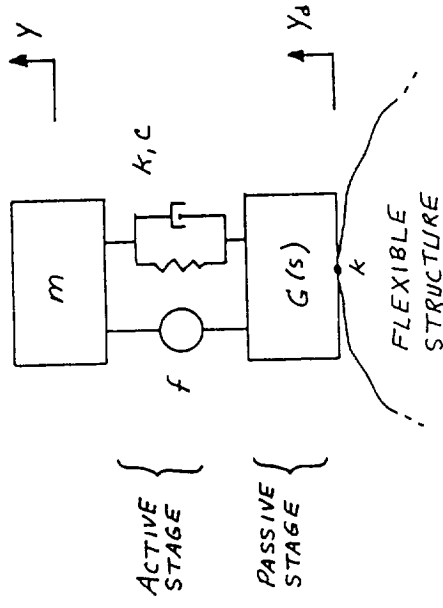
Problem A: Given the prescribed displacement disturbance of a flexible base structure, design an active interface to reduce transmissibility of displacement to a rigid payload. 214z

Problem B: Given the prescribed clamped force and output impedance of a vibrating machine, design an active interface to reduce transmissibility of force to a flexible base structure.

Thesis will study:

- relative performance of passive and active isolation designs
- choice of feedback sensors and passive design to decouple flexible base dynamics
- active isolation as an element of CST process:
 - disturbance attenuation
 - simultaneous isolation mounts
 - isolation and pathlength control together
- implementation of MDOF isolators on testbed

Model: Base Flexibility Coupling into Isolation Feedback Loop



Structural admissibility at k :

$$H_k(s) = \sum_{i=1}^{\infty} \frac{(\phi_i)^2}{s^2 + 2\zeta_i\omega_i s + \omega_i^2}$$

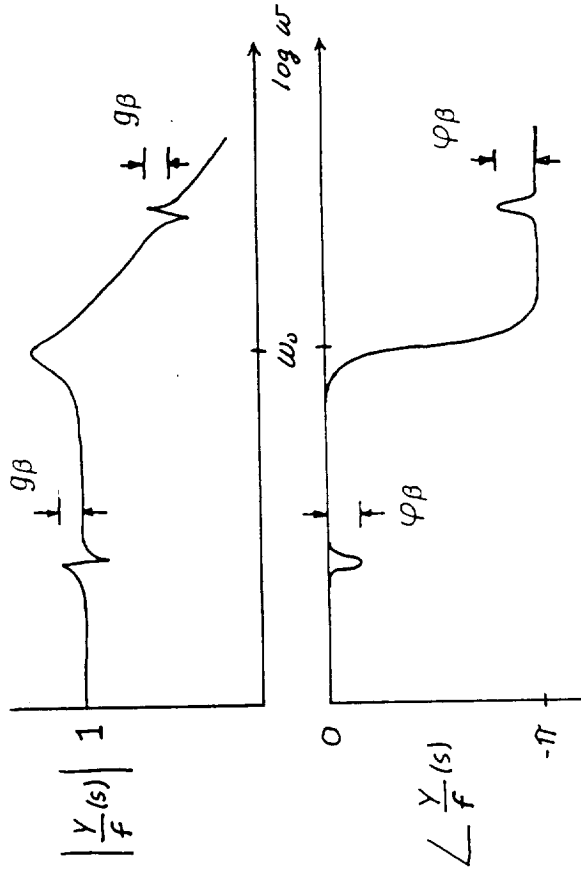
$$\omega_o = \frac{k}{m}$$

- Plant transfer function: $y(s)/f(s)$
- Non-dimensional parameter governing flexible coupling of i^{th} mode:

$$\omega_r \ll \omega_o : \quad \beta_L = \frac{m(\phi_i)^2}{2\zeta_i}$$

$$\omega_r \gg \omega_o : \quad \beta_H = \frac{m(\phi_i)^2}{2\zeta_i} \left(\frac{\omega_r}{\omega_o} \right)^2$$

$$g\beta = (1 + \beta)^{1/2} \quad \varphi\beta = 2\text{atan}(\beta/2)$$

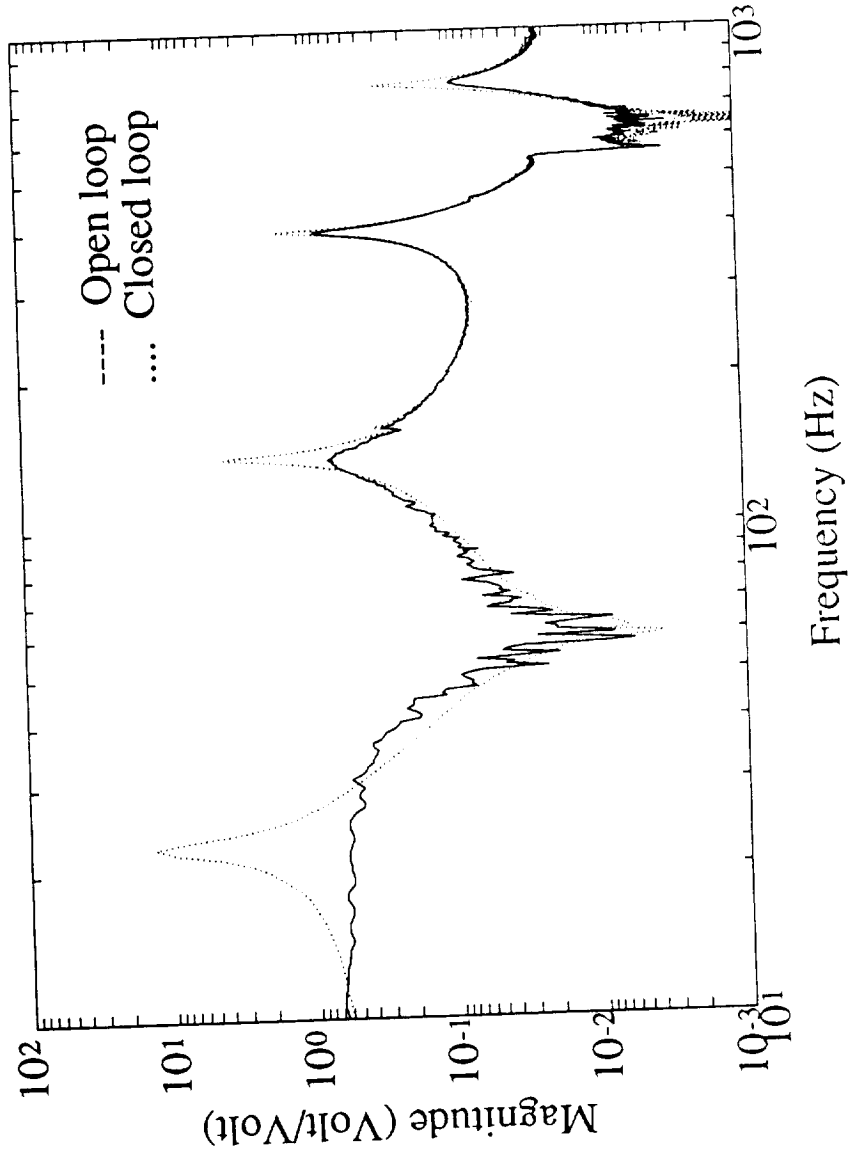


A Phase 0 Testbed

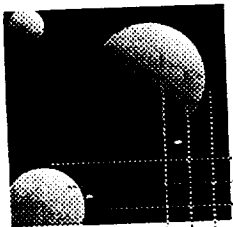
- 33 cm cantilevered beam, initially developed as a deformable mirror testbed.
- Designed to test the sensor, actuator, modelling, and control issues associated with nanometer resolution requirements.
- Sensors/actuators: tip laser displacement, PZT, and PVDF.
- High Authority/Low Authority controller:
 - passive damping (resistive piezoelectric shunting)
 - LAC: strain rate feedback (PVDF to PZT), applied to same actuators as HAC, analog
 - HAC: constrained order LQG (4), two loop feedback (laser measurement to PZT), digital.

Closed Loop Results

- Transfer function from disturbance (mid beam) to tip displacement:



MIT
Space
Engineering
Research
Center



A Stochastic Approach to Robust Broadband Structural Control

Douglas G. MacMartin
Steven R. Hall

January 22, 1992

160332
N93-27892

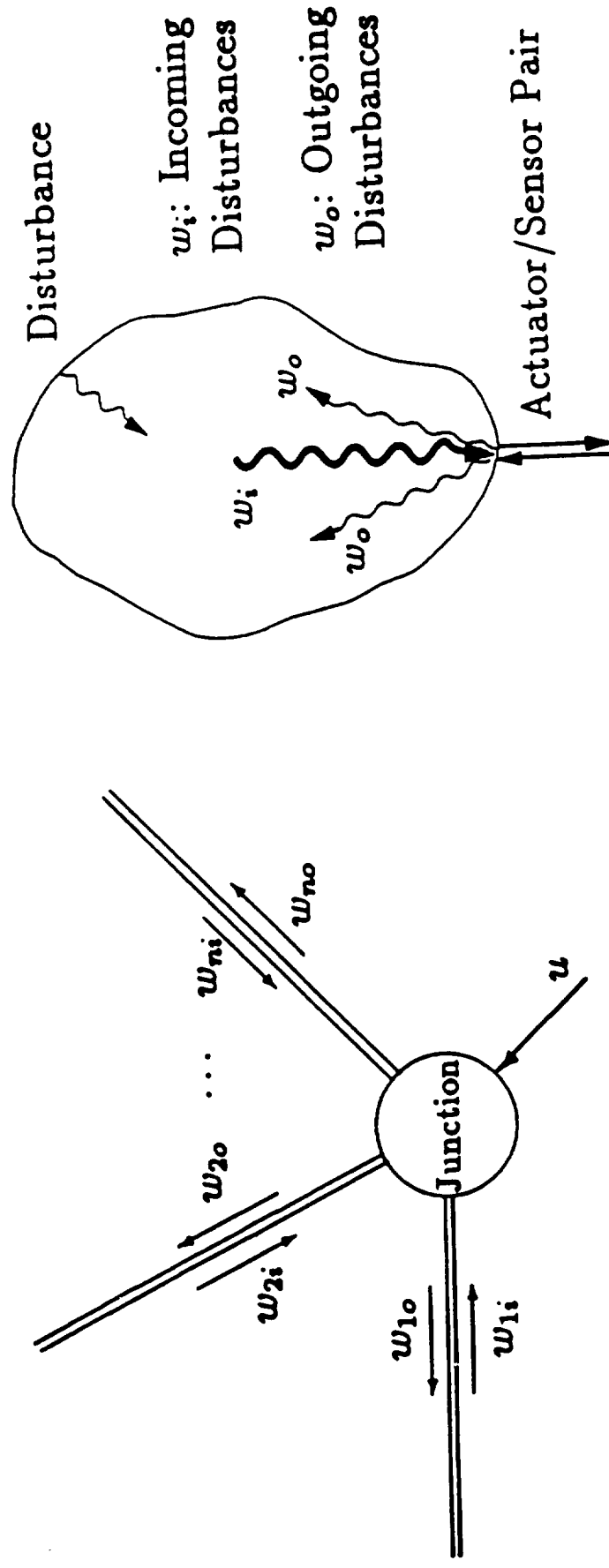
D, 18

Goal

- Active broadband control of uncertain modally dense structures.
- Use collocated feedback.
 - Positive real controller guarantees stability.
 - Low authority or local control (“active damping.”)
- Use local acoustic or statistical model of structure.
- Maximize power dissipation.
 - Equivalent to impedance matching.
 - Cannot match impedance exactly at all frequencies due to causality constraint.
- Experimental demonstration on complex structures.

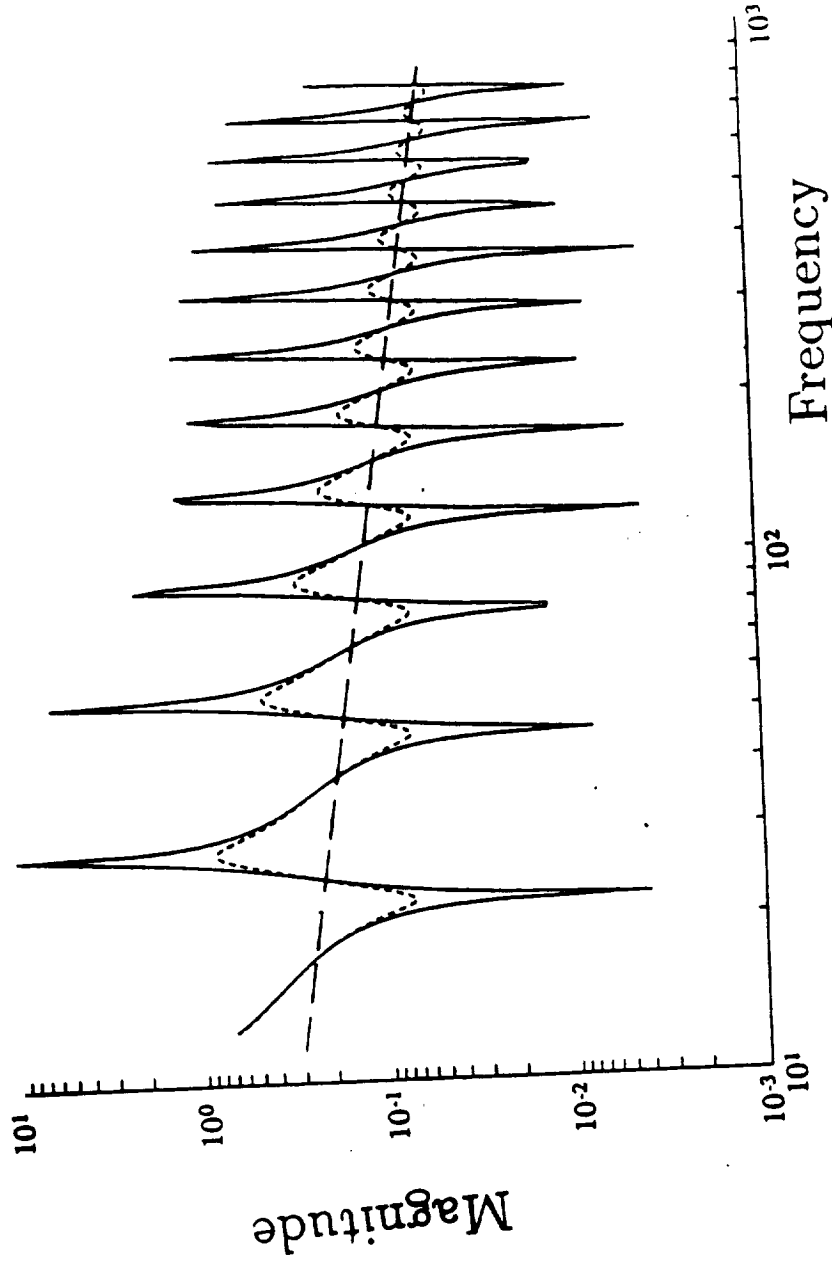
Local Models

Travelling wave model Dereverberated mobility model



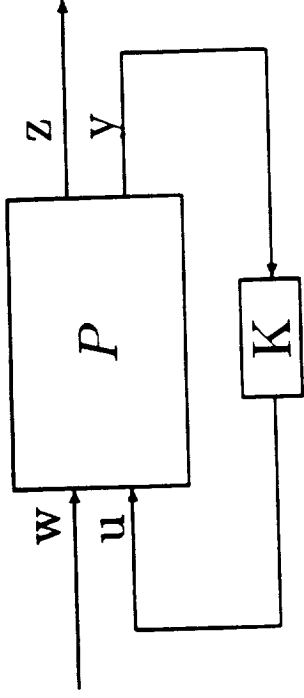
Computation of Dereverberated Mobility

- From averaging transfer function:



Power Flow

- Use local model only.
- Power dissipation related to input mobility G :



$$\begin{Bmatrix} z \\ y \end{Bmatrix} = \begin{bmatrix} G_1 I & G_1 \tilde{G}_0 \\ G_0 & G \end{bmatrix} \begin{Bmatrix} w \\ u \end{Bmatrix}$$

- Define $H(s) = \frac{z(s)}{w(s)}$.
 - Analogous to reflection coefficient
 - Reflected power is $(H^* H) w^* w$
 - Dissipated power is $(I - H^* H) w^* w$

Impedance Matching

- Maximum power dissipation is obtained if the compensator is the conjugate of the structural impedance.
 - This is noncausal \Rightarrow need best causal approximation.
- \mathcal{H}_2 optimization: No guarantee of stability on actual structure.
- \mathcal{H}_∞ optimization: guarantees stability, but doesn't minimize desired performance metric.
- Goal: minimize actual rms cost and guarantee stability using only local information.

Stochastic Systems

- Investigate systems of the form

$$\dot{x} = A(\sigma)x + w$$

- σ is a random variable with known probability distribution.
- Uncertainty is only in the imaginary part of the eigenvalues.
- The average covariance $\langle xx^T \rangle_{\sigma, w}$ satisfies
 - Incoherence: the amplitudes of distinct modes are uncorrelated,
 - Equipartition: the average kinetic and potential energy of each mode is the same, and
 - Conservation of energy (for an undamped system.)
- These are the key assumptions made in Statistical Energy Analysis.

Control Problem

- Minimize “global” mean-square performance metric $\langle y^T y \rangle$
using only local knowledge, local control.
- Use characteristics of stochastic systems.
- Use conservation of energy!

Handwritten notes:
- Inherent - different means are used to find the same result
- In preparation: say $P \leq 1$ (if $P > 1$, then you need to be more careful)

Control of Stochastic Systems

- Incoherence \Rightarrow

$$\langle y^T y \rangle = \sum_{n=0}^{\infty} C_n E_n \simeq \int_{-\infty}^{\infty} C(\omega) E(\omega)$$

- Incoherence & Equipartition \Rightarrow incoming structural power is proportional to structural energy.
 - Total power dissipated is therefore

$$\Pi_{diss} = \underbrace{(I - H(j\omega)^* H(j\omega))}_{\text{Relative Dissipation}} E(\omega)$$

- Conservation of energy \Rightarrow

$$\Pi_{diss} = \Pi_{in}$$

- The average (over uncertainty) cost is therefore:

$$J = \frac{1}{2\pi} \int_{-\infty}^{\infty} C(\omega) [(I - H^* H)^{-1} H^* H] \Pi_{in}(\omega) d\omega$$

Properties

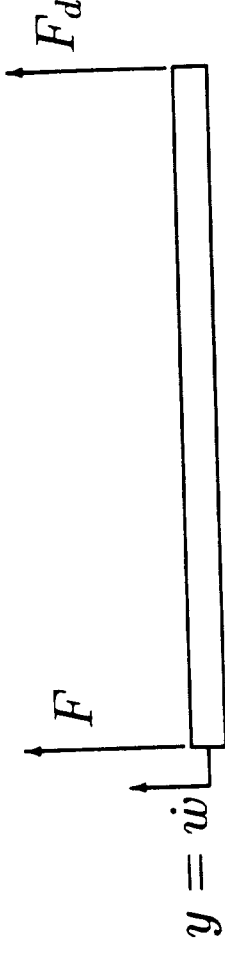
- Guarantees \mathcal{H}_∞ norm bound, $\|H\|_\infty < 1$.
 - Guarantees $\left\{ \begin{array}{l} \text{positive real} \\ \text{dissipates power} \\ \text{stable closed loop} \end{array} \right.$
- Overbounds weighted \mathcal{H}_2 cost.
 - Minimizes desired performance metric.

Using Cost Functional

- Cost is related to other $\mathcal{H}_2/\mathcal{H}_\infty$ approaches, and to differential games.
- Can evaluate cost for a state space system with solution to a Riccati equation and a Lyapunov equation.
- Can optimize cost using Lagrange multiplier approaches
 - Yields coupled Riccati and Lyapunov equations.
 - Cannot be solved explicitly.
 - Can be solved using numerical optimization.

Example: Bernoulli-Euler Beam

- Free-free beam, force actuator and velocity sensor at left end, disturbance force at right end.
- Minimize difference between end-point displacements.



- Dereverberated mobility: (describes local dynamics)

$$G(s) = \frac{\sqrt{2}}{(\rho A)^{3/4} (EI)^{1/4}} \cdot \frac{1}{\sqrt{s}}$$

- Non-causal impedance match: (maximum dissipation)

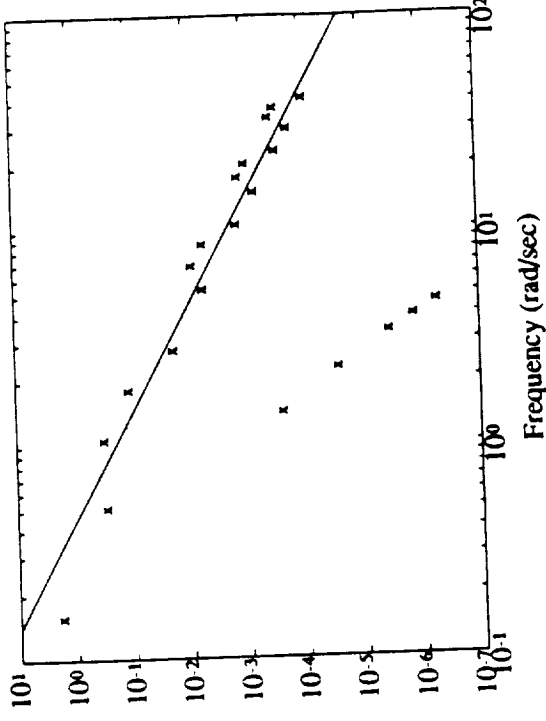
$$K(s) = \frac{(\rho A)^{3/4} (EI)^{1/4}}{\sqrt{2}} \cdot \sqrt{-s}$$

Compensator Design

- Choose $\Pi_{in}(\omega)$ based on disturbance spectrum $V(\omega)$ and dereverberated input mobility at disturbance location $G_d(\omega)$.

$$\Pi_{in} = (G_d + G_d^*)V$$

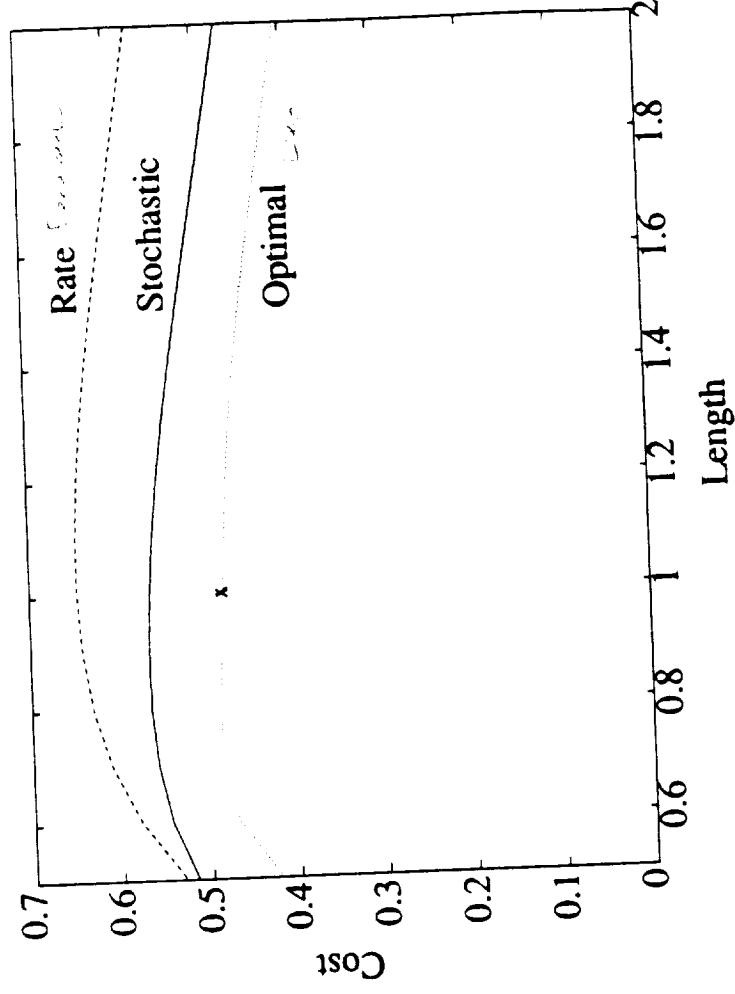
- Choose $C(\omega)$ to approximate modal cost:



- Choose desired compensator order and use numerical optimization.

Performance

- Compare cost versus length of beam for various compensators.
 - LQG compensator unstable for small changes in length.



“Power” Dual Variables

- Force into structure and relative velocity across active strut are dual.
- Piezo stack stiffness is high \Rightarrow commands displacement.
 - Can also command relative velocity.
- Want compensator $K(s)$ such that

$$\begin{aligned}\dot{x} &= K(s)f \\ \Rightarrow x &= K(s)\left(\frac{f}{s}\right)\end{aligned}$$

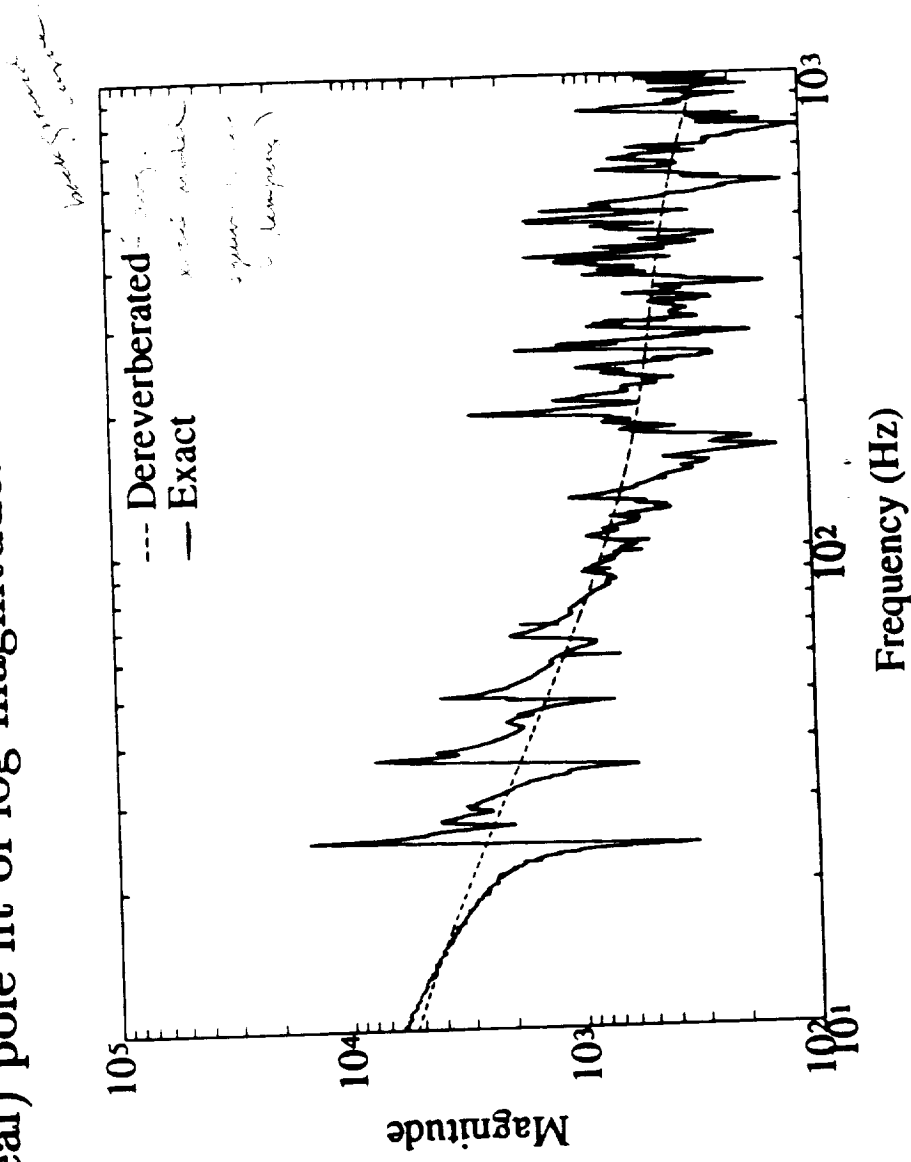
- Use integral of force feedback.

Dereverberation of Complex Structure

- Wave approach: truss behaves like a beam at low frequencies.
- Compute “best” fit of log magnitude using only real poles and zeroes.
- Fit transfer function using complex poles and zeroes, and add damping to resulting model.

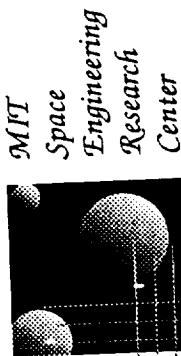
Dereverberated Transfer Function

- Open loop transfer function from displacement to integrated force.
- Three (real) pole fit of log magnitude.



Conclusions

- Use local model of structure for broadband control.
 - Dereverberated mobility or travelling wave model.
 - Ideal compensator is a non-causal impedance match.
- Parameter-robust control for structures must take advantage of conservation of energy.
- Average covariance exhibits equipartition and incoherence.
- A cost functional can be obtained that uses these properties, and guarantees both stability and performance robustness.



THE MIDDECK 0-GRAVITY DYNAMICS EXPERIMENT (MODE):

Prof. Edward F. Crawley

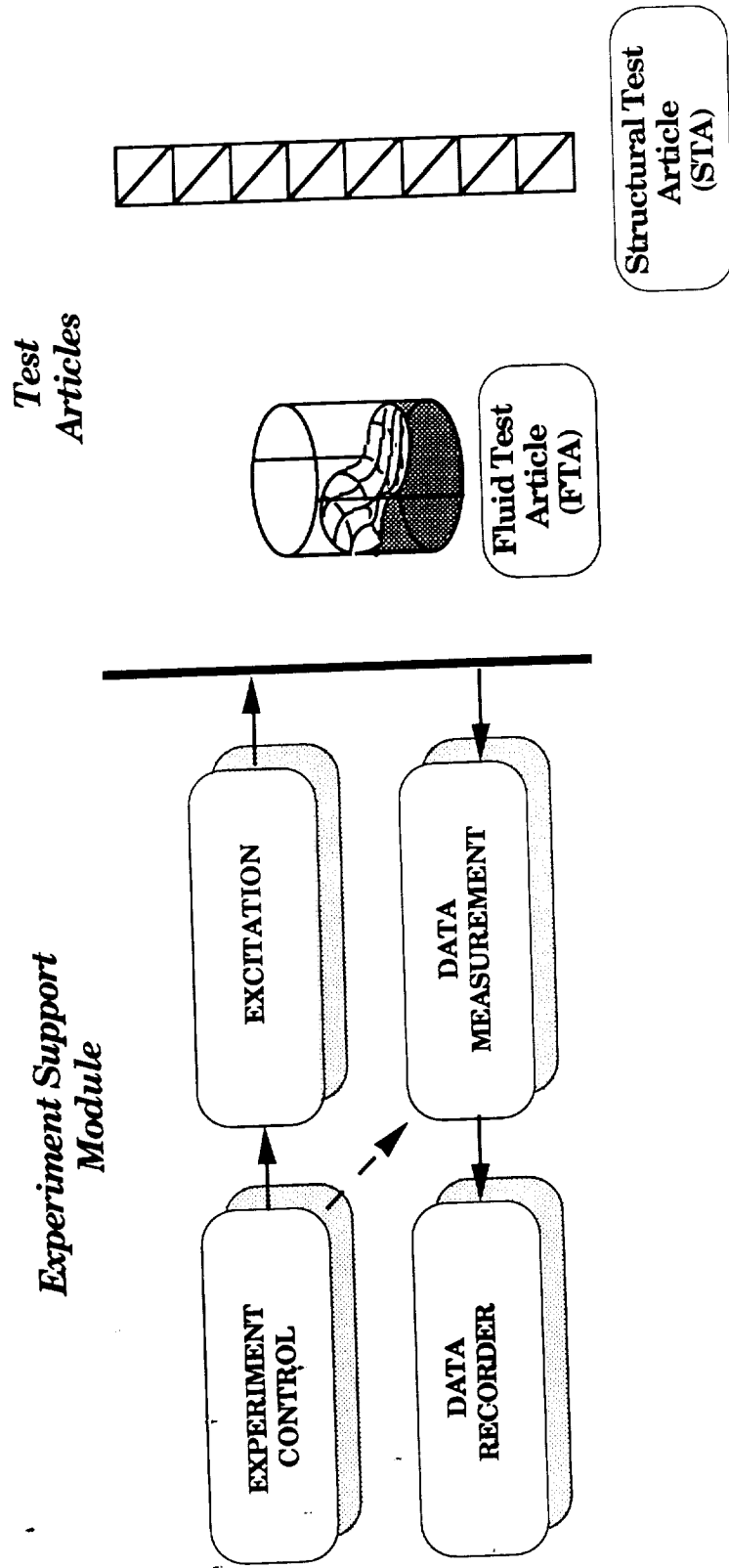
Dr. Javier de Luis

SERC Steering Committee

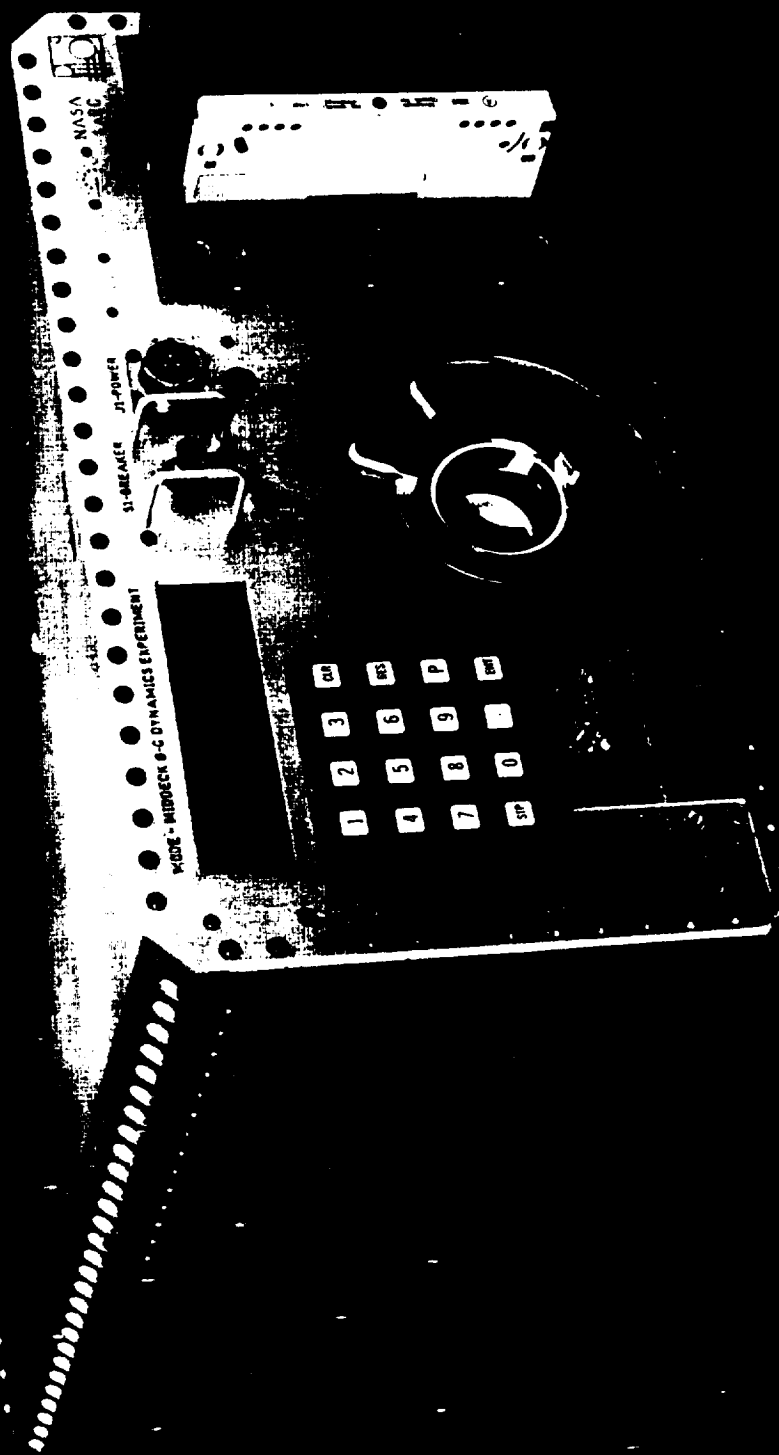
January 22, 1992

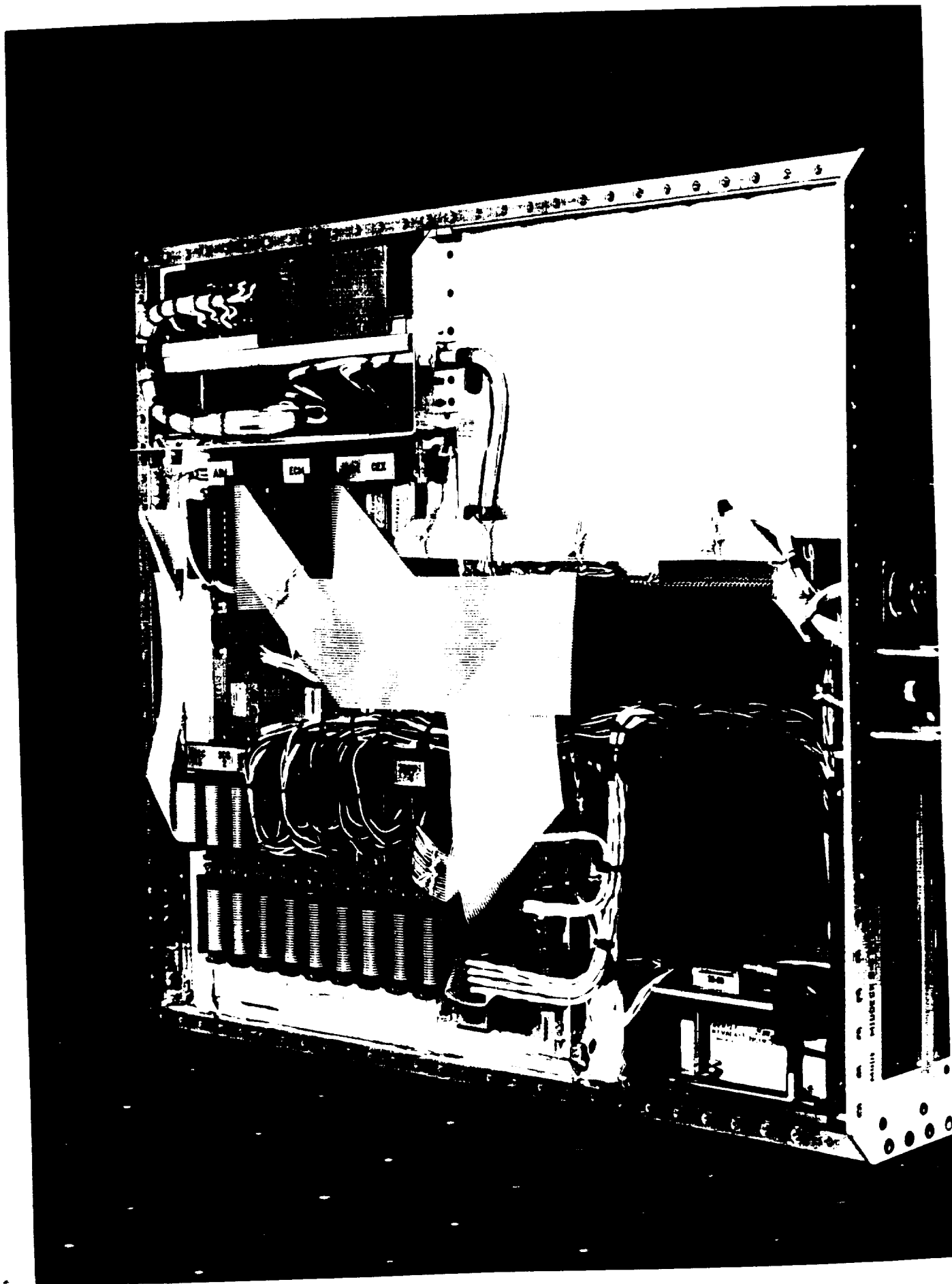
15-29
160314
N93-427893

MODE FLIGHT HARDWARE ELEMENTS

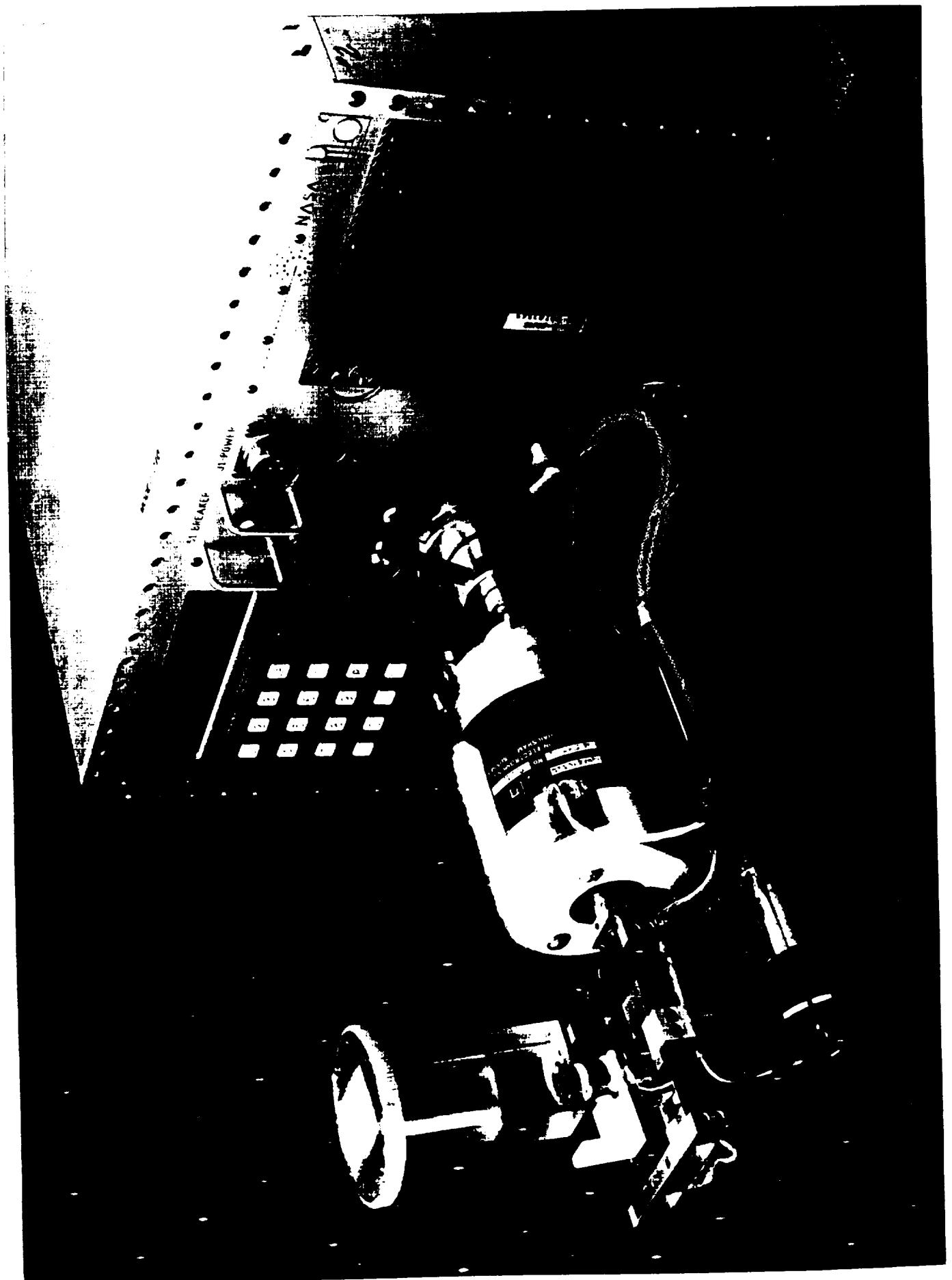


ORIGINAL PAGE IS
OF POOR QUALITY





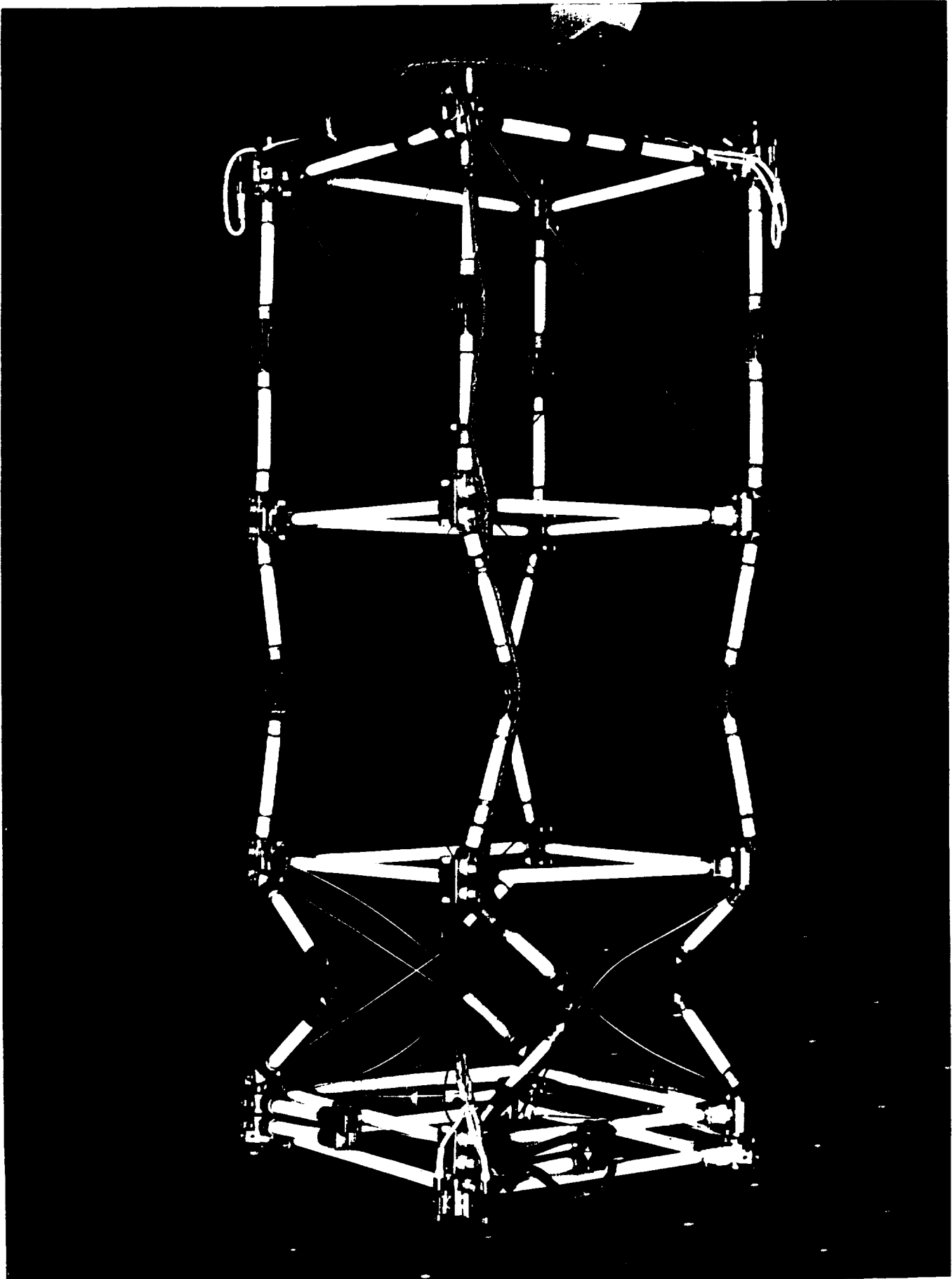
ORIGINAL PAGE IS
OF POOR QUALITY



ORIGINAL PAGE IS
OF POOR QUALITY



ORIGINAL PAGE IS
OF POOR QUALITY



ORIGINAL PAGE IS
OF POOR QUALITY



MODE SCIENCE OBJECTIVES

- Investigate two gravity-dependent nonlinear dynamic phenomena affecting future spacecraft:

Fluid Test Article (FTA)	Fluid slosh in a tank, uncoupled and coupled to spacecraft motions.
-----------------------------	---

Structural Test Article (STA)	Nonlinear dynamics of truss structures.
----------------------------------	--

- Both investigations complement OAST R&D base and enhance future space station/exploration missions.

MODE SCIENCE OBJECTIVES (CONT.)

Science objectives for both test articles include:

- Establishing a data base of dynamic response data in the ground and orbital gravity regimes.
- Understanding truss joint and fluid interactions with spacecraft motion.
- Using test results to verify nonlinear computer models developed at MIT.
- Using the knowledge obtained to more efficiently design spacecraft and their control systems.

MODE TEAM

Flight experiment funded by the NASA HQ In-Space Technology Experiments Program (In-Step)

Principal Investigator and science development team	M.I.T. Space Engineering Research Center
Sponsor	NASA Office of Aeronautics, Science, and Technology
Program monitor	NASA Langley Research Center
Hardware fabrication and integration team	Payload Systems Inc.
Co-Investigator	McDonnell Douglas Space Systems Co.

MODE IN THE UNIVERSITY ENVIRONMENT

- MODE provided focus and motivation for engineering education:
 - 20 undergraduate students
 - 7 graduate students
 - 2 postdoctoral students
- Student participation involved basic research and actual flight hardware fabrication and testing

FLIGHT OPERATIONS

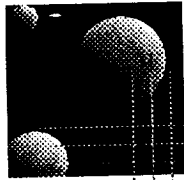
- MODE was launched on-board Discovery, STS-48, on Sept. 12, 1991. Hardware was deployed in the Middeck by the crew during operations.
- Flight operations began on Friday, September 13.
- MODE operations occurred on Flight Days 2, 4 and 5.
- Operations were supported at JSC by a 10 person MIT/PSI/MDSSC/LaRC team.
- All planned test operations plus an additional 3 hours of testing were successfully completed yielding over 600 Mbytes of on-orbit data.
- Hardware was recovered within 24 hours after landing.
- Hardware is currently being used at MIT for ground science tests.

FLIGHT OPERATIONS (CONT.)

- Fluid data was obtained on :
 - silicone oil, uncoupled, flat bottom tank
 - silicone oil, uncoupled, spherical bottom tank
 - water, uncoupled, flat bottom tank
 - water, coupled, flat bottom tank
 - water, uncoupled, spherical bottom tank
 - water, coupled, spherical bottom tank.
- Structural data was obtained on:
 - straight, 3 amplitudes, 3 pretension settings
 - straight with α -joint, 3 amplitudes, 2 friction settings
 - L-shape, 2 amplitudes, 2 friction settings
 - L-shape with flex. appendage

SUMMARY

- MODE exploits the unique 0-g laboratory environment provided by the Space Shuttle.
- Provides NASA with a reusable dynamic test facility for testing dynamic systems in space.
- Complements OAST R&D base and enhances future Space Station/exploration missions.
- Team represents a unique consortium of university, industry, and government.
- Cost-effective flight experiment developed on schedule by a small core group of scientists, engineers, and students
- Provides mission relevant focus for engineering education.



MIT
Space
Engineering
Research
Center

MODE: STRUCTURAL TEST ARTICLE (STA)

Prof. E. Crawley
Mr. Brett Masters

MIT
MIT

2629
165315
N93-271894

Space Engineering Research Center

MODE: Structural Test Article Motivation

- DETAILED MODEL AND UNDERSTANDING OF ON-ORBIT STRUCTURAL DYNAMICS IS IMPORTANT SINCE:

Resonant and transient response influence on-board vibration / acoustic environment.

Incorrect modeling of dynamics can cause inadvertent CSI with attitude dynamics.

Detailed modelling is vital for robustness / performance of precision controlled structures.

- NEED TO CORRECTLY MODEL AND UNDERSTAND NON-LINEAR EFFECTS ON A COMPONENT AND SUB-COMPONENT LEVEL.

- UNDERSTANDING ON-ORBIT DYNAMICS WILL REDUCE UNCERTAINTIES
BY:

comparison of earth test results with 0-gravity test results.

verifying and validating analytical models.

adding to the scant data base of quality data available on the dynamics of large flexible space structures in 0-gravity.

Why Test STA In Space?

- GROUND BASED SIMULATIONS HAVE BEEN EXPLOITED

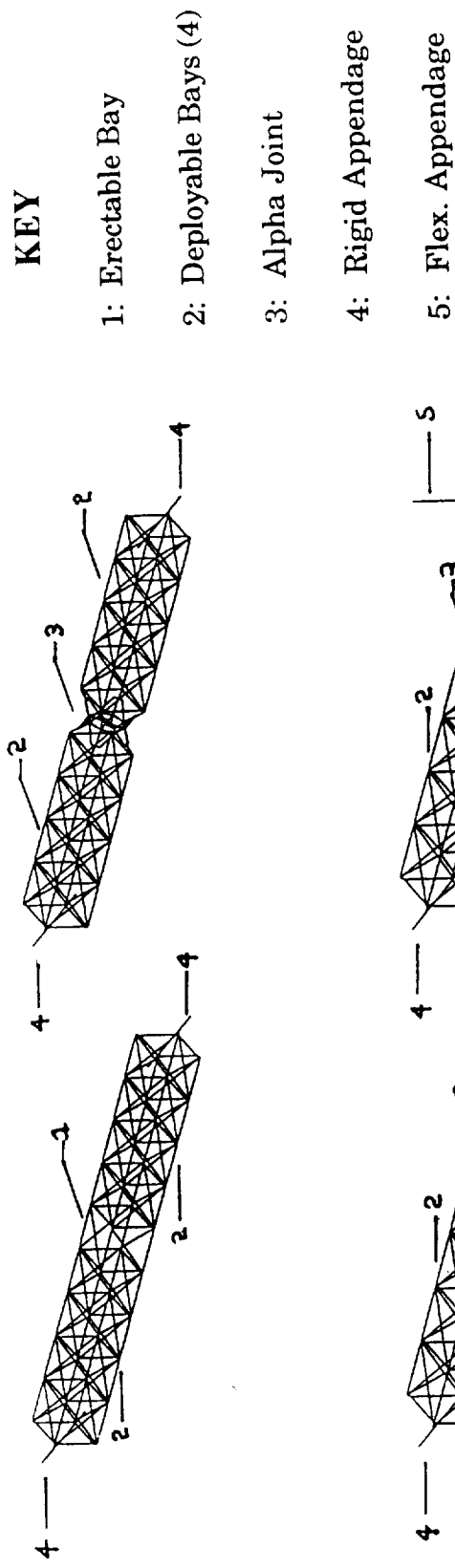
Options

- (a) Suspended in air
- (b) Suspended in vacuum
- (c) Lofted in vacuum (Free-fall)

BUT:

- (a) Air damping undesirable, suspension systems corrupt modal measurements, and the gravity field causes pre-loads and pre-deflections in the structure.
- (b) Suspension and gravity!
- (c) Short time periods of free-fall reduce accuracy of modal identification due to
 - (i) Uncertain initial conditions (inhomogeneous terms)
 - (ii) Difficulty in exciting the structure
 - (iii) Poor signal-to-noise ratio

Hardware

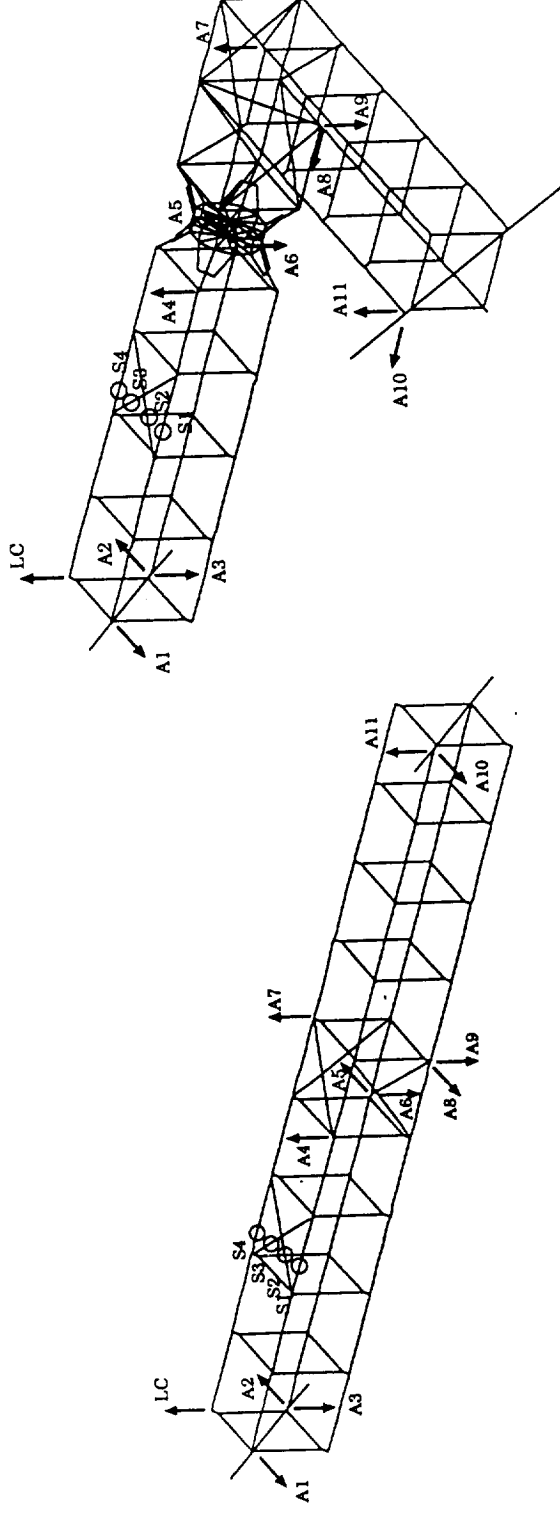


Four Test Configurations of the STA

Sensors and Actuator

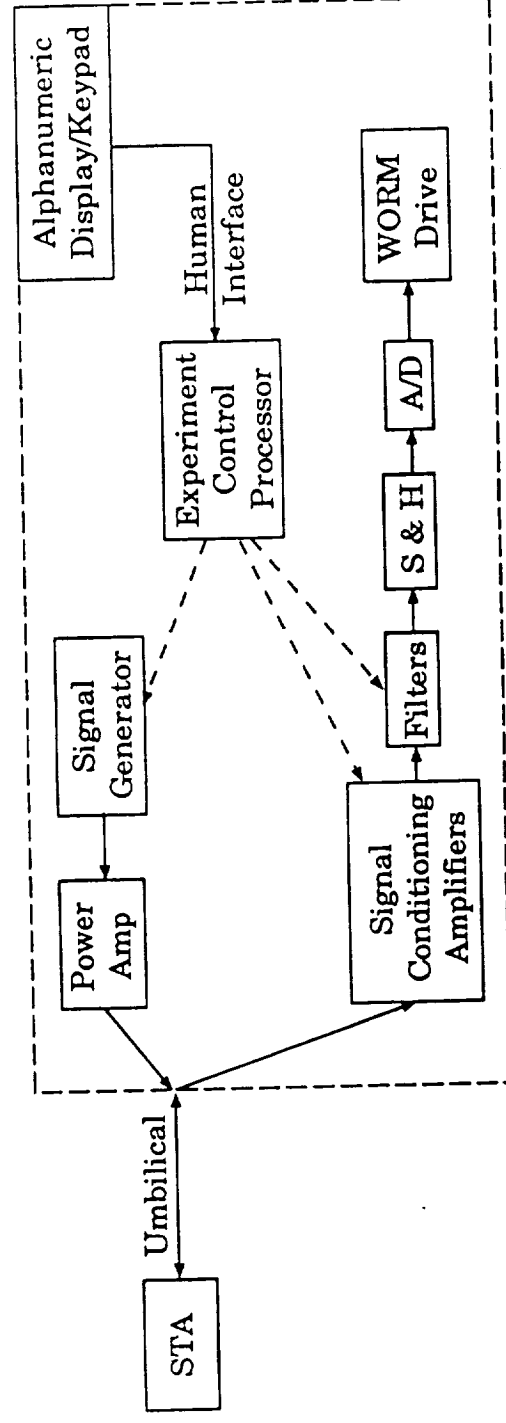
Sixteen sensor channels arranged and conditioned as full-bridge resistive gages

- four strain gage pairs located on one face of adjustable preload bay
- eleven accelerometers (piezoresistive) at predetermined locations
- one load cell located in the proof-mass actuator housing



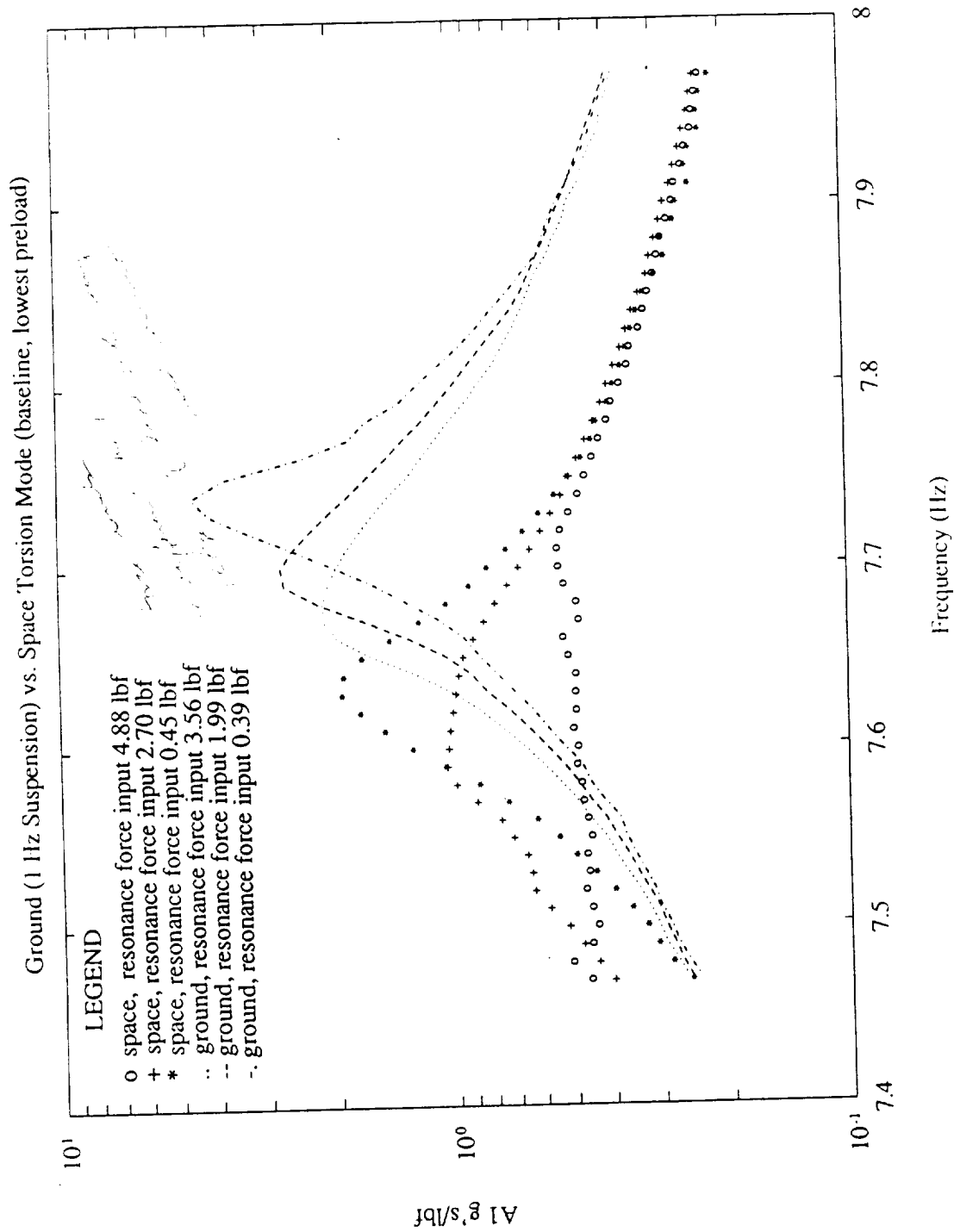
Sensor and actuator locations for Straight and L configurations.

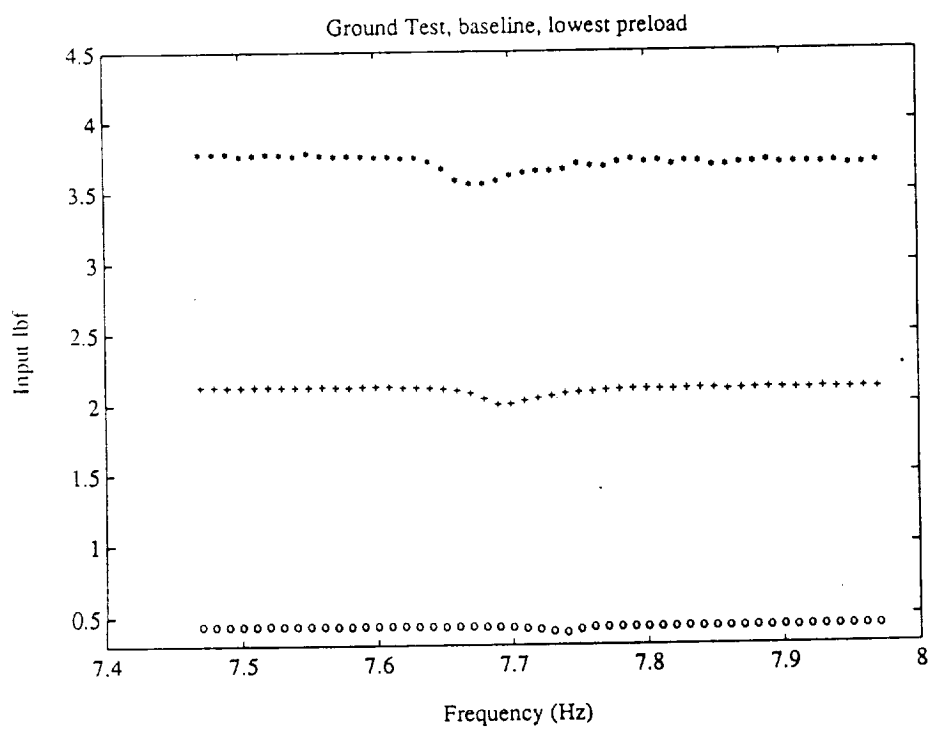
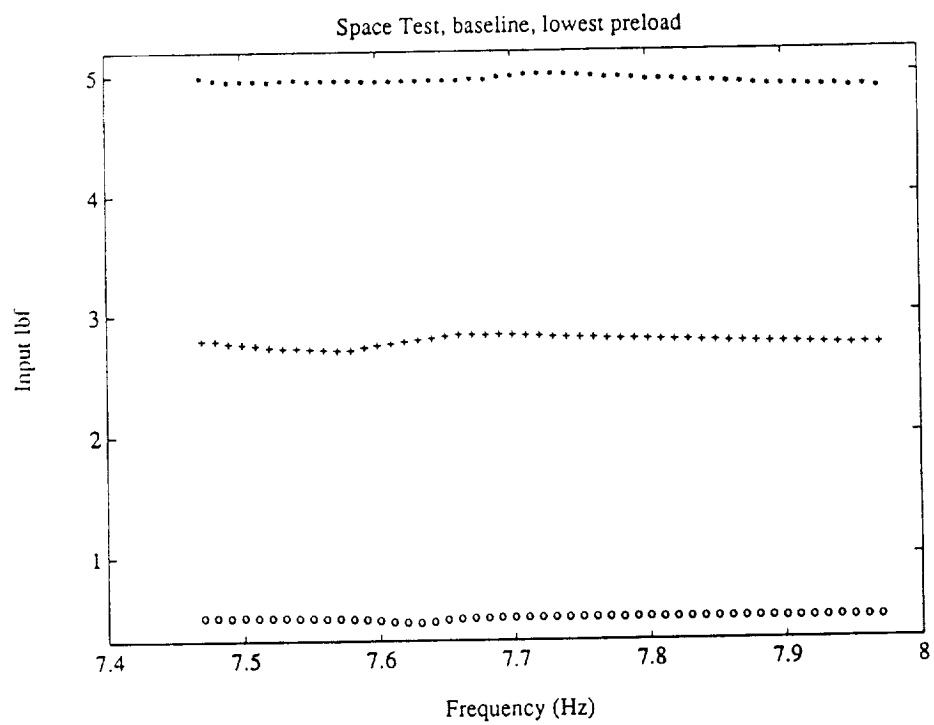
Experimental Support Module



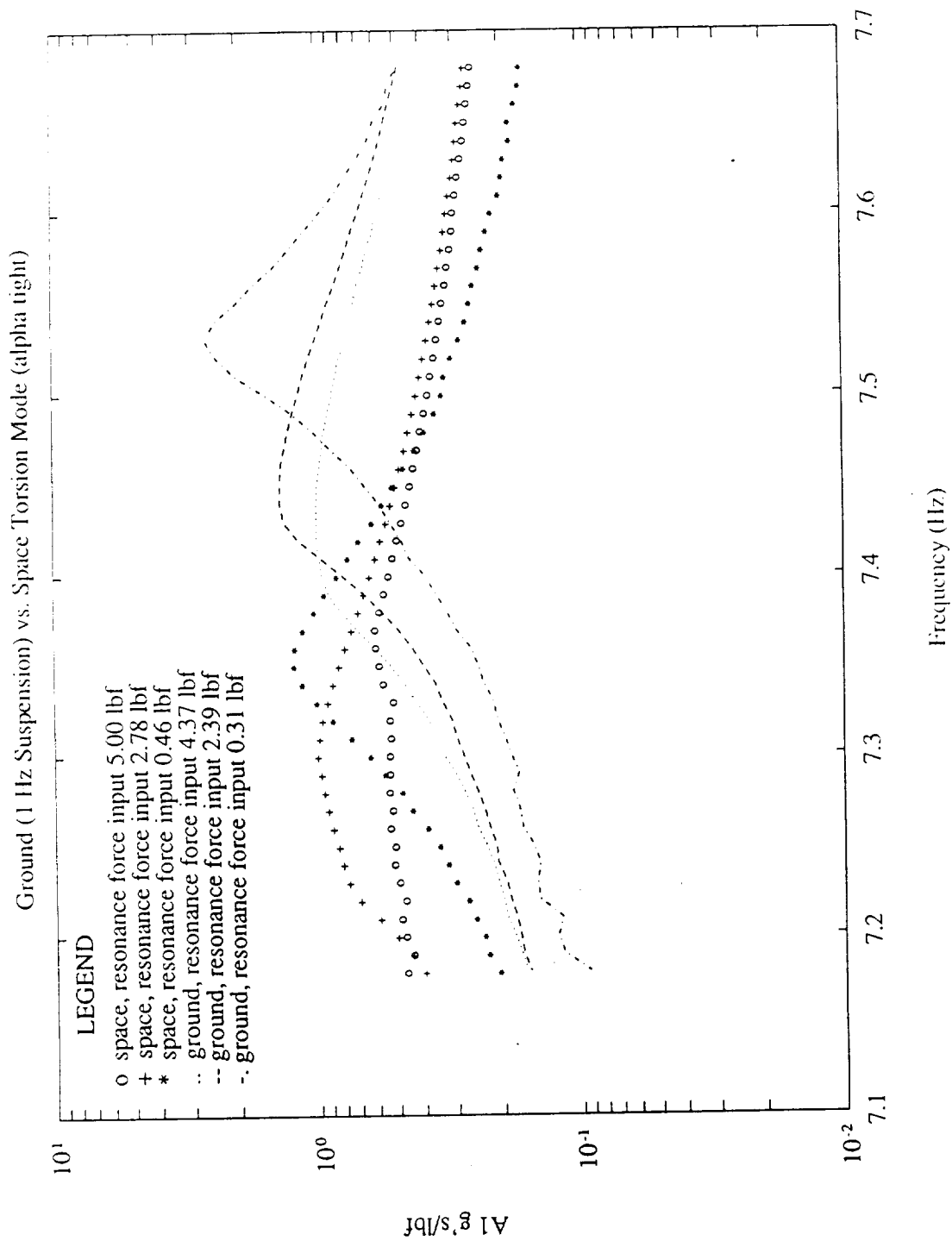
ESM Driven Flow Diagram

Data





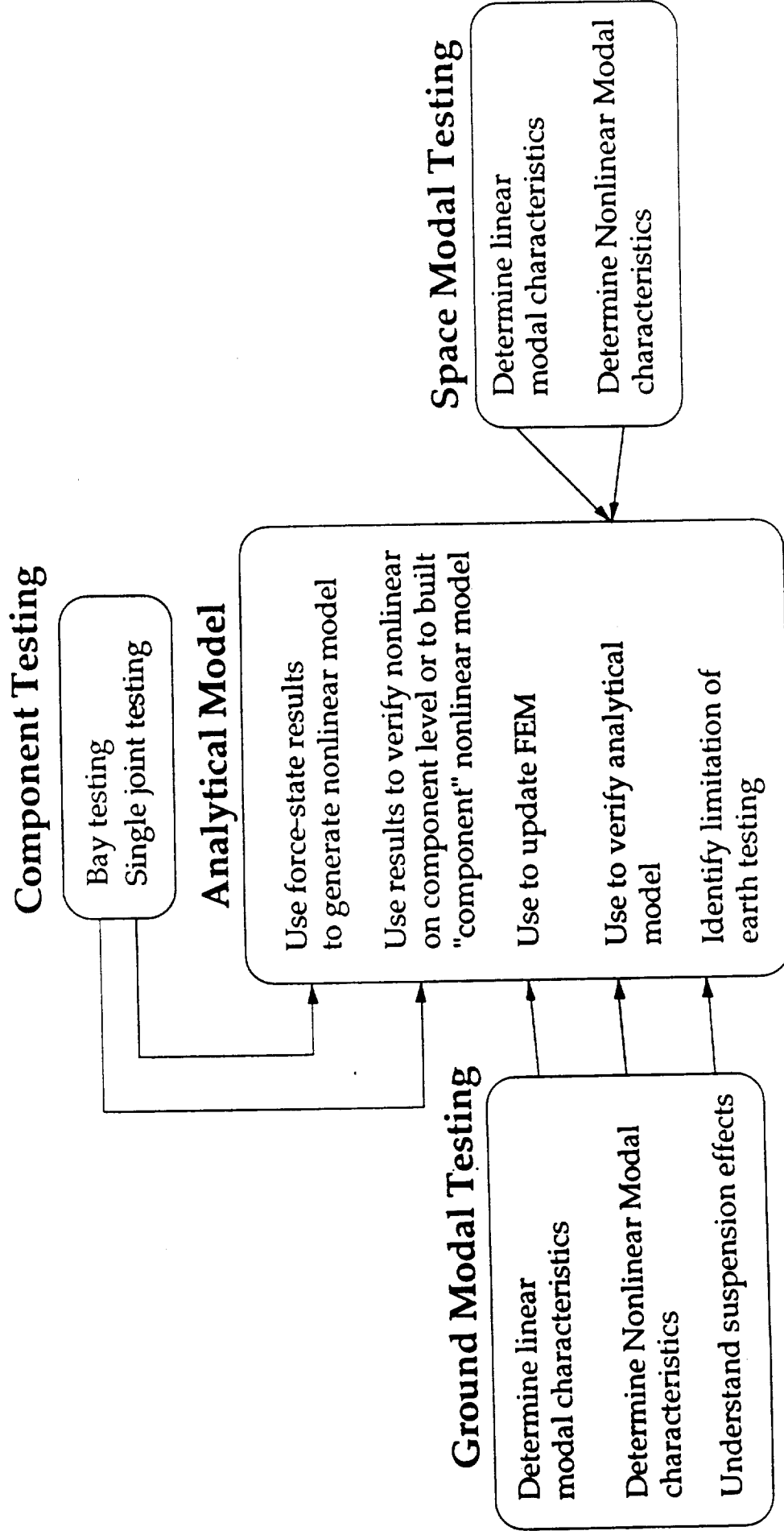
Data (cont.)



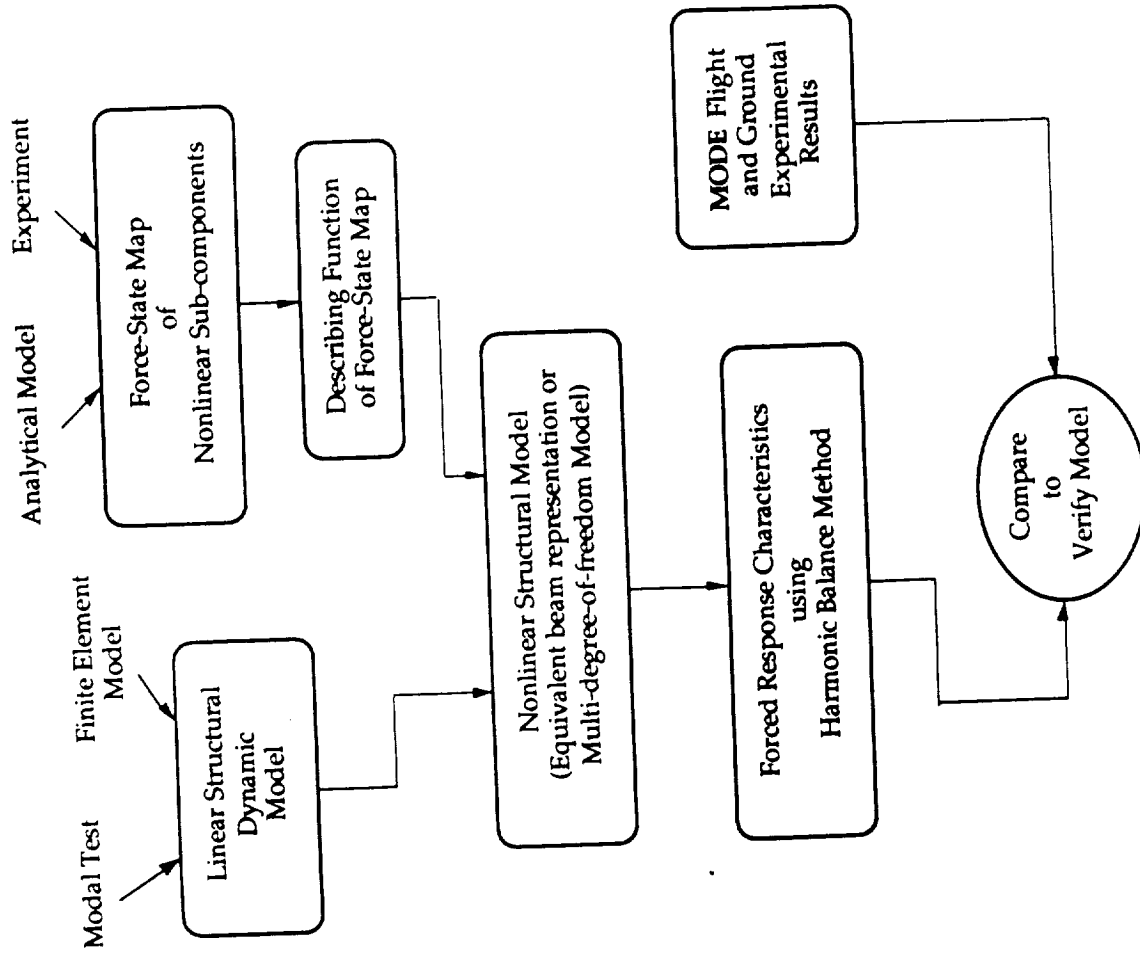
Preliminary Results

- MODES GENERALLY APPEAR SOFTER IN 0-GRAVITY
- RESONANCES EXHIBIT SIMILAR SHIFTS, ON THE GROUND AND IN 0-GRAVITY, RELATIVE TO INPUT FORCING LEVEL.
- MODES ARE GENERALLY MORE DAMPED IN 0-GRAVITY.
- DATA EXHIBIT SOME ANOMALIES, TO BE EXPLAINED BY NON-LINEAR ANALYSIS?
- SOME MODES OUT OF 0-GRAVITY TEST WINDOWS!

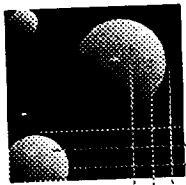
Supporting Analysis Program



Modelling Approach



MIT
Space
Engineering
Research
Center



MIDDECK 0-GRAVITY DYNAMICS EXPERIMENT

FLUID SLOSH EXPERIMENTS

Dr. Marthinus C. van Schoor

University of Pretoria
South Africa

January 1992

57-21
160316
N 9 3 7 27-8/95

Space Engineering Research Center

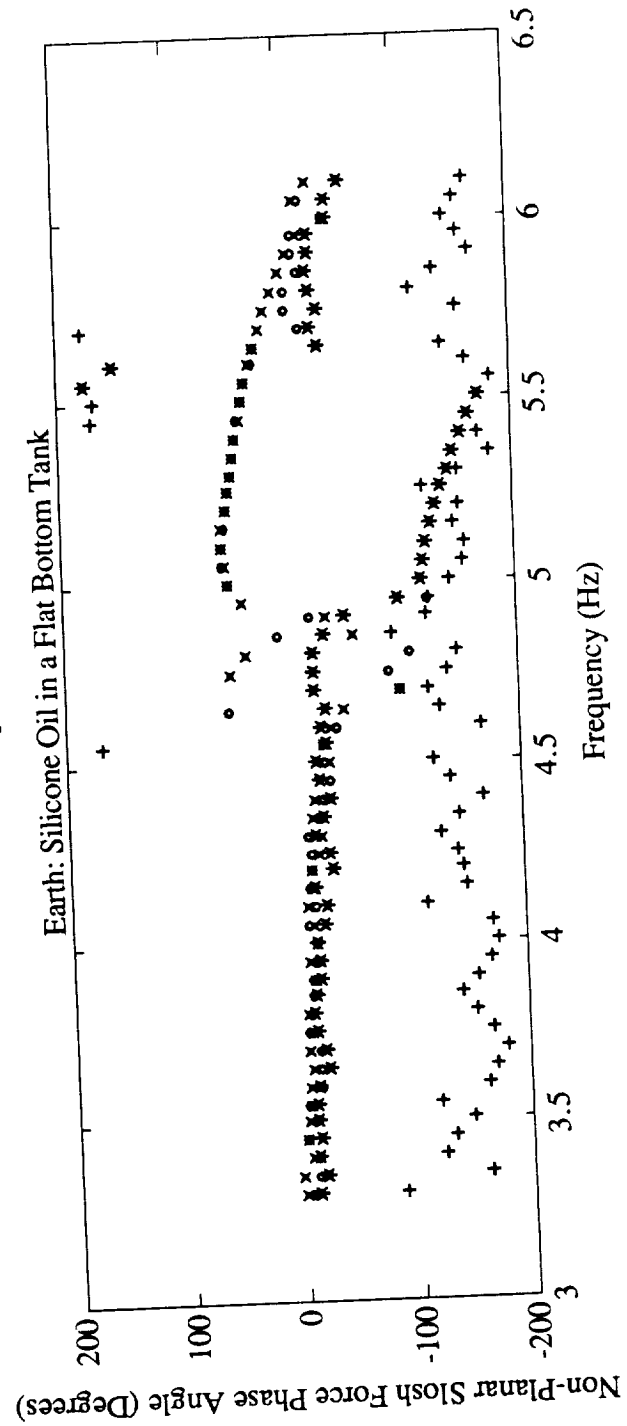
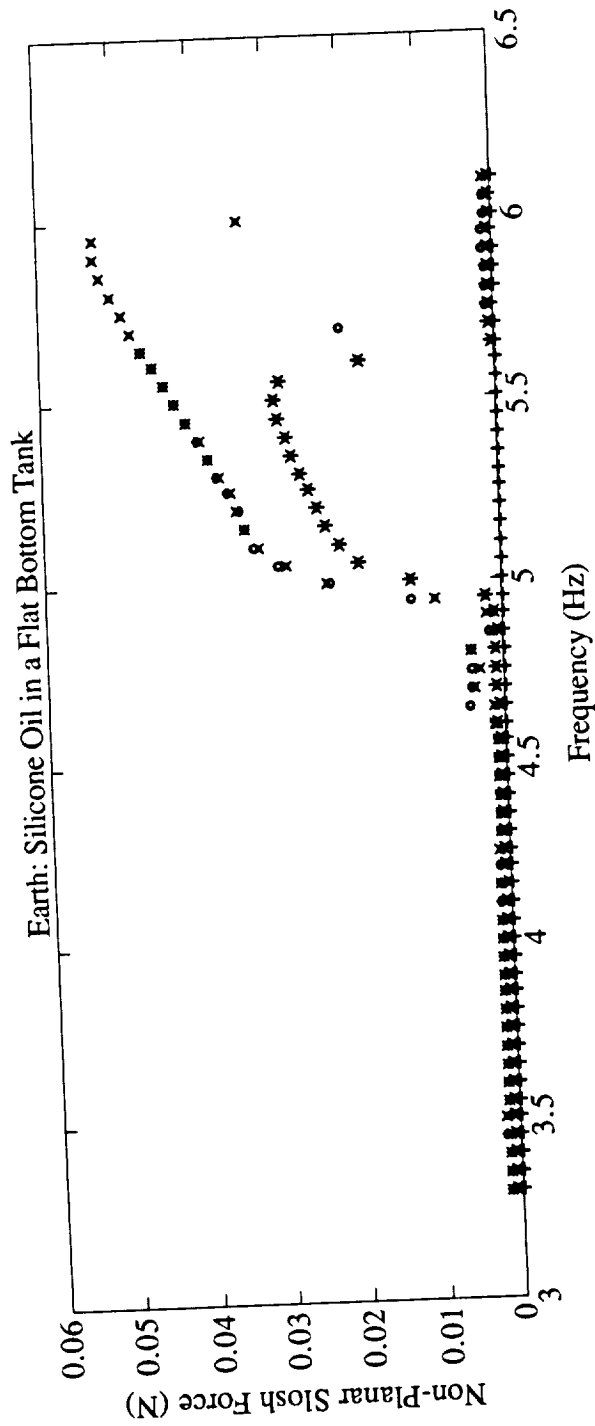
Summary Preliminary Results

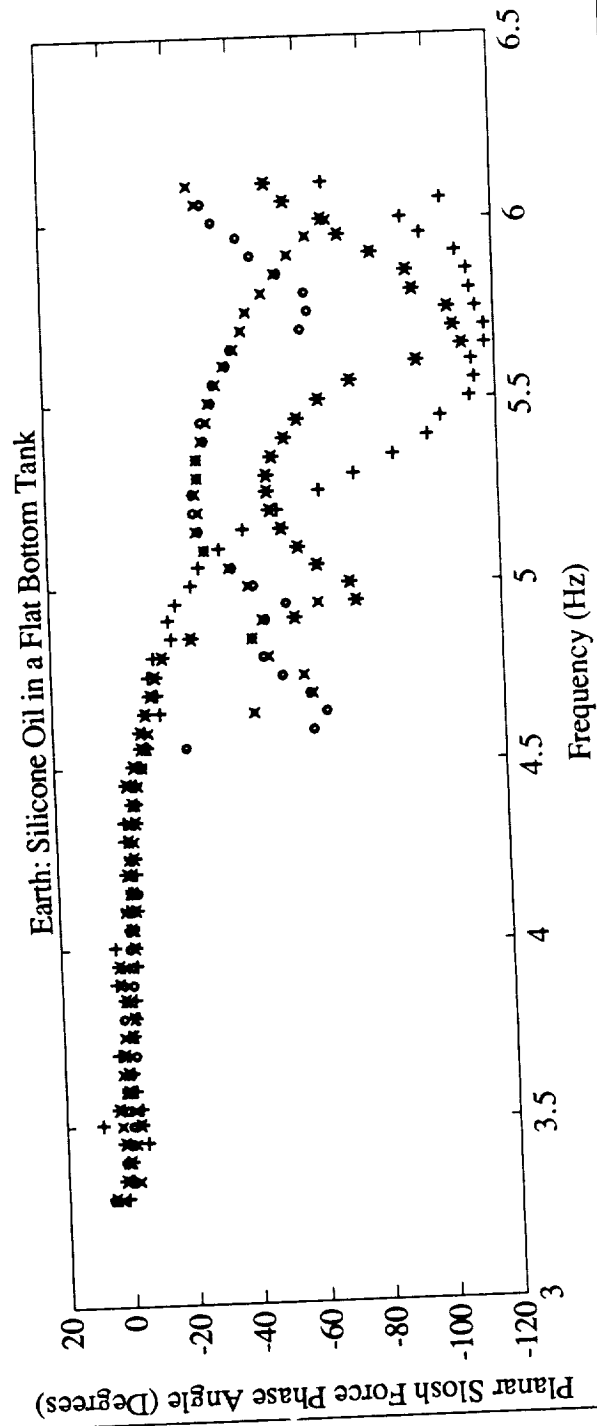
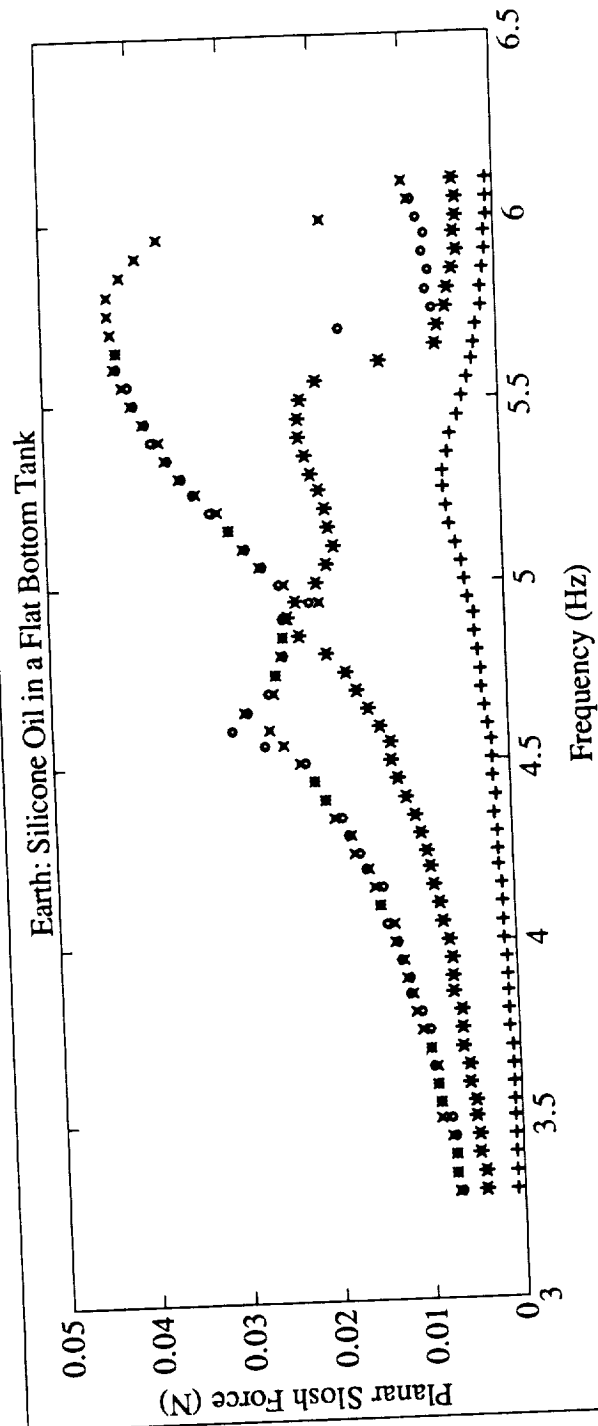
- More benign nonlinear behavior than observed on earth
- Modal damping ratios and frequencies different from predicted

Typical Results

Silicone Oil (3.1 cm Cylindrical Tank with a Flat Bottom):

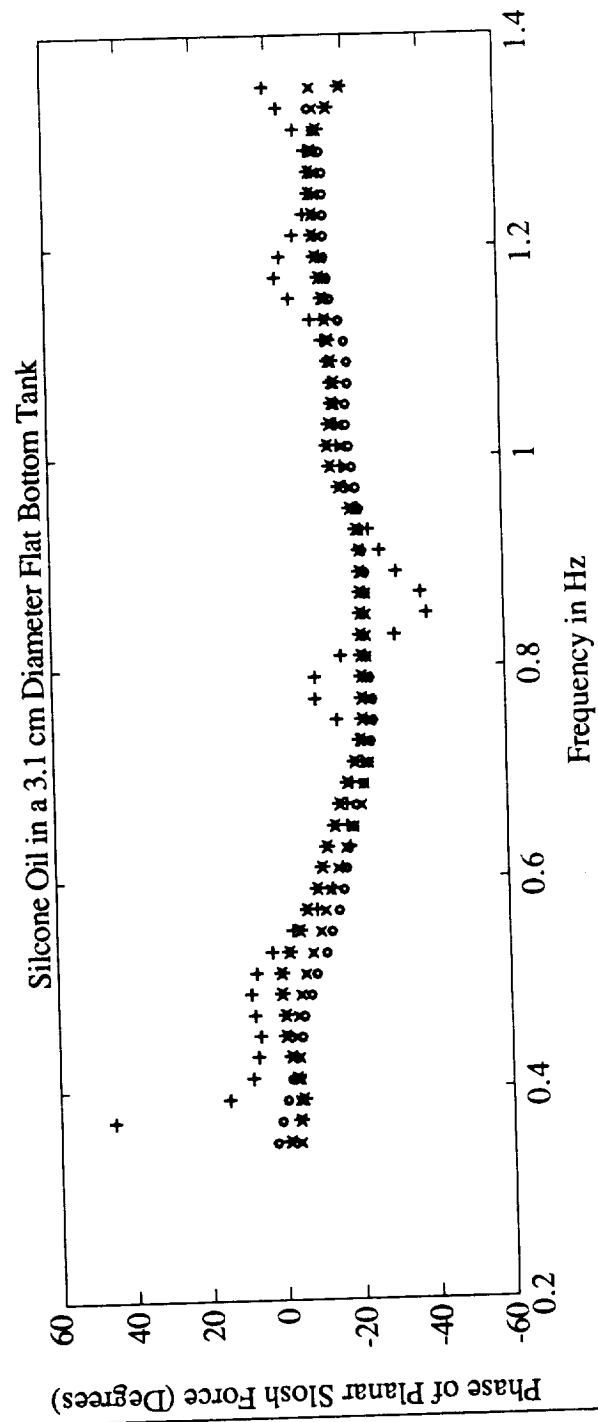
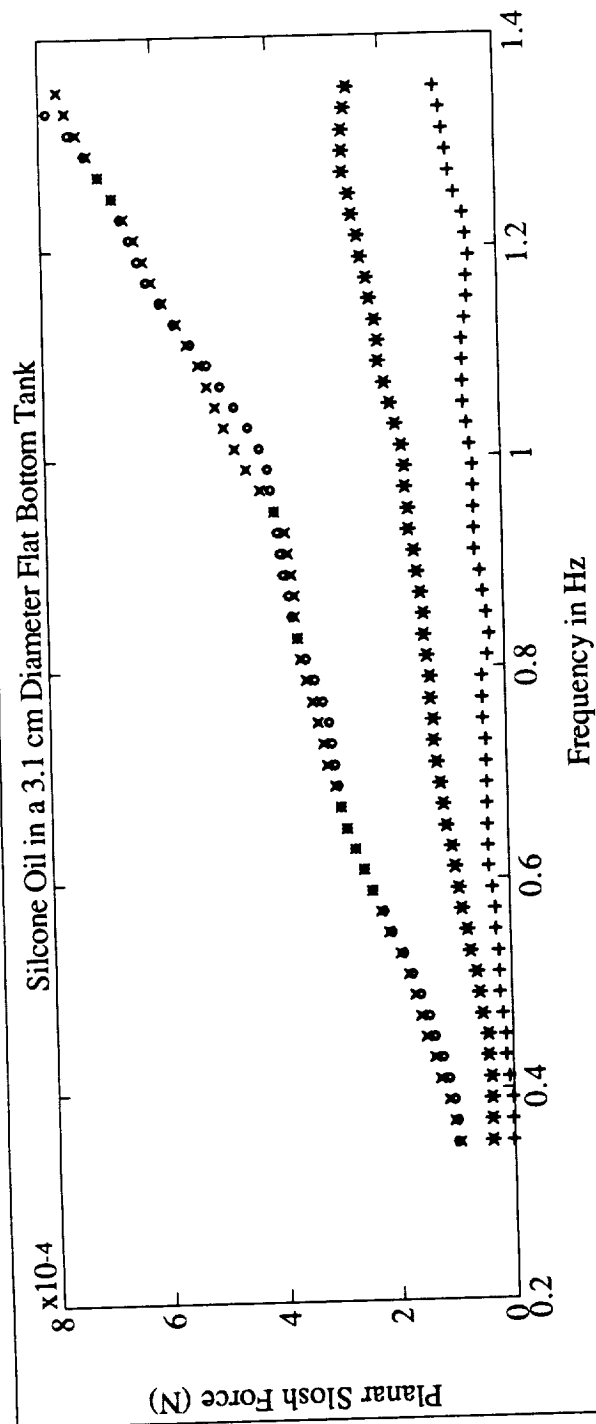
Earth:

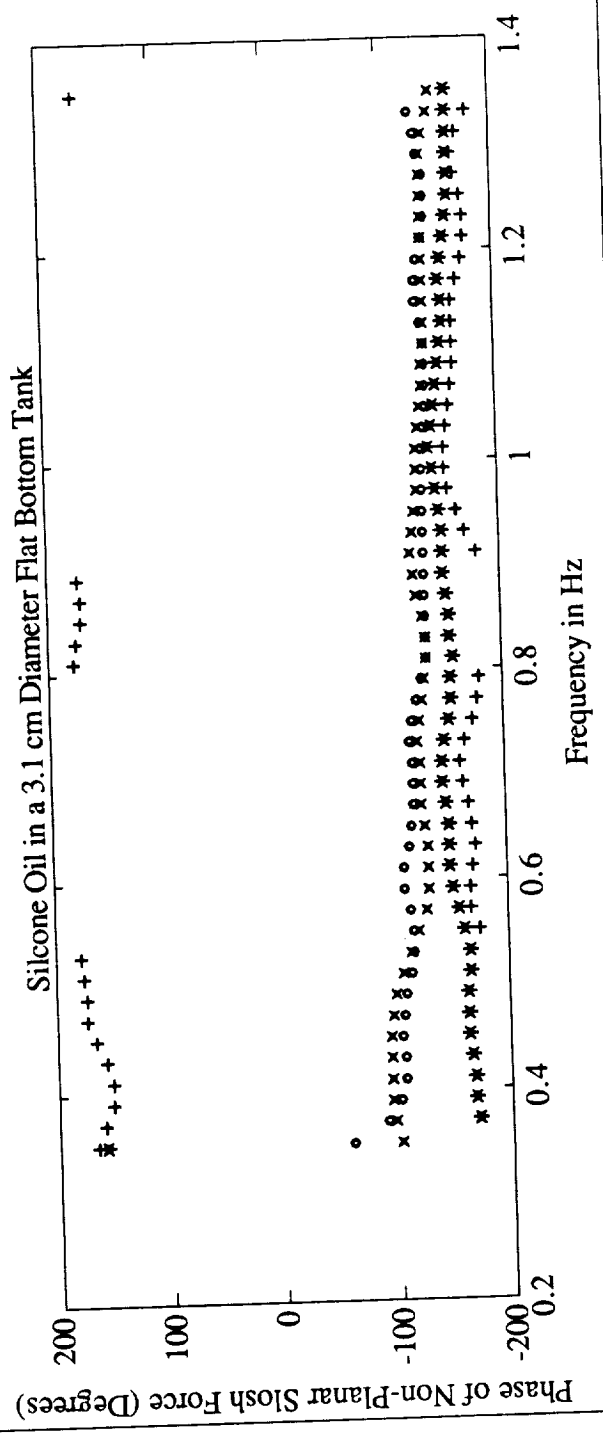
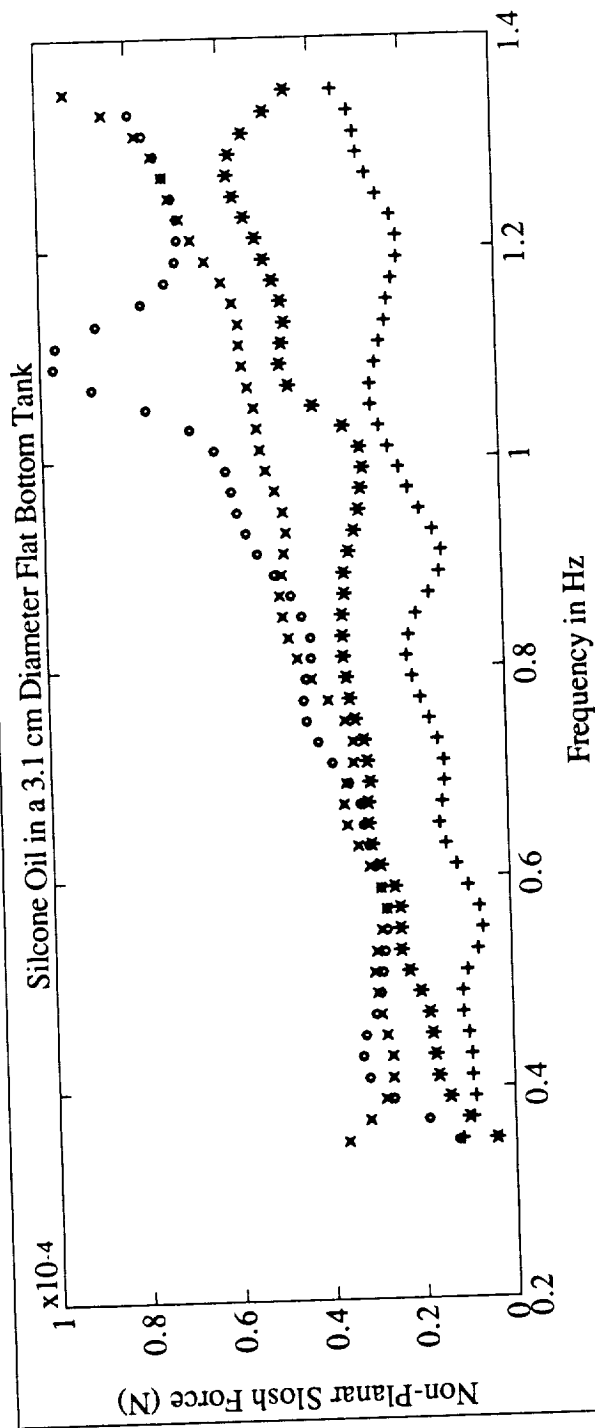




Silicone Oil (3.1 cm Cylindrical Tank with a Flat Bottom):

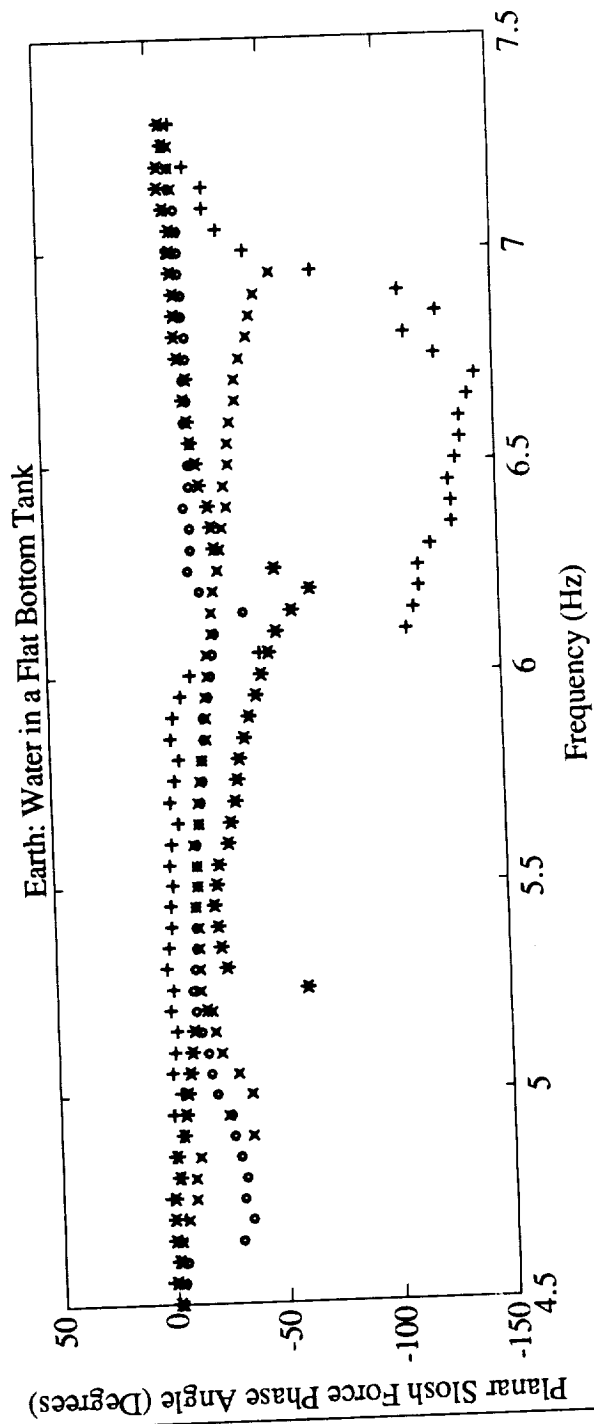
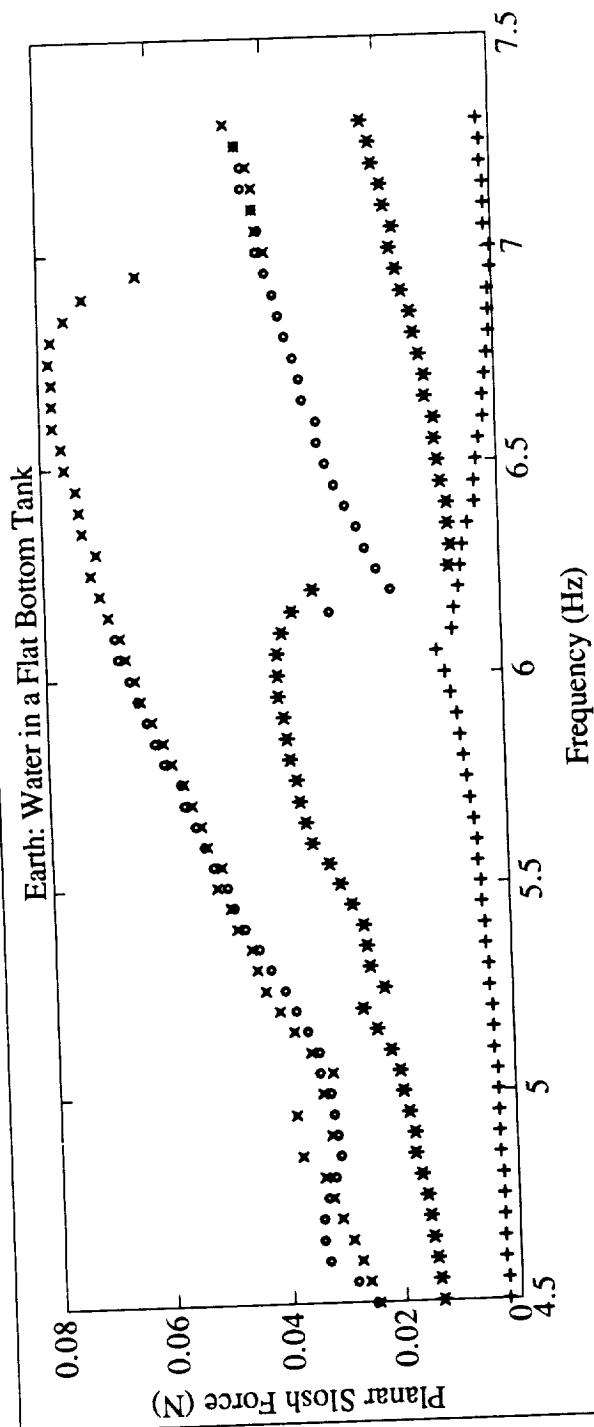
Space:





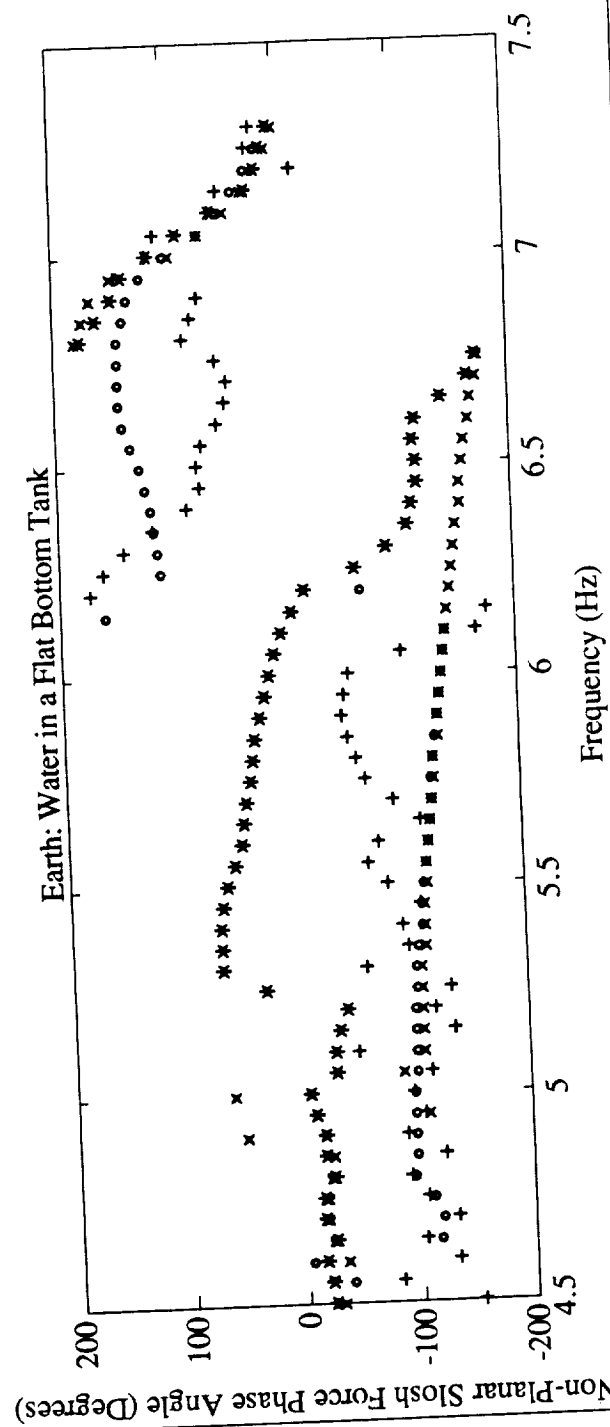
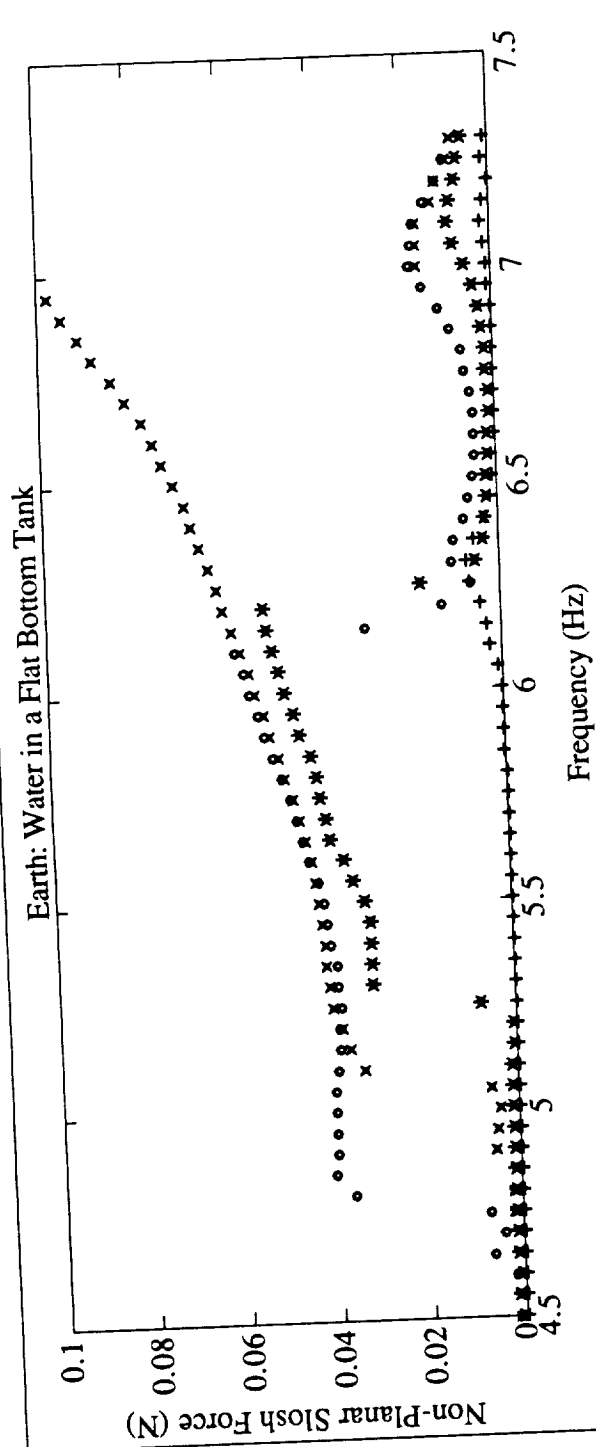
Water (3.1 cm Cylindrical Tank with a Flat Bottom):

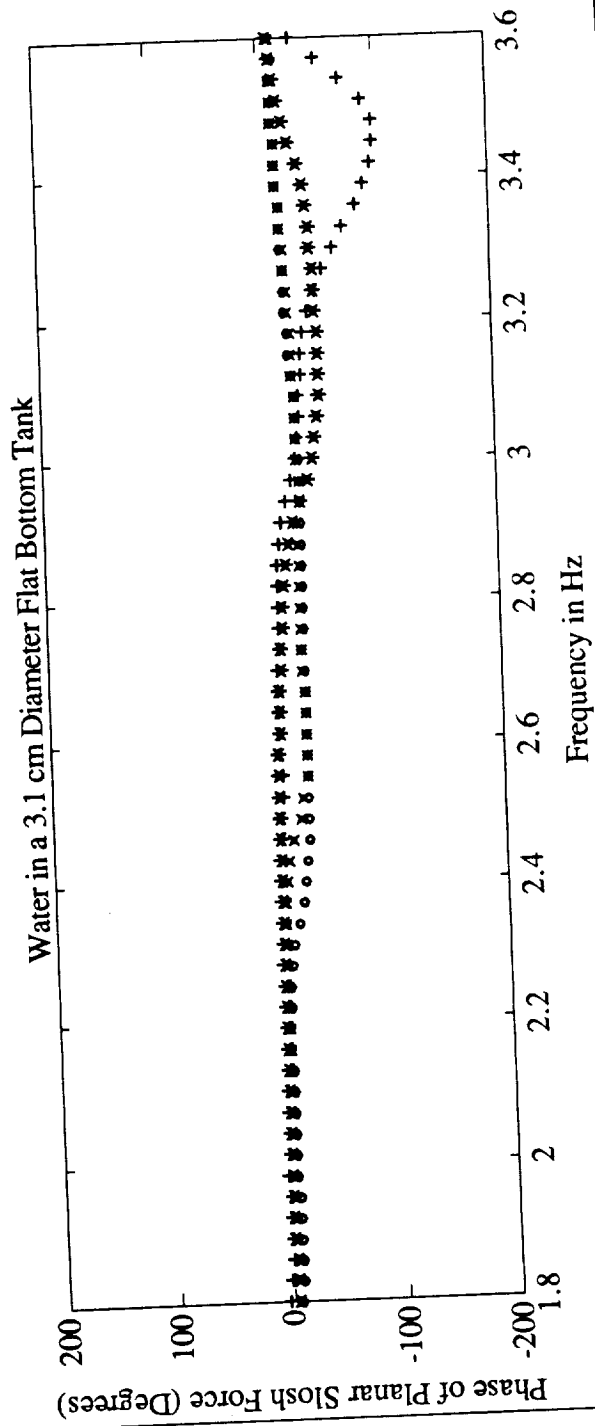
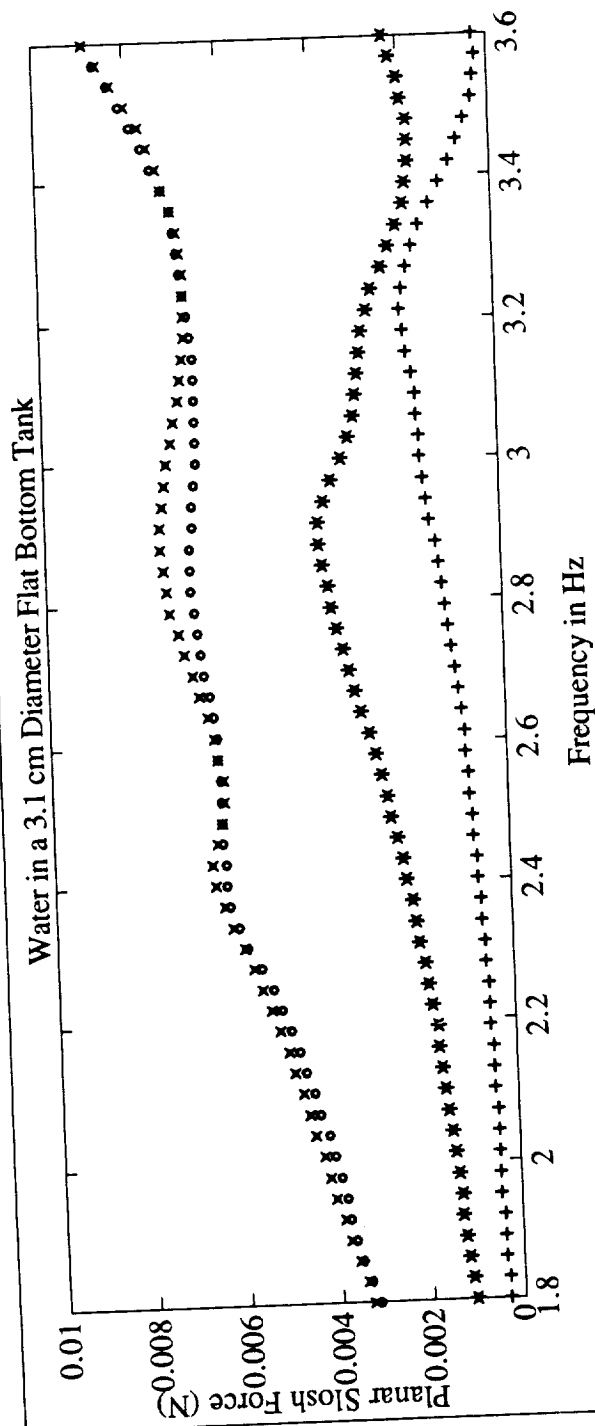
Earth:

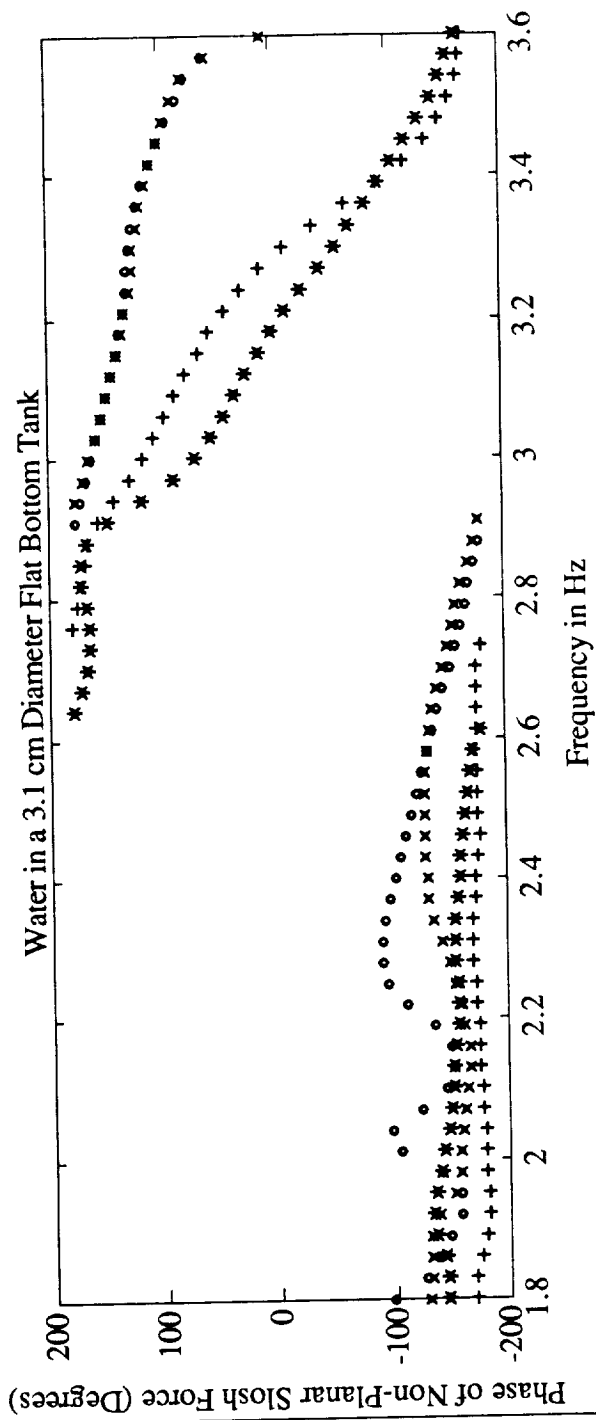
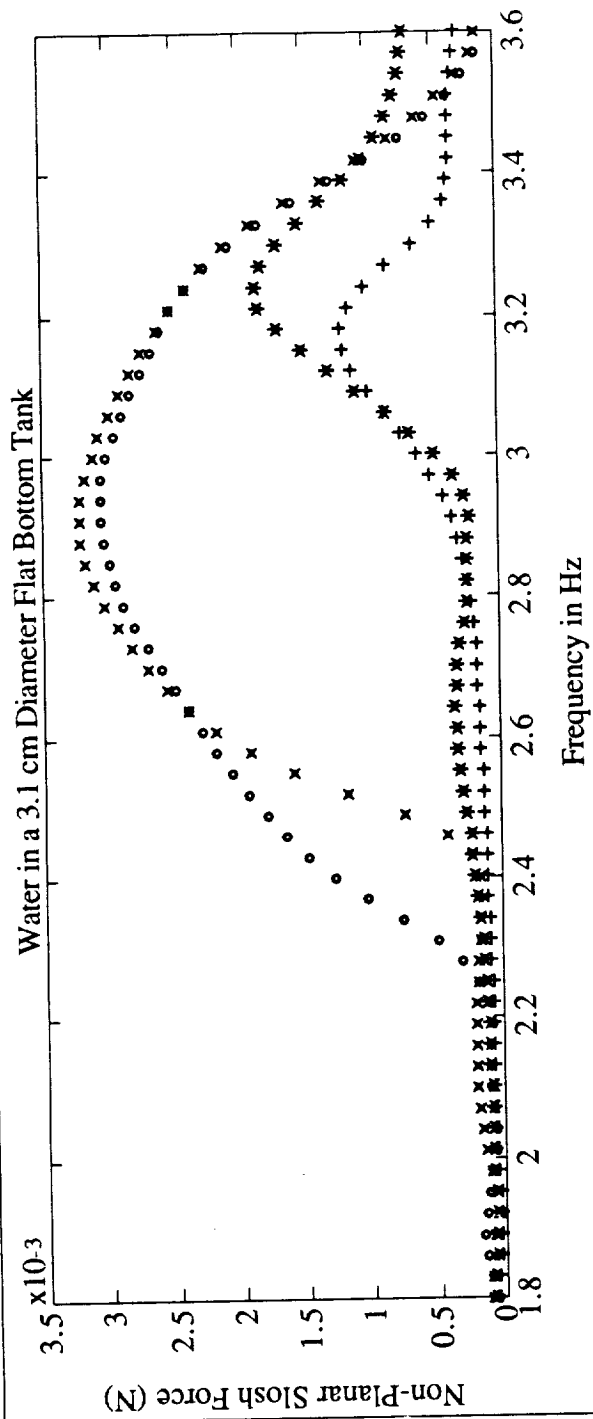


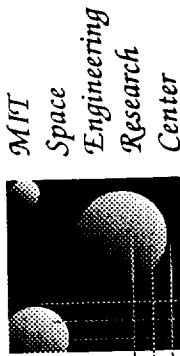
Water (3.1 cm Cylindrical Tank with a Flat Bottom):

Space:









THE MIDDECK ACTIVE CONTROL EXPERIMENT (MACE):

Dr. David W. Miller

MIT

SERC Steering and Technical Representative Meeting

January 1992

58-39
165317
N 93-127896

Space Engineering Research Center

PROGRAM OBJECTIVES

- Science Objective

To develop a verified set of methods that will allow designers of CSI/CST spacecraft, which cannot be dynamically tested on the ground in a sufficiently realistic 0-g simulation, to have confidence in the eventual orbital performance of such spacecraft.

- Implications

Understand direct and indirect gravity effects and the relation between control authority and manifestation.

Develop procedures for predicting on-orbit performance.

Quantify prediction accuracy achievable through analysis and ground tests.

Develop techniques for on-orbit identification.

Quantify performance improvement through control redesign based upon on-orbit identification.

PROGRAM FEATURES

Milestones

Preliminary Design Review (PDR)	April, 1992
Critical Design Review (CDR)	December, 1992
Launch	July, 1994

Participants

M.I.T. SERC	PI and science development
Payload Systems Inc.	Fabrication and Integration
Lockheed, Sunnyvale	Co-Investigator
McDonnell Douglas	Co-Investigator
Integrated Systems Inc.	AC-100 and design tools
CSA	Suspension

Hardware Phases

Development Model	science development
Engineering Model	flight prototyping
Flight Model	two flight hardware units

FLIGHT EXPERIMENT FEATURES

- Middeck experiment stored in four lockers
- Test article deployed on middeck with umbilical connection to Experiment Support Module (ESM)
- ESM contains:
 - experiment and realtime control computers
 - actuator power amplifiers and sensor signal conditioning data storage
 - human and host computer interfaces
- Duration of three 8-hour days
- On-orbit timeline
 - Identification Day 1
 - Downlink ID data Day 1
 - Implement same algorithms as on ground Day 1
 - Implement algorithms adjusted for lack of gravity Day 2
 - Uplink ID based control algorithms Day 3
 - Implement new measurement based algorithms Day 3
- ESM provides reusable realtime control facility

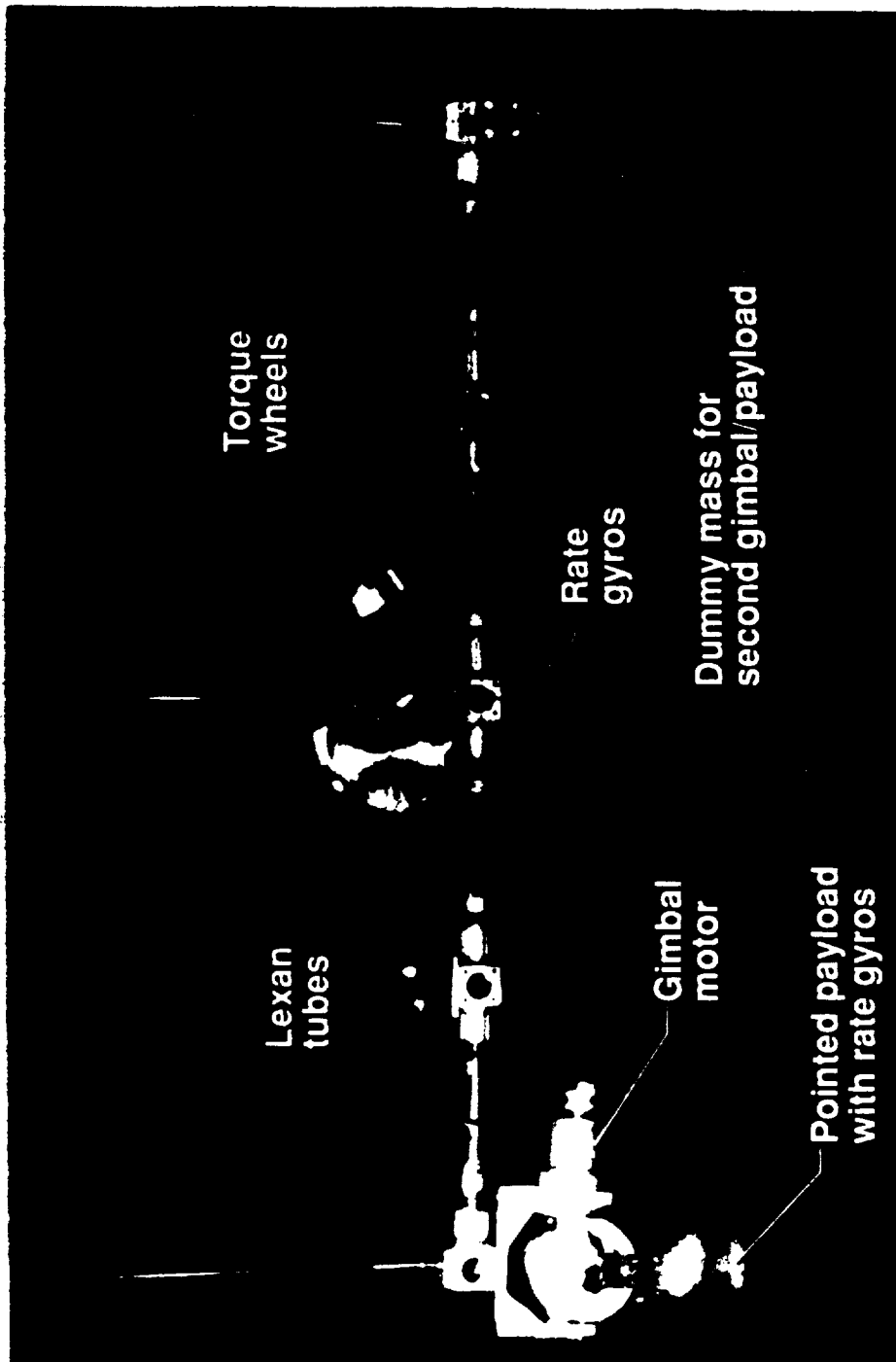
CURRENT ACTIVITIES

- Preliminary flight hardware design (PSI)
- Engineering Model gimbal acquisition (PSI, LMSC)
- Selecting on-orbit test configurations based upon desire to have gravity effects cause significant performance deviation from ground near midrange of control authority (Sepe)
- Incorporating gravity effects in Finite Element model (Rey)
- Development Model (DM) modern closed-loop control (Saarmaa, Miller)
- Command input shaping tests on DM (Chang)
- Formulation of 1-g and 0-g identification procedures (Karlova, Douglas)
- Study of multibody gravity effects (Quadrelli)
- Fabrication of active strut (PSI)

MIDDECK ACTIVE CONTROL EXPERIMENT (MACE)

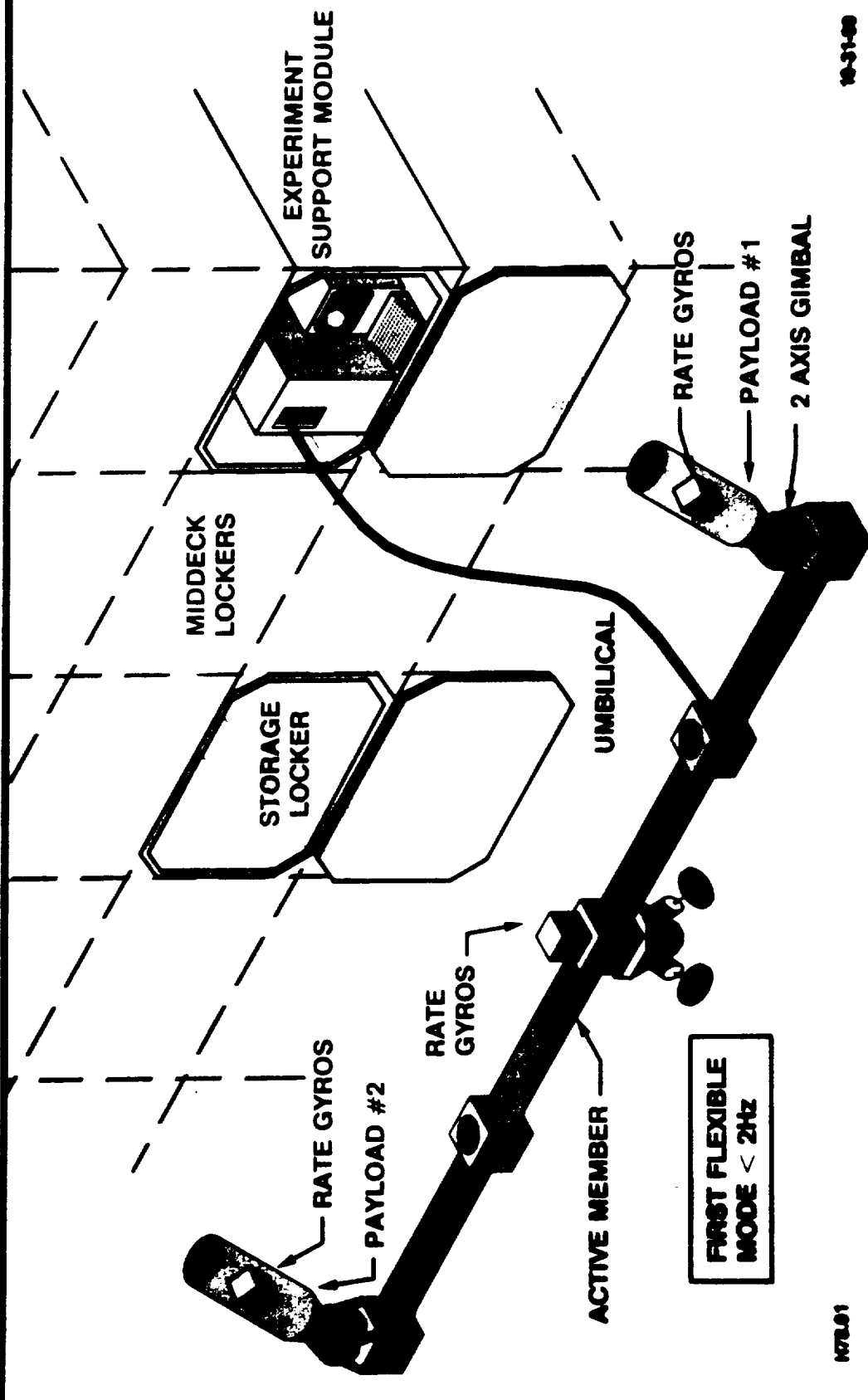
Development Model Lab Testing

(Flight unit will have smaller torque wheels and gimbal motors)



ORIGINAL PAGE IS
OF POOR QUALITY

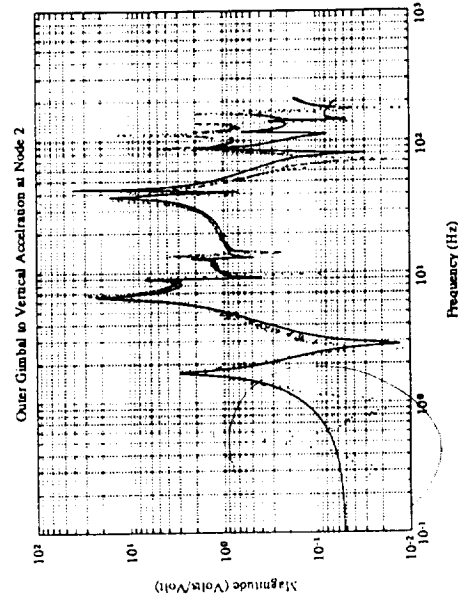
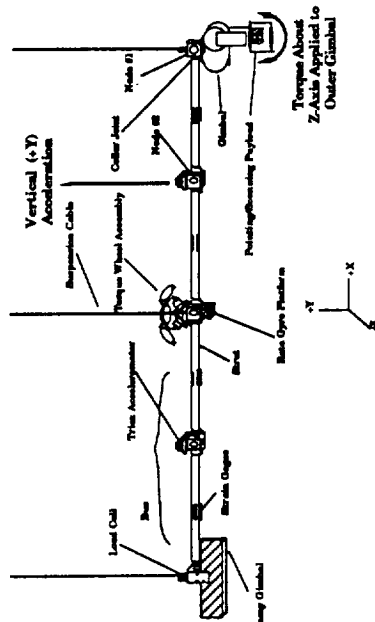
MACE TEST ARTICLE DEPLOYED ON THE STS MIDDECK



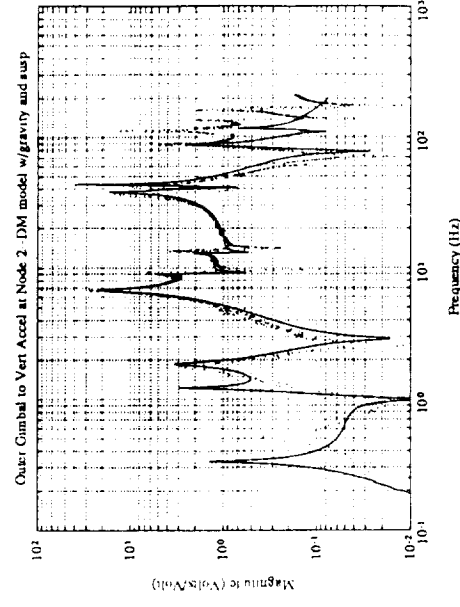
1470.01

10-31-60

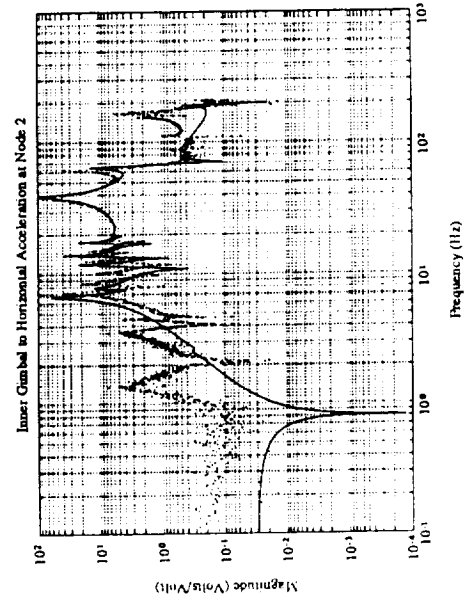
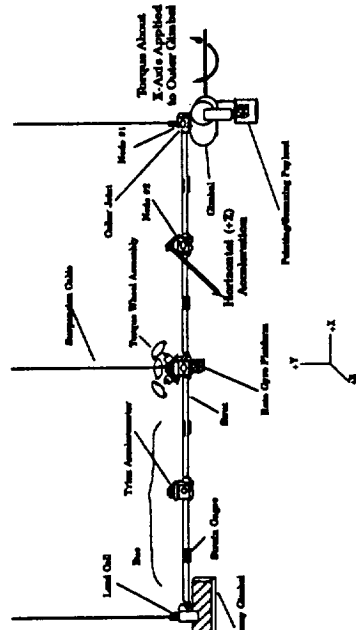
Data Channel



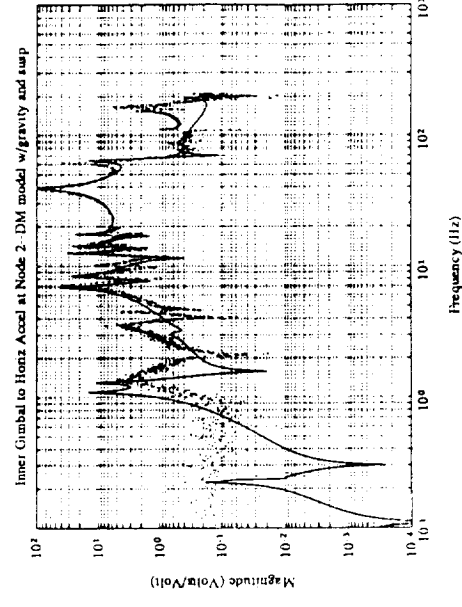
0-g model, 1-g data



1-g model, 1-g data



Inner Gimbal to Horizontal Acceleration at Node 2

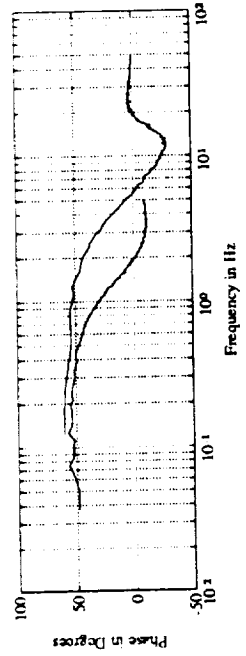
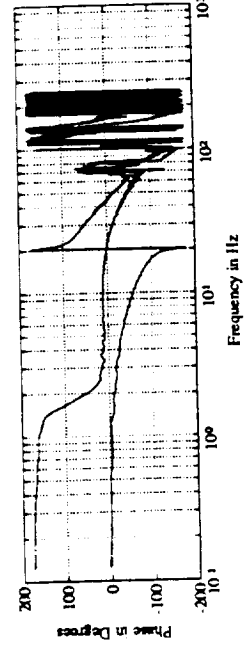
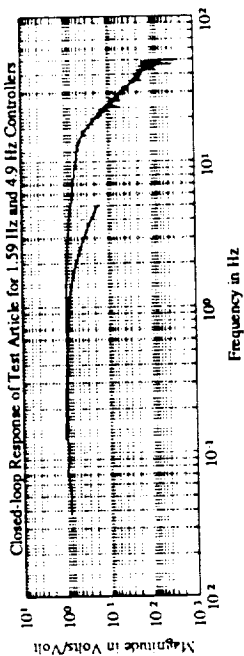
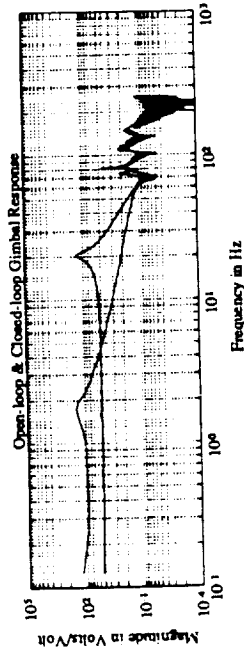


Inner Gimbal to Horiz Accel at Node 2--DM model w/gravity and wind

DEVELOPMENT MODEL TESTING

Component Control Work

Gimbal Control Torque Wheel Control Baseline Control



Torque Input Axis	Z	Z	Z	Y
Input Voltage RMS (volts)	0.1	0.3	0.1	0.2
Input Torque RMS (Nm)	0.00969	0.02606	0.00969	0.017371
Payload Output Axis	Z	Z	Z	X
Payload Angle RMS (degrees)	0.0389	0.0968	0.0357	0.1420
Payload Angle 3RMS (degrees)	0.1166	0.2904	0.1070	0.4529
Payload Clamped Angle	+45 deg about Z	+45 deg about Z	-45 deg about Z	0 deg (down)

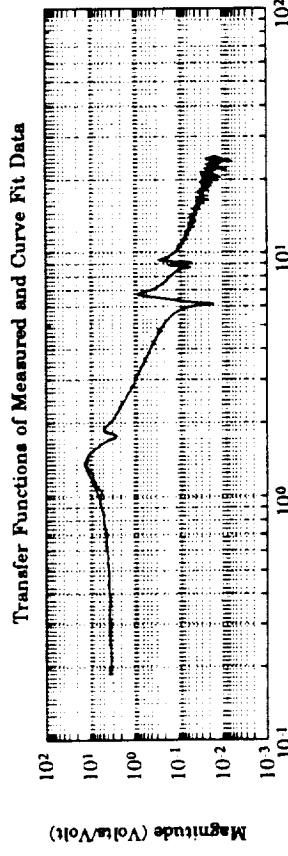
DEVELOPMENT MODEL TESTING

Single Input, Single Output Control (localized topology)

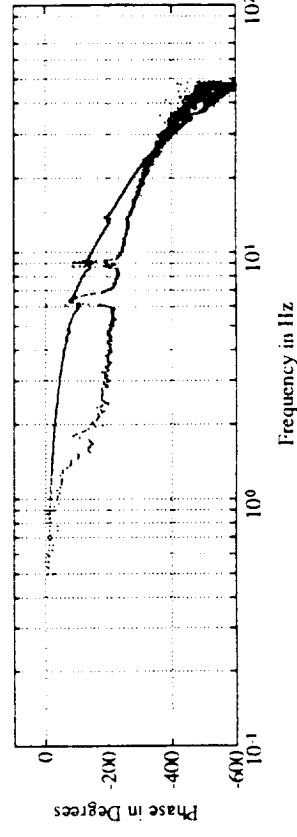
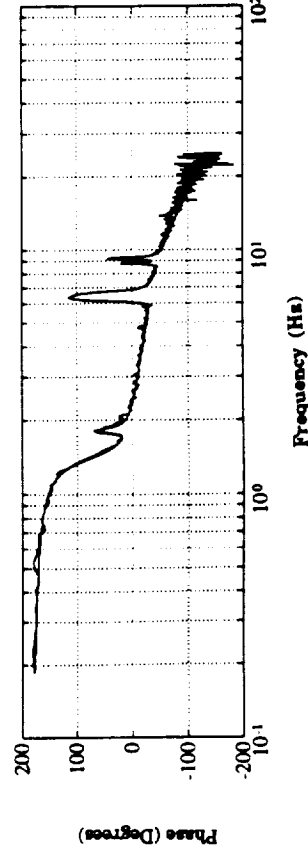
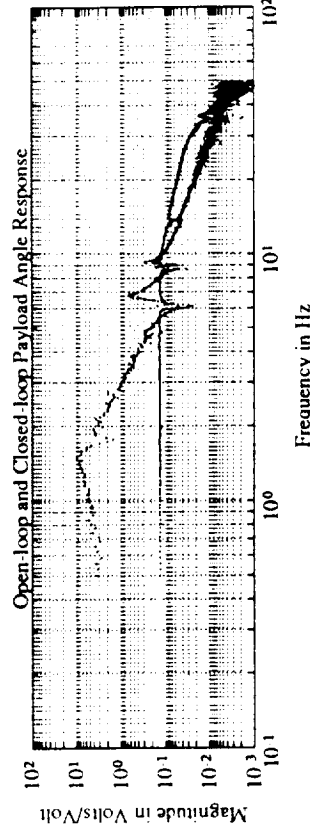
Description:

- Penalize payload inertial angle
- Feed payload inertial angle to gimbal outer stage motor
- Torque disturbance additive with gimbal control signal
- Formulate Linear Quadratic Gaussian Control (LQG)

Measurement Model



Performance



DEVELOPMENT MODEL TESTING

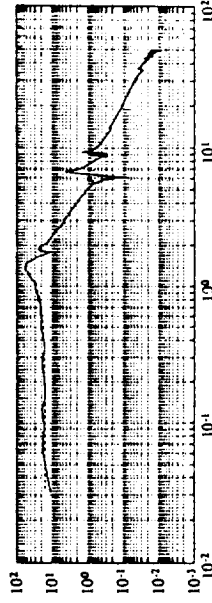
Single Input, Two Output Control (centralized topology)

Description:

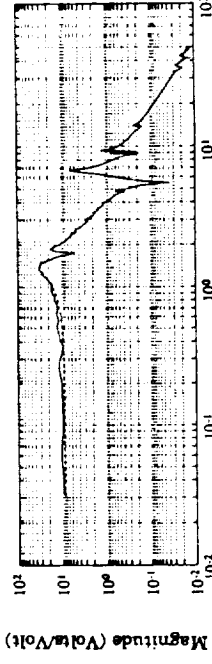
Feed relative gimbal and inertial bus angles to gimbal outer stage motor
Torque disturbance additive with gimbal control signal
Since poles common to all transfer functions, must be averaged

measurement model

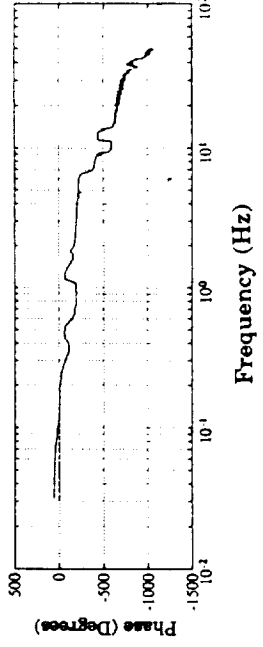
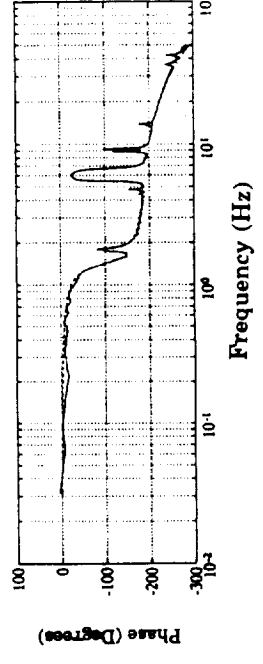
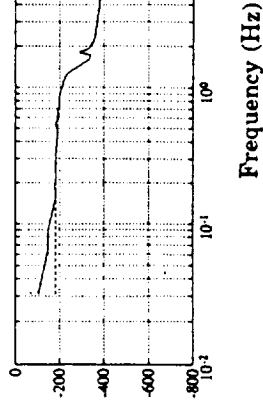
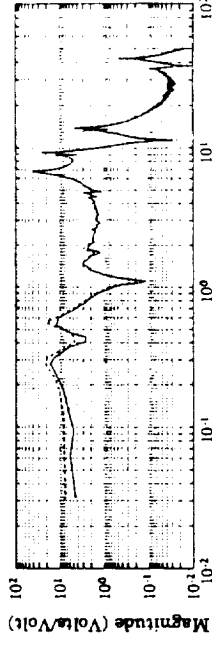
Payload Inertial Angle



Encoder Relative Angle



Bus Inertial Angle



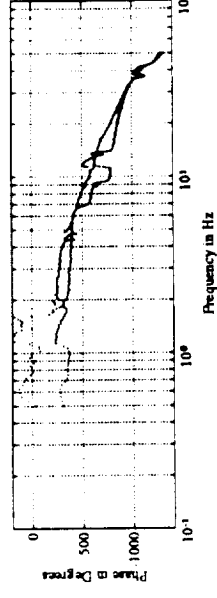
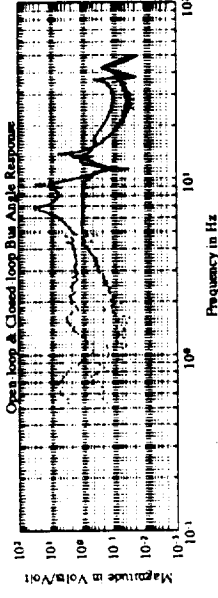
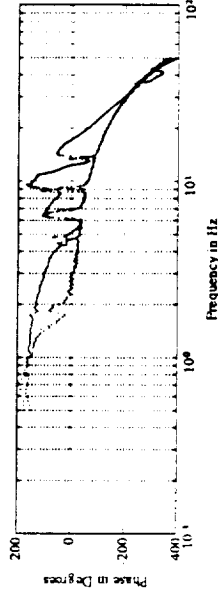
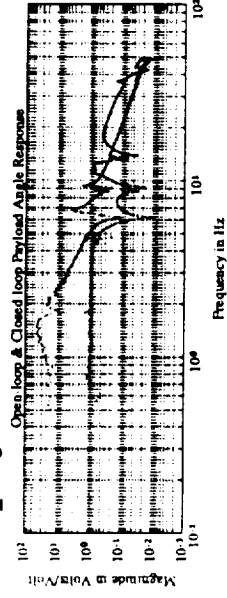
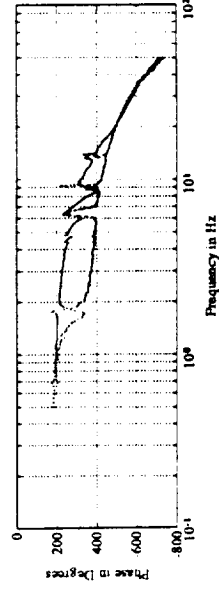
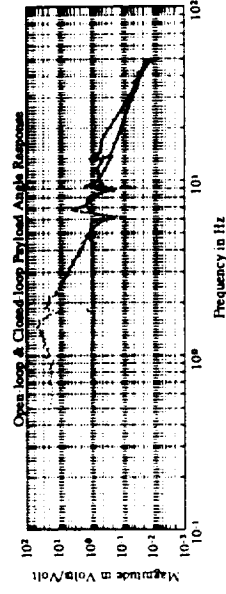
DEVELOPMENT MODEL TESTING

Single Input, Two Output Control (cont'd)

Description:

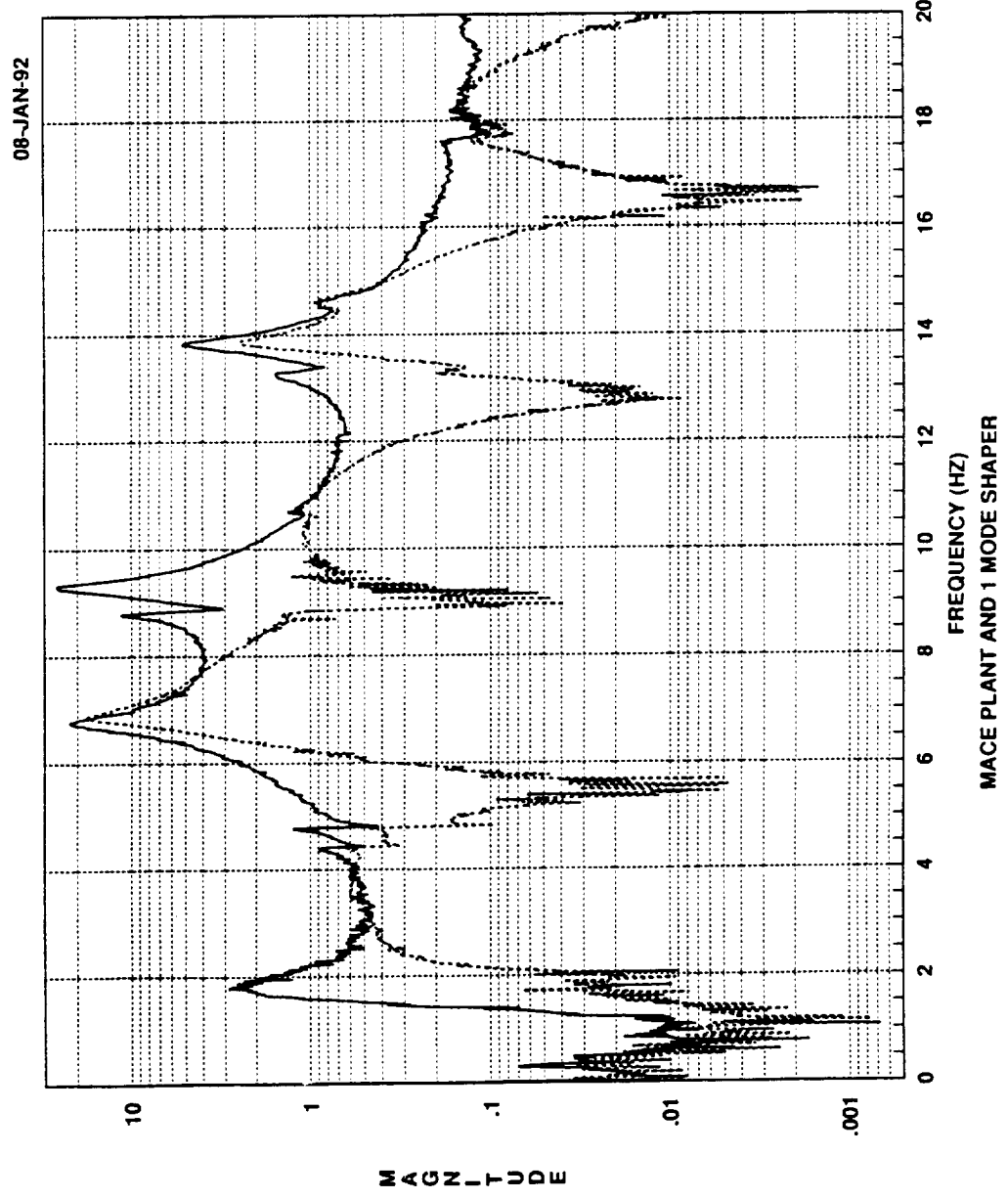
Formulate Linear Quadratic Gaussian control (LQG)

penalize payload inertial angle penalize payload and bus inertial angles



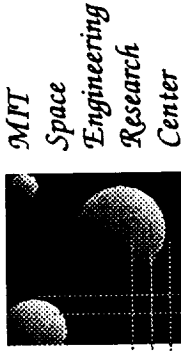
DEVELOPMENT MODEL TESTING

Slew Command Shaping



FUTURE DEVELOPMENT MODEL WORK

- Closed-loop control based on finite element model (Grocott, Glaese, Miller)
- Development of multi-input, multi-output measurement models (Karlof, Douglas, Athans)
- Classical control design using successive loop closure (Campbell, Crawley)
- Robust control using multi model and other uncertainty approaches (MacMartin, Hall)
- Constrained order and topology control (Mercadal, Vander Velde)
- Slew command shaping for minimizing excitation of flexibility (Chang, Seering)



THE MIDDECK ACTIVE CONTROL EXPERIMENT:

GRAVITY AND SUSPENSION EFFECTS

Dr. E. F. Crawley
Dr. H. Alexander
Mr. Daniel Rey

MIT
MIT
MIT

SERC Steering Committee Workshop
January 22 and 23, 1992

37-29
N93-7827897
p. 18

OUTLINE

- Motivation and Objectives
- Approach
- Overview of Gravity and Suspension Effects
- Modelling of Gravity and Suspension Effects
 - Effects on Structure
 - Effects on Sensors and Actuators
- Application to MACE
 - EM Configuration Study and DM Modelling
 - Objectives
 - Approach
 - Results
- Conclusions
- Future Work

GRAVITY AND SUSPENSION INFLUENCES

Motivation:

The need to perform closed-loop tests for performance verification of controlled structures and the reality of largely being limited to ground-based tests motivate the study of the impact of gravity and suspension effects on the closed-loop system behavior.

Objectives:

To identify and understand the effects of gravity and of a suspension system on the dynamics of a controlled structure.

To develop and codify modelling techniques for the prediction of potential changes in the plant dynamics due to the presence or absence of gravity.

To develop rule-of-thumb predictions for the magnitude of the various gravity effects based on beam equivalent approximations of the suspended structure.

APPROACH

Motivate research with a simple example of gravity field perturbation to closed-loop performance.

Identify and categorize gravity and suspension system effects.

Develop an understanding of how to incorporate gravity effects into the system variational principle and its finite order approximation.

Verify modelling techniques by applying them to sample problems.

Perform parametric variation studies and experimental validation.

Develop rules-of-thumb for when gravity and suspension system effects become important for suspended structures.

OVERVIEW: Gravity and Suspension Effects on Structure

The following are direct effects on the structure and its model
(i.e. the A matrix of the controlled structure model.)

GRAVITY FIELD EFFECTS	SUSPENSION SYTEM EFFECTS
<p>1) FINITE DEFLECTIONS</p> <ul style="list-style-type: none"> distributed gravity loads will cause initial deformations of the suspended structure. <p>2) GRAVITY STIFFENING/DESTIFFENING</p> <ul style="list-style-type: none"> distributed gravity loads stress the deformed structure which leads to eigenfrequency shifts and eigenmode coupling. 	<p>3) STATIC B. C. PERTURBATIONS</p> <ul style="list-style-type: none"> static translational stiffnesses in the horizontal and vertical directions are prescribed by the suspension system at each attachment point. <p>4) DYNAMIC B.C. PERTURBATIONS</p> <ul style="list-style-type: none"> modal coupling with the suspension dynamic modes results in dynamic impedances at the attachment points.
<p>5) DYNAMIC LOADING DUE TO GRAVITY FIELD AND SUSPENSION CONSTRAINTS</p> <ul style="list-style-type: none"> dynamic torques which result from center of mass axis offsets with respect to the suspension support plane(s). 	

OVERVIEW: Gravity Effects on Sensors and Actuators

Sensors and actuators are also sensitive to gravity field effects.

Perturbations to their performance result in changes to the control, output and feed-forward matrices (i.e. B, C and D matrices) of the model. Two types of effects can be identified:

1) Direct Effects:

The harmonic rotation of a translating ~~mass~~ device in a gravity field results in an additive perturbation to its ideal performance. To date, the only devices identified as being susceptible to this effect ~~are~~ the accelerometer and the proof-mass actuator.

Gravity loading can also result in non-ideal sensor and actuator performance; e.g. gravity induced friction in device.

2) Indirect Effects:

Perturbations to the structure (i.e. the A matrix) can result in perturbations to the sensor and actuator performance depending on their location and the extent of the perturbation to the structure.

MODELLING OF GRAVITY AND SUSPENSION EFFECTS ON STRUCTURE

Gravity

The effect of a constant stress on a structure in equilibrium is to alter its stiffness.

In a FEM this change to the stiffness matrix can be called the differential stiffness matrix or the geometric stiffness matrix.

The geometric stiffness matrix is a function of the applied loading and to comprehensively incorporate the effect of gravity loading on the homogeneous system one should include its effects in the initial deformation calculations.

Suspension System

The effects of the suspension system on the structural dynamics are captured by including the suspension system in the system model before incorporating the effects of gravity.

Geometric stiffness theory and initial static deformation calculation

The geometric stiffness matrix is obtained from the non-linear strain terms in the potential energy expression for an elastic structure in equilibrium:

$$U_p = \int_V \left\{ \frac{1}{2} (\epsilon_l^T E \epsilon_l + 2 \epsilon_l^T E \epsilon_q + \epsilon_q^T E \epsilon_q) - (\epsilon_l^T E \epsilon_{l0} - \epsilon_l^T E \epsilon_{q0} - \epsilon_q^T E \epsilon_{l0} - \epsilon_q^T E \epsilon_{q0}) \right\} dV \\ + \int_V \{ \epsilon_l^T \sigma_0 + \epsilon_q^T \sigma_0 \} dV - \int_V u^T F dV - \int_S u^T \phi dS$$

For finite deflections the initial static deformation calculation is a non-linear problem as both the deflection and the stiffness are functions of the loads. Iterations are therefore required to solve for the final equilibrium state:

$$q_{i+1} = [K(q_i) + Kg(q_i, Q(q_i))]^{-1} Q(q_i)$$

MODELLING GRAVITY'S EFFECT ON ACCELEROMETERS AND PMAs

Harmonic rotation of an accelerometer or proof-mass actuator about an axis other than the vertical axis or the device's sensitivity/actuation axis results in an additive perturbation to the device's output/input.

The harmonic rotation can be as a result of harmonic bending or torsional vibration of the supporting structure.

The output/input is either attenuated or amplified depending on the relative phasing of the coupled translation and rotation of the supporting structure, (with a possible phase reversal in the attenuation case).

In the case of torsion the output/input perturbation is about zero such that gravity makes torsional modes observable and gravity causes the PMA force actuator to induce torques.

The effects of gravity on the B and C matrices have been identified and non-dimensional sensitivity measures show that these effects are especially important at low frequencies but are only significant with near-horizontal oriented devices and at those points where the rotations are large with respect to the displacements.

MODELLING GRAVITY'S EFFECT ON ACCELEROMETERS AND PMAs

The output of an accelerometer mounted to a beam in uncoupled bending and torsion vibration is given by:

$$a_i = \sum_{r=1}^{N_t} \left\{ \left(g \sin \left(\Phi_r^t(x_i) \right) \kappa_i^t \right) \eta_r^t(t) \right\} + \sum_{r=1}^{N_b} \left\{ \left(g \sin \left(\Phi_r^b(x_i) \right) \kappa_i^b - \omega_j^2 \Phi_r^b(x_i) \right) \eta_r^b(t) \right\}$$

In modal modelling terms this yields the following C matrix type terms:

$$X = \left[\begin{array}{c|c|c} \eta^t & \dot{\eta}^t & \eta^b \\ \hline & \eta^b & \dot{\eta}^b \end{array} \right]^T \quad C_{ij}^T = g \kappa_i^t \Phi_j^t(x_i) \quad C = \left[\begin{array}{c|c|c} C^T & 0 & C^B \end{array} \right]$$

$$C_{ij}^B = g \Phi_j^b(x_i) \kappa_i^b - \omega_j^2 \Phi_j^b(x_i)$$

The non-dimensional gravity effect ratio is thus:

$$\Gamma = \frac{g \hat{\Phi}_j^b \left(\frac{x_i}{l} \right) \kappa_i^b}{\omega_j^2 \hat{\Phi}_j^b \left(\frac{x_i}{l} \right)}$$

Similar expressions hold for the effective input of a PMA mounted to a beam in bending and torsion vibration.

APPLICATION TO MACE

MACE EM Configuration Study

Objectives:

Select a MACE Engineering Model baseline configuration based on open-loop and closed-loop susceptibility to gravity and suspension effects.

MACE DM Modelling

Objectives:

Develop a high fidelity model of the MACE DM for use in control system design.
Experimentally verify the gravity and suspension modelling techniques.

MACE EM CONFIGURATION STUDY

Approach:

Develop set of 0g and 1g models of various fundamental MACE EM geometries.

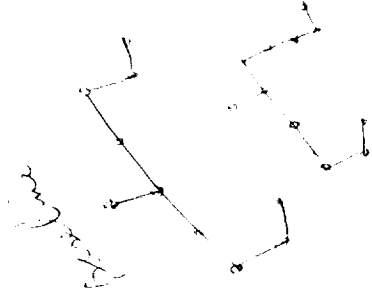
Study open-loop impact of gravity and suspension system using eigensystem and transfer function references.

Study closed-loop impact of gravity and suspension system by applying LQG to system with PD stabilized bus attitude and gimbal pointing loops.

Configurations studied:

Baseline - circular section struts, 1.7 Hz fundamental, payloads at 45° from vertical, planar system (i.e. suspension plane).

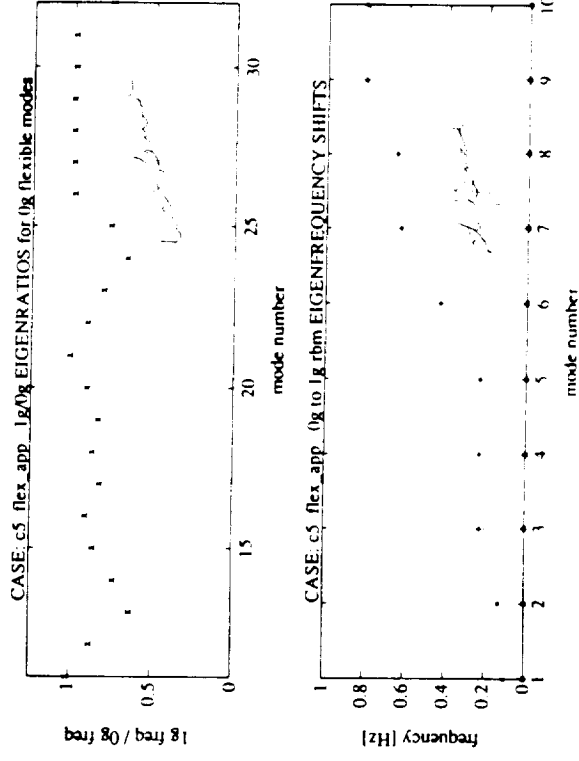
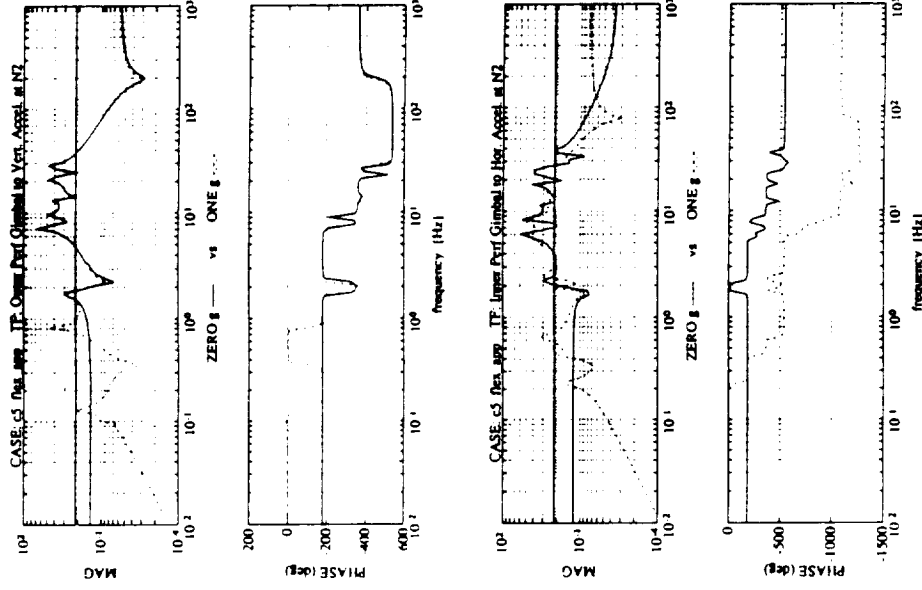
- | | |
|--------------------|--|
| $f = 1 \text{ Hz}$ | - stiffness change to obtain 1 Hz fundamental. |
| $EI_z/EI_y = 3$ | - rectangular section struts, stiffened about z. |
| $EI_z/EI_y = 1/3$ | - rectangular section struts, destiffened about y. |
| Out-of-plane | - performance payload is swung 45° out-of-plane. |
| Flex. App. | - flap-type flexible appendages added to node 1. |
| L-shaped | - downward 90° bend is put in bus at node 2. |



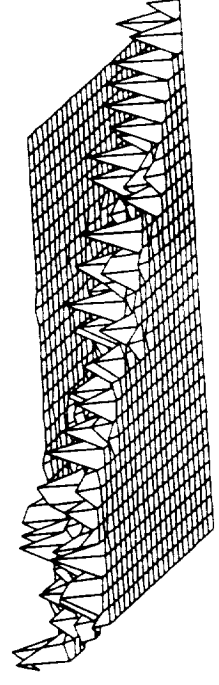
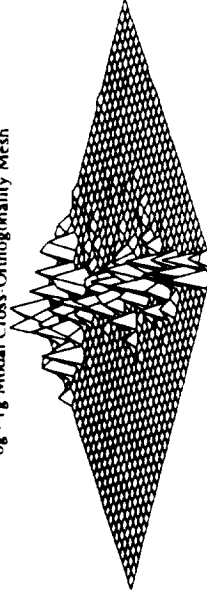
MACE EM CONFIGURATION STUDY

Sample Open-Loop Results:

c5 - ONE g: MACE test article
with Flexible Appage Pair
Mode 17, Frequency 5.9100 Hz.



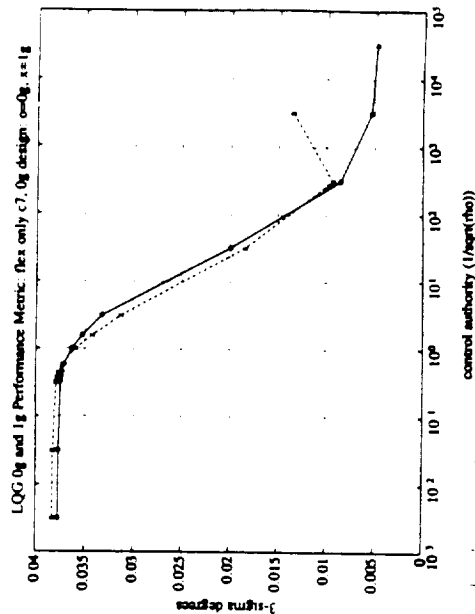
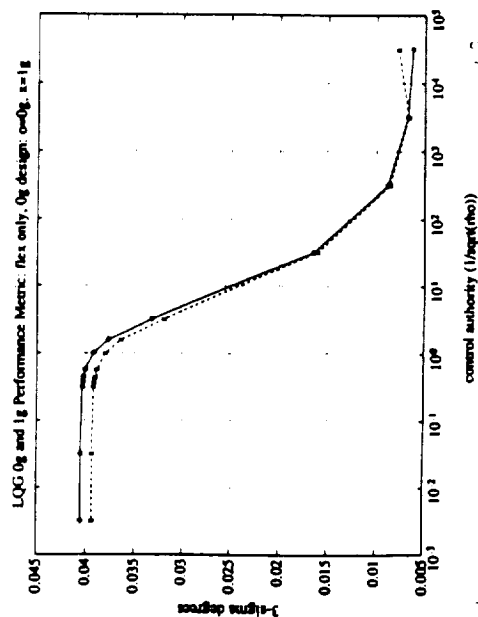
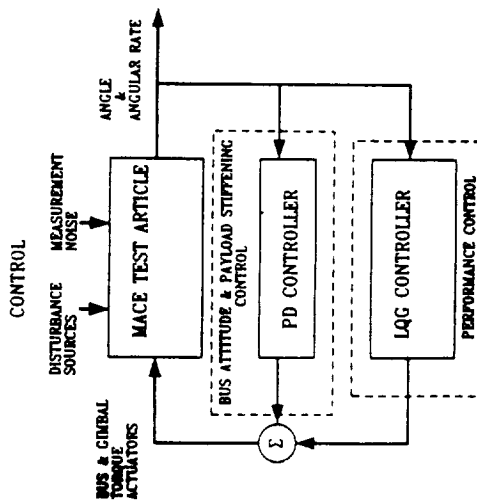
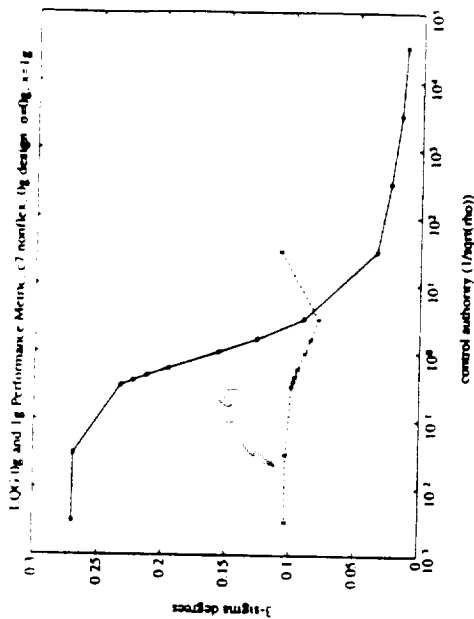
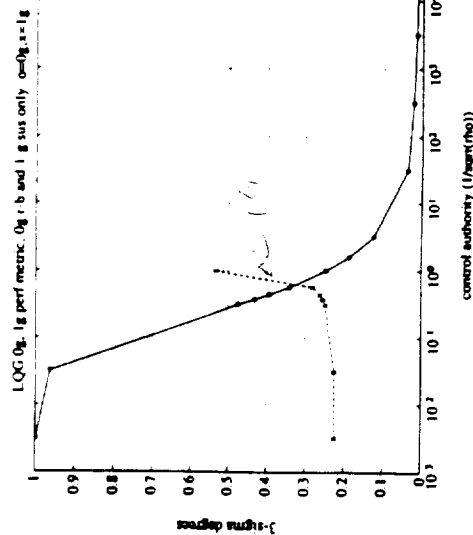
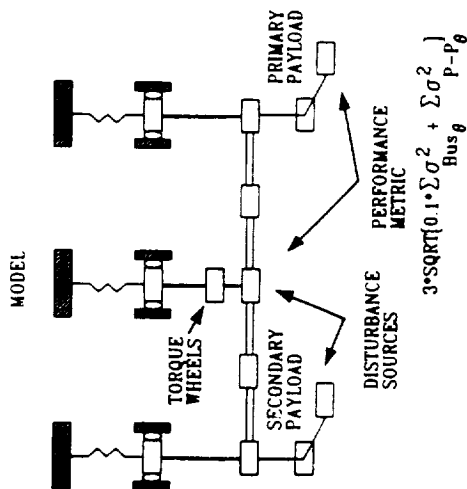
0g - 1g Modal Cross Orthogonality Mesh



MACE EM CONFIGURATION STUDY

Sample Closed-Loop Results:

Sample Closed-Loop Results:



flex only better performance

Space Engineering Research Center

MACE DM CONFIGURATION STUDY

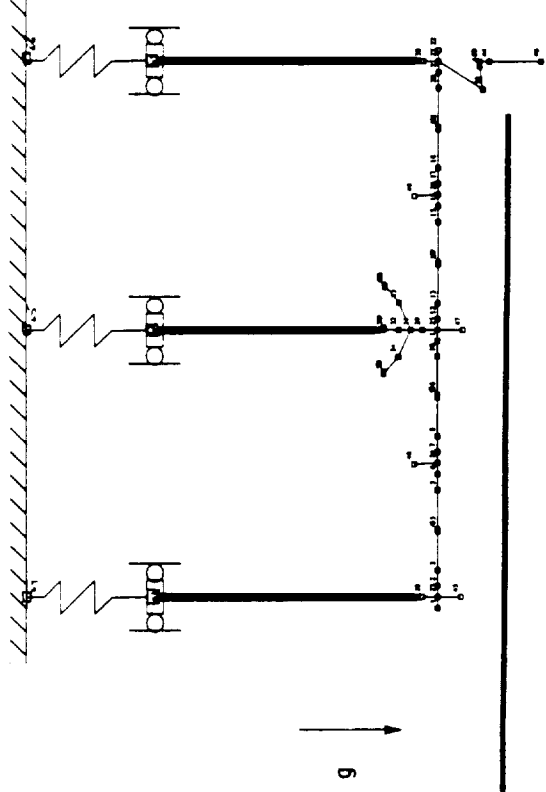
Approach:

Add a basic model of suspension system to 0g model and incorporate static pre-deformation and geometric stiffening effects.

Model pneumatic-electric suspension devices as soft tuned springs between ceiling and suspension carriages, constrain suspension carriages to vertical translation and attach structure to carriages via stiff pinned-pinned rods.

Compare low-frequency modal I.D. data with predicted transfer functions and tune if required.

MACE 1g DM Model Schematic:

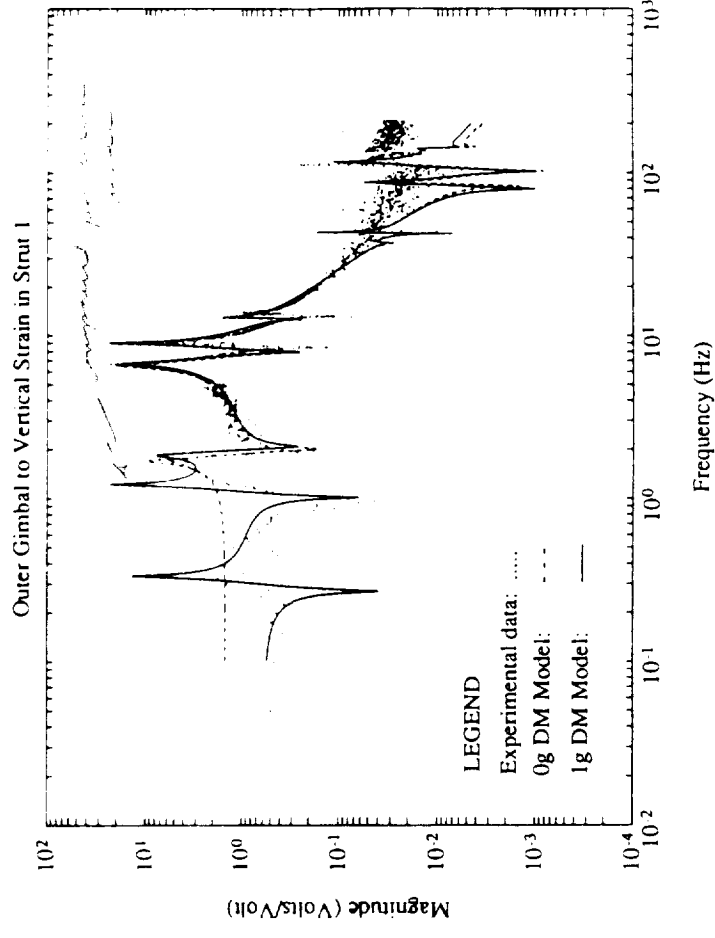
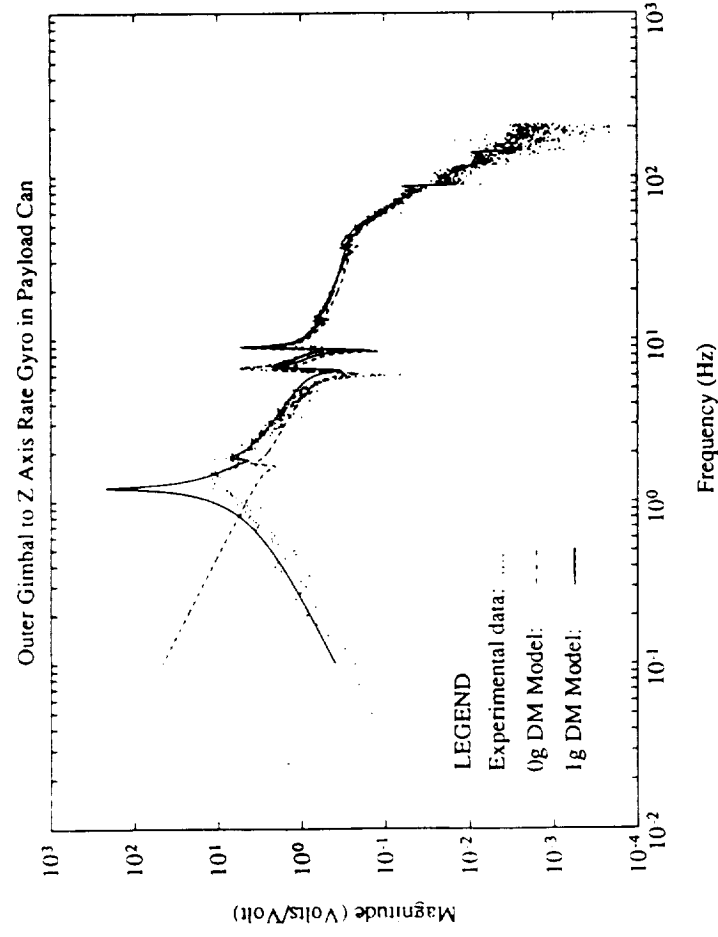


MACE DM CONFIGURATION STUDY

Status:

First iteration complete. Low frequency predictions have improved but some tuning is required including the addition of a higher order suspension model.

Sample Transfer Function Results:



CONCLUSIONS

The MACE test article is a valuable and effective test-bed for the research of gravity and suspension system effects.

The result of this research will be:

- a set of verified gravity effect and suspension system modelling techniques for application to detailed models of suspended controlled space structures, and
- a set of general gravity effect rules-of-thumb based on non-dimensional parameter descriptions of a suspended space structure.

FUTURE WORK

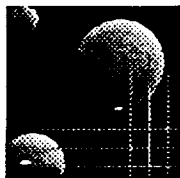
Paper - “Direct Effects of Gravity on the Control and Output Matrices of Controlled Structure Models.”

Investigate impact of not reforming the mass matrix in the case of large deflections.

Tune the 1g DM model and continue experimental validation using the MACE test article.

Derivation of gravity/suspension effect rules of thumb.

S.M. Thesis - “Gravity and Suspension Effects on Controlled Structure Models”



THE MIDDECK ACTIVE CONTROL EXPERIMENT (MACE):

IDENTIFICATION FOR ROBUST CONTROL

Dr. Valery I. Karlov

Moscow Aviation Institute (MAI)

9/0-37
16-53
N 93-27898
p. 12

Three Levels of Identification

	1	2	3
A l g o r i t h m	<ul style="list-style-type: none"> • Empirical Transfer Function Estimate • Eigen Value Analysis • 	<ul style="list-style-type: none"> • Least Square • Maximum Likelihood • Prediction Error •Methods 	<ul style="list-style-type: none"> • Extended Kalman-type filters (state and parameter estimation)
M o d e l	<ul style="list-style-type: none"> • SISO • MIMO (deterministic) 	<ul style="list-style-type: none"> • TF • ARMAX $A(q)y(t)=B(q)u(t) + e(t)$ $t = 0, \dots, K$ 	<ul style="list-style-type: none"> • State-space $\dot{x} = A(\alpha)x + B(\beta)u + \xi$ $y = C(\beta)x + D(\beta)u + \eta, \quad t \in (0, T)$
P r o d u c t	<ul style="list-style-type: none"> • Model structure (number of modes, preliminary estimates) 	<ul style="list-style-type: none"> • Fitted estimates [but of "indirect" parameters $\gamma = \phi(\alpha, \beta)$] 	<ul style="list-style-type: none"> • High-precision estimates of "direct" parameters: <ul style="list-style-type: none"> - α (frequencies, damping ratios) - β (mode shapes, masses) • Realistic bounds

Basic Elements of The Approach

1. Non-linear problem of Riccati equation control for augmented covariance matrix:

$$\begin{bmatrix} P_x & P_{x\alpha} \\ P_{\alpha x} & P_\alpha \end{bmatrix}$$

2. Equivalent linear problem
(Received on the basis of non-traditional usage of RE analytical properties)
3. Converge numerical algorithm of optimization
4. Extended Kalman filter
5. Robust control problem
(Solution on the basis of decomposition with respect to frequencies)
 - Cost averaging techniques (use the "Post-ID" bounds directly)
 - Petersen -Hollot's bounds (need modification)

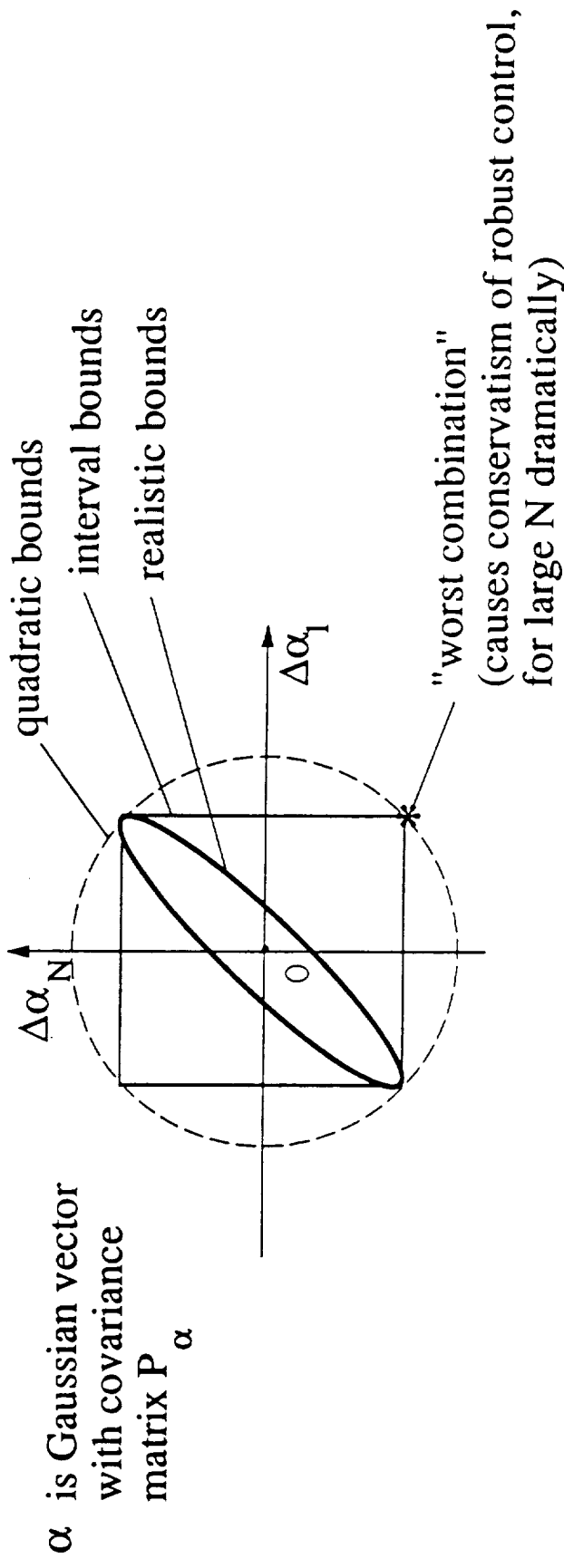
$$\begin{aligned} \text{a). } & SA_0^T + A_0^T S + (K + \beta \gamma N W N^T) - S(BR^{-1}B^T - \beta \gamma^{-1}LVL^T)S = 0 \\ & \beta < 1, \quad VW = P_\alpha \end{aligned}$$

- b). Duality principle for design of dynamical feedback

Why the Approach Provides

- **Realistic statistical model of uncertainty**
(accuracy characteristics are received in the state-space model with "separated" noises in sensors and actuators)
- **Active ID:** Optimization of open- and close-loop inputs directly with respect to robust control performance
- **Taking into account constraints on excitation**
(desirable ID accuracy can be achieved with much less excitation, extremely important for experiments in the space)
- **Possibility to identify time-varying parameters**
(in case of moving rigid payloads)

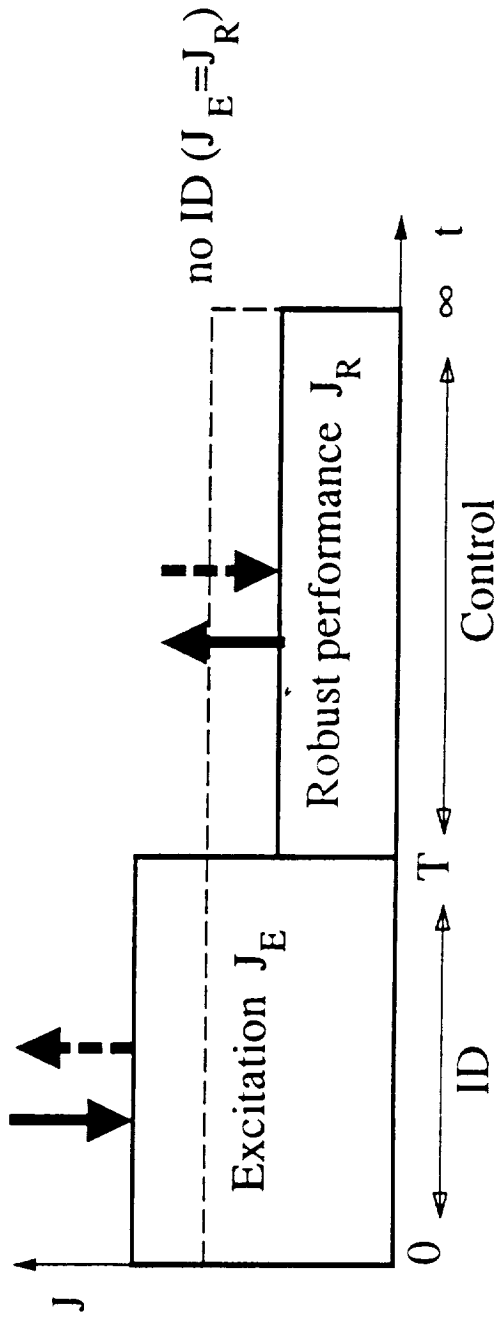
Advantages of "Post-ID" Model of Uncertainty



- Reveals "cost" of different errors
- Reveals covariances between parameters
- Prevents non-realistic "worst combination" of parameters
(degrades conservatism of robust control)

Advantages of Optimization

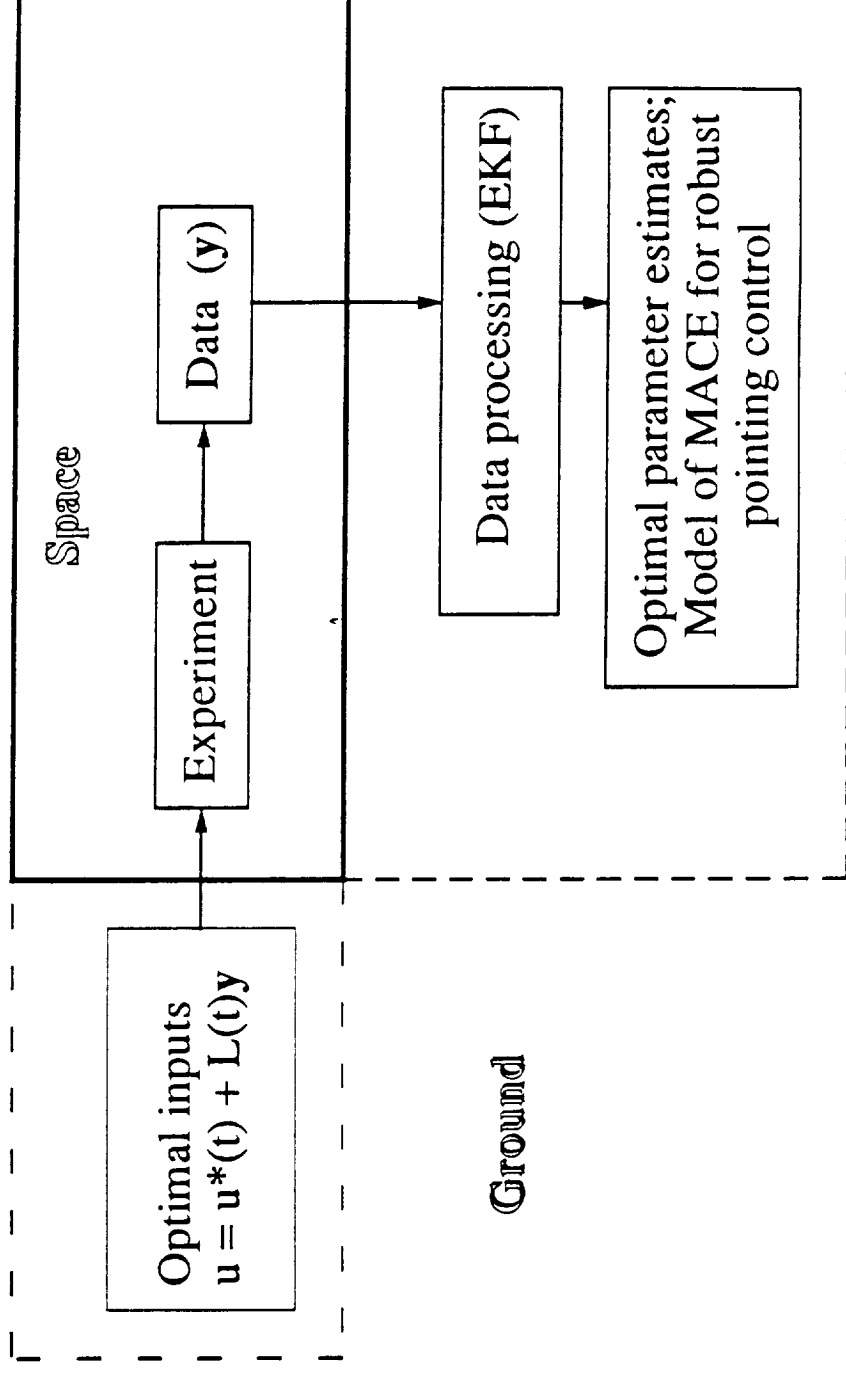
- Further degrading the conservatism
- Better coping with "difficulties" in the model, e.g. close modes (*excitation in optimal directions amplifies the difference between modes*)
- The best compromise between excitation and robust control performance

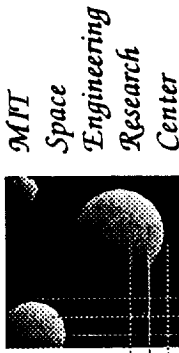


$J = J_R + pJ_E$ where p is a "price" of ID
All J are quadratic forms

Practical Realization

- Simulation of identification and robust control processes for MACE
(important for confirming convergence of parameter estimates to "true" ones)
- Ground experiment
- Experiment in space





SUMMARY OF ADDITIONAL RESEARCH IN MULTIVARIABLE IDENTIFICATION AND CONTROL

Michael Athans
Frank Agguiero
Edward Bielecki
Josef Bokor
Joel Douglas
Kirk Gilpin
Leonard Lublin

January 23, 1992

ROBUST MULTIVARIABLE CONTROL WITH PARAMETRIC UNCERTAINTY

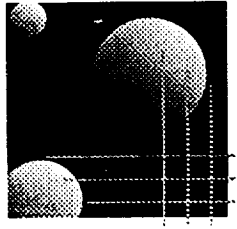
- Novel Robust LQR control strategy derived by J. Douglas (SM thesis, two ACC papers) under assumption of full state feedback.
- Uncertain energy interpretation continuing by J. Douglas and E. Bielecki.
- Extension to Robust H_2/H_∞ version, with output feedback and dynamic compensation, topic of J. Douglas Ph.D. thesis with applications to MACE.

MULTIVARIABLE IDENTIFICATION

- Systematic procedure for MIMO identification, together with required software, developed (K. Gilpin SM thesis; Gilpin, Athans, Bokor 1992 ACC paper). Blends:
 - Model reduction using Hankel matrix tools.
 - Initial SISO models using ordinary least squares and sinusoidal inputs.
 - Selective model refinement using nonlinear least squares.
 - Integration into MIMO model via residue matrix methods.
 - MIMO zero refinement using maximum likelihood identification based on white noise signals. Constrain MIMO poles, refine MIMO zeros.
 - Generation of singular values vs frequency.
- Methodology tested on interferometer testbed using accelerometer measurements. Extended to laser measurements (R. Jacques, F. Agguiero, and others). Will be used by Douglas for MACE.

MIMO DESIGN UNDER PARAMETRIC AND OTHER DYNAMIC UNCERTAINTY

- Goal is how to deal with complex dynamic plant errors in MIMO feedback control designs (e.g. interferometer) and to study impact of scaling and frequency weights.
- Developed H₂ (frequency-weighted LQG) MIMO controller for a 2D truss using truncated beam model. Topic of L. Lublin SM thesis (being written right now). Simulation study; no hardware tests as yet.
- Parametric and high-frequency dynamics model errors limit superior disturbance-rejection performance.
- Phase information from Singular Value Decomposition provides partial information for stability-robustness.
 - We could not obtain significant reduction in conservatism associated with unstructured stability-robustness tests using this MIMO phase information.



MIT
Space
Engineering
Research
Center

Multivariable Identification for Control

Joel Douglas

January 23, 1992

omit

MOTIVATION

- We want to study the design of robust multivariable controllers.
- Need a state-space model of system for design.
- How do we derive a minimal multivariable model?

SISO Identification

- Well known techniques for Identifying SISO models.

- Output Error/Nonlinear Least Squares

$$Y(z) = G(z, \theta_f)U(z) + e_{oe}(z)$$

- Equation Error/Linear Least Squares

$$G(z) = G(z, \theta_f) + e(z)$$

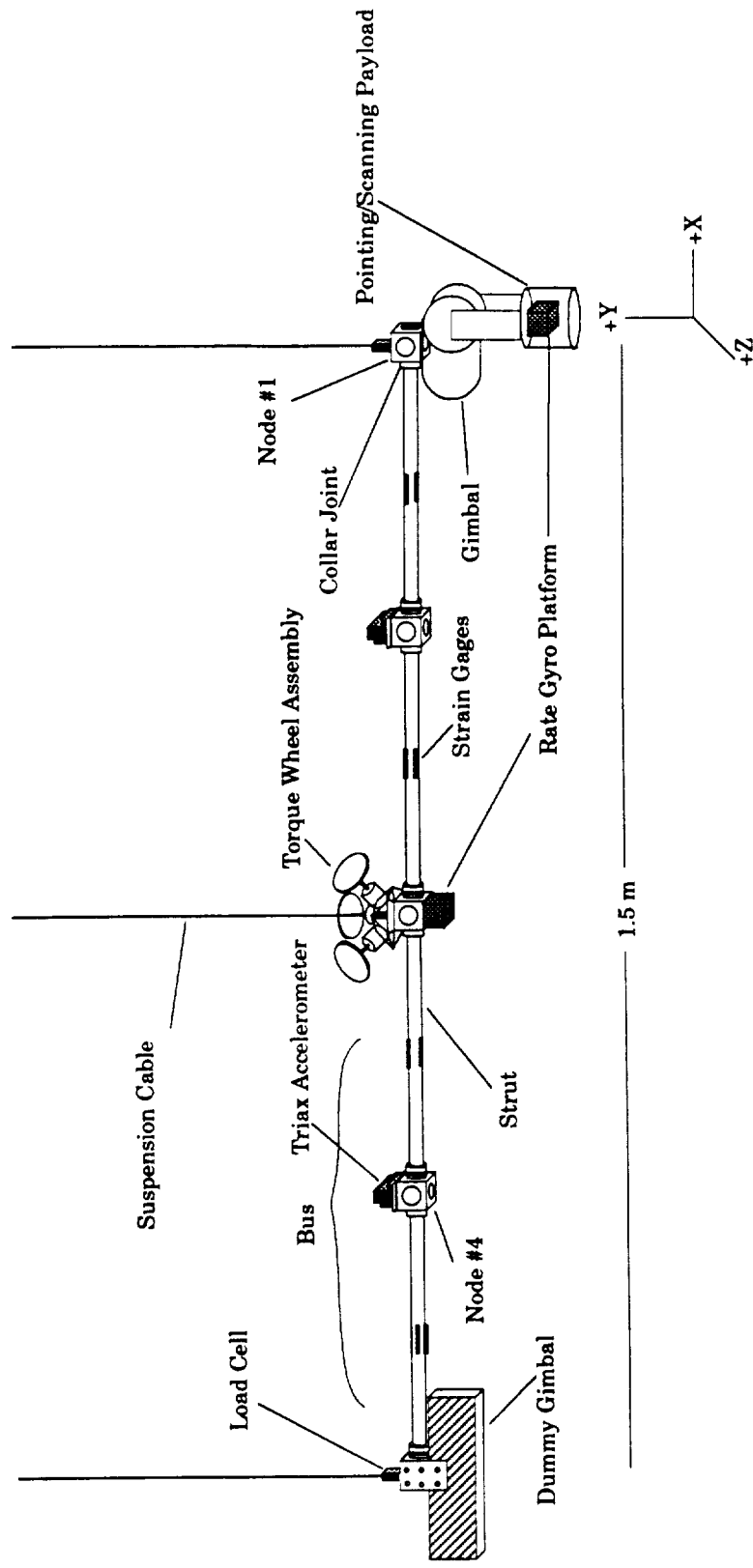
- Results in a set of poles/zeros for each SISO loop.

- Example on MACE

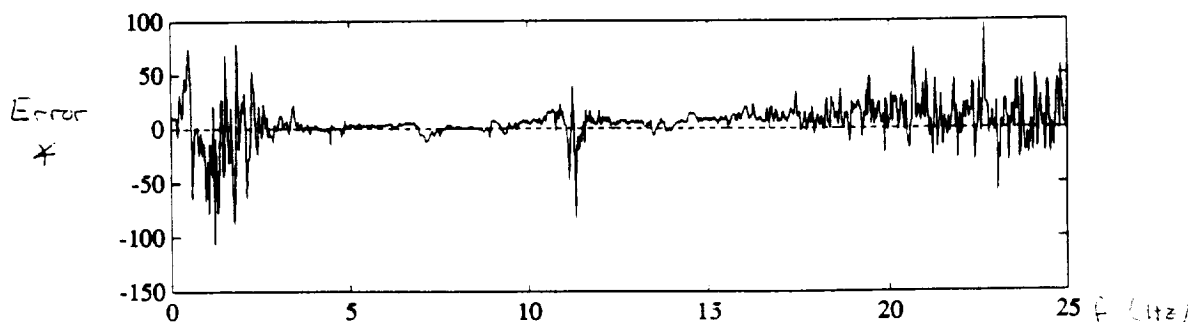
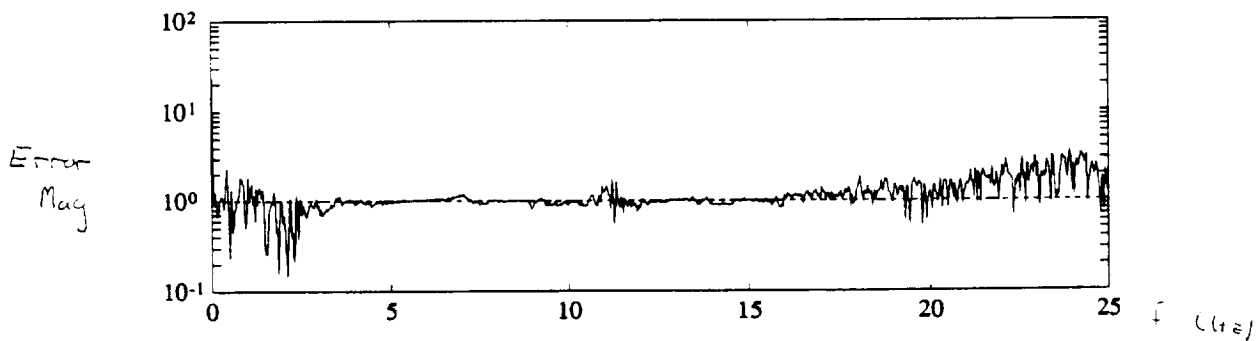
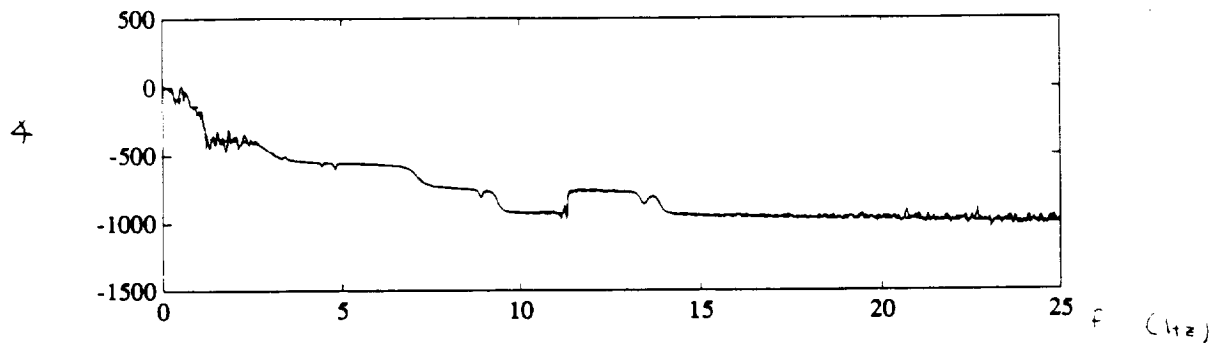
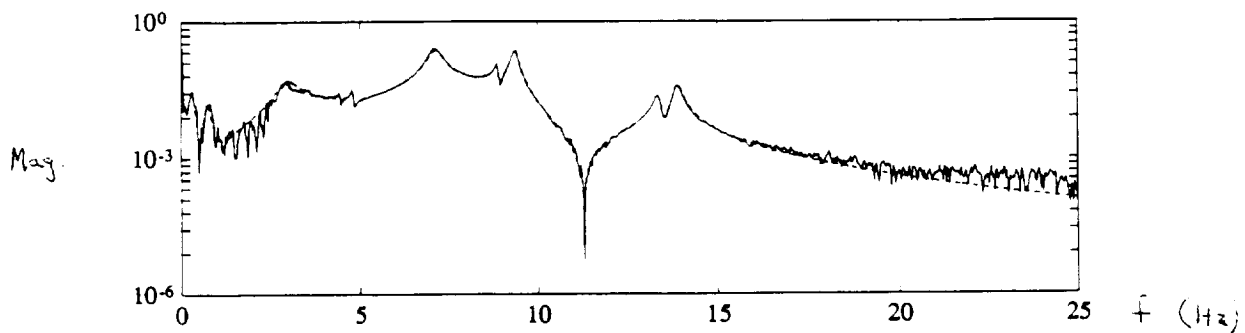
- Inputs: gimbal torque, torque wheel
- Outputs: payload angle, encoder angle, bus angle
- Nonlinear method with new cost function (Jacques):

$$J = \|\log G - \log G_m\|_2$$

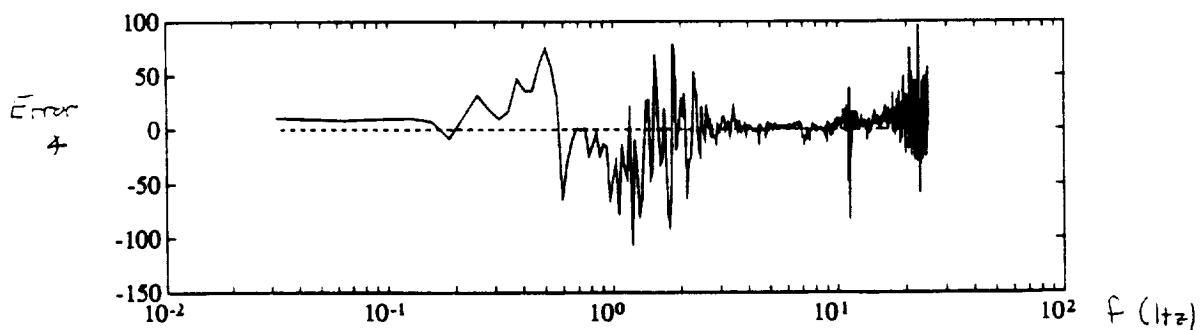
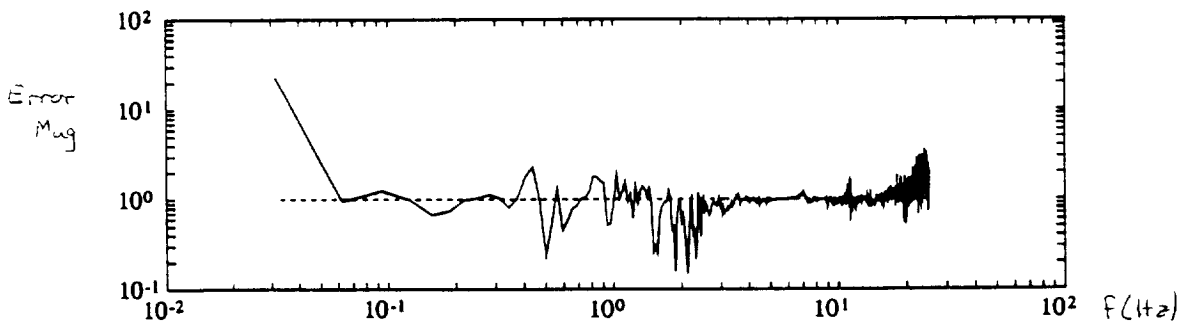
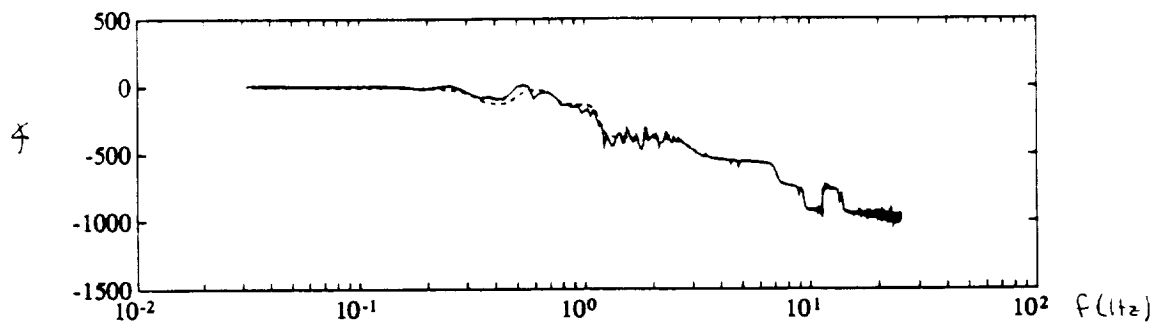
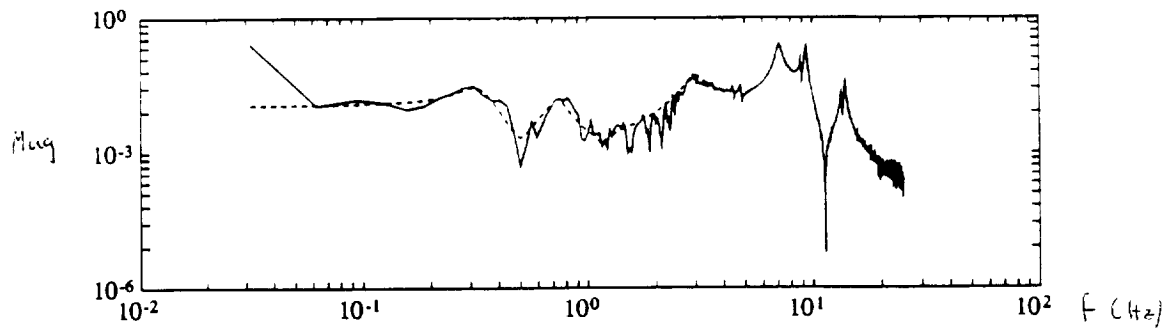
MACE SCHEMATIC



MACE EXAMPLE: TORQUE WHEEL TO ENCODER



MACE EXAMPLE: TORQUE WHEEL TO ENCODER

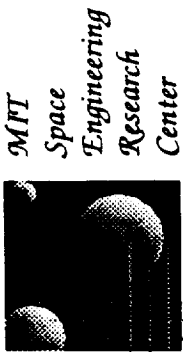


MIMO STATE SPACE MODEL

- State Space desired for ease of implementing control algorithms
- Goal is to determine minimal representation w/o truncation
- SM thesis by Gilpin

FUTURE WORK

- Identification
 - Combine SISO transfer functions using Gilpin's procedure.
 - Learn about identifying bounds on errors in frequencies, damping, mode shapes.
- Multivariable Control
 - Close a multivariable loop on MACE.
 - Extend robust full state feedback procedure of SM thesis to output feedback.
- Combine ID and robust control for overall procedure.



STRAIN ACTUATED AEROELASTIC CONTROL

Kenneth B Lazarus

January 23, 1992

Project Sponsors:

General Dynamics Corporation
NASA Langley Research Center
National Science Foundation

91137
N93-27899
100

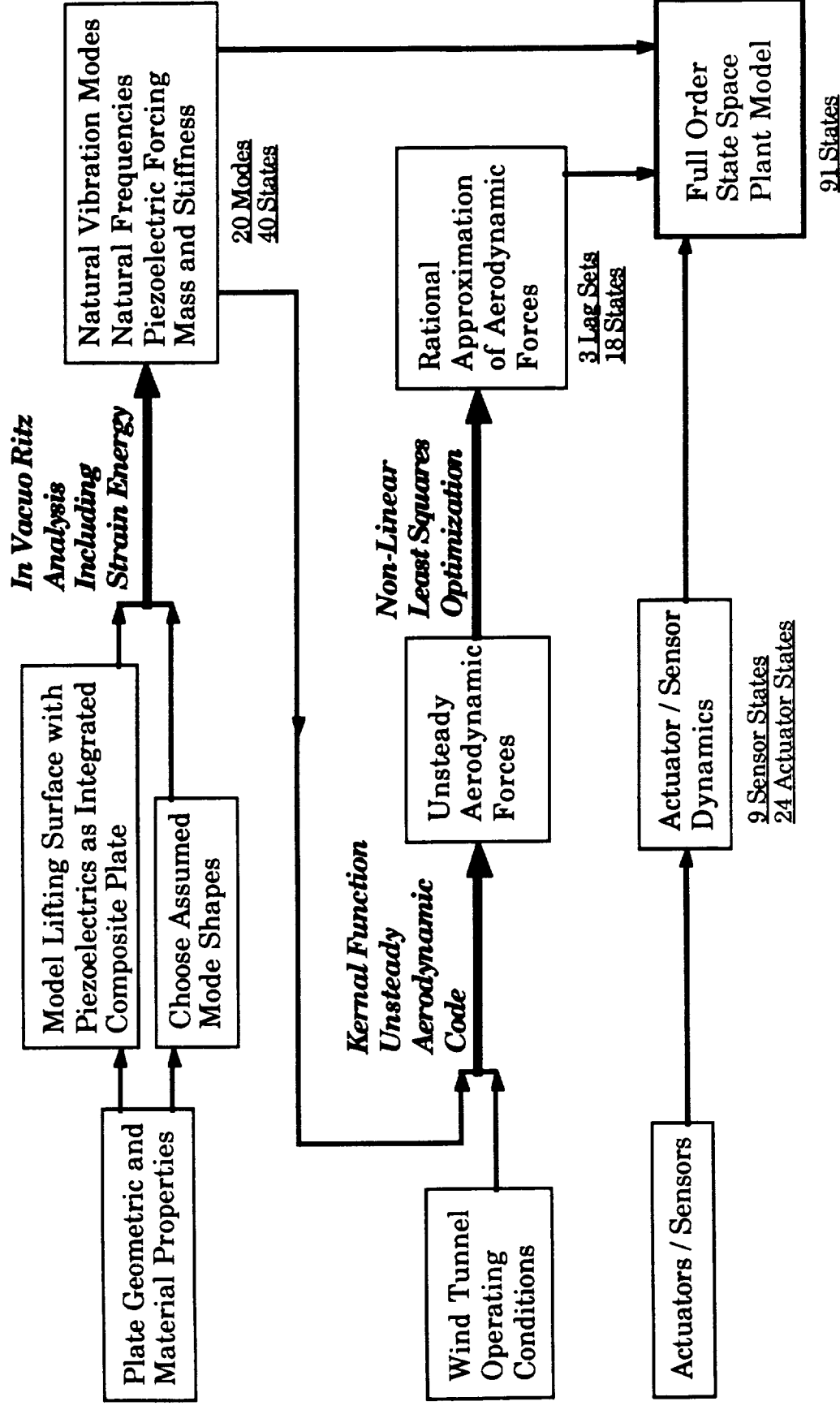
PROJECT GOAL

- **Develop and Demonstrate Strain Actuated Lifting Surface Technology for Aeroelastic Control**
 - Induced Strain Actuation, rather than conventional articulated methods, allows for:
 - Control of the Lifting Surface Shape for Altering the Aerodynamic Forces
 - Direct Control of the Strain in the Structure and Dynamic Mode Shapes

SPECIFIC OBJECTIVES

- **Develop a Capability for Analyzing Plate-Like Aeroelastic Lifting Surfaces**
- **Develop MIMO Control Laws for the Strain Actuated Adaptive Wing**
- **Demonstrate that Strain Actuation is an Effective means of Achieving Aeroelastic Control**

STRUCTURAL AND AERODYNAMIC MODELLING

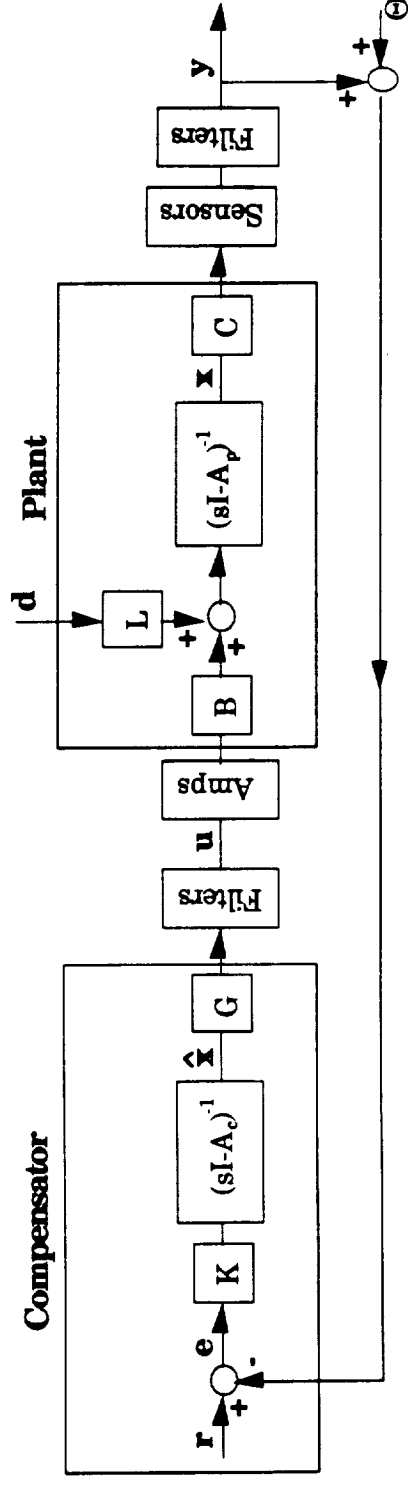


CONTROL LAW DESIGN METHODOLOGY

- **Reduce 'Full' Order Model to 'Design' Model**
 - Obtain Minimum Realization
 - Find Hankel Singular Values
 - Retain Modes with Largest Hankel SV's and DC Components of Others
- **Design Linear Quadratic Gaussian Compensator**
 - Cost Minimization
 - Loop Shaping
- **Reduce 'Design' Model to "Controller" Model**
 - Same Procedure as Above
 - Optimal Projection

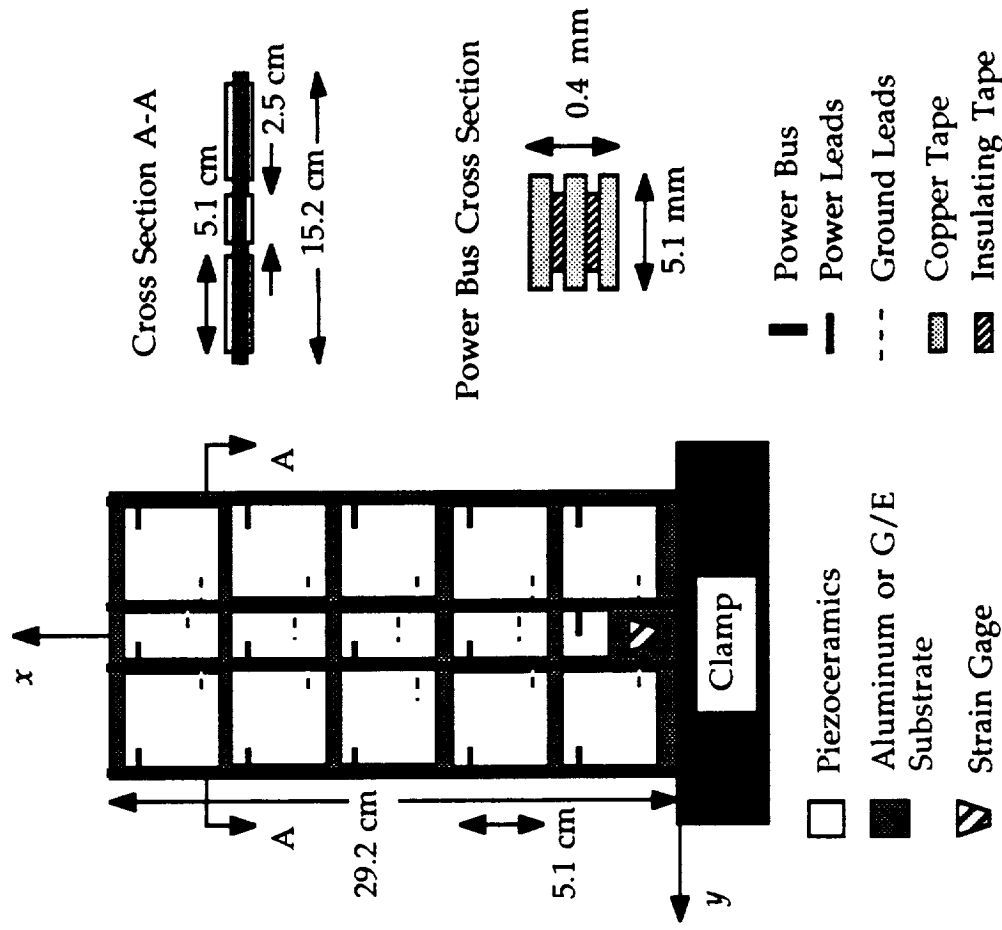
SYSTEM BLOCK DIAGRAM

- Plant Model from Raleigh-Ritz and Unsteady Aerodynamic Analysis
- Sensor, Amplifier and Filter Dynamics Included in “Full” System
- Magnetic Shaker (Bench) or Gust Generator (WT) Disturbance Source
- MIMO Compensators Designed using Reduced Order LQG or Optimal Projection Theory
- Compensators Implemented by a Real Time Digital Control Computer



ADAPTIVE WING TEST ARTICLE

- Cantilever Plate Configuration: Actuators Cover 71% of Plate



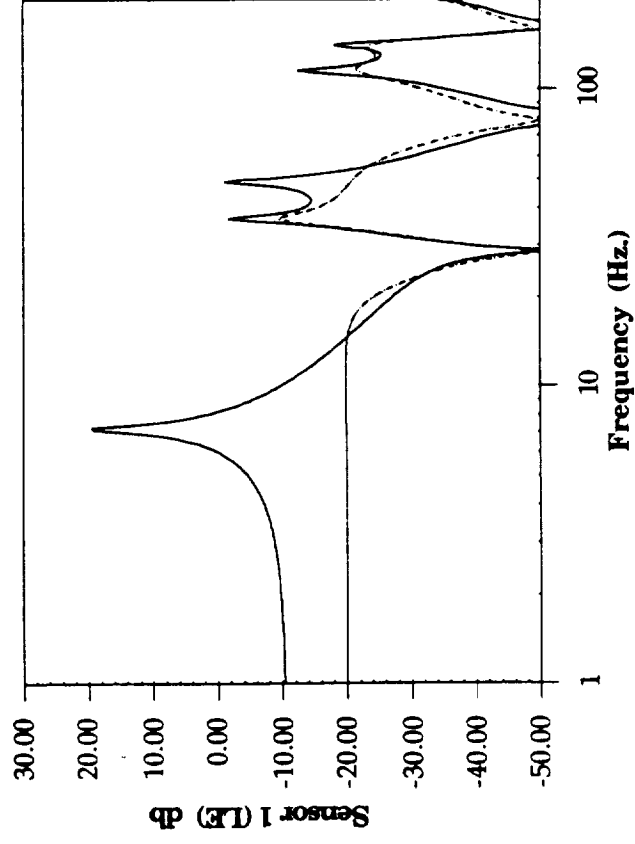
BENCH - TOP EXPERIMENTS

- **Correlate Analytic Model and Check Hardware Functionality**
- **Verify Control Law Design Procedure and Gain Necessary Controller Design Experience**
- **Demonstrate High-Authority Large-Bandwidth Disturbance Rejection Capabilities**

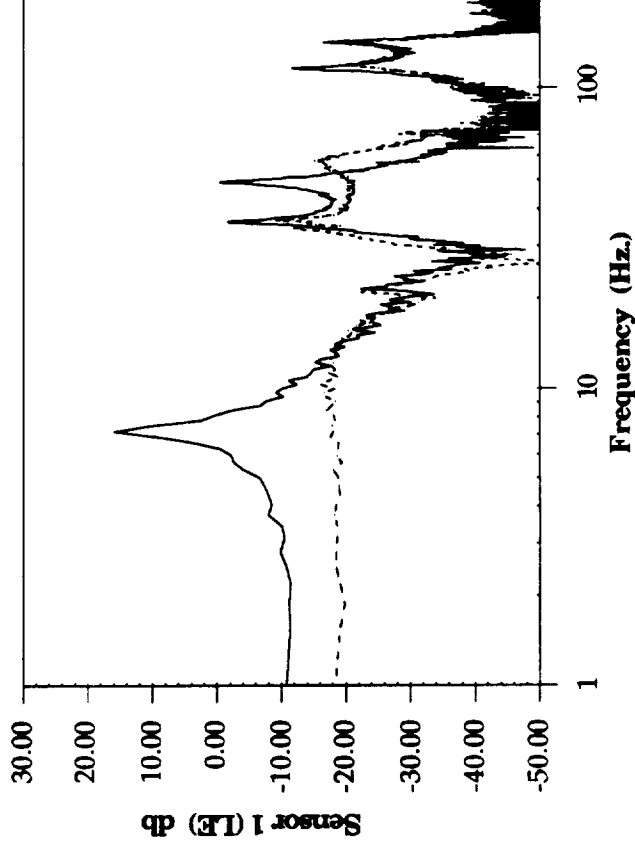
BENCH-TOP DISTURBANCE REJECTION: OPEN AND CLOSED LOOP RESPONSE

- Aluminum Bench Mark Specimen
- Reduced Order LQG Design: $\rho = 1e-2$ Sensor Noise = 3.0%

Analytic Model



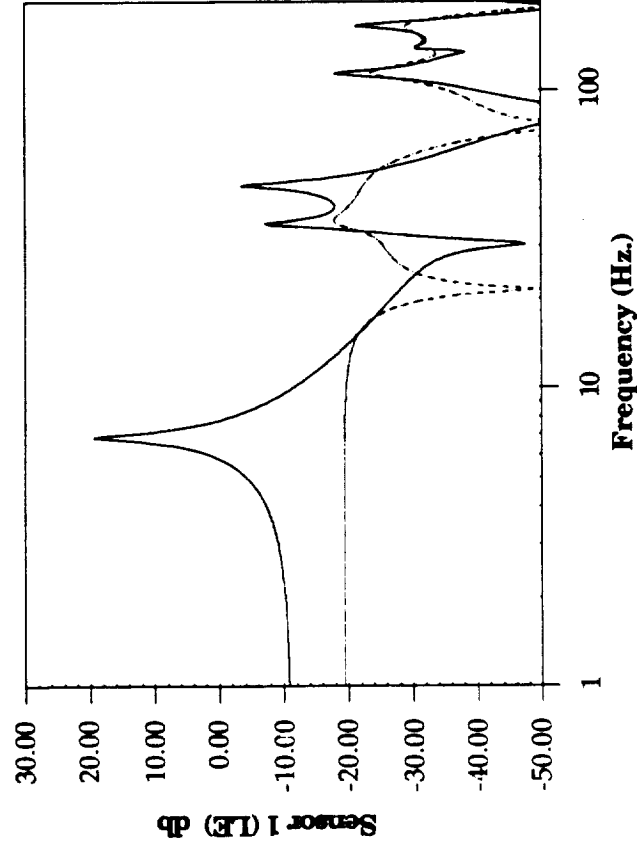
Bench-Top Experiments



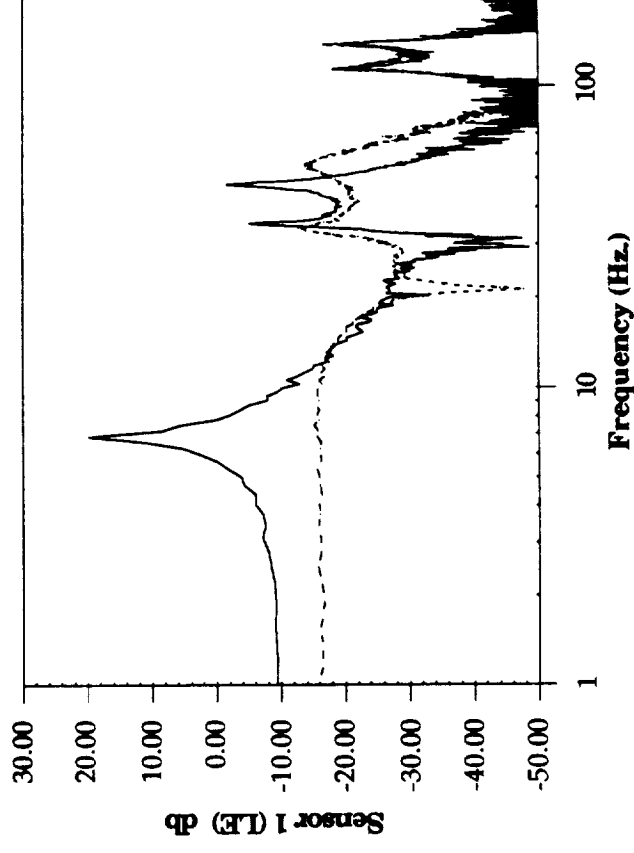
BENCH-TOP DISTURBANCE REJECTION: OPEN AND CLOSED LOOP RESPONSE

- Graphite/Epoxy Bend/Twist Coupled Specimen
- Reduced Order LQG Design: $\rho = 1e-2$ Sensor Noise = 3.0%

Analytic Model

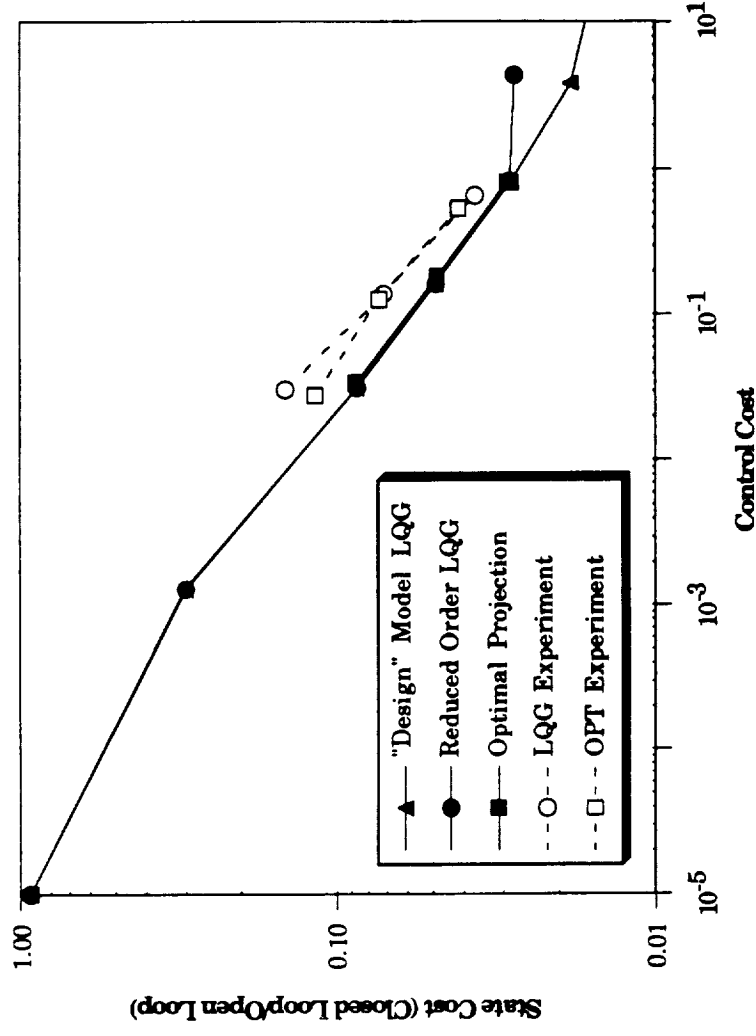


Bench-Top Experiments



BENCH-TOP DISTURBANCE REJECTION: STATE COST VERSUS CONTROL COST

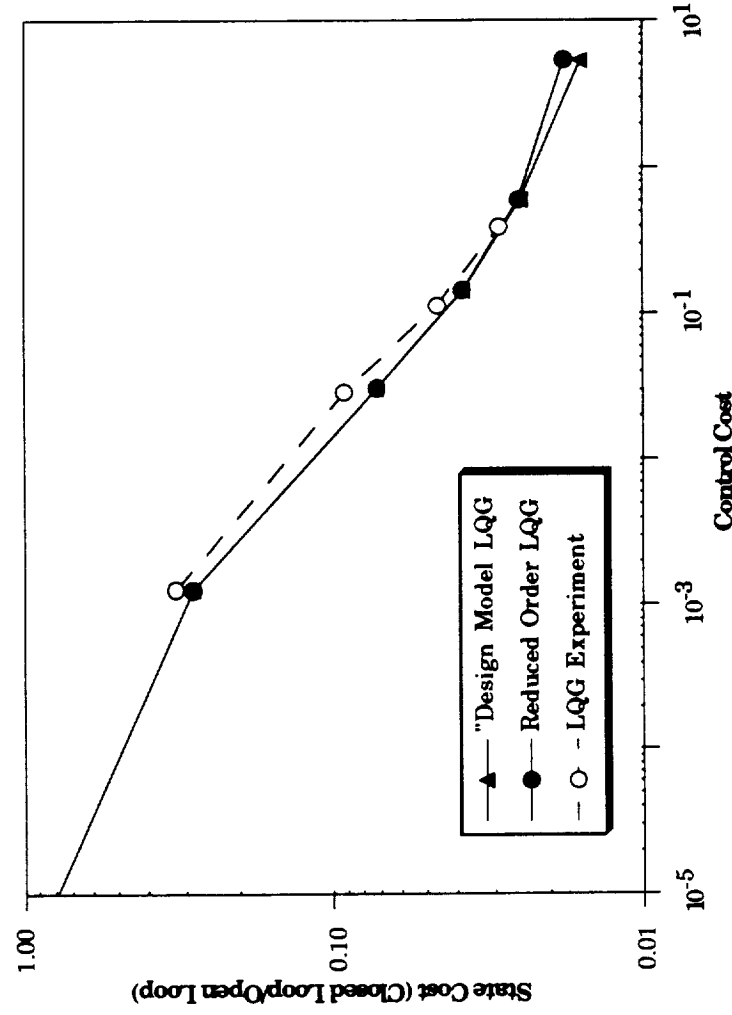
- Aluminum Bench Mark Specimen
- Reduced Order LQG & OPT Designs: Sensor Noise = 3.0%



- State Cost Reduced by 96% (14 db RMS)

BENCH-TOP DISTURBANCE REJECTION: STATE COST VERSUS CONTROL COST

- Graphite/Epoxy Bend/Twist Coupled Specimen
- Reduced Order LQG Design: Sensor Noise = 3.0%



- State Cost Reduced by 96% (14 db RMS)

WIND TUNNEL EXPERIMENTS

- **Aeroelastic Control Issues**

Performance Objectives

Flutter Suppression
Vibration Suppression
Gust Alleviation
Maneuverability

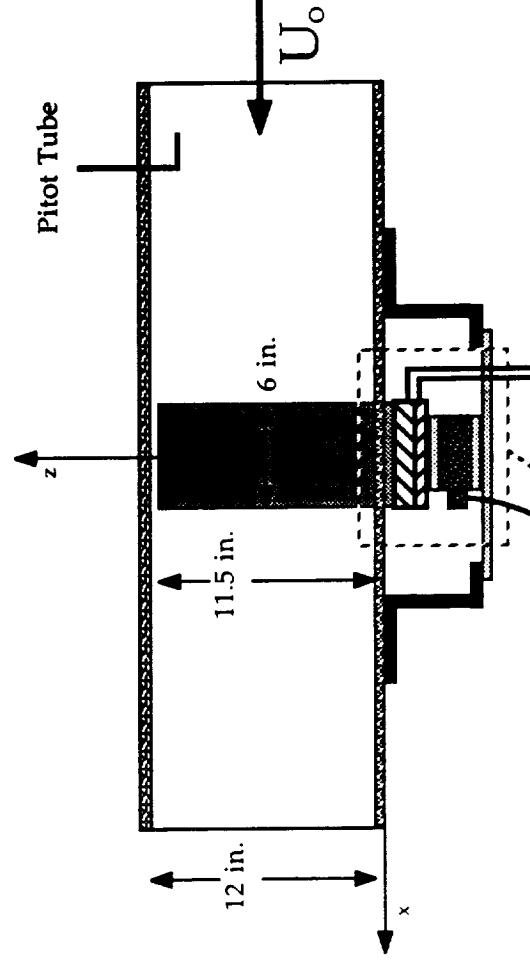
Control Law Objectives

Stability
Plant Regulation
Disturbance Rejection
Low Frequency Command Following

- **Result: A Well Regulated Plant with High Loop Gain in the Low Frequency Regime is Desired**

WIND TUNNEL SET-UP

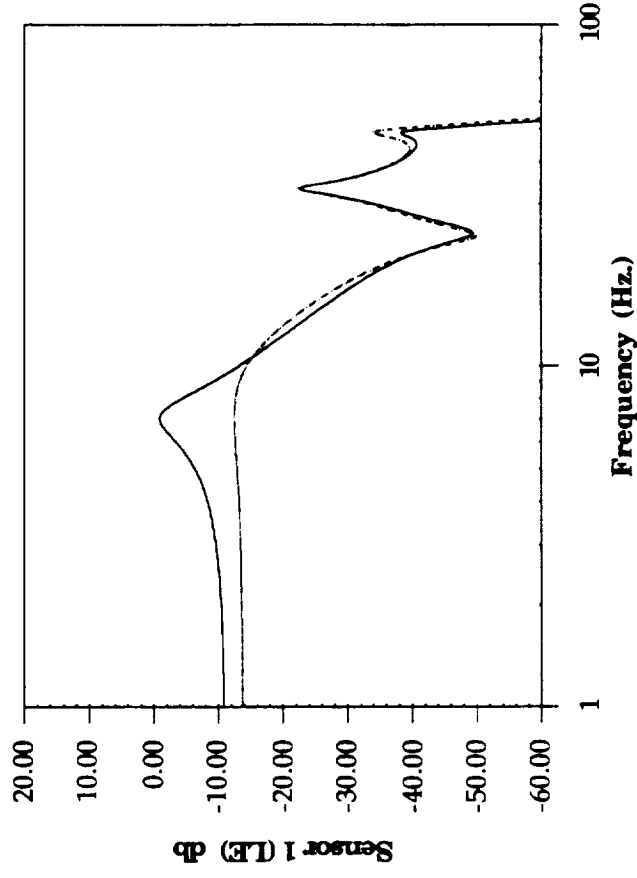
- **1 Foot Low Turbulence Tunnel**
 - Test Section: 8" x 12"
 - Maximum Speed: 100 MPH
- **Gust Generator 1 Semi-Chord Ahead of Leading Edge**
- **Laser Displacement Sensors Built Into Side of Test Section**



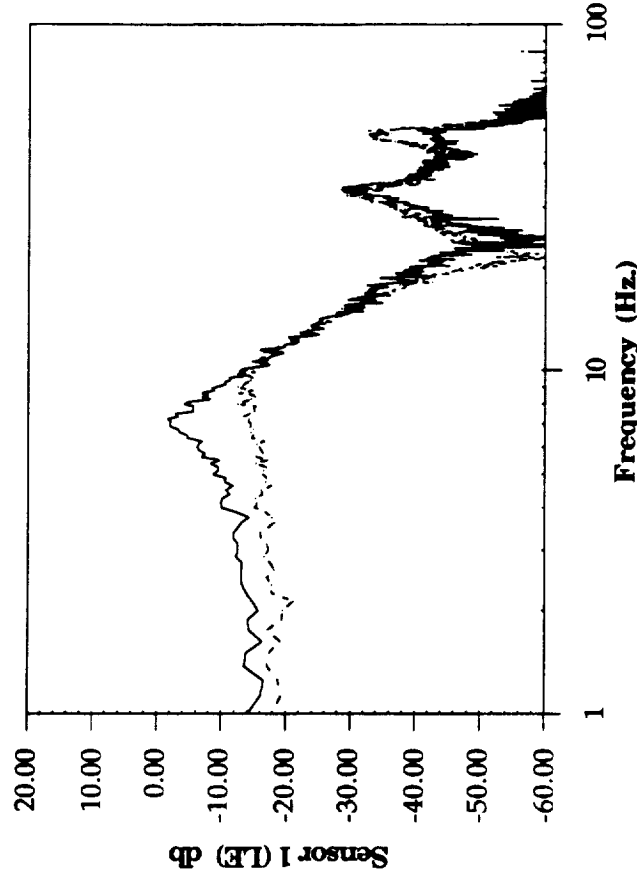
WIND TUNNEL GUST ALLEVIATION: OPEN AND CLOSED LOOP RESPONSE AT 60 MPH

- Aluminum Bench Mark Specimen
- Reduced Order LQG Design: $\rho = 1e-1$ Sensor Noise = 1.0%

Analytic Model



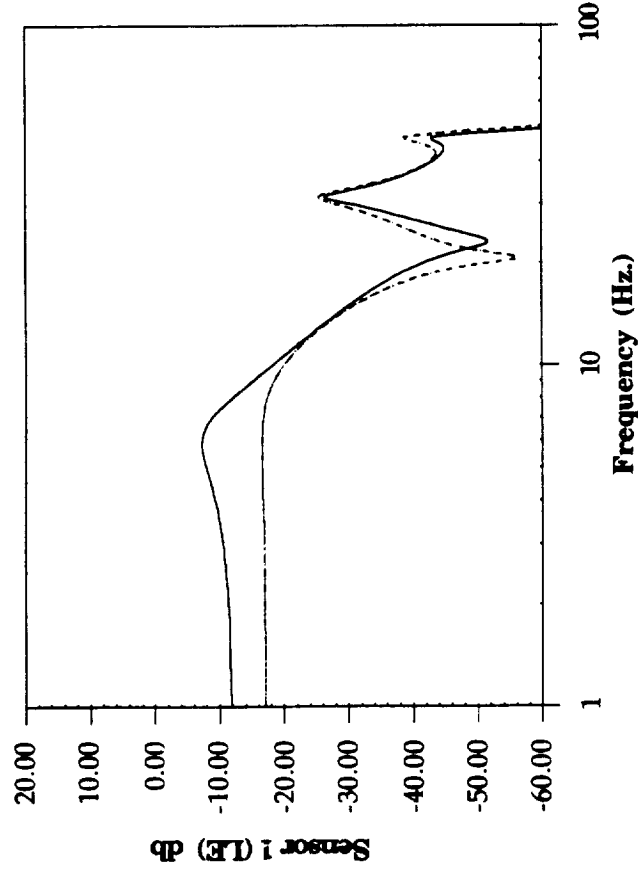
Bench-Top Experiments



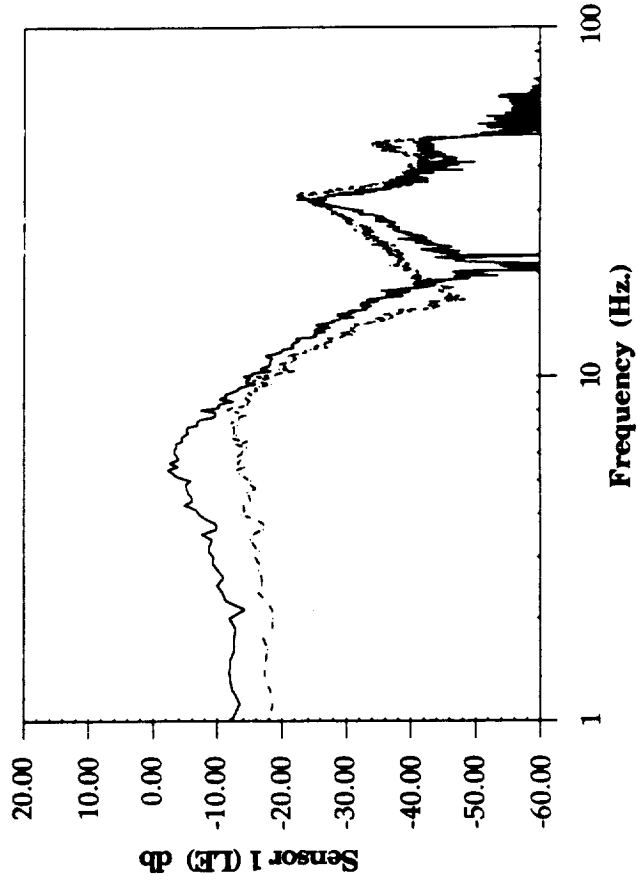
WIND TUNNEL GUST ALLEVIATION: OPEN AND CLOSED LOOP RESPONSE AT 60 MPH

- Graphite/Epoxy Bend/Twist Coupled Specimen
- Reduced Order LQG Design: $\rho = 1e+0$ Sensor Noise = 0.5%

Analytic Model

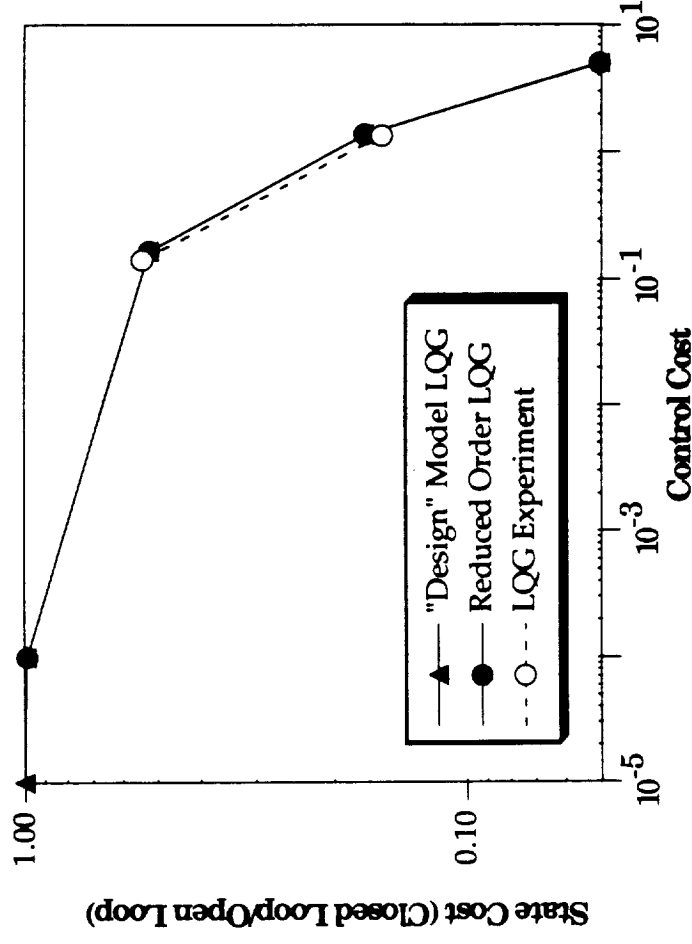


Bench-Top Experiments



WIND TUNNEL GUST ALLEVIATION: STATE COST VERSUS CONTROL COST AT 60 MPH

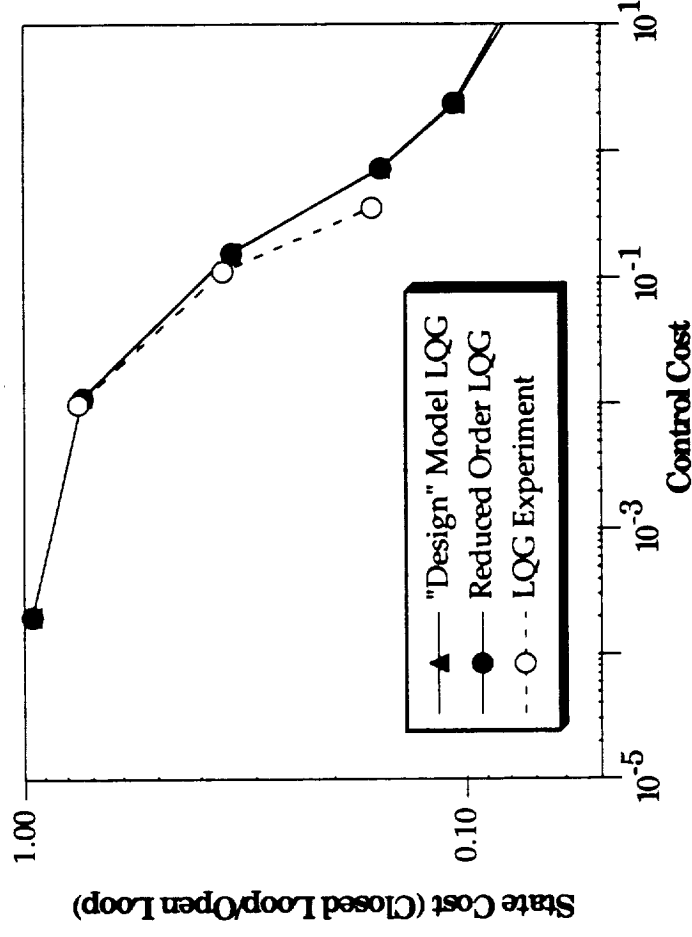
- Aluminum Bench Mark Specimen
- Reduced Order LQG Design: Sensor Noise = 0.5%



- State Cost Reduced by 84% (8 db RMS)

**WIND TUNNEL GUST ALLEVIATION:
STATE COST VERSUS CONTROL COST AT 60 MPH**

- Graphite/Epoxy Bend/Twist Coupled Specimen
- Reduced Order LQG Design: Sensor Noise = 1.0%

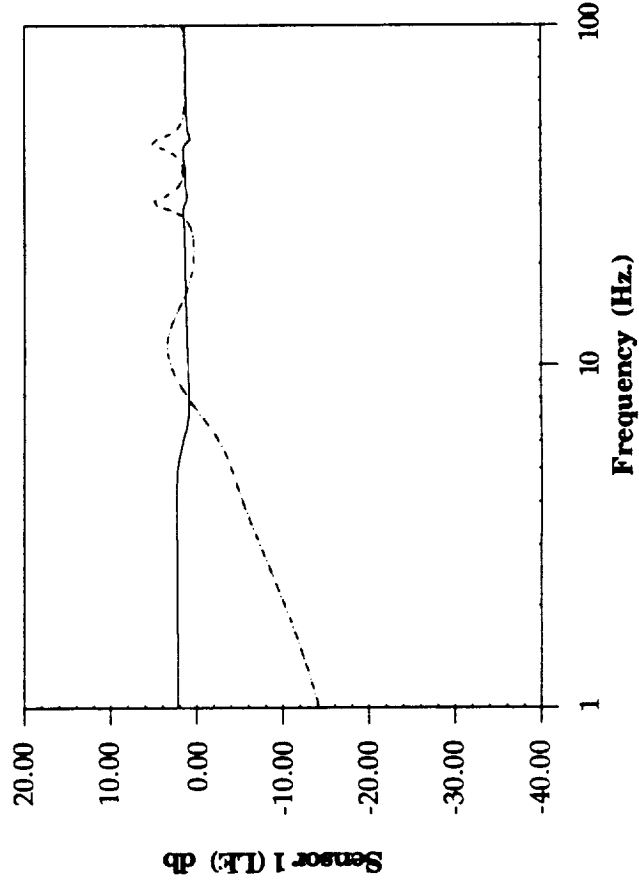


- State Cost Reduced by 84% (8 db RMS)

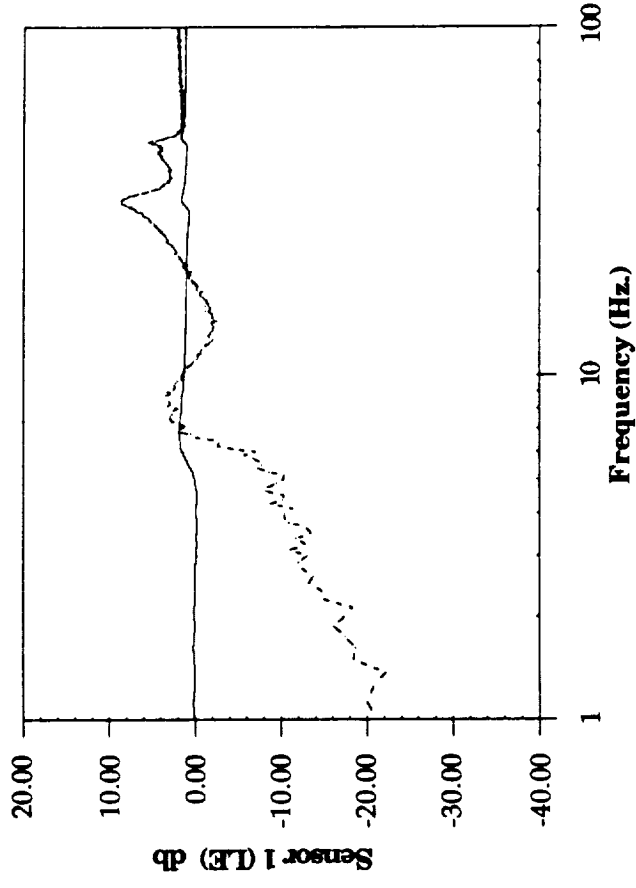
**WIND TUNNEL COMMAND FOLLOWING:
OPEN AND CLOSED LOOP ERROR AT 60 MPH**

Graphite/Epoxy Bend/Twist Coupled Specimen: Low Bandwidth

Analytic Model



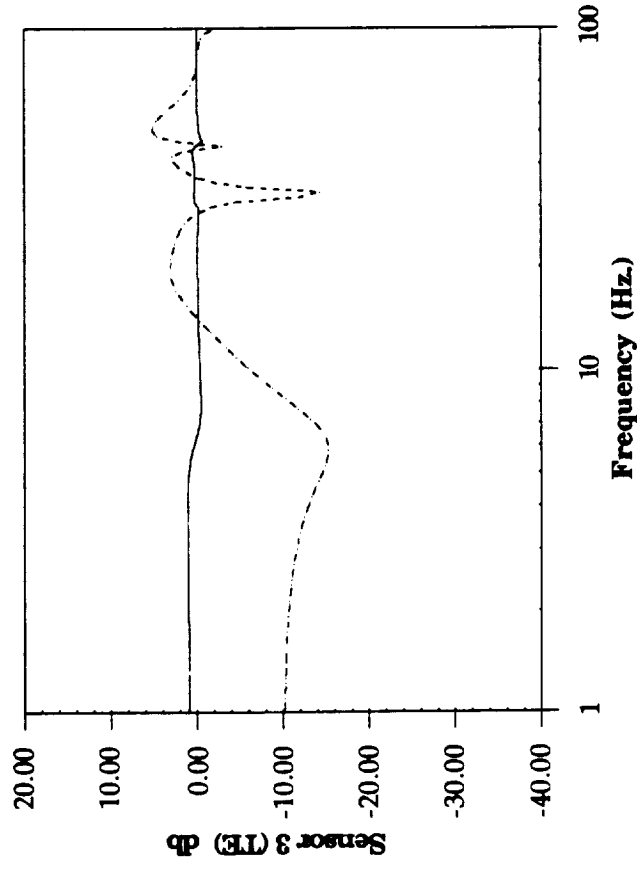
Bench-Top Experiments



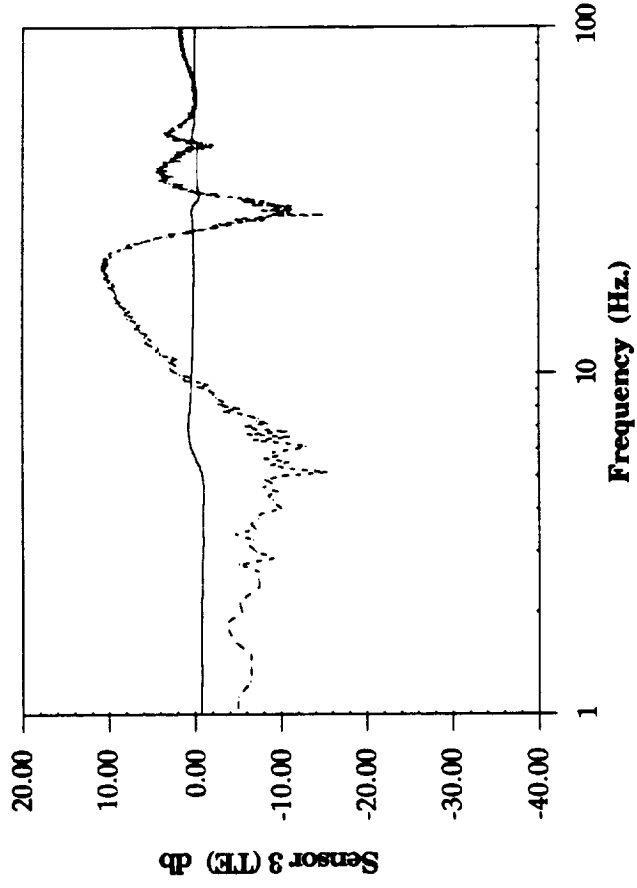
WIND TUNNEL COMMAND FOLLOWING: OPEN AND CLOSED LOOP ERROR AT 60 MPH

Graphite/Epoxy Bend/Twist Coupled Specimen: High Bandwidth

Analytic Model

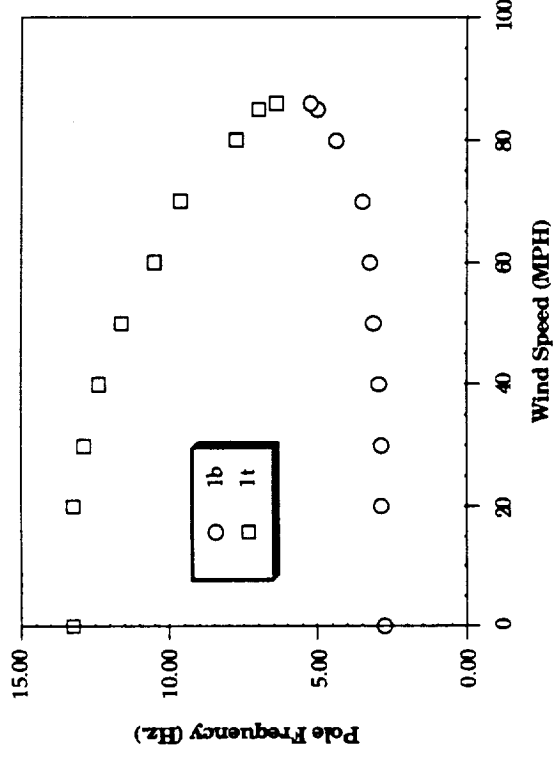


Bench-Top Experiments



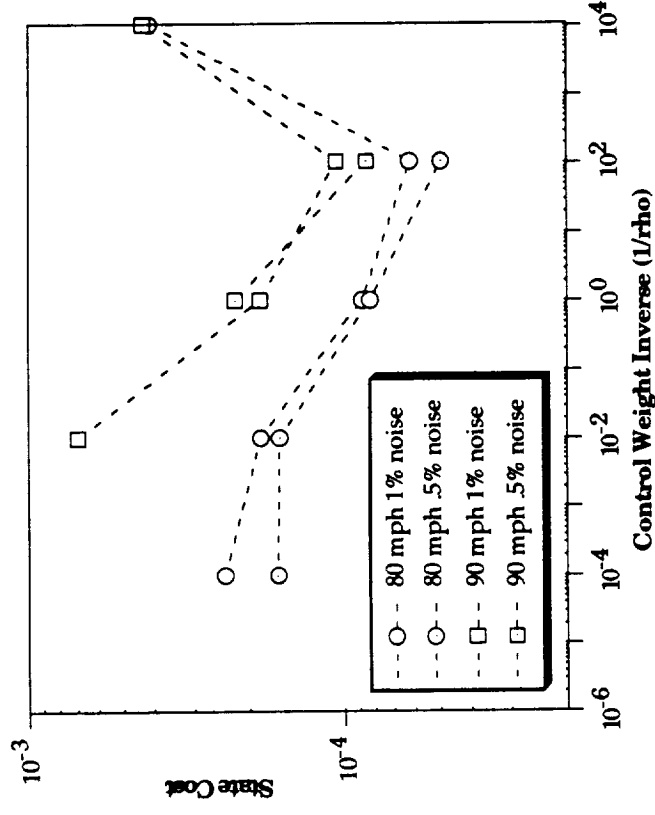
WIND TUNNEL FLUTTER SUPPRESSION: OPEN LOOP FLUTTER SPEED

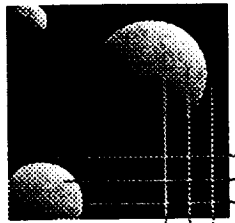
- Aluminum Plate Original Flutter Speed About 125 MPH
- Flutter Speed Lowered to 88 MPH by:
 - Adding 1.6x Original Weight
 - 0.8 Semi-Chords Behind the TE



WIND TUNNEL FLUTTER SUPPRESSION: CLOSED LOOP STATE COST CURVES

- Finite State Cost (stable system) for Any Control Weight
- High Frequency Modes Are Destabilized as Gain Becomes Large





MIT
Space
Engineering
Research
Center

Sensor and Actuator Technology Development

Eric Anderson and Nesbitt W. Hagood

January 23, 1992

512-35

160320

Ψ93727900

Outline

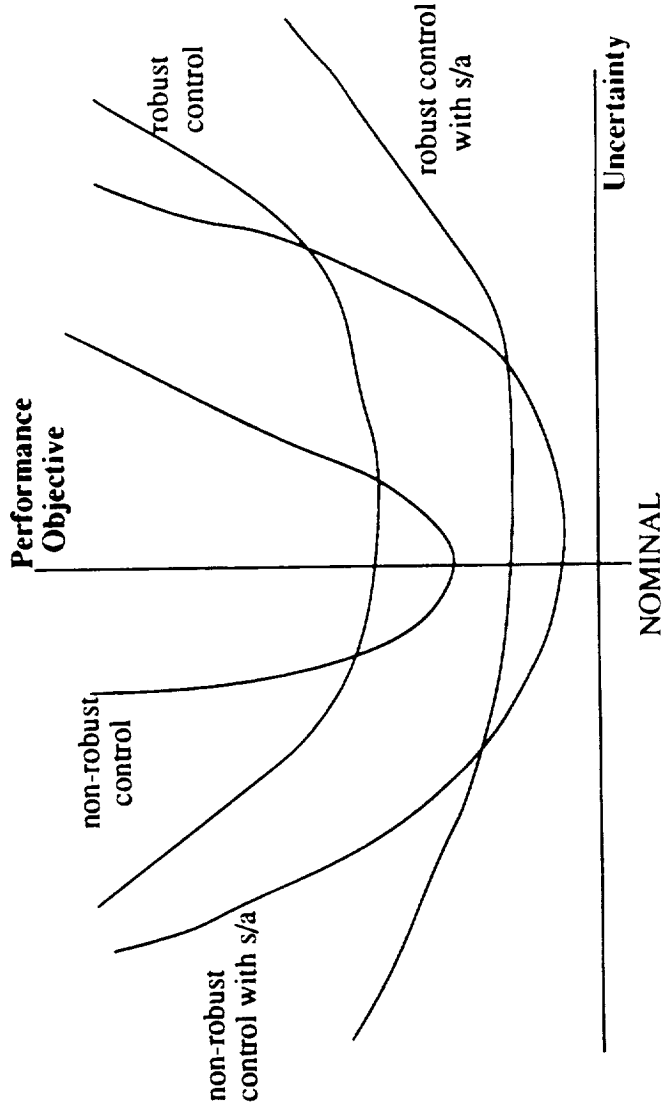
- Sensor and Actuator Placement for Robustness
- Self-Sensing Actuators
- Nonlinear Actuation Models

Sensor/Actuator Selection for Robustness

- Concept: Select sensors and actuators to minimize impact of model inaccuracies on achievable performance and stability.
- Motivation:
 - Placement and resulting closed-loop performance \stability are a strong function of model.
 - Only have uncertain model on which to base placement decisions.
 - Implies large uncertainties in *achievable* closed-loop performance or robustness.
- Method: Incorporate model uncertainty information into open or closed loop placement algorithms.

Achievable Performance Robustness

- Control design must use actuator and sensors it is given.
 - Example: Loss of controllability when actuator is unwittingly placed at a node.
- Can enable control task by introducing performance robustness through s/a set.



Representing the Uncertain System

- All system matrices affected by model uncertainty
- Focus on finite element errors, not ID errors
- Determine eigenvector uncertainty to expected errors:
 - Stiffness of components
 - Boundary conditions
 - Mass distribution
- Two approaches:
 - *Range* of possible plants/systems over all uncertain parameters
 - *Sensitivity* of nominal plant/system to uncertain parameters

Figures of Merit

- Open loop analysis of sensor/actuator options used to reduce number of choices to manageable number
- Use controllability and observability gramians

$$W_c(t_0, t_1) = \int_{t_0}^{t_1} \phi(t_1, \tau) B(\tau) \phi^T(t_1, \tau) d\tau$$

- Calculate with Lyapunov equation for each value of uncertainty

$$0 = A_i W_{c_i} + W_{c_i} A_i^T + B_i \sum_{ww} B_i^T ;$$

- Closed loop cost

$$J_{cl} = \text{tr} \{ \langle Q C_i^T C_i \rangle \}$$

where

$$0 = A_i Q_i + Q_i A_i^T + B_i B_i^T$$

Design Algorithms

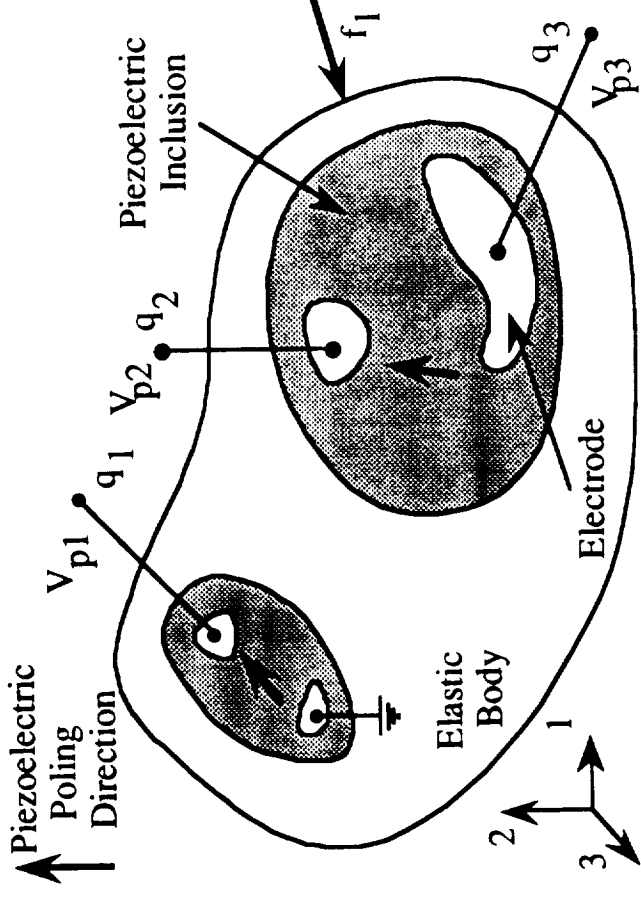
- Open loop
 - Compute expected value of gramians over entire uncertainty set
 - Reduce number of s/a options by straight ranking
- Closed loop
 - Use existing techniques for optimization
 - Cost is expected value over uncertainty set
- Trade off degree of open loop reduction vs. size of set for closed loop optimization

Current Efforts

- Analytical sample problem: cantilevered beam
 - 6 sensors, 6 actuators
 - LQG control (SISO and TITO)
- Interferometer testbed
 - Analysis based on finite element model
 - Uncertainty description provided from system ID data
 - Main focus is active strut placement problem
 - Experimental demonstration of improved closed loop performance based on sensor/actuator location and type

Piezoelectric Actuation and Sensing

- Structure with piezoelectric actuators/sensors.



- Governing Equations of Motion:

$$(\mathbf{M}_s + \mathbf{M}_p) \ddot{\mathbf{r}} + (\mathbf{K}_s + \mathbf{K}_p) \mathbf{r} - \Theta \mathbf{v} = \mathbf{B}_f \mathbf{f} \text{ Actuator Eq.}$$

$$\Theta^T \mathbf{r} + \mathbf{C}_p \mathbf{v} = \mathbf{B}_q \mathbf{q} \text{ Sensor Eq.}$$

Simultaneous Sensing and Actuation

- Concept: Use the same piece of piezoelectric simultaneously as both a structural sensor and an actuator.
- Motivation:
 - Eliminates need for separate sensor. Reduced signal conditioning.
 - Perfectly collocated dual sensor useful for structural control.
- Modelling: If the applied current and piezoelectric electrode voltage is known, one can reconstruct the mechanical strain or strain rate.

$$\Theta^T \mathbf{r} = \mathbf{q} - \mathbf{C}_p \mathbf{v} \quad \Theta^T \dot{\mathbf{r}} = \dot{\mathbf{q}} - \mathbf{C}_p \dot{\mathbf{v}}$$

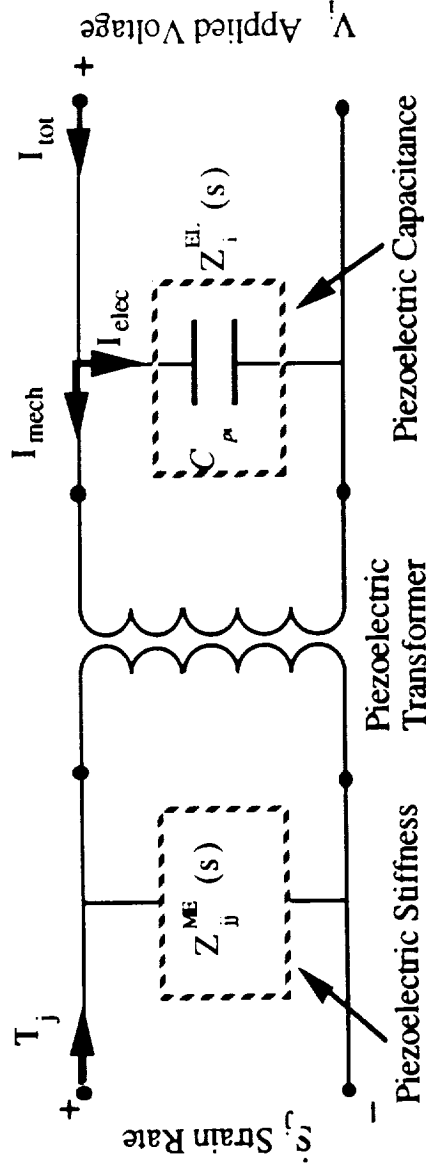
- The $\Theta^T \mathbf{r}$ term is proportional to averaged strain state as for the charge based sensor.

$$\Theta^T \mathbf{r} = \int_{V_p} [\mathbf{e}_{31} S_1 + \mathbf{e}_{31} S_2 + \mathbf{e}_{33} S_3] dv$$

- More insight can be gained on the physical significance of the terms by using a piezoelectric circuit analogy.

Physical Interpretation

- The piezoelectric transformer analogy is useful for determining the physical significance of the terms. The piezoelectric element is represented as a transformer converting mechanical energy to electrical and vice versa.

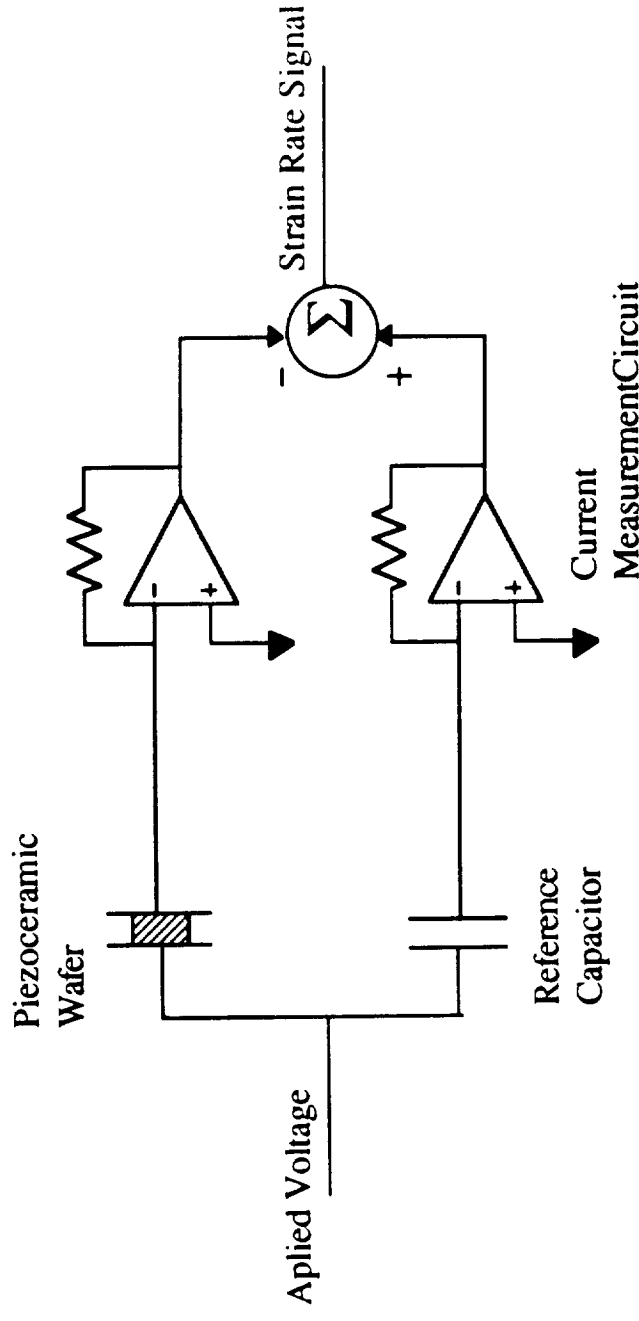


- The sensor equation can be interpreted physically as measuring the difference in between applied current and the capacitance current.

$$\Theta^T \dot{\mathbf{r}} = \underbrace{\mathbf{i}}_{\mathbf{i}_{mech}} - \underbrace{C_p \dot{\mathbf{v}}}_{\mathbf{i}_{elec}}$$

Simple Circuit Implementation

- Strain Rate Circuit

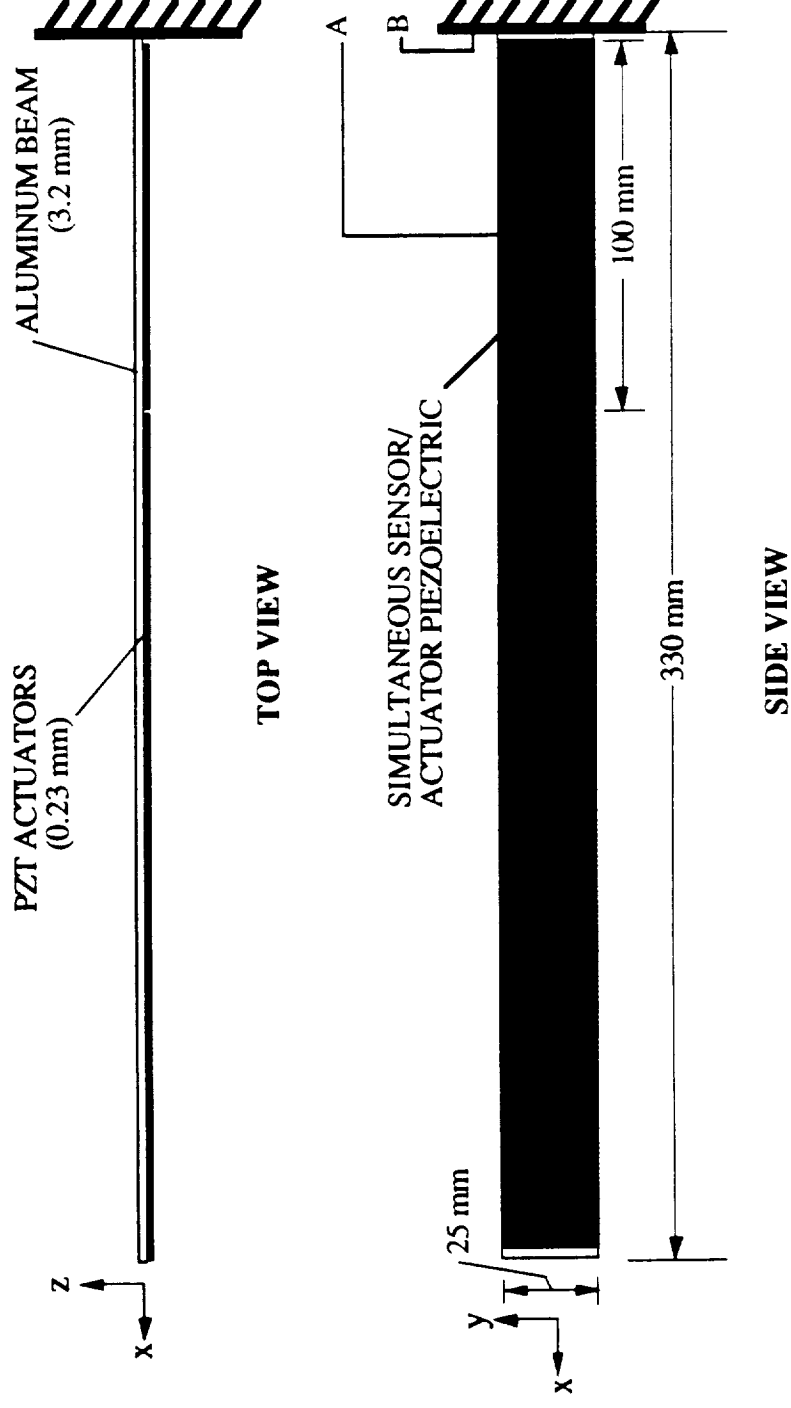


B) Strain-Rate Sensing Configuration

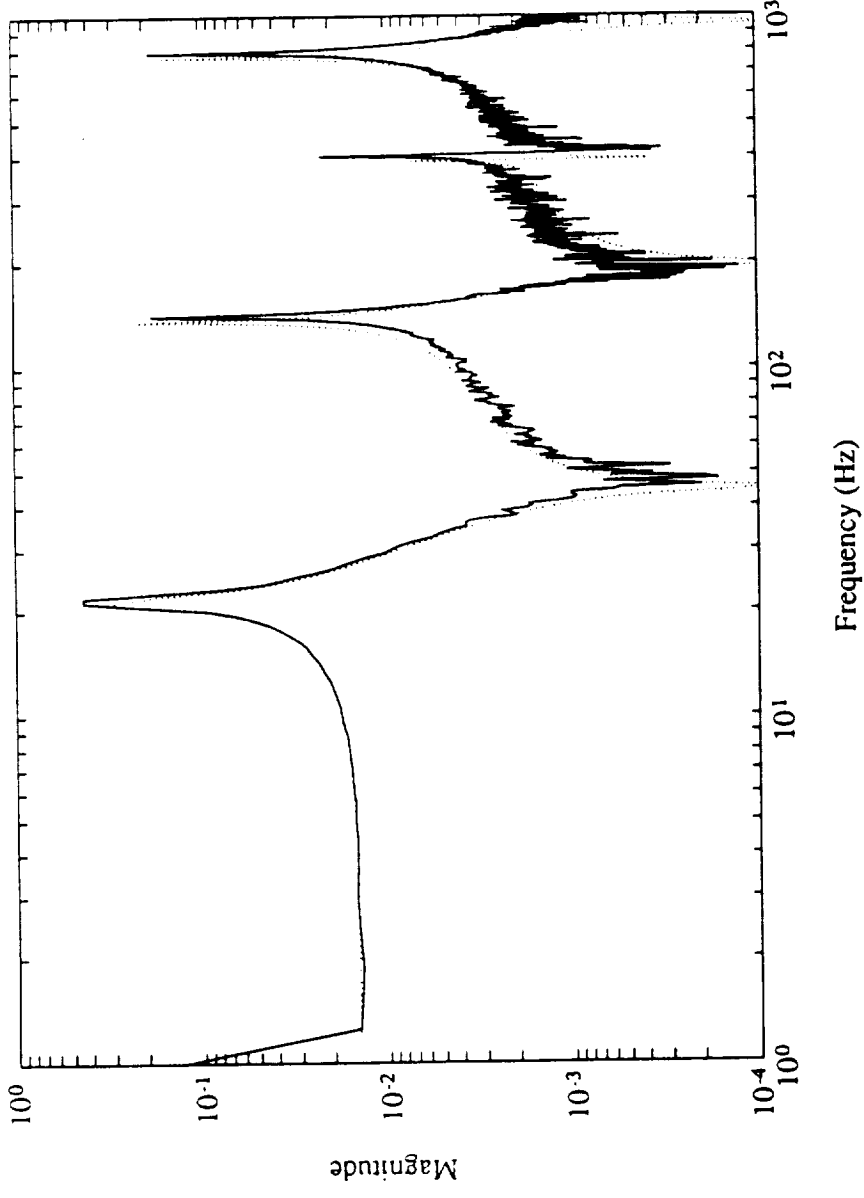
- Also possible to implement simple strain sensing circuit by measuring applied charge rather than current.

System for Experimental Demonstration

- Cantilevered beam with PZT wafers on the surface.



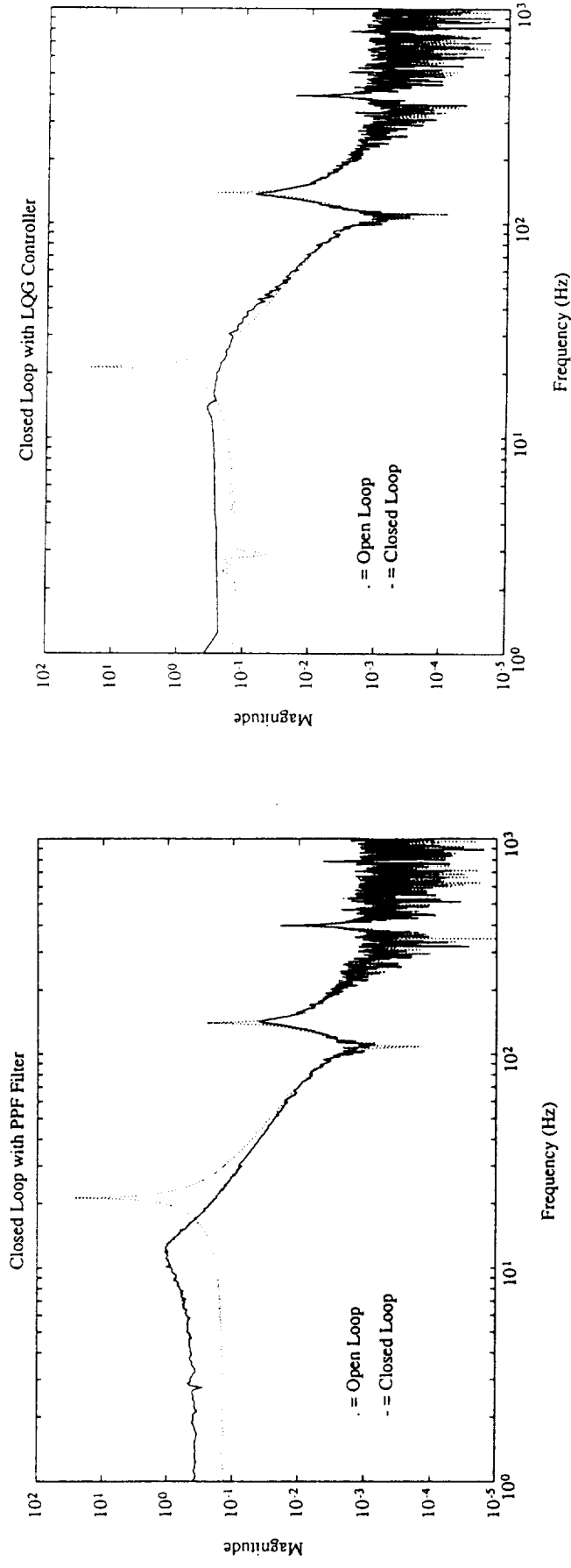
Open Loop Results



- Model compares well with measurement
- Zero location matching hindered by PZT hysteresis

Closed Loop Results

- Tip displacement/force input with “sensuator” loop closed



- Positive position feedback (PPF)
- LQG

Applications

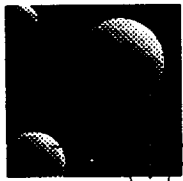
- Retrofit of sensing capability on existing actuator systems
 - Information on local deformation
 - Information for collocated control (addition of damping)
- Linearization of actuator response
- Health monitoring and system identification
- Active structural control (high gain collocated loops)

Nonlinear Actuation Models

- Concept: Develop models of actuated structures capable of handling actuation material nonlinearities
- Motivation:
 - Piezoelectric material properties are nonlinear at high strains.
 - Higher actuation performance available from inherently nonlinear materials.
 - Electrostrictive materials
 - New high-strain, shape-memory ceramics.
- Approach:
 - Microscopic material models for capturing relevant physics.
 - Macroscopic phenomenological models for nonlinear structural response using energy methods.

Conclusions

- Ongoing work in three areas:
 - Robust Actuator and Sensor Placement
 - Self-Sensing Actuation
 - Nonlinear Actuation Modeling
- Robust actuator and sensor placement addresses a clear need but faces the difficulty of good error model development.
- Self-sensing actuation has been demonstrated and modeled, works well in active control systems for simple structures, and is being applied to built up structures.
- New research on nonlinear actuation models holds promise for high fidelity modeling of high strain actuation materials.



MIT
Space
Engineering
Research
Center

IMPLEMENTATION OF INPUT COMMAND SHAPING TO REDUCE VIBRATION IN FLEXIBLE SPACE STRUCTURES

Kenneth W. Chang
Professor Warren P. Seering
B. Whitney Rappole

SERC Steering Committee Meeting
January 23, 1992

513 81
N 98-27901

P-37

Space Engineering Research Center

GOALS OF RESEARCH

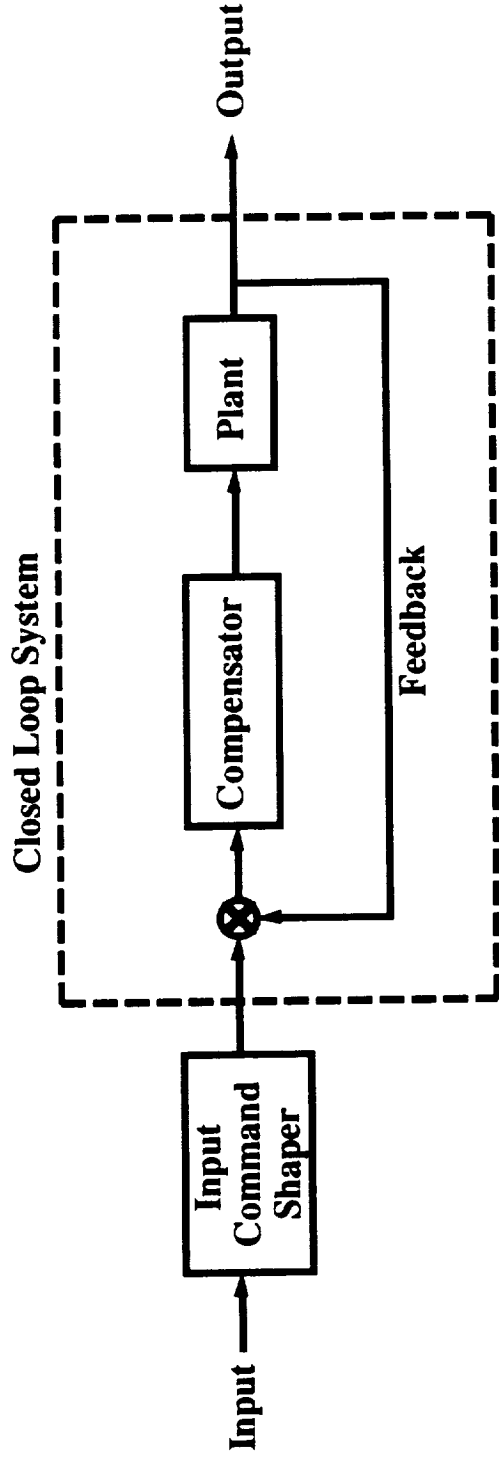
- Explore theory of input command shaping to find an efficient algorithm for flexible space structures.
- Characterize MACE test article.
- Implement input shaper on the MACE structure; interpret results.

OUTLINE

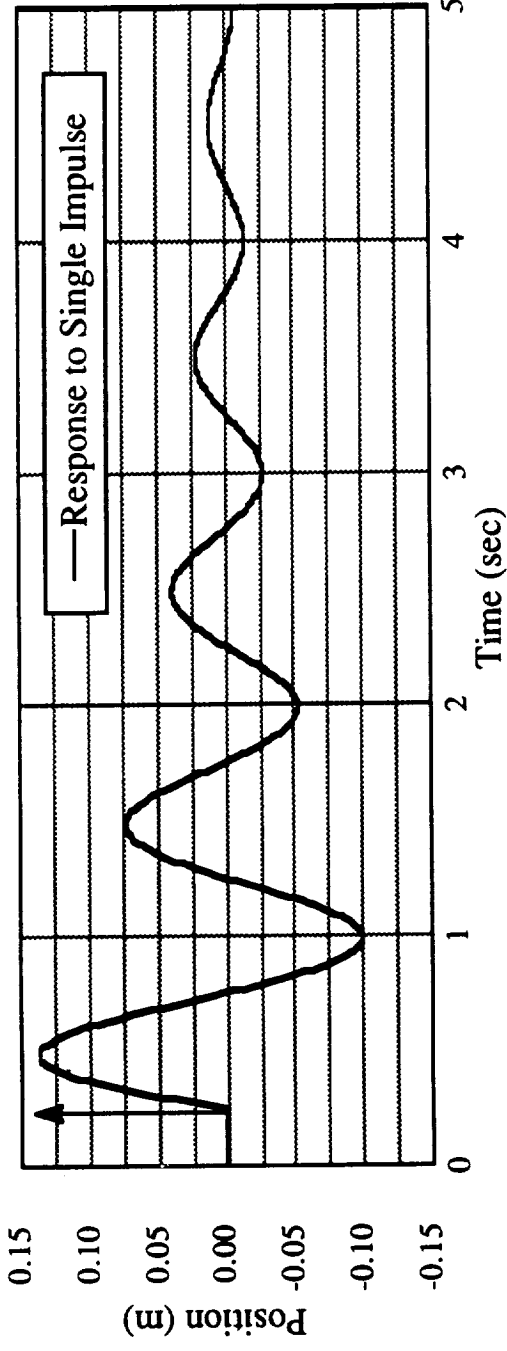
- Background on Input Shaping.
- Simulation Results.
- Experimental Results.
- Future Work.

WHAT IS INPUT COMMAND SHAPING?

An **OPEN-LOOP** method of reducing residual vibration by manipulating the input to a dynamic system.



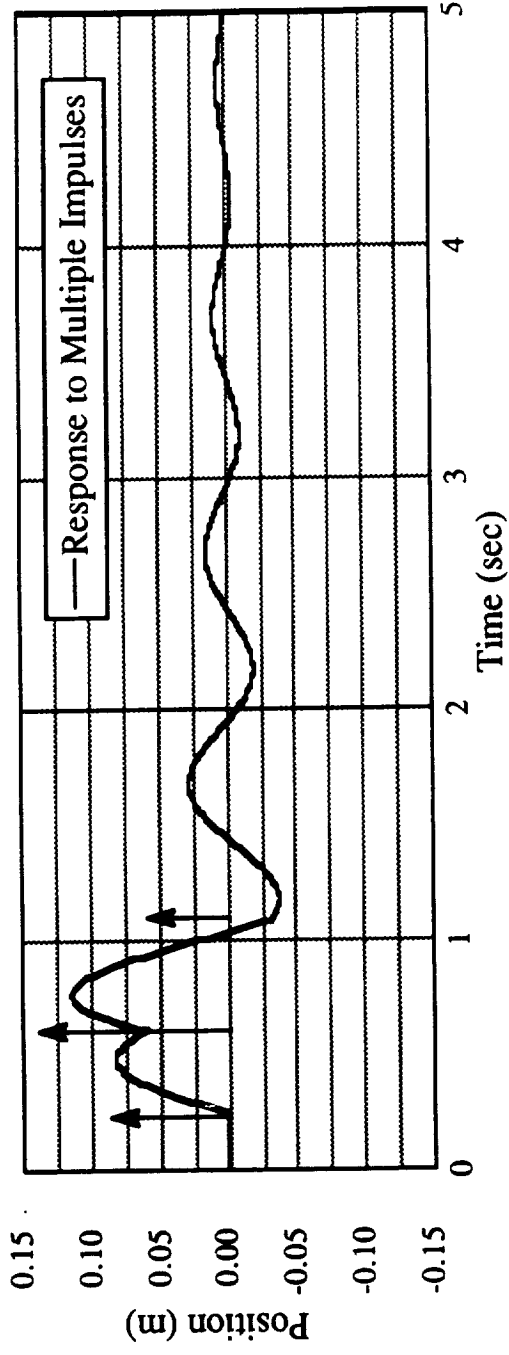
IMPULSE COMMAND SHAPING ASSUMES SECOND ORDER LINEAR RESPONSE.



$$y_i(t) = A_i e^{-\zeta \omega (t - t_i)} \sin((t - t_i) \omega \sqrt{1 - \zeta^2})$$

y_i	Response to Impulse i
A_i	Magnitude of Impulse i
t_i	Time of Impulse i
ω	System Natural Frequency
ζ	System Damping Ratio

BY SUPERPOSITION, WE CAN CALCULATE THE RESPONSE TO MULTIPLE IMPULSES.



$$y_i(t) = \sum_{i=1}^N A_i e^{-\zeta \omega (t-t_i)} \sin((t-t_i) \omega \sqrt{1-\zeta^2})$$

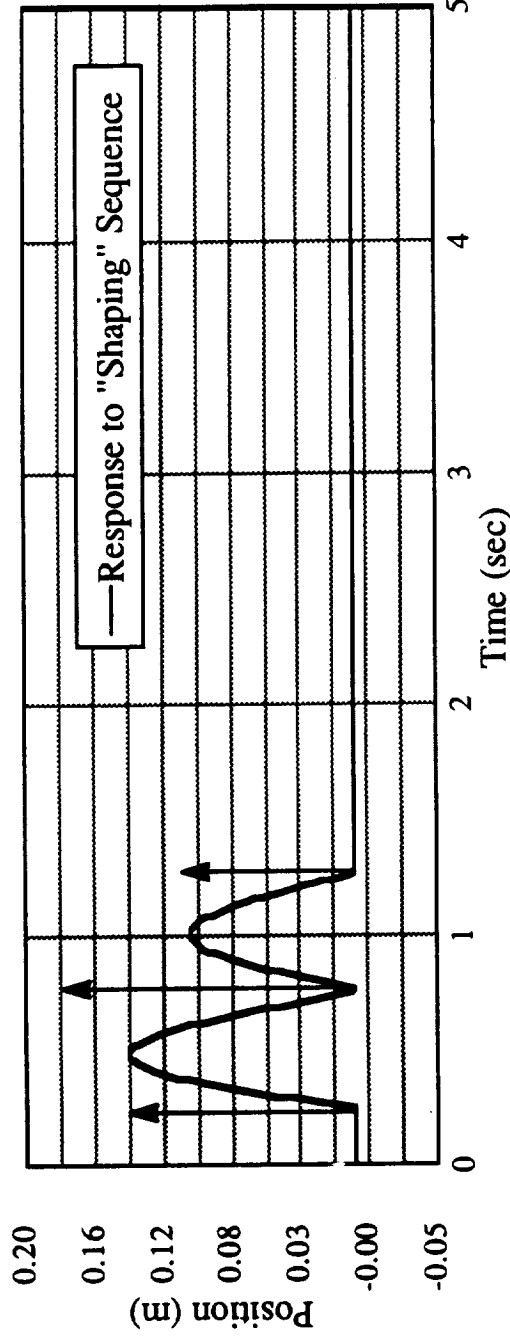
i Impulse Counter
 N Number of Impulses

AN EXPRESSIONS FOR THE AMPLITUDE OF RESIDUAL VIBRATION.

$$\text{Amp} = \left[\left(\sum_{i=1}^N A_i e^{-\zeta \omega (t_N - t_i)} \sin(t_i \omega \sqrt{1 - \zeta^2}) \right)^2 + \left(\sum_{i=1}^N A_i e^{-\zeta \omega (t_N - t_i)} \cos(t_i \omega \sqrt{1 - \zeta^2}) \right)^2 \right]^{1/2}$$

Expression for envelope amplitude at t_N ,
the time of the final impulse.

TO ELIMINATE RESIDUAL VIBRATION, THESE CONSTRAINTS MUST BE MET.



$$\sum_{i=1}^N A_i e^{-\zeta \omega t_i} \sin(t_i \omega \sqrt{1 - \zeta^2}) = 0 \quad \sum_{i=1}^N A_i t_i e^{-\zeta \omega t_i} \sin(t_i \omega \sqrt{1 - \zeta^2}) = 0$$

$$\sum_{i=1}^N A_i e^{-\zeta \omega t_i} \cos(t_i \omega \sqrt{1 - \zeta^2}) = 0 \quad \sum_{i=1}^N A_i t_i e^{-\zeta \omega t_i} \cos(t_i \omega \sqrt{1 - \zeta^2}) = 0$$

WE CAN EXTEND THIS METHOD TO MULTIPLE MODES.

$$\sum_{i=1}^N A_i e^{-\zeta_j \omega_j t_i} \sin(t_i \omega_j \sqrt{1 - \zeta_j^2}) = 0$$

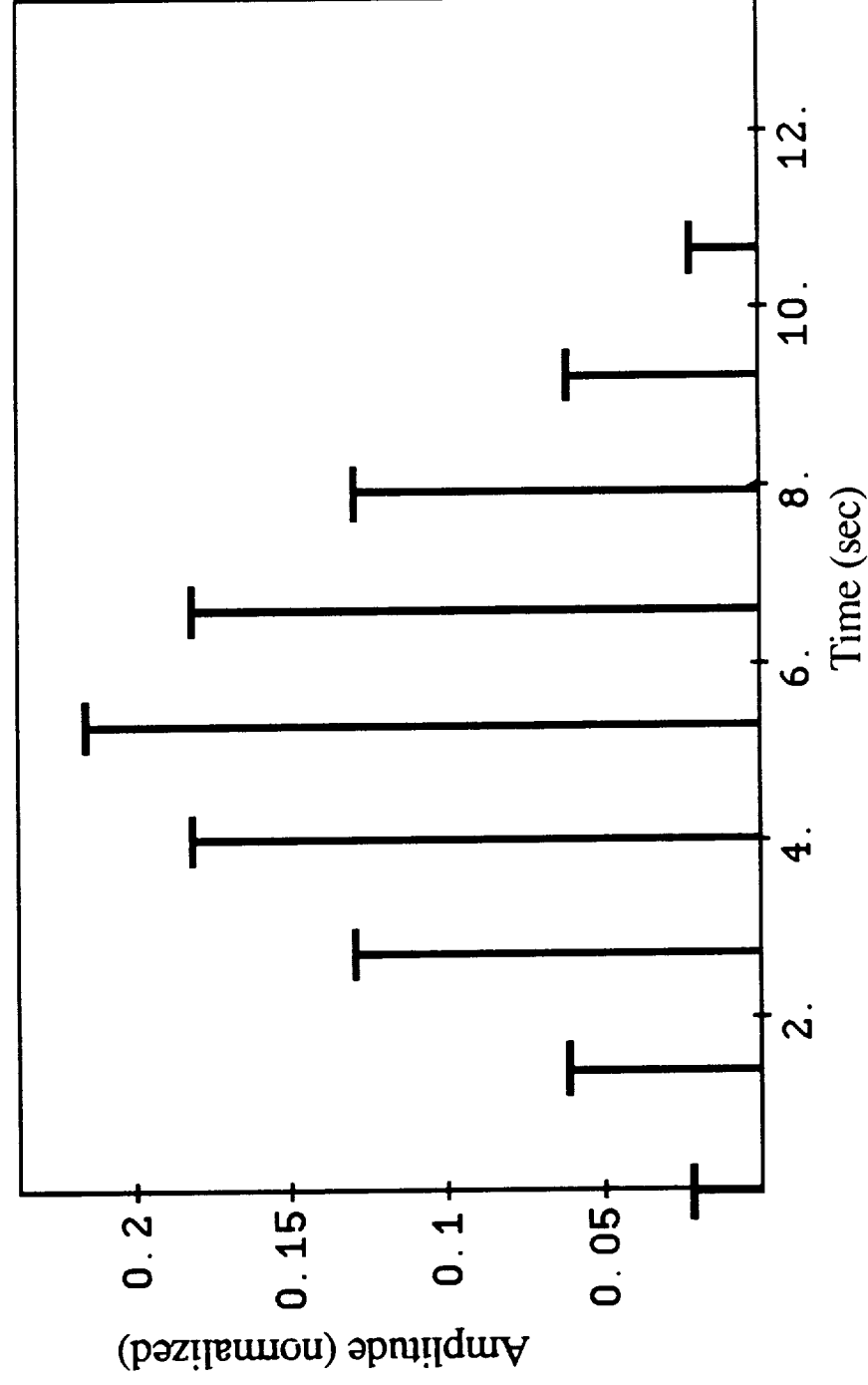
$$\sum_{i=1}^N A_i e^{-\zeta_j \omega_j t_i} \cos(t_i \omega_j \sqrt{1 - \zeta_j^2}) = 0$$

$$\sum_{i=1}^N A_i t_i e^{-\zeta_j \omega_j t_i} \sin(t_i \omega_j \sqrt{1 - \zeta_j^2}) = 0$$

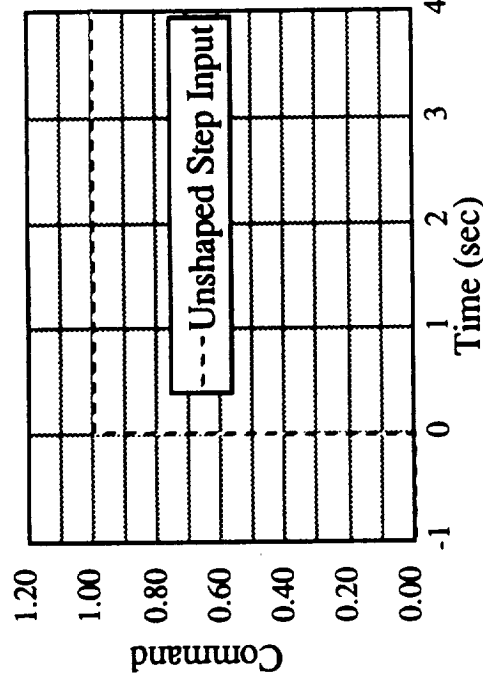
$$\sum_{i=1}^N A_i t_i e^{-\zeta_j \omega_j t_i} \cos(t_i \omega_j \sqrt{1 - \zeta_j^2}) = 0$$

These four equations are repeated for each mode "j"

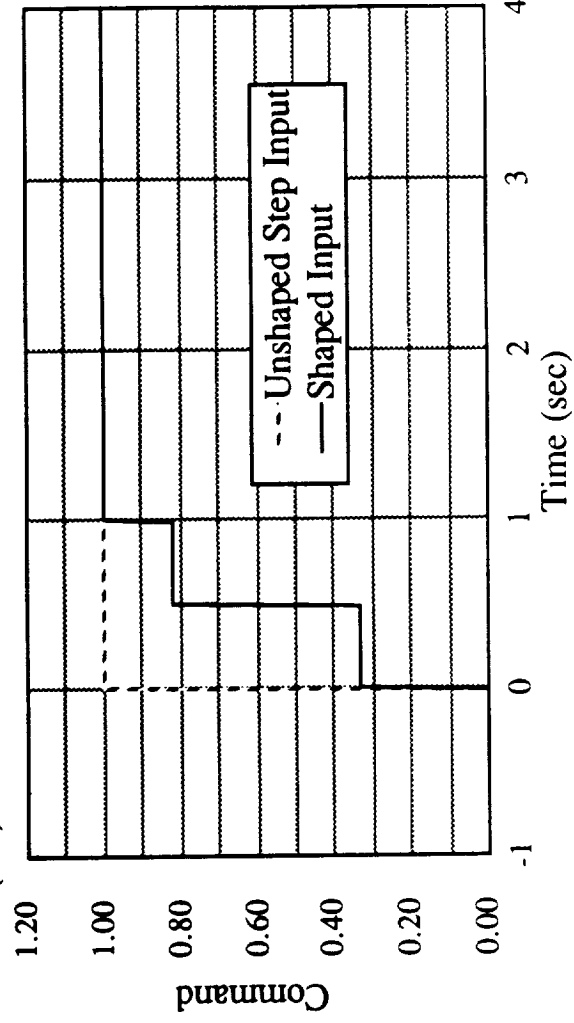
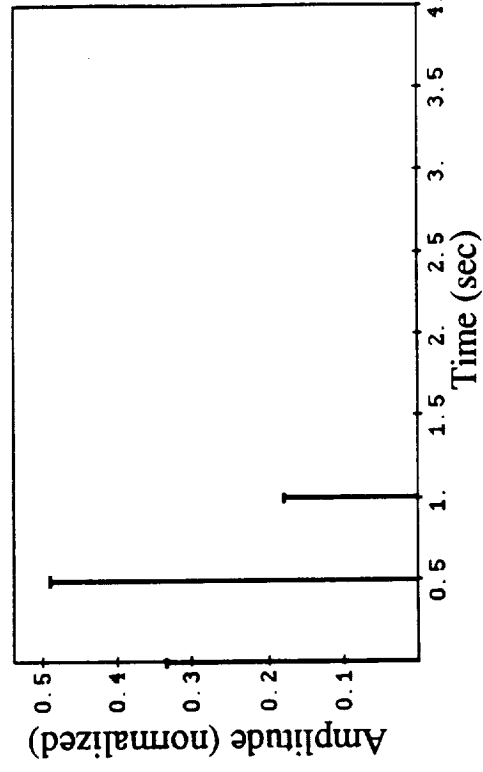
AN EXAMPLE SOLUTION OF IMPULSES FOR A 4 MODE PROBLEM.



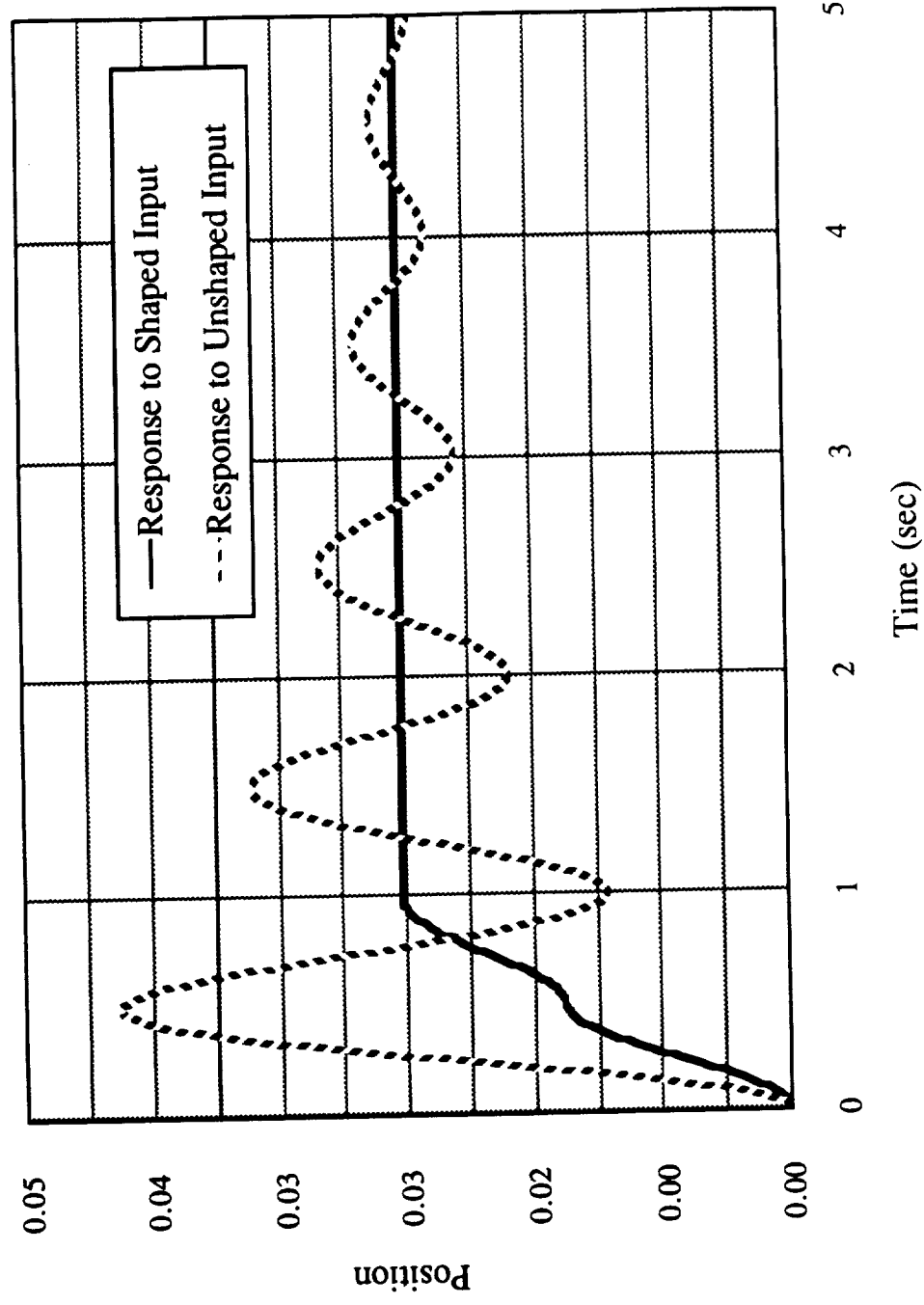
THE SHAPER IS IMPLEMENTED BY CONVOLVING THE INPUT WITH THE IMPULSES.



*

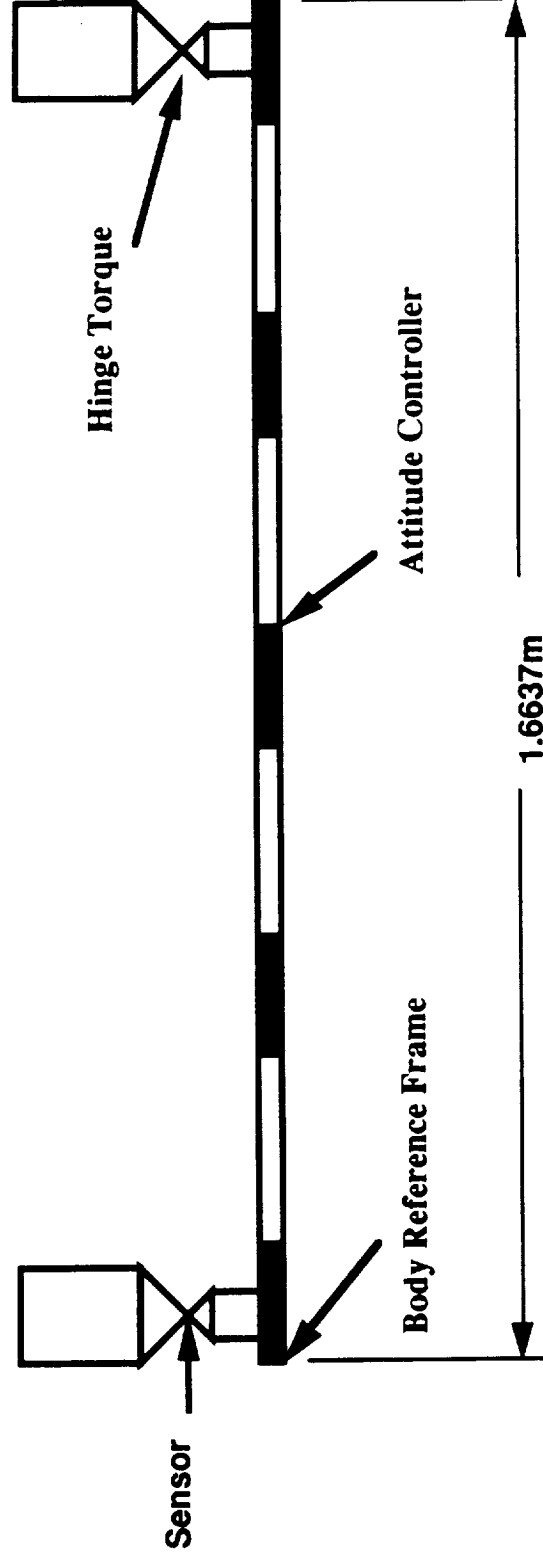


RESPONSE TO INPUTS FOR A SIMPLE 1 MODE SYSTEM.



DISCOS SIMULATION RESULTS.

DISCOS MODEL OF MACE.



Body 1 = Bus + Gimbals + Torque Wheels

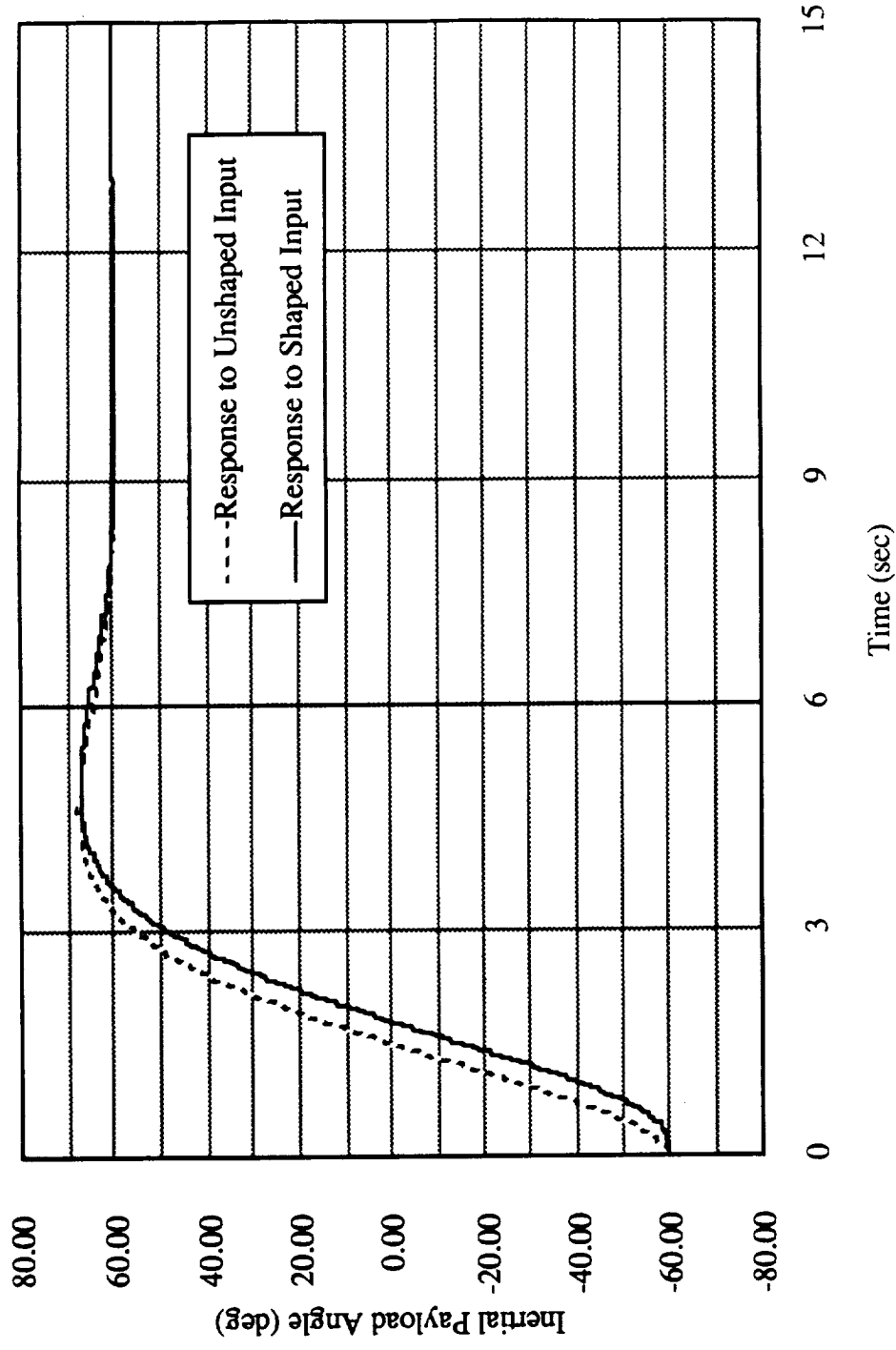
Body 2 = Payload 1 (Rigid)

Body 3 = Payload 2 (Rigid)

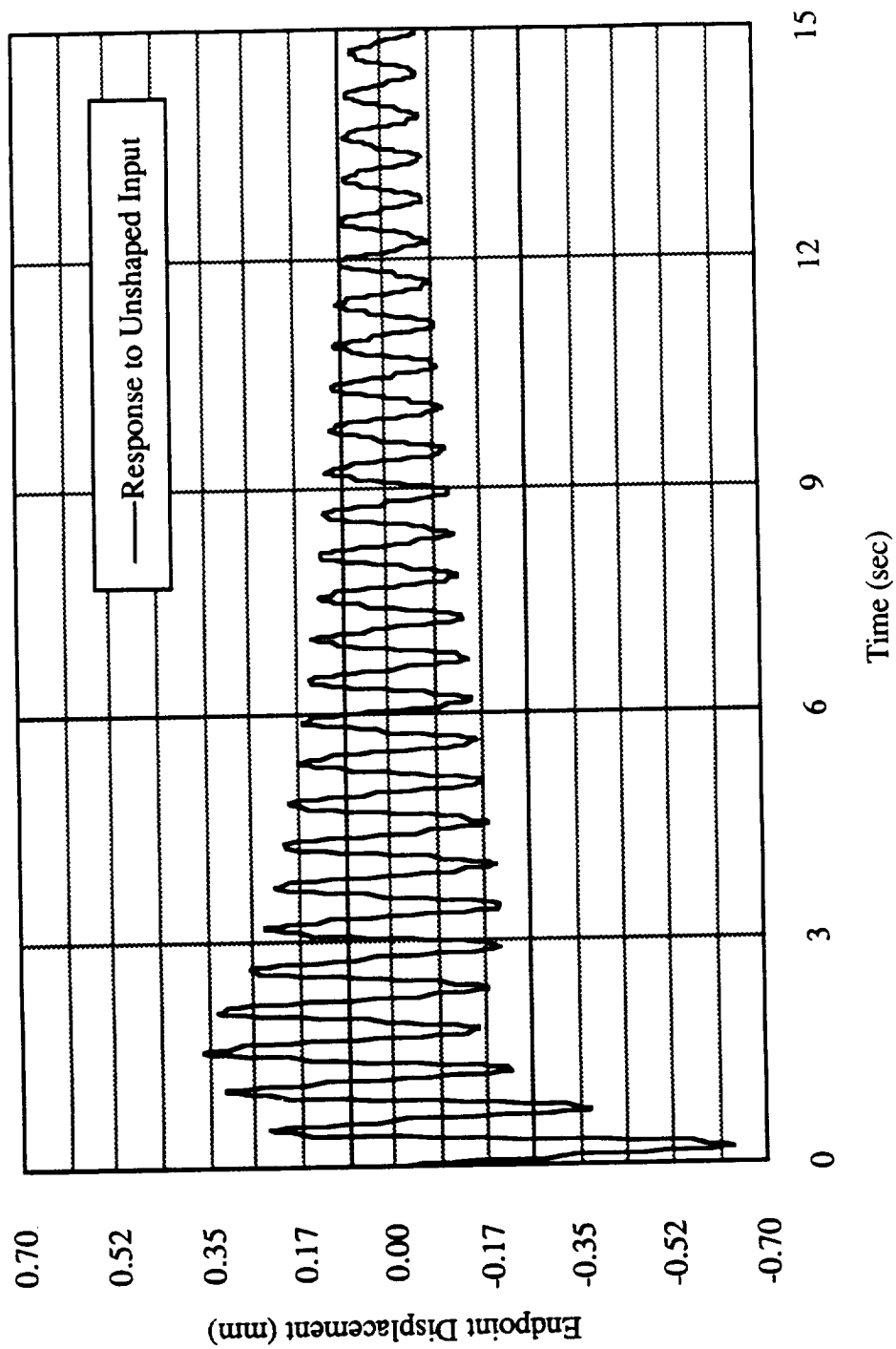
IDENTIFIED CLOSED LOOP FREQUENCIES (NON-LINEAR DISCOS MODEL)

<i>60° Outboard (Hz) (Beginning of 120° Slew)</i>	<i>60° Inboard (Hz) (End of 120° Slew)</i>
<i>2.18</i>	<i>1.88</i>
<i>14.25</i>	<i>13.40</i>
<i>15.25</i>	<i>14.20</i>
<i>15.90</i>	<i>15.90</i>

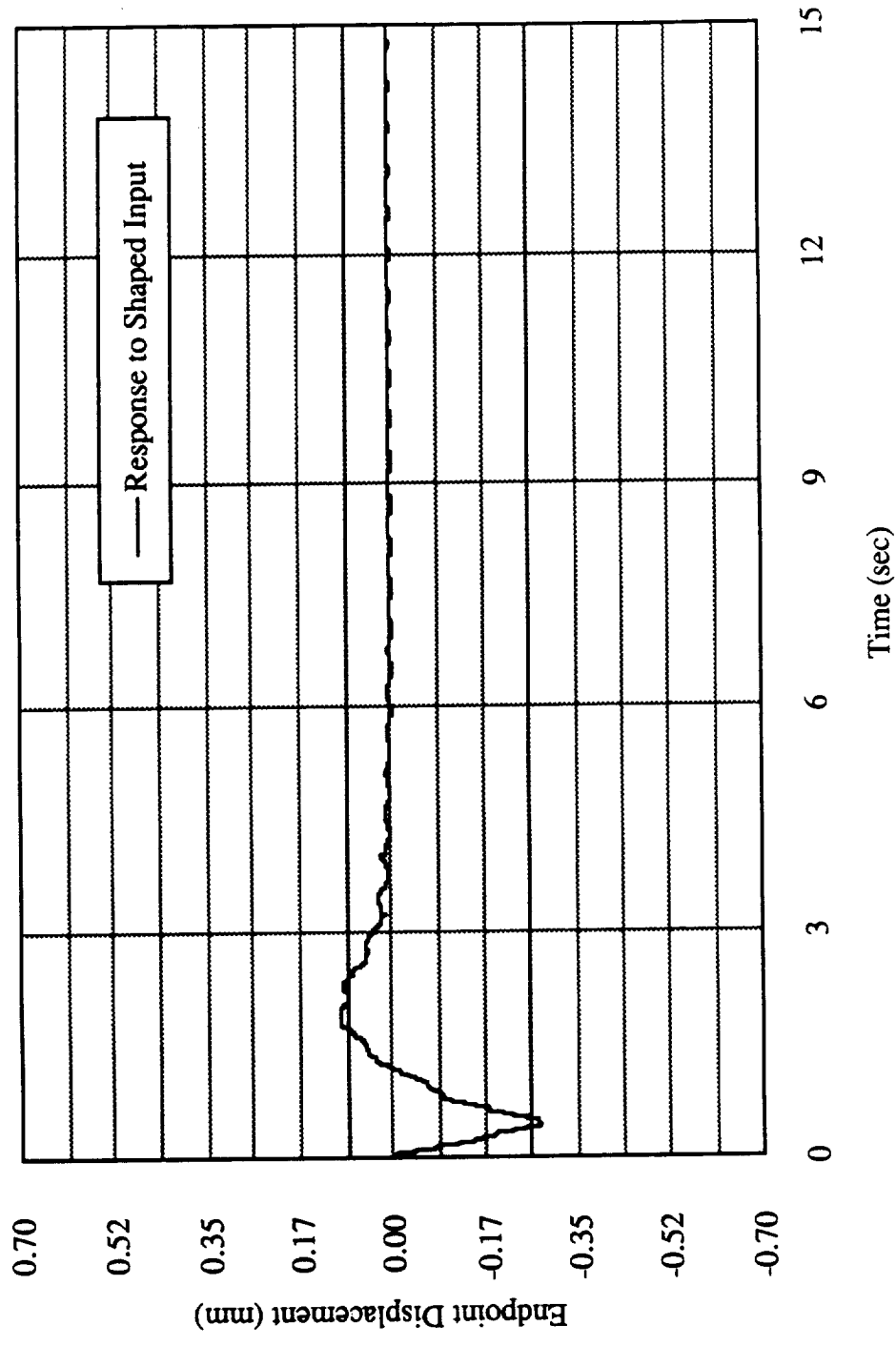
TIME TRACE OF 120° PAYLOAD SLEW



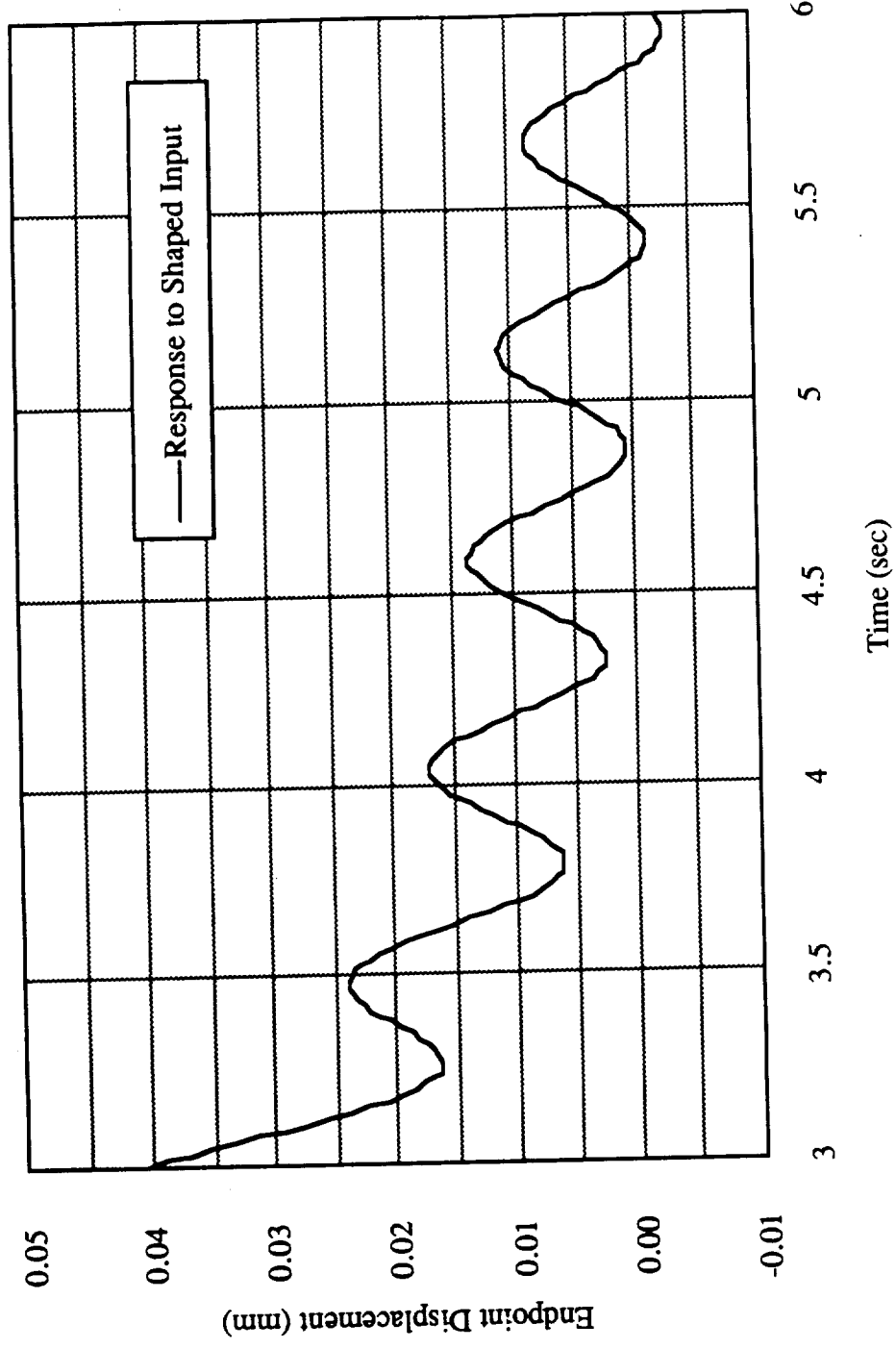
ENDPOINT RESPONSE TO UNSHAPED SLEW



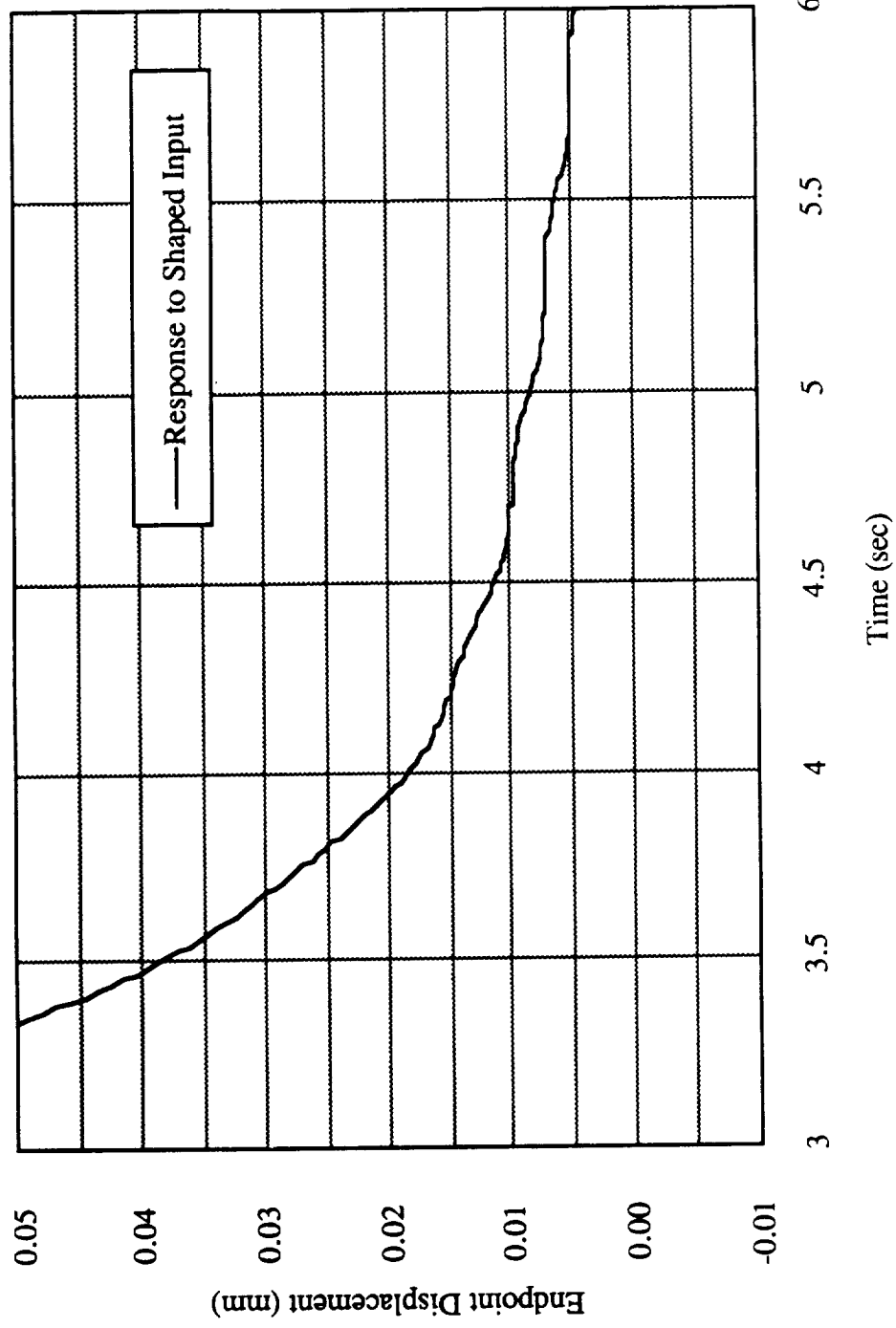
ENDPOINT RESPONSE TO SHAPED SLEW



SHAPED RESPONSE DETAIL

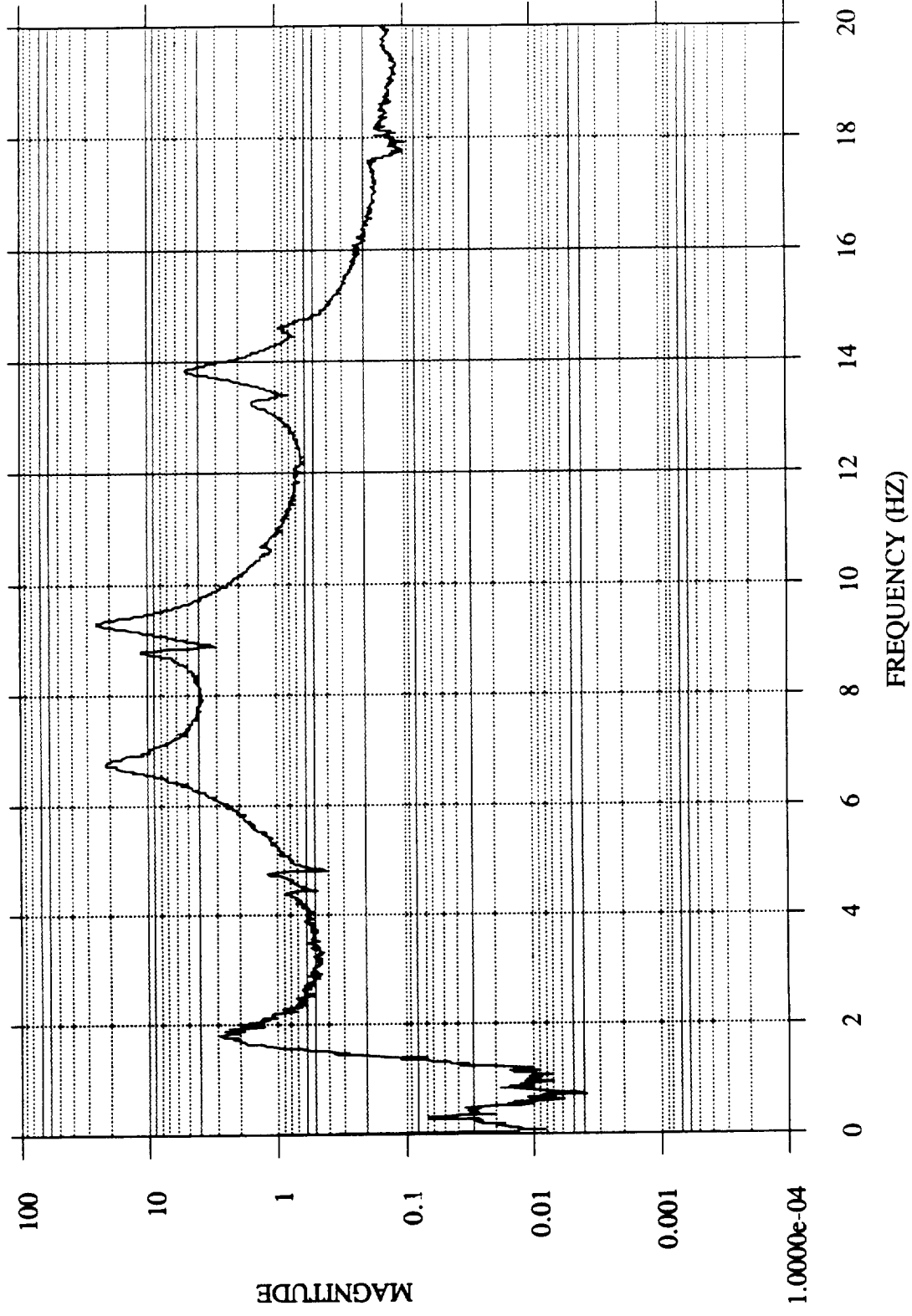


RESPONSE DETAIL FOR SHAPER WITH ADDITIONAL MODES.



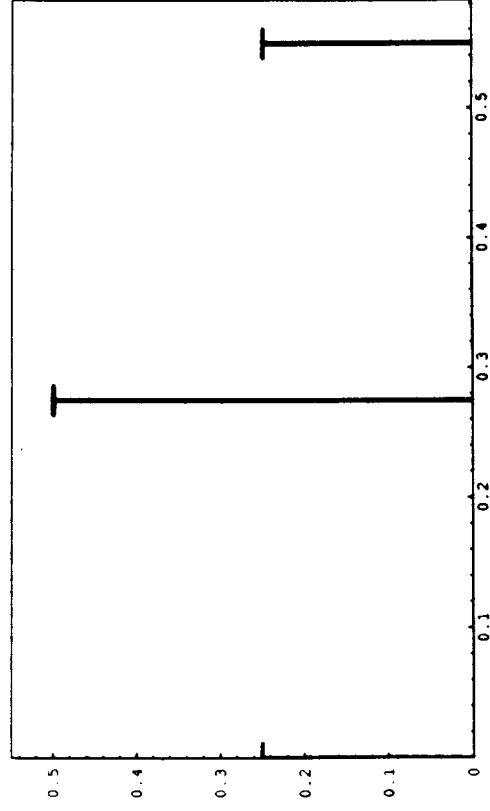
EXPERIMENTAL RESULTS

MACE PLANT FREQUENCY RESPONSE

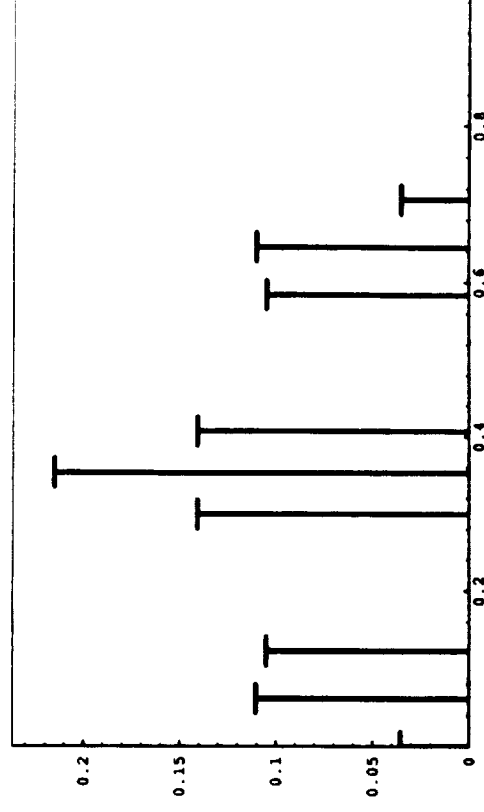


IMPULSE SHAPERS CALCULATED FOR FIRST FOUR MODES.

1.82 hz
6.82 hz
8.79 hz
9.29 hz

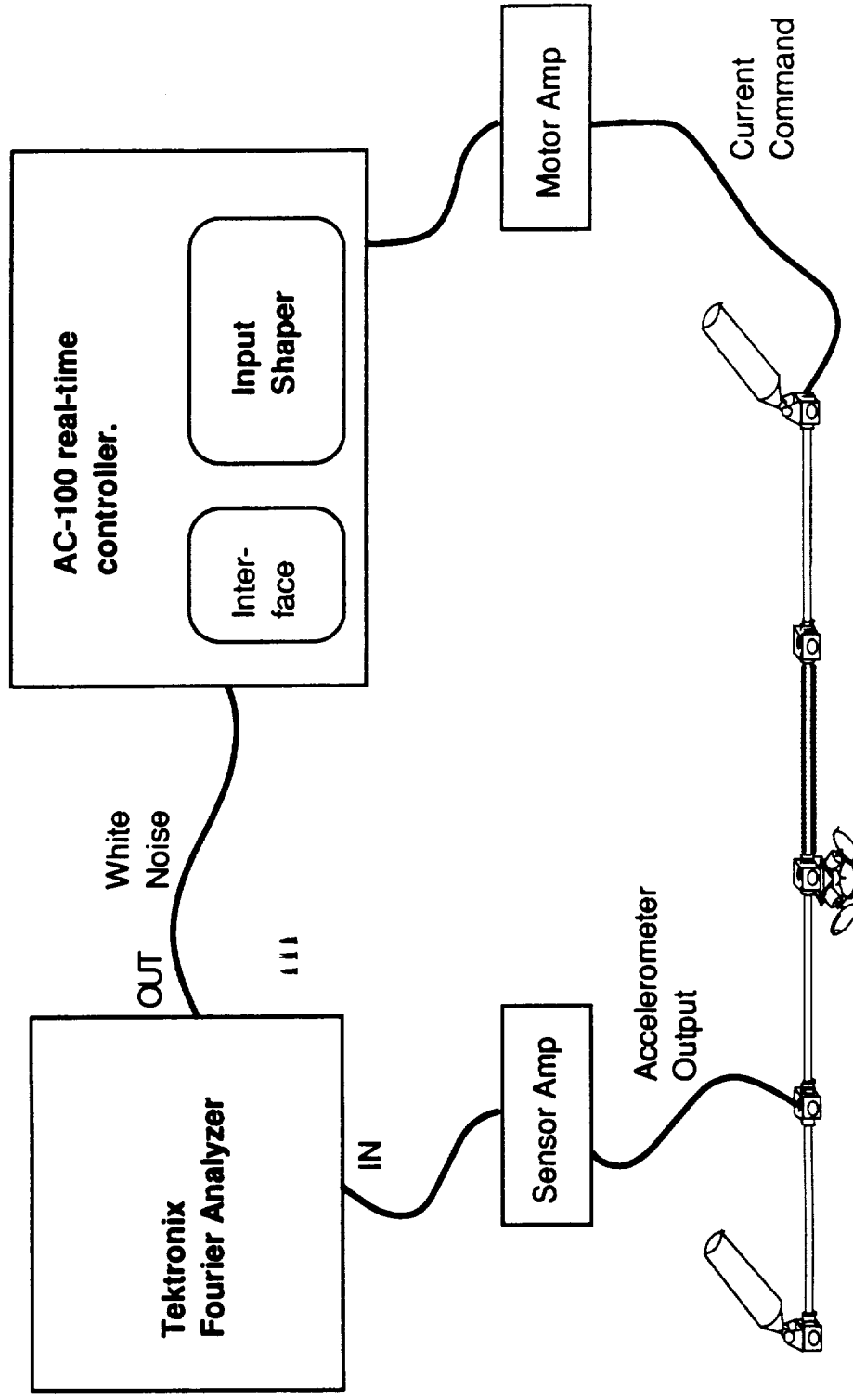


FIRST MODE ONLY

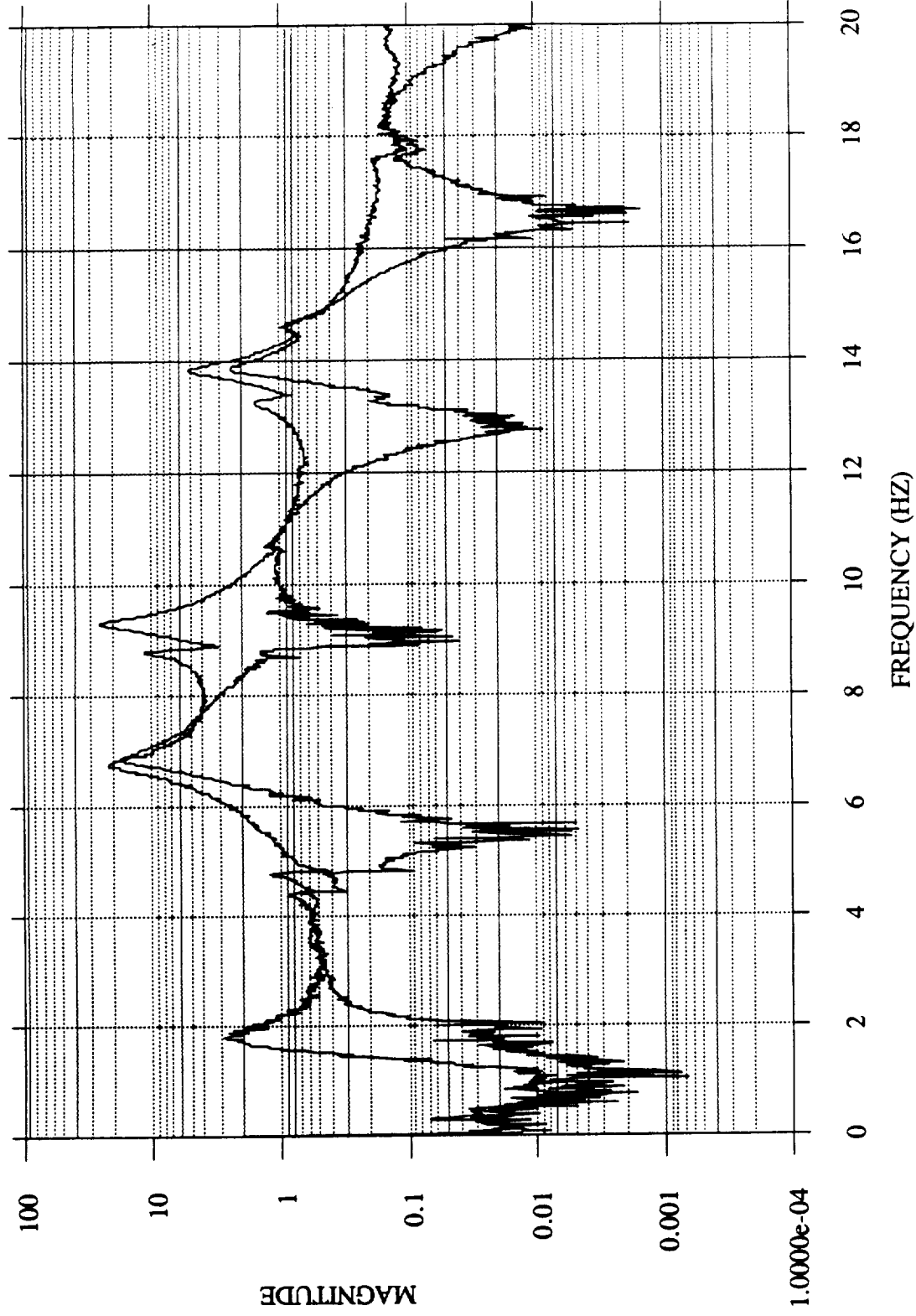


FOUR MODES

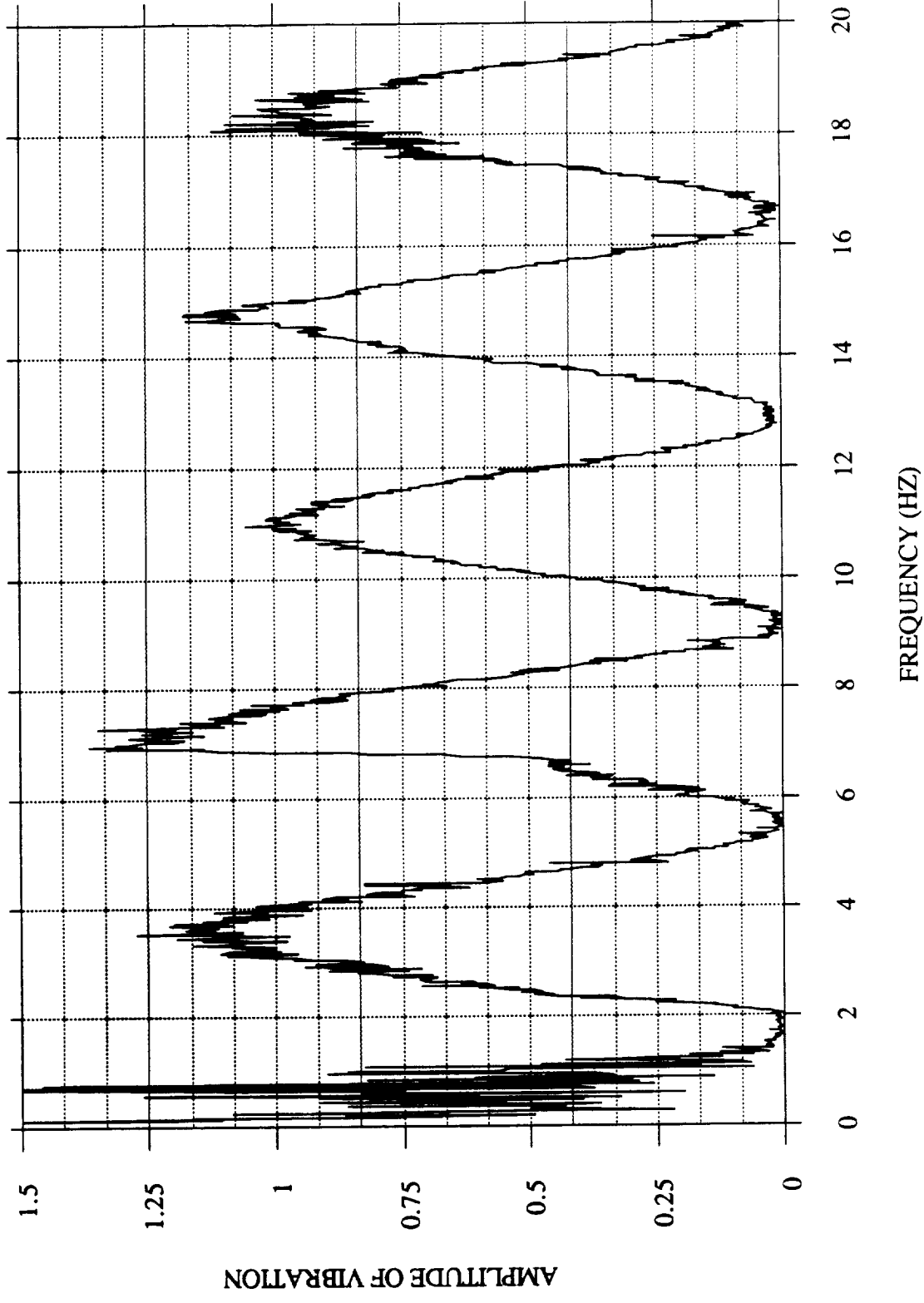
EXPERIMENTAL SETUP



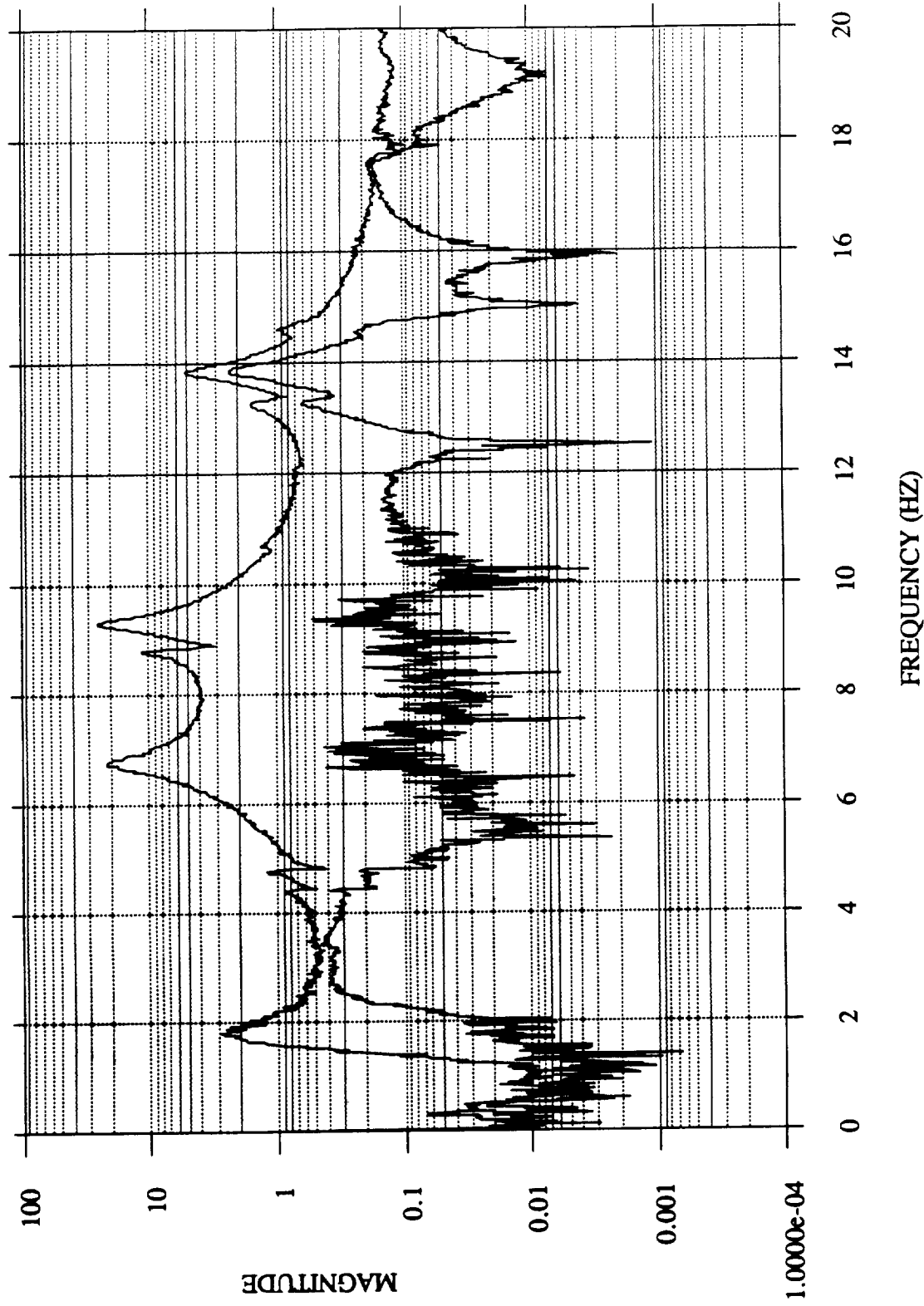
MACE PLANT WITH SHAPER FOR 1ST MODE



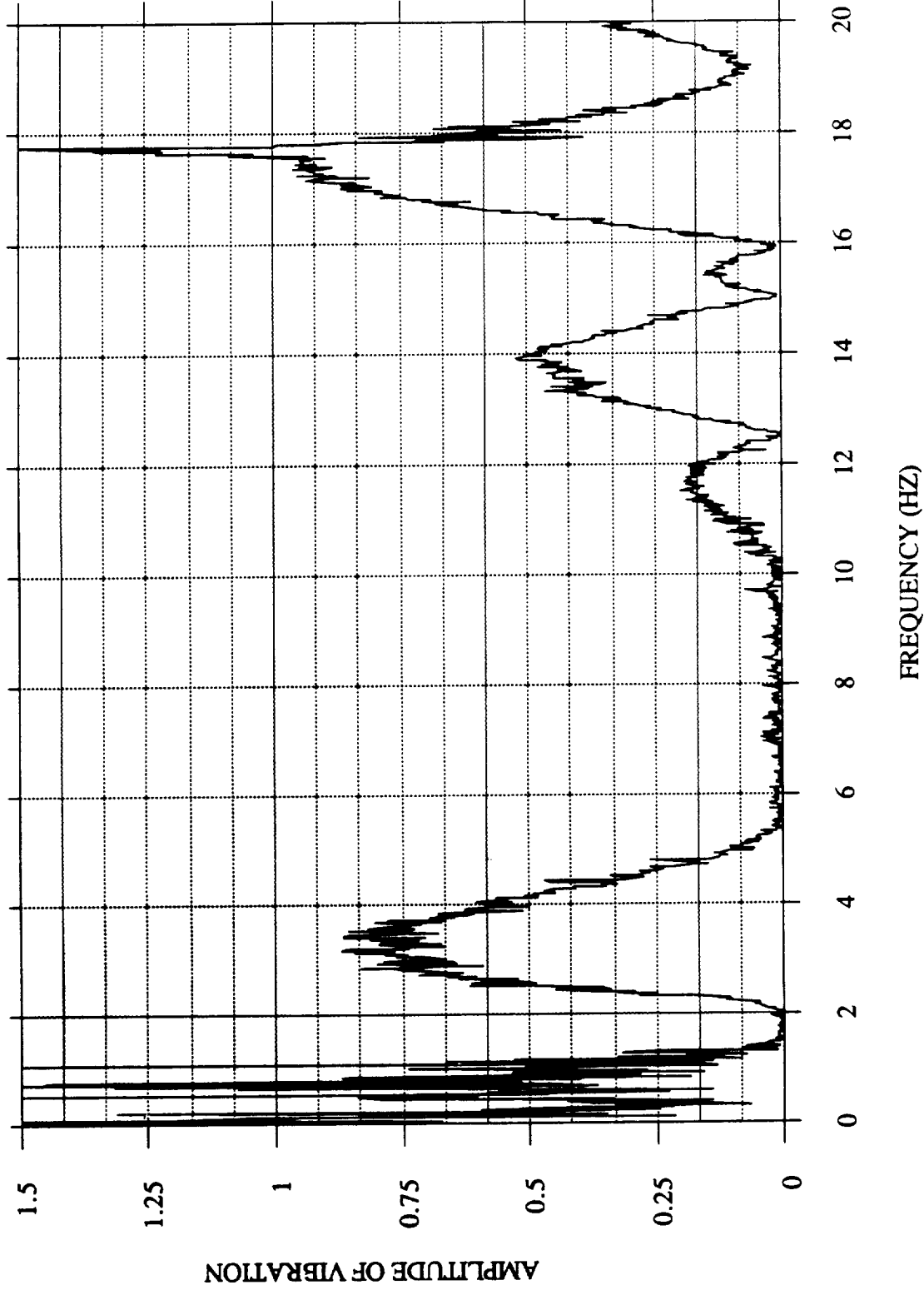
INSENSITIVITY CURVE FOR ONE MODE SHAPER



FREQUENCY RESPONSE WITH SHAPER FOR FIRST FOUR MODES



INSENSITIVITY CURVE FOR 4 MODE SHAPER



CONCLUSIONS

- Input shaping can reduce vibration in multiple-mode systems (MACE).
- Real system non-linearities decrease effectiveness of impulse shaping.

FUTURE WORK

- Identify relevant non-linearities in MACE test article. (friction, kinematic changes in frequency, gravity effects ...)
- Implement an input shaper which most efficiently reduces residual vibration in the presence of non-linearities.
- Generalize observations for all systems.

Embedded Electronics for Intelligent Structures

Recent work in the center has established potential advantages of distributing and embedding large numbers of sensors, actuators, and processors for precision control of flexible structures

A technique to embed electronic devices in addition to sensors and actuators in structural members has been demonstrated

Current research is focusing on the distribution of power and signals to embedded electronic components

- Thermal, structural, and electrical design models of a prototypical intelligent structure are being developed to explore functional requirements for embedded components
- These requirements will drive the custom design of an efficient, single-chip amplifier suitable for driving piezoelectric actuators

The work is expected to culminate in a graphite/epoxy beam test article in which both an actuator and an amplifier are embedded, possibly with additional control circuitry

METHODS OF IDENTIFICATION AND MODELING OF THE INTERFEROMETER TESTBED

- **OBJECTIVE:**

To become familiar with the data acquisition and system identification techniques of the interferometer testbed, and to integrate suspension modes of the interferometer into the finite element code.

- **APPROACH:**

Use interferometer data acquisition equipment to record four transfer functions. The transfer functions correspond to two active strut inputs to the plant and two laser displacement measurements, as the output.

Linearize displacement dynamics of suspended interferometer in order to come up with a first cut model of suspension modes to incorporate in finite element code.

- **STATUS:**

Transfer function data taken and analyzed

Verification of predicted suspension modes in progress

PRESSURE ACTUATOR WITH VISCOUS FLUID DAMPING

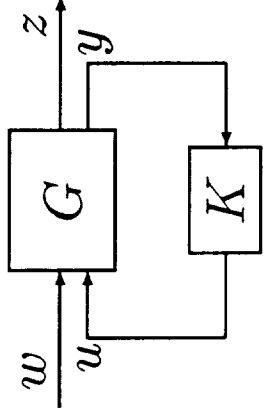
- **OBJECTIVE:** The design, manufacture, and testing of a pressure-controlled actuator with viscous fluid damping
- **PRINCIPLE:** Controlled pressurization will alter the dimensions of the structure while eliminating high frequency excitations
- **APPROACH:**
 - Application of theory to a first generation design including actuator size, shape and critical subcomponents
 - Design and manufacture of an actuator based on an isotropic (Aluminum) pressure cavity
 - Testing and analysis of first generation design
 - Second generation design and manufacture based on an anisotropic (composite) cavity to maximize axial stroke and hoop stress tolerance
 - Incorporation of actuator into a controlled truss structure
- **STATUS:** Initial component design completed

Passive Control/Damping: Spangler, Hall

- Objective: Design and implementation of optimal structural control using integral piezoelectrics shunted with strictly passive electrical networks.

- Approach

- Modeling for Control Design:



- * Controller input/output are voltage/current at piezo electrodes.
 - * Piezo is both sensor and actuator, *truly* collocated.
 - * G_{22} is an electrical impedance which exhibits the combined effects of the piezo capacitance and the structure's dynamics.

Passive Control: Spangler, Hall (cont.)

- Control Design:
 - * Passivity constraint is formulated in terms of constraints on the state-space realization of the controller network.
 - * Cost (some functional of z) is optimized numerically over the constrained controller.
- Status:
 - Frequency domain modeling technique developed - extension of [Hagood '91] - and examples worked.
 - \mathcal{H}_2 controllers developed for benchmark examples, with networks restricted to RC.
- Future:
 - Develop a more fundamental, elegant solution technique for the \mathcal{H}_2 /RC design problem (riccati equations).
 - Experiment on the Interferometer Testbed.

END-POINT CONTROL OF FLEXIBLE MANIPULATOR ARMS

Objective:

- To achieve high-bandwidth, robust, end-point position control of a two-link, planar manipulator with distributed flexibility in the links.

Approach:

- Model distributed flexibility using assumed modes.
- Investigate maximum performance achievable.
- Obtain analytical stability and performance results for desired controllers.
- Design controllers for robustness to model uncertainties, both structured and unstructured.
- Exploit the use of simplified models when possible.
- Conduct simulations.

Status:

- Simulation of planar, two-link flexible manipulator has been created.
- Investigation of nonlinear system dynamics, degree of nonlinearity of desired trajectories, and choice of mode shapes for control design are under way.
- Theory of output regulation for nonlinear systems used as a framework to elucidate tradeoffs between Feedforward and Feedback control.
- Performance limitations inherent in nonlinear nonminimum phase (NMP) systems made transparent in this way and are reducible locally to limits of performance on linear NMP systems.
- Concepts from Lyapunov-based Sliding Control and Adaptive control for rigid robots and robots with flexible joints are combined with differential geometric concepts to extend results to flexible link robots.
- Hamiltonian approach to Lyapunov function selection promises stabilizing control results without neglecting higher order dynamics through modal truncation.
- Extensions to tracking control and to controllers with robustness to parameter uncertainty seem possible.